eman ta zabal zazu

Universidad del País Vasco
Euskal Herriko Unibertsitatea

DOKTOREGO TESIA

A geometric and physical study of Riemann's non-differentiable function

Riemannen funtzio ez-diferentziagarriaren azterketa geometriko eta fisikoa

Estudio geométrico y físico de la función no diferenciable de Riemann

Egilea:
Daniel ECEIZABARRENA

Zuzendaria:
Luis VEGA

Bilbon, 2020ko maiatzean

PHD THESIS

A geometric and physical study of Riemann's non-differentiable function

Author:
Daniel ECEIZABARRENA

Advisor:
Luis VEGA

Bilbao, May of 2020

This PhD thesis has been carried out at BCAM, the Basque Center for Applied Mathematics and supported by the Ministry of Education, Culture and Sport (Spain) under grant FPU15/03078 - Formación de Profesorado Universitario, by the ERCEA under the Advanced Grant 2014 669689 - HADE, by the Ministry of Science, Innovation and Universities under the BCAM Severo Ochoa accreditations SEV-2013-0323 and SEV-2017-0718 and by the Basque Government through the BERC 2014-2017 and 2018-2021 programs.

Abstract

A geometric and physical study of Riemann's non-differentiable function

Daniel ECEIZABARRENA

Riemann's non-differentiable function is a classic example of a continuous but almost nowhere differentiable function, whose analytic regularity has been widely studied since it was proposed in the second half of the 19th century. But recently, strong evidence has been found that one of its generalisation to the complex plane can be regarded as the trajectory of a particle in the context of the evolution of vortex filaments. It can, thus, be given a physical and geometric interpretation, and many questions arise in these settings accordingly.

It is the purpose of this dissertation to describe, study and prove geometrically and physically motivated properties of Riemann's non-differentiable function. In this direction, a geometric analysis of concepts such as the Hausdorff dimension, geometric differentiability and tangents will be carried out, and the relationship with physical phenomena such as the Talbot effect, turbulence, intermittency and multifractality will be explained.

Laburpena

Riemannen funtzio ez-diferentziagarriaren azterketa geometriko eta fisikoa

Daniel ECEIZABARRENA

Edonon jarraituak baina inon deribagarriak ez diren funtzioen artean ospetsuenetarikoa dugu Riemannen funtzio ez-diferentziagarria. XIX. mendearen amaieran proposatu zutenez geroztik, haren inguruan egindako azterketa analitikoa sakona izan da. Edonola ere, analisitik at ere protagonismo esanguratsua duela aurkitu dute duela gutxi; izan ere, funtzioa plano konplexura orokortuz gero, zurrunbilo-filamentu jakin batzuen ibilbidearen antz handia du. Jatorrian analitikoa den objektu honek, beraz, interpretazio fisiko eta geometriko argia onartzen du, eta bere azterketarako bide berri eta interesgarri ugari sortzen dira ondorioz.

Ikuspuntu horri helduz, Riemannen funtzio ez-diferentziagarriaren propietate geometriko eta fisikoak aztertzea da tesi honen helburua. Geometriari dagokionez, haren Hausdorffen dimentsioa, diferentziagarritasun geometrikoa eta ukitzaileak aztertuko dira, eta fisikaren aldetik, Talboten efektua, turbulentzia, intermitentzia eta multifraktaltasuna bezalako fenomenoekiko erlazioa nabarmendu eta ikertuko da.

Resumen

Estudio geométrico y físico de la función no diferenciable de Riemann

Daniel ECEIZABARRENA

La función no diferenciable de Riemann es uno de los ejemplos clásicos de funciones que, a pesar de ser continuas, no son diferenciables en ningún punto. Su regularidad analítica ha sido objeto de estudio constante desde que fue propuesta en la segunda mitad del siglo XIX. Sin embargo, se ha mostrado recientemente que esta función admite una interpretación física y geométrica en paralelo a su naturaleza analítica, dado que una de sus generalizaciones al plano complejo se asemeja a una trayectoria en la evolución de ciertos filamentos de vórtice. En este contexto, surgen nuevas preguntas desde perspectivas que no han sido exploradas hasta ahora.

El objetivo de esta tesis es analizar propiedades de la función no diferenciable de Riemann motivadas por esta nueva interpretación. Así, teniendo en cuenta la semejanza a la trayectoria mencionada, se estudian aquí su dimensión de Hausdorff, su diferenciabilidad geométrica y la existencia de tangentes. Por otro lado, se han analizado las conexiones con fenomenos físicos tales como el efecto de Talbot, la turbulencia, la intermitencia y la multifractalidad.

Acknowledgements - Esker onak - Agradecimientos

To everyone that has been near me at some moment or another, thank you.

Eskerrak eman nahi dizkiot azken lau urte hauetan nire inguruan egon den pertsona orori. Ondorengo lerroetan aipatu behar nuen inor aipatu gabe utzi badut, jaso ditzala nire eskerrak eta barkamena aldi berean.

Ante todo, quiero ofrecer mi más sincero agradecimiento a todas las personas que me han acompañado y que, de una u otra manera, han contribuido a mi bienestar durante estos últimos cuatro años. A los que nombro y a los que no, muchas gracias.

Muchas gracias a Luis Vega por haber dirigido esta tesis. Desde luego, yo me quedo muy satisfecho con el trabajo realizado.

Merci à Valeria Banica de m'avoir reçu à Paris pour le stage de trois mois et d'avoir eu le temps de m'écouter quand j'étais en pleine préparation de mes papiers.

Thank you, Andrea Nahmod and Bob Jerrard, for having taken the time to read the manuscript of this thesis and to write the corresponding reports.

Many thanks to my collaborators. Merci à Alex Boritchev et Victor Vilaça da Rocha. Grazie mille a Renato Lucà.

Zein eskertuta nagoen Naiara Arrizabalaga eta Aingeru Fernández! Zer konfidantza eta askatasuna eman didaten hasiera-hasieratik, baita ikasleen aurrean jarri nintzen lehendabiziko aldian ere. Eskerrik asko bene-benetan.

Eskerrak BCAMi eta bertako langileei. En especial, agradezco enormemente la labor de Miguel Benítez, que me ha ayudado con mil y una gestiones. Muchísimas gracias, Miguel.

Gracias a las variopintas gentes de BCAM y de la universidad. ¡Qué inmenso placer haber podido compartir con vosotros todo este tiempo! Gracias a mi gran compañero de cueva primero y de oficina después, don Sandeep Kumar. Gracias a mis contemporáneos doctorandos: a Javi Martínez, a Massi, a Natalia, a Bruno, a Xuban, a Martina, a Javi Canto, a Isabella, siempre cerca desde el principio hasta el final. Nola ez, baita unibertsitateko gaztetxoagoei, Andoni eta Igorri, ere. Gracias también a Luz, a David, a Julia, a Mario, a Fabio, a Dae-Jin, a Antsa, a Simone, a Andrea. Y no me olvido de los que a pesar de llegar los últimos, me parece que están desde el principio: de Tomás, de Martín y de Lorenzo. Más de uno envidiaría una kuadrilla así.

Y qué fácil fue también pasar los tres meses en París en compañía de Eli, Jaime, Giorgina, Santi, Nacho, Chals y demás. ¡Gracias, chicos! And of course, I can't forget about that crazy Minnesotan guy who dares to wear shorts and sandals in freezing temperatures. Thanks a lot, Allen!

Los últimos meses, y en particular la redacción de la mayor parte de esta tesis, han estado marcados por la crisis de la COVID-19. Encerrados en casa a cal y canto durante mucho tiempo, duro para quienes disfrutan del aire fresco en compañía, sin poder aprovechar el buen tiempo de primavera para hacer excursiones a lo largo de la geografía vasca y alrededores. Sin poder ir a tomar algo en Somera. ¡Sin poder ir a la sidrería que ya teníamos reservada, después de lo que nos costó encontrar sitio! Me

pregunto cómo veremos todo esto cuando tengamos la perspectiva temporal necesaria. En cualquier caso, se merecen por mi parte una mención muy especial Martina Conte y Javi Canto, que me han brindado una compañía constante y han hecho que haya sido muy llevadero. Muchísimas gracias a los dos.

Zinez bestelakoa den Torontoko lagun taldeari ere badoakio nire esker ona. Horren desberdinak izanda eta elkar horren gutxi ikusita, benetan miresgarria egiten zait harremana horrenbeste denboran zehar mantentzea lortu izana. Denak erdi pitzatuta gaudelako ote da? Batek daki... Batez ere, azkeneko hilabete hauetan emandako konpainiarengatik, Ainara, Ander, Maialen eta Jon, eskerrik asko.

Nola ez, eskerrik asko kuadrilako lagunei. Bai Tolosan daudenei eta baita kanpoan zaudetenoi, nahiz eta horren maiz ez ikusi. Bereziki, zenbat oxigeno eta energia eman didaten Pirinioetako, Asturiasko eta Oropesako bidaiek! Ez ditzagun ohitura onak galdu!

Ezin ahaztu etxeko giroan gertu izan dudan elementu parea. Hiruon artean, ezin esan zein zoroago. Lagun onak lehenagotik, lagun hobeak elkarrekin bizi garenetik, ea lortzen dugun progresioa mantentzea gure bideak aldentzen direnean. Markel eta Iker, eskerrik asko!

Gertukoenei, gehien maite ditudanei, zer esango diet ba? Nire esker on mugagabea dute Aitor, Aita eta Amak. Asko maite zaituztet!

Amaitzeko, azken hilabete gogor hauetan amonak utzi gaitu, eta ni urruti harrapatu nau. Baina bakean joan omen zen, eta horrek pozten nau. Orain konturatzen naiz ez dudala gogoratzen keinu txarrik bere aurpegian. Bat ere ez. Zeinen umore eta esker oneko emakumea! Beti irribarrea zuen niretzat. Eta zeinen poz handia haren oroitzapen horrekin geratzea. Tesi hau hari eskaini nahi nioke.

Danik 2020ko maiatzean Bilbon idatzia

Contents

Outline of the thesis

Riemann's non-differentiable function

$$f(x) = \sum_{n=1}^{\infty} \frac{\sin(n^2 x)}{n^2} \tag{1}$$

is undoubtedly one of the most famous among the functions that are continuous but nowhere differentiable. Devised and proposed as an analytically pathological example in the 1870s against general beliefs of the time, it is not surprising that it has been traditionally studied from an analytical point of view; even less, taking into account that its differentiability was not completely solved until 1970. It is worthwhile to mention Gerver's result [42], who concluded that f is indeed differentiable in points of the form odd/odd, and nowhere else. Later, the study of Riemann's function continued its natural course by tackling more subtle regularity properties, like Hölder regularity.

Even if a few geometry-flavoured properties were also proved, it was in the work of De la Hoz and Vega [26] when Riemann's function was put in direct connection with a physical experiment. This experiment concerns the evolution of vortex filaments that have been produced by polygonal jets. A practical and common example is given by the smoke rings that smokers can produce with their mouth. Physically more consistent would be to generate such rings with a circular smoke cannon. We all know from experience that these rings travel in space with their shape almost unchanged, but then, what would happen if the cannon were of a regular polygonal shape? This is precisely what underlies the mathematical terms in [26], where they analysed the evolution of a regular polygonal curve which evolves according to the binormal flow, or the vortex filament equation (VFE),

$$\boldsymbol{X}_t = \boldsymbol{X}_s \times \boldsymbol{X}_{ss},$$

where $\boldsymbol{X} = \boldsymbol{X}(s,t)$ is a curve in arclength s and time t. This is a model for one-vortex filament dynamics that was derived for the first time by Da Rios [20] in 1906 from the Euler equation, and according to the experiments in [66], it seems to adapt well enough to the real evolution of polygons, at least qualitatively. One of the findings in [26] is that the trajectory of a corner of the polygon is very similar to

$$\phi(t) = \sum_{k\in\mathbb{Z}} \frac{e^{-4\pi^2 i k^2 t} - 1}{-4\pi^2 k^2}, \tag{2}$$

a generalisation of Riemann's non-differentiable function (1) to the complex plane. Moreover, this approximation seems to improve when the number of sides of the polygon is increased.

The above shows that Riemann's non-differentiable function, at least in its version ϕ, can be regarded as a purely and intrinsically geometric and physical object, and also to be in direct connection to the theory of turbulence. In this sense, the study of geometric properties of the image set $\phi(\mathbb{R})$ that represents the trajectory, as well as of physically motivated properties in the setting of turbulence such as intermittency and multifractality, seems natural and interesting. In this dissertation, it has been my objective to contribute with some advances in these directions.

In what follows, let me offer a short outline of the contents in the present document.

Of the introduction. Chapter 1

Chapter 1 is devoted to a general introduction where the appearance of Riemann's non-differentiable function in geometric and physical settings is explained in detail.

First of all, Section 1.1 concerns the historic development of the regularity of functions that led to the definition of Riemann's function and the consequent revolution in the foundations of mathematics. Also, we will discuss the establishment of its differentiability and other analytic properties during the 20th century, as well as the few geometric results that started appearing.

In Section 1.2, we review the contribution by De la Hoz and Vega [26] that shows the connection of Riemann's function with the experiment of vortex filaments. Based on the solution of the VFE that corresponds to a regular polygonal and planar vortex, some heuristic arguments yield ϕ as an approximation to the trajectory of a corner of the polygon. Numerical simulations show that even if rudimentary, these arguments are apparently effective, since the matching between ϕ and the actual trajectory of a corner of the polygon is very accurate. This strongly motivates the interest in learning about its geometric properties.

The Talbot effect is the central element of discussion in Section 1.3. To begin with, I have chosen to relate the historic account of this beautiful optical effect and to explain it in detail. This is not strictly for mathematical reasons, but rather because it has allowed me to share my work with the general public. Indeed, the Talbot effect has been the gate to the dissemination of my work for almost four years, and thus I considered it fair that its physical and historical description be part of this dissertation as a humble tribute. It is not, however, the only reason to do it; indeed, it having been traditionally studied by physicists, many arguments lack of mathematical rigour. Hence, we will try to rigorously establish these arguments, to the extent possible, in Appendix A. This path, however, leads to very weak convergence results that consist in somewhat humble mathematical arguments, hence its inclusion as an appendix and not as a chapter in the body of the text.

In any case, the Talbot effect is the optical phenomenon that happens when light crosses an equidistant diffraction grating. There is a distance, called the Talbot distance, in which the grating is exactly reproduced due to the interference of the luminous waves produced in each slit. Moreover, and more astonishingly, the grating is reproduced with q times more slits in every fraction of the Talbot distance, where q is the denominator of the fraction in question. Incredible as it may seem, this effect is also observed in the evolution of regular polygons by the binormal flow. In every rational multiple of some fixed time that depends on the number of sides of the initial polygon, the vortex filament is also a polygon which now has a number of sides proportional to the denominator of the fraction and which is not necessarily planar anymore. Somehow, slits in the optical experiment are identified with corners in the evolution of polygonal vortices. A more detailed description, with the corresponding mathematical expressions, is given in Subsection 1.3.2.

The connection of Riemann's function with the Talbot effect may seem indirect, since if the evolution of the polygonal vortex is taken as the central experiment, then the Talbot effect appears when time is fixed, while Riemann's function shows up when space is fixed. However, the Talbot effect will play a role in the heuristic argument which motivates the method to obtain the asymptotic behaviour of ϕ, critical to prove geometric results.

Finally, in Section 1.4 we will explore the relationship of Riemann's function with concepts related to turbulence such as multifractality and intermittency. Multifractality originated in the study of of fully developed turbulence, when observing that

the velocity of the fluid under consideration suffers very large variations even in a very reduce amount of space. Hence, it is expected that its regularity, measured usually in terms of Hölder regularity, changes drastically. In other words, it is reasonable to expect that the velocity admits very different scaling laws in very close points. This phenomenon is usually called intermittency. In this situation, physicists look for the the spectrum of singularities

$$d(\alpha) = \dim_{\mathcal{H}} D_\alpha,$$

the Hausdorff dimension of the sets D_α which are the sets of points where the velocity is approximately α-Hölder regular,

$$D_\alpha = \{\, x \in \mathbb{R}^3 \,:\, |v(x+l) - v(x)| \approx l^\alpha, \quad \forall l \text{ small} \,\}.$$

If different Hölder exponents produce sets of different dimension, or similarly, if $d(\alpha)$ takes an open set of values, then it is said that the velocity is multifractal. Unfortunately, the spectrum of singularities is technically difficult to measure in experiments. In this sense, Frisch and Parisi [41] proposed a method to obtain it by measuring the so-called structure functions

$$S_p(l) = \langle |v(x+l) - v(x)|^p \rangle, \qquad x, l \in \mathbb{R}^3$$

where $\langle \cdot \rangle$ stands for some ensemble average, easier to track in practice. More precisely, assuming that the structure functions scale like $S_p(l) \approx |l|^{\zeta(p)}$, they related the spectrum of singularities with $\zeta(p)$ in terms of the Legendre transform

$$d(\alpha) = \inf_p \{\alpha p - \zeta(p) + 3\}, \tag{3}$$

which receives the name of multifractal formalism. The arguments leading to this, though, are heuristic, and its mathematical validity, unclear. Hence, after adapting all these concepts to mathematically rigorous objects such as measures or functions, it became a popular problem in the 1990s to determine the range of validity of (3). For instance, it is reasonable to redefine the sets D_α as

$$D_\alpha = \{\, x \in \mathbb{R}^3 \,:\, \alpha_v(x) = \alpha \,\}, \qquad \text{where} \qquad \alpha_v(x) = \sup\{\alpha \,:\, v \in C^\alpha(x)\},$$

and the structure functions as

$$S_p(l) = \|f(\cdot + l) - f(\cdot)\|_{L^p}^p. \tag{4}$$

In this setting, Jaffard [55] proved that the multifractal formalism holds for Riemann's non-differentiable function. In the same spirit, we will see how the concept of intermittency can also be adapted to the setting of functions using the structure functions (4), or alternatively some Fourier high-pass filters, based on the probabilistic concept of kurtosis or flatness. The result of Jaffard thus motivates the analysis of the intermittency of Riemann's function.

Of the body of the dissertation. Chapters 2 to 5

The results concerning the geometric analysis of Riemann's function are discussed in Chapters 2, 3 and 4.

In Chapter 2, we will first establish the mathematical setting and notation that we will use all along the geometric analysis of ϕ, and then we will compute the asymptotic behaviour of ϕ around rational multiples of its period as a tool for the coming results.

This was already done by Duistermaat in [29] for the function

$$\phi_D(x) = \sum_{n=1}^{\infty} \frac{e^{i\pi n^2 x}}{i\pi n^2},$$

which is trivially related to ϕ, and his results could thus be translated. However, I chose to compute them from scratch for ϕ here, firstly so that this dissertation remains as self-contained as possible, and secondly because we will follow a path which I found to be more intuitive. It is (very) slightly different from Duistermaat's and we will keep track of the connection to his computations often and remark the pros and cons of each approach. The proof is based on the very deep connection of Riemann's function with Jacobi's θ function, whose interaction with the modular group is key to success. The main results in this chapter, too long and technical to state here, are written in Propositions 2.12 and 2.15.

In Chapter 3, in the setting of ϕ being a representative of a trajectory in the experiment of vortex filaments, we look for the Hausdorff dimension of the image set $\phi(\mathbb{R})$. This is specially motivated by the computer-made plot in Figure 1.5, which shows a certain self similar pattern and therefore suggests fractality. The main result is the following theorem, which corresponds to Theorem 3.1.

Theorem. *Let ϕ be Riemann's non-differentiable function defined in (2). Then,*

$$1 \leq \dim_{\mathcal{H}} \phi(\mathbb{R}) \leq 4/3.$$

The lack of exact self similarity makes the finding of the correct lower bound a difficult task that will be subject of future research.

This theorem can be generalised to the multifractal setting explained above; indeed, when Jaffard proved the validity of the multifractal formalism for Riemann's function, he was able to show

$$d(\alpha) = \dim_{\mathcal{H}} D_\alpha = 4\alpha - 2, \qquad \forall \alpha \in [1/2, 3/4].$$

We may, thus, wonder about the dimension of the image of these sets D_α. In this sense, we will show the following result, which corresponds to Theorem 3.2.

Theorem. *Let ϕ be Riemann's non-differentiable function defined in (2). Then,*

$$\dim_{\mathcal{H}} \phi(D_\alpha) \leq \dim_{\mathcal{H}} \phi\Big(\bigcup_{\beta \leq \alpha} D_\beta \Big) \leq \frac{4\alpha - 2}{\alpha}, \qquad \forall \alpha \in [1/2, 3/4].$$

The proofs of both theorems are based on the asymptotic expansion of ϕ around rational multiples of its period and also on the approximation of irrational numbers by continued fractions.

Following with the fact that ϕ represents the trajectory of some particle, we may wonder about the velocity in which it moves. It seems clear that some mean velocity can be computed, since the motion of the particle is deterministic and determined by ϕ. But can we decide this infinitesimally? In other words, can the velocity and, in particular, the direction of the particle be determined at any precise moment? This is what we may call the geometric differentiability of ϕ and which we tackle in Chapter 4. The main result is the following.

Theorem. *Let ϕ be Riemann's non-differentiable function defined in (2). There does not exist a point $x \in \mathbb{R}$ such that $\phi(\mathbb{R})$ has a tangent in $\phi(x)$.*

Two are the issues to be noted here. One is that this result is meaningful because there is not a clear relationship between analytic and geometric differentiability of ϕ. Computer-made plots show that in rational points where ϕ has no derivative, $\phi(\mathbb{R})$ has two side tangents that are perpendicular and thus do not coincide. On the other hand, in points where ϕ is differentiable, a spiralling pattern is observed in $\phi(\mathbb{R})$ such that no tangent can exist. In what concerns to irrationals, a preliminary analysis like this is more complicated to do. The second issue is that there is a need to define a proper concept of tangent, since the usual definitions from differential geometry are of no use because ϕ is not differentiable in any open set. A purely geometric definition seems most reasonable, but a parametric definition is more convenient in terms of computations. Thus, we give two definitions, one in each setting, and show that the result for the parametric definition implies the geometric result. Hence, it will be enough to prove the theorem from the parametric point of view. I refer the reader to Section 4.3 for the precise statements of the results we will prove and from which we will deduce the theorem above stated.

We change topics in Chapter 5 to the analysis of the intermittency of Riemann's function. For that, following the motivation given in the introduction, we will adapt the definitions of structure functions, high-pass filters, flatness and intermittency to the setting of functions and prove the following theorem.

Theorem. *Riemann's non-differentiable function is intermittent.*

I refer the reader to Chapter 5 for the precise definition of intermittency. The precise results that correspond to this theorem are Corollaries 5.7 and 5.11. Indeed, they are nothing but special cases of the wider Corollaries 5.5 and 5.10.

Of the appendices

As already mentioned, the expression that is usually used to describe the Talbot effect is obtained by arguments that, even if maybe reasonable physically, are not correct from a mathematical point of view. The objective in Appendix A is to clarify to what extent these arguments can be made rigorous. For that, we begin by reviewing the physical arguments used and explaining why they make sense for approximations in a laboratory. After that, we first need to find a suitable mathematical environment, which by the restrictions posed by the objects themselves, will need to be spaces of distributions. Consequently, the results we will establish are very weak convergence results.

In Appendix B, we will review the basics of the theory of continued fractions, widely used along the whole text. We will define them first and give the motivation of their existence, and then we will state and prove several basic but important properties.

In Appendix C, a very brief account of some symmetries of the Schrödinger equation is offered, emphasising in the Galilean and the pseudoconformal symmetry used at some point in the text.

Tesiaren nondik norakoak

Zalantzarik gabe, Riemannen funtzio ez-diferentziagarria, hots,

$$f(x) = \sum_{n=1}^{\infty} \frac{\sin(n^2 x)}{n^2},$$

jarraituak baina inon diferentziagarriak ez diren funtzioen artean famatuenetarikoa da. Horien adibide gisa proposatu zuten 1870eko hamarkadan, eta garai hartako uste guztien kontra zijoan heinean, ez da harritzekoa gaur egun arte haren inguruan egindako lan gehiena perspektiba analitiko batetik egin izana. Funtzioaren berezko konplexutasunak azterketa horretan eragindako zailtasuna dela medio, bere diferentziagarritasuna ez zuten guztiz argitu 1970era arte; orduan frogatu zuen Gerverrek [42], hainbat urte lehenago Hardyk [47] lortutako emaitzak erabiliz, f funtzioak deribatua duela soilik p/q zenbaki arrazionaletan, eta gainera p eta q biak bakoitiak direnean besterik ez. Guztiz zuzenak izateko, beraz, *Riemannen funtzio ia-inon diferentziagarria* litzateke; baina, tira, bere izen originala mantenduko dugu sinpletasunaren izenean besterik ez bada ere. Edozein kasutan, deribagarritasunaren problema nagusia ebatzita, funtzioaren erregulartasun analitikoa sakonago aztertzen hasi ziren. Posible ote zen, adibidez, deribaturik ez duen puntuetan funtzioaren Hölder erregulartasuna zehaztea?

Bide horretaz gain, XX. mendearen amaiera aldean emaitza geometriko batzuk argitaratu zituzten, poliki-poliki analisitik kanpoko alorretako kontzeptuak lantzen hasiz. Baina 2014an, ikuspuntu guztiz berri eta harrigarria eman zitzaion Riemannen funtzioari; izan ere, EHUko irakasle diren Patxi de la Hoz eta Luis Vegak [26] fisikarekin erlazionatu zuten, zurrunbilo-filamentuekin egindako esperimentu batekin, zehazki. Zurrunbilo-filamentu hauek ezagunak zaizkigu; horien adibide dira erretzaile batek egiten dituen kezko eraztunak, edota zientziarako egoera hobean, ke-kanoi batek laborategi batean sorturikoak. Dakigunez, eraztun horiek airean mugitzen dira beraien itxura zirkularra aldatu gabe, tarte batean behintzat, sakabanatzen hasten diren momentura arte, eta egoera ideal batean bageunde, segurasko ez ginateke harrituko eraztuna bere horretan betirako mantenduko balitz. Baina imagina al dezakegu zer gertatuko litzatekeen kanoiak itxura triangeluarra izango balu itxura zirkularraren ordez? Horixe da, hain zuzen ere, De la Hoz eta Vegak aztertutako egoera: fluxu binormala edo zurrunbilo-filamentuen ekuazioa (VFE) jarraitzen duen hasierako *eraztun* triangeluar honen eboluzioa aztertu zuten matematikoki. Ekuazio hori,

$$\boldsymbol{X}_t = \boldsymbol{X}_s \times \boldsymbol{X}_{ss}$$

hain zuzen ere, zurrunbilo-filamentu baten dinamikarako eredua da, 1906an proposatua [20] eta Eulerren ekuaziotik datorrena. Hemen, $\boldsymbol{X} = \boldsymbol{X}(s,t)$ hiru dimentsioko espazioan dagoen kurba bat da, eta s arku-luzera eta t denbora aldagaiak ditu. Zenbait esperimenturen arabera [66], eredu hau nahiko ondo moldatzen da zurrunbilo poligonalen eboluziora, kualitatiboki behintzat. Egoera honetan, hara zer aurkitu zuten De la Hoz eta Vegak beraien artikuluan [26]: poligono horien edozein erpinen ibilbidea Riemannen funtzioarekin begi-bistako erlazioa duen

$$\phi(t) = \sum_{k\in\mathbb{Z}} \frac{e^{-4\pi^2 i k^2 t} - 1}{-4\pi^2 k^2} \tag{5}$$

funtzioaren oso antzekoa dela! Are gehiago, zenbakizko simulazioen bidez ikusi zuten antzekotasun hori areagotu egiten dela hasierako poligonoaren alde kopurua handitzen

den heinean.

Honen guztiaren arabera, esan genezake Riemannen funtzio ez-diferentziagarriak, edo behintzat bere ϕ aldaerak, berezko egitura fisiko eta geometrikoa dituela, eta zurrunbilo-filamentuen esperimentuetan azaltzen denez, turbulentziaren teoriarekin ere erlazionatuta dagoela. Horregatik, ibilbide fisiko baten ordezkaria den aldetik, $\phi(\mathbb{R})$ multzoaren azterketa geometrikoa egitea naturala da, eta bestalde, inspirazio fisikoa duten ϕ funtzioaren propietateak aztertzeak ere interes handia du. Tesi honen helburua izan da bide horiek jorratzea.

Behin gaia aurkeztuta, hona hemen tesiaren egitura eta eduki nagusien laburpena.

Sarrerarena. 1. kapitulua

Tesi hau Riemannen funtzio ez-diferentziagarriaren historia eta garapenari buruzko sarrerarekin hasten da bere 1. kapituluan.

Hasteko, funtzioen erregulartasunaren garapenaren historia jorratuko dugu 1.1 atalean. Izan ere, gaur egun hain ohikoak zaizkigun jarraitutasun eta deribagarritasunaren definizio zehatzak XIX. mendean zehar ezarri ziren, urte askoren bueltan eta matematikari askoren lanari esker. Garai hartan, funtzio jarraitu batek deribatua eduki behar zuela uste zuten; beraz, ez da harritzekoa Riemannen funtzioaren aurkezpenak iraultza sortu izana. Gertaera honen ondorioak aztertu ondoren, XX. mendean zehar funtzioaren deribagarritasuna eta propietate analitikoei buruzko lana errepasatuko dugu, eta haren inguruko lehen emaitza geometrikoak ezagutuko ditugu.

1.2. atalean De la Hoz eta Vegaren ekarpena [26] jorratuko dugu, Riemannen funtzioaren eta zurrunbilo-filamentuen arteko erlazioari buruzkoa. Lehenik, ikusiko dugu VFE ekulazioaren soluzioaren adierazpen bat kalkula daitekeela hasierako datua zurrunbilo lau eta poligonal bat bada. Adierazpen horri helduz eta zenbait argudio heuristikori esker, ϕ funtzioa lor dezakegu poligonoaren erpin baten ibilbidearen hurbilpen modura. Nahiz eta asko landu gabeko kalkuluak izan, zenbakizko simulazioek erakusten dute nahiko ondo moldatzen direla errealitatera, ϕ funtzioaren irudia eta zenbakizko ibilbideak oso antzekoak baitira, hainbeste non ezin baitira begiz atzeman, adibidez, hamar aldeko hasierako poligonoaren kasuan. Ez da arrazoi eskasa, nire ustetan, Riemannen funtzioa ikuspuntu geometriko batetik aztertzeko.

Talboten efektuari buruzkoa da 1.3. atala. Hasteko, efektu optiko bitxi eta eder honen historia kontatzea erabaki dut. Hori egiteko arrazoi nagusia ez da matematikoa; aitzitik, Talboten efektuak nire lanaren dibulgazioa egitea ahalbidetu dit azken lau urte hauetan zehar. Hitzaldiak eman eta elkarrizketak egin ahal izan ditut, eta horien artean asko euskaraz izan dira. Hori dela eta, bidezkoa iruditu zait tesi honen zati bat efektu hau deskribatzeko erabiltzea. Edonola ere, beste arrazoiak ere baditut; izan ere, espero dezakegun bezala, tradizionalki fisikariek landu dute efektu hau, eta nahiz eta aurkikuntza interesgarri asko egin, erabilitako kalkulu eta argudio asko ez dira matematikoki onargarriak. Matematikari batek segituan du galdera bere aurrean: posible al da hori guztia formalizatzea? Egindako lanaren zati bat izan da hauxe, baina zinez ahulak diren konbergentzia ematzak lortu ditut, argudio nahiko xumeak erabiliz. Horregatik, lan hau A eranskinean jaso dut tesiko gorputzean idatzi beharrean.

Azaldu ditut Talboten efektua tesian sartzearen arrazoiak, baina ez dut oraindik zer den esan. Labur-labur, Talboten efektua fenomeno optiko bat da, argiak zirrikitu zuzen eta paraleloak dituen difrakzio-sareta erregular bat zeharkatzen duenean gertatzen dena. Argia, noski, difraktatu egiten da zirrikitu bakoitzean, eta sortzen diren uhin guztiek elkarrekin interferitzen dute. Interferentzia honen emaitzak harrigarriak

dira. Adibidez, saretatik distantzia jakin batean, argiak hasierako sareta berbera eratzen du haren eraginez. Distantzia honi Talboten distantzia deritzo, eta bere edozein p/q frakziotan, hasierakoa baino q aldiz estuagoa den sareta eratzen da, interferentziak eraginda berriz ere. Baina are harrigarriagoa da efektu hau zurrunbilo-filamentuen esperimentuan agertzen dela ikustea; izan ere, hasierako poligonoaren alde kopuruaren menpekoa den denbora baten multiplo arrazional orotan, filamentuak itxura poligonala hartzen du nahiz eta oro har laua ez izan, eta alde kopurua frakzio horren izendatzailearen menpekoa da. Paralelismoa argia da: efektu optikoko zirrikituak filamentuen erpinei dagozkie. Honen guztiaren deskribapen zehatza idatzi dut 1.3.2 azpiatalean.

Ez dirudi Talboten efektuaren eta Riemannen funtzioaren arteko lotura begibistakoa denik, zurrunbilo-filamentuaren esperimentuan Talboten efektua denbora finkatuz agertzen baita, eta Riemannen funtzioa, ordea, espazioa finkatuz. Hala ere, Talboten efektua garrantzitsua izango da Riemannen funtzioaren portaera asintotikoa kalkulatzeko erabiliko ditugun argudio heuristikoetan. Honek guztiak berebiziko garrantzia izango du funtzioaren propietate geometrikoak aztertzerako garaian.

Azkenik, 1.4 atalean turbulentziarekin erlazionatuko dugu Riemannen funtzioa, multifraktaltasunarekin eta intermitentziarekin, hain zuzen ere. Multifraktaltasunaren jatorria guztiz garatutako turbulentziaren azterketan aurkituko dugu, non fluido baten abiadurak aldaketa bortitzak jasaten dituen nahiz eta behatzen dugun espazio tartea oso txikia izan. Horren ondorioz, bere erregulartasuna oso aldakorra izatea espero dugu. Ohikoa da egoera horretan abiaduraren Hölder erregulartasuna neurtzea, eta kasu horretan, behatutako puntuarekiko oso sentikorrak diren eskala-legeak izatea espero dugu. Fenomeno honi intermitentzia deritzo. Normalean, fisikariek abiaduraren singulartasun-espektroa deritzon

$$d(\alpha) = \dim_{\mathcal{H}} D_\alpha$$

funtzioa, hots, D_α multzoaren Hausdorffen dimentsioa bilatzen saiatzen dira, non

$$D_\alpha = \{\, x \in \mathbb{R}^3 \,:\, |v(x+l) - v(x)| \approx l^\alpha, \quad l \text{ txikia denean} \,\}.$$

Beste hitzetan, D_α multzoko puntuetan fluidoaren abiadurak α-Hölder erregulartasuna du. Fluidoaren abiadura multifraktala dela esaten da baldin eta α desberdinei dimentsio desberdineko D_α multzoak badagozkie, edo zertxobait zehatzago esateaarren, $d(\alpha)$ funtzioaren irudiak behintzat tarte ireki bat badu. Zoritxarrez, ordea, esperimentuetan zaila da singulartasun-espektroa zuzenean neurtzea, eta arazo honi erantzuna eman nahian, Frisch eta Parisik ordezko metodo bat proposatu zuten [41]. Horretarako, neurtzeko errazagoak diren egitura-funtzio deritzen

$$S_p(l) = \langle |v(x+l) - v(x)|^p \rangle, \qquad x, l \in \mathbb{R}^3,$$

funtzioekin lan egitea proposatu zuten, non $\langle \cdot \rangle$ egoeraren eta beharren arabera alda litekeen batez-besteko moduko bat den. Funtzio hauek $S_p(l) \approx |l|^{\zeta(p)}$ eskala-legea betetzen dutela suposatuz, proposatu zuten $\zeta(p)$ funtzioa $d(\alpha)$ singulartasun espektroarekin erlazionatuta dagoela formalismo multifraktala deritzon

$$d(\alpha) = \inf_p \{\alpha p - \zeta(p) + 3\} \tag{6}$$

formularen bitartez. Hala ere, formula honetara iristeko erabili zituzten argudioak heuristikoak eta matematikoki oso ahulak dira, eta horrek bere baliotasun matematikoaren azterketara bultzatu zituen matematikari asko 1990eko hamarkadan. Kontestu

horretan, lehenengo lana definizio fisikoak lengoaia matematikora egokitzean datza. Adibidez, helburua (6) adierazpena zein funtziok betetzen duen ikustea bada, orduan D_α multzoak

$$D_\alpha = \{\, x \in \mathbb{R}^3 \,:\, \alpha_v(x) = \alpha \,\}, \qquad \text{non} \qquad \alpha_v(x) = \sup\{\alpha \,:\, v \in C^\alpha(x)\}$$

adierazpenaren bitartez definitzea da begi-bistako aukera, eta antzeko modu batean,

$$S_p(l) = \|f(\cdot + l) - f(\cdot)\|_{L^p}^p \tag{7}$$

ezartzea. Helburu honekin, Jaffardek Riemannen funtzio ez-diferentziagarriaren kasuan formalismo multifraktala egia dela frogatu zuen [55]. Ildo berean, probabilitatean agertzen den kurtosi kontzeptua erabiliz, ikusiko dugu intermitentzia funtzioetara egoki daitekeela (7) egitura-funtzioak erabiliz, edo bestela, aztertu nahi dugun funtzioaren Fourierren koefiziente altuak iragaziz. Jaffarden emaitza ikusita, Riemannen funtzioaren intermitentzia aztertzeak itxura oneko lana dirudi.

Tesiaren gorputzarena - 2, 3, 4 eta 5 . kapituluak

Tesiaren 2, 3 eta 4. kapituluetan Riemannen funtzio ez-diferentziagarriaren azterketa geometrikoa jorratuko dugu.

2. kapituluaren hasieran, ϕ funtzioaren azterketan erabiliko dugun notazioa ezarriko dugu, eta ondoren bere portaera asintotikoa kalkulatuko dugu bere periodoaren multiplo arrazional guztietan. Emaitza honek garrantzi handia izango du hurrengo kapituluetan frogatuko ditugun propietateetan. Kalkulu hau ez da berria, Duistermaatek egin baitzuen

$$\phi_D(x) = \sum_{n=1}^{\infty} \frac{e^{i\pi n^2 x}}{i\pi n^2}$$

funtzioaren kasuan [29]. Gure ϕ funtzioarekin daukan erlazio zuzena ikusita, bere emaitzak gurera itzul daitezke, agian zenbait kalkulu astun baina tribialen bidez. Ez da hori hemen egingo duguna; aitzitik, kalkuluak ϕ funtziorako berregitea erabaki dut bi arrazoi nagusi direla medio. Bata, tesi hau ahal den heinean kanpoko beharrik gabe irakurtzeko testu bat izan dadin. Bestea, intuitiboagoa deritzodan bide bat jarraituko dugulako, nahiz eta Duistermaatenaren oso antzekoa den. Gure bidea harenaren paraleloa izango da, eta bakoitzak dauzkan alde onak eta txarrak nabarmenduko ditugu. Froga hau Riemannen funtzioak Jacobiren θ funtzioarekin eta talde modularrarekin daukan erlazio sakonean oinarritzen da. Emaitza teknikoa eta luze samarra denez, ez dut hemen idatziko argitasunaren izenean. Irakurleak 2.12 eta 2.15 proposizioetan aurkituko du.

3. kapituluan, $\phi(\mathbb{R})$ multzoaren Hausdorffen dimentsioa kalkulatzea izango da helburua. Esan bezala, Riemannen funtzioaren aldaera hau zurrunbilo-filamentuen esperimentuko ibilbide baten ordezkaria den aldetik, galdera zilegi da, eta are gehiago 1.5 irudia begiratu ondoren, bertan nolabaiteko autoantzekotasuna nabaria baita. Jakina denez, autoantzekotasuna fraktalen ohiko ezaugarria da. Kapituluko emaitza nagusia honakoa da, testu nagusiko 3.1 teoremari dagokiona.

Teorema. *Izan bedi ϕ Riemannen funtzio ez-diferentziagarria, (5) ekuazioan definitutakoa. Orduan,*

$$1 \leq \dim_{\mathcal{H}} \phi(\mathbb{R}) \leq 4/3.$$

Aipatutako autoantzekotasuna zehatza ez izateak arazoak sortzen ditu dimentsioaren behe-borne on bat lortzerako garaian. Nire ustez, problema interesgarri eta zail hau etorkizunean lantzea merezi du.

Goiko teoremak orokorpen multifraktala onartzen du. Hasteko, Riemannen funtzioaren azterketa multifraktala egin zuenean, Jaffardek

$$d(\alpha) = \dim_{\mathcal{H}} D_\alpha = 4\alpha - 2, \qquad \forall \alpha \in [1/2, 3/4]$$

frogatu zuen. Posible ote da multzo horien irudien dimentsioa kalkulatzea? Erantzunaren zati bat datorren teoreman jaso dut, testu nagusiko 3.2 teoremari dagokiona.

Teorema. *Izan bedi ϕ Riemannen funtzio ez-diferentziagarria, (5) ekuazioan definitutakoa. Orduan,*

$$\dim_{\mathcal{H}} \phi(D_\alpha) \leq \dim_{\mathcal{H}} \phi\Big(\bigcup_{\beta \leq \alpha} D_\beta \Big) \leq \frac{4\alpha - 2}{\alpha}, \qquad \forall \alpha \in [1/2, 3/4].$$

Bi teorema hauen frogak ϕ-k zenbaki arrazionalen inguruan duen portaera asintotikoan ez ezik, zenbaki irrazionalen frakzio jarraituen bidezko hurbilpenean oinarritzen dira.

Bestalde, ϕ ibilbide fisiko baten ordezkaria bada, zentzua du, printzipioz behintzat, bere abiadurari buruz hitz egiteak. Zein da partikularen abiadura? Eta zein norabidetan mugitzen da? Argi dago bi punturen arteko batez besteko abiadura kalkula dezakegula: hartu bi puntu horiek, neurtu egindako distantzia eta horretarako denbora-parametroa mugitu dena, eta zatiketa egin. Dena ϕ funtzioak berak finkatuta dago. Baina errepika al daiteke hauxe bera distantzia infinitesimalean? Hau da, partikularen abiadura eta norabidea jakin al dezakegu ibilbidearen puntu bakoitzean? Hauxe bera, funtzioaren diferentziagarritasun geometrikoaren azterketa alegia, 4. kapituluko aztergaia da, eta honakoa, berriz, bertako emaitza nagusia:

Teorema. *Izan bedi ϕ Riemannen funtzio ez-diferentziagarria, (5) ekuazioan definitutakoa. Ez da existitzen $x \in \mathbb{R}$ non $\phi(\mathbb{R})$ multzoak ukitzailea duen $\phi(x)$ puntuan.*

Bi gauza aipatu nahiko nituzke hemen. Lehenik, emaitza hau esanguratsua da, ez baitago lotura zuzenik ϕ-ren diferentziagarritasun analitiko eta geometrikoaren artean. Ordenagailuz egindako irudiek erakusten dute ϕ diferentziagarria ez den puntu arrazionaletan $\phi(\mathbb{R})$ irudiak albo ukitzaileak dituela, baina ez dutela bat egiten perpendikularrak direlako. Ordea, ϕ diferentziagarria den puntuetan $\phi(\mathbb{R})$ multzoak itxura espiraleko portaera dauka eta beraz ezin du bertan ukitzailerik eduki. Irrazionalen kasuan, zailagoa da horrelako azaleko azterketa irudiei begiratuz egitea. Bigarrenik, azterketa geometriko zuzena egiteko behar-beharrezkoa da bektore ukitzailearen definizio egoki bat aurkitzea. Hau ez da guztiz tribiala, geometria diferentzialeko ohiko definizioak ez baitira erabilgarriak funtzioa tarte ireki batean ere diferentziagarria ez delako. Bestalde, neurriaren teoria geometrikoak ematen dizkigun ohiko definizioak ezin ditugu erabili, horretarako beharrezkoa baita multzoaren dimentsioa ezagutzea. Multzoaren itxurak definizio geometrikoa eskatzen duela dirudi, baina aldi berean, bere adierazpen analitikoak definizio parametriko bat eskatzen du. Honela, bi definizio erabiliko ditugu, bakoitza ikuspuntu batetik, eta beraien arteko erlazioa aztertuko dugu, definizio parametrikorako emaitzak definizio geometrikorako emaitza inplikatzen duela ikusiz. Honela, teorema definizio parametrikorako frogatzea nahikoa izango da. Hau guztia 4.3 atalean idatzi dut; bertan definizioak eta erlazio hauek garatu eta teoremaren adierazpen zehatza irakur daitezke.

5. kapituluan, gaia aldatu eta Riemannen funtzioaren intermitentziaren azterketara joko dugu. Horretarako, sarrerako ideiei helduz, egitura-funtzioen, Fourierren iragazkien, kurtosiaren eta intermitentziaren definizioak funtzioen testuingurura egokituko ditugu honako teorema frogatzeko:

Teorema. *Riemannen funtzio ez-diferentziagarria intermitentea da.*

Irakurleak 5. kapituluan bertan aurkituko du intermitentziaren definizio zehatza. Goiko teorema 5.7 eta 5.11 korolarioei dagokie, eta hauek, berriz, 5.5 eta 5.10 korolarioen kasu bereziak besterik ez dira.

Eranskinena

Lehenago esan dut Talboten efektua matematikoki deskribatzen duen adierazpena ondorioztatzeko erabili izan diren argudioak ez direla matematikoki zuzenak, nahiz eta fisikoki onargarriak izan. A eranskinean, nire helburua izan da zein neurritan kalkulu hauek matematikoki justifika daitezkeen ikustea. Horretarako, uhinen ekuaziotik efektuaren adierazpen nagusia lortzeko argudio fisikoak errepasatu eta fisikoki onargarriak izatearen arrazoiak aztertuko ditugu. Horiek formalizatzeko, beharrezkoa da lehenik egitura matematiko egokia aurkitzea. Problemak berak eragiten du egitura horiek distribuzioen espazioak izatea, eta ondorioz, lortzen diren emaitzak konbergentzia emaitza nahiko ahulak dira.

B eranskinean frakzio jarraituen oinarrizko teoria bildu dut, testu nagusiko atal batean baino gehiagotan garrantzi handia baitute. Definiziotik eta haien jatorrizko motibaziotik hasiz, oinarrizkoak diren baina berebiziko garrantzia duten propietateen enuntziatuak eta frogak idatzi ditut.

Amaitzeko, C eranskinean Schrödingerren ekuazioak onartzen dituen zenbait simetria idatzi ditut oso era laburrean. Haien artean, simetria galilearra sasikonformea dira aipatzekoak, testu nagusiko zatiren batean garrantzizkoak direnak.

Líneas generales de la tesis

Sin duda alguna, la función no diferenciable de Riemann

$$f(x) = \sum_{n=1}^{\infty} \frac{\sin(n^2 x)}{n^2} \tag{8}$$

es una de las más célebres funciones continuas que no son derivables en nungún punto. Fue propuesta en la década de 1870 como un ejemplo analíticamente patológico que dejaba en evidencia las convicciones de la comunidad matemática de la época, por lo que no es de extrañar que haya sido tradicionalmente estudiada desde un punto de vista analítico. Sus propiedades de derivabilidad no se supieron con precisión hasta la contribución de Gerver [42] en 1970, donde quedó demostrado que la función sí tiene derivada en ciertos puntos, en concreto en los puntos racionales que consisten en un cociente entre dos números impares. Por tanto, la conjetura mayoritaria que predecía su no derivabilidad en todo punto fue descartada, dado que la función es no diferenciable *tan solo* en casi todo punto. A partir de ese momento, el estudio profundizó en cuestiones de regularidad más finas como en determinar la regularidad Hölder.

En años posteriores, se empezaron a publicar unos pocos resultados de naturaleza geométrica sobre el grafo de la función de Riemann. Sin embargo, fue en 2014 cuando De la Hoz y Vega [26] mostraron una conexión directa con un experimento físico donde la función puede ser considerada como un objeto puramente geométrico. El experimento consiste en observar la evolución de filamentos de vórtice generados por boquillas poligonales, que aun pudiendo sonar ligeramente esotérico, no es más que una versión teórica de los muy cotidianos aros de humo que los fumadores habilidosos lanzan al aire mientras disfrutan de un cigarrillo. No hay duda, sin embargo, de que siempre será científicamente más fiable generar dichos aros en un laboratorio a través de un cañón de humo circular. Sabemos, por experiencia, que estos aros se trasladan en el espacio sin variar mucho su forma, al menos hasta que se empiezan a dispersar, lo cual sugiere que bajo condiciones ideales el aro mantendría su forma indefinidamente. Pero ¿qué pasaría si el cañón tuviera forma triangular en vez de circular? Esta es, precisamente, la situación tratada en [26], donde se analiza la evolución de una curva con forma de polígono regular que sigue las leyes del flujo binormal, o lo que es lo mismo, de la ecuación de filamentos de vórtice (VFE)

$$\boldsymbol{X}_t = \boldsymbol{X}_s \times \boldsymbol{X}_{ss}.$$

Aquí, $\boldsymbol{X} = \boldsymbol{X}(s,t)$ es una curva tridimensional parametrizada por su longitud de arco s y el tiempo t. Este modelo fue propuesto por Da Rios [20] en 1906 a partir de las ecuaciones de Euler, y comparándolo con experimentos como los realizados por Kleckner, Scheeler e Irvine [66], se puede decir que se adapta bastante bien a la realidad, al menos cualitativamente. Uno de los descubrimientos en [26] es que la trayectoria de las esquinas del polígono inicial se asemeja a la función

$$\phi(t) = \sum_{k\in\mathbb{Z}} \frac{e^{-4\pi^2 i k^2 t} - 1}{-4\pi^2 k^2}, \tag{9}$$

que podemos ver como una generalización de la función no diferenciable de Riemann (8) al plano complejo. Además, dicha aproximación mejora a medida que se aumenta el número de lados del polígono en cuestión.

Estas afirmaciones muestran que la función no diferenciable de Riemann, o al menos su versión ϕ, puede ser considerada como un objeto intrínsecamente geométrico y físico. Además, la relación con la teoría de la turbulencia parece evidente, dado que esta juega un papel importante en el estudio de los filamentos de vórtice. Desde este punto de vista, el estudio de propiedades geométricas del conjunto $\phi(\mathbb{R}) \subset \mathbb{C}$ que representa la trayectoria, así como de propiedades con motivación física y origen en el estudio de la turbulencia, es natural y diría que interesante. Mi objetivo en esta tesis ha sido contribuir con algunos avances en esta dirección.

Procedo, pues, al resumen de las partes que componen este documento.

De la introducción. Capítulo 1

El primer capítulo de esta tesis corresponde a una introducción general cuyo objetivo es explicar con cierto detalle la naturaleza original de la función no diferenciable de Riemann, así como su recientemente descubierta relación con fenómenos físicos.

Comenzaremos en la sección 1.1 con el relato del desarrollo histórico de la regularidad de las funciones, origen y motivación indudables de la función de Riemann que provocó una verdadera revolución en los cimientos teóricos de las matemáticas. También repasaremos brevemente los resultados analíticos sobre ella durante el siglo XX, así como los primeros resultados de perfil geométrico.

En la sección 1.2, analizaremos la conexión de la función de Riemann con el experimento de los filamentos de vórtice poligonales dada por De la Hoz y Vega [26]. A partir de la solución de la VFE para un vórtice poligonal, regular y plano, veremos cómo gracias a argumentos heurísticos podemos llegar a la función ϕ como una aproximación de la trayectoria de sus esquinas. Se ha observado en simulaciones numéricas que estos cálculos rudimentarios son más fiables de lo que en principio cabría esperar, dado que la imagen de ϕ y la trayectoria numérica coinciden de manera muy precisa, indistinguible por el ojo humano a partir de polígonos de unos 10 lados. Todo ello supone una gran motivación para el estudio geométrico de la función de Riemann.

El efecto de Talbot es el elemento central de la sección 1.3, que comienza con la exposición histórica de este bello efecto óptico y con una detallada explicación de su naturaleza. Más que por razones estrictamente matemáticas, así lo he decidido en parte porque el efecto de Talbot me ha permitido compartir mi trabajo con el público en general durante estos últimos cuatro años. Ha sido la puerta que me ha abierto el camino a la divulgación en charlas para públicos diversos y a entrevistas en varios medios de comunicación, y por ello considero que su descripción histórica y física deben estar incluídos en este trabajo. Sirva ello como un humilde tributo. Sin embargo, no es esta la única razón para hacerlo. Y es que, como cabe esperar, este efecto ha sido estudiado mayoritariamente por físicos cuyos argumentos, o al menos una parte de ellos, carecen de rigor matemático. Así pues, he revisado estos razonamientos y he intentado ver hasta qué punto se pueden demostrar matemáticamente. Sin embargo, los resultados obtenidos son en convergencia muy débil y se basan en razonamientos que podríamos catalogar como humildes, por lo que he decidido incluir este trabajo en el apéndice A al final del texto.

Pero aún no he explicado en qué consiste este efecto, ni cuál es su relación con la función de Riemann. Así pues, el efecto de Talbot es un fenómeno óptico que sucede cuando la luz atraviesa una rejilla de difracción equidistante y como consecuencia de la interferencia entre las ondas difractadas que surgen de cada rendija. En esta situación, existe una distancia en la que la interferencia produce un patrón de luz idéntico al de la rejilla. Es más, en toda fracción p/q de esta distancia, el patrón

de luz creado se corresponde con una rejilla q veces más estrecha que la original, es decir, con q veces más rendijas. Aunque parezca increíble, este fenómeno se observa también en la evolución de los filamentos de vórtice poligonales del experimento antes mencionado, dado que en toda fracción p/q de un tiempo particular, el filamento se convierte en un polígono regular y no necesariamente plano de q veces más lados que el original. El paralelismo es claro: las rendijas del experimento óptico se corresponden con las esquinas del experimento de los filamentos de vórtice poligonales. Veremos una descripción más detallada de todo esto en la subsección 1.3.2 a través de las correspondientes expresiones matemáticas.

La conexión de este efecto con la función de Riemann puede parecer indirecta, ya que en el experimento del filamento de vórtice poligonal, el efecto de Talbot aparece cuando fijamos el tiempo, mientras que la función de Riemann aproxima la trayectoria temporal cuando fijamos la variable espacial. De todos modos, el efecto de Talbot juega un papel importante en los argumentos heurísticos que motivan el método que utilizaremos para conseguir el comportamiento asintótico de ϕ, que será vital a la hora de demostrar los resultados geométricos.

Finalmente, en la sección 1.4 exploraremos la conexión entre la función de Riemann y varios conceptos relacionados con la turbulencia, tales como la multifractalidad y la intermitencia. La primera tiene su origen en el estudio del flujo de un fluido turbulento completamente desarrollado, cuya velocidad puede sufrir grandes variaciones aun cuando el espacio analizado es muy pequeño. Se espera, pues, que su regularidad, habitualmente medida en términos de la regularidad Hölder, varíe drásticamente de punto a punto. En otras palabras, es razonable esperar que la velocidad obedezca leyes de escala muy diferentes en puntos muy cercanos entre sí, un fenómeno al que se llama intermitencia. En esta situación, los físicos intentan calcular el espectro de singularidades

$$d(\alpha) = \dim_{\mathcal{H}} D_\alpha,$$

es decir, la dimensión de Hausdorff de los conjuntos

$$D_\alpha = \{\, x \in \mathbb{R}^3 \,:\, |v(x+l) - v(x)| \approx l^\alpha, \quad \forall l \text{ pequeño} \,\}$$

formados por los puntos en los que la velocidad es aproximadamente Hölder de grado α. En el caso de que diferentes valores de α generen conjuntos de dimensiones diferentes, o alternativamente, si $d(\alpha)$ toma todos los valores de un intervalo abierto, se dice que la velocidad es multifractal. Desafortunadamente, el espectro de singularidades es difícil de medir en los experimentos, por lo que Frisch y Parisi [41] propusieron un método para calcularlo a través de las funciones de estructura

$$S_p(l) = \langle |v(x+l) - v(x)|^p \rangle, \qquad x, l \in \mathbb{R}^3,$$

más fáciles de calcular. Aquí, denotamos por $\langle \cdot \rangle$ alguna media en conjunto que varía según el contexto y las necesidades. En concreto, asumiendo que dichas funciones de estructura se comportan como $S_p(l) \approx |l|^{\zeta(p)}$ para alguna función $\zeta(p)$, entonces esta se relacionaría con el espectro de singularidades mediante la transformada de Legendre

$$d(\alpha) = \inf_p \{\alpha p - \zeta(p) + 3\}. \tag{10}$$

El formalismo multifractal, nombre con el que se conoce a esta fórmula, se basa en razonamientos heurísticos cuya validez matemática no está clara en absoluto. Por ello, en la década de 1990 se empezó a investigar sobre el rango de validez de la fórmula (10), después de adaptar todos los conceptos mencionados a objetos matemáticos

rigurosos como medidas o funciones. Por ejemplo, es razonable redefinir los conjuntos D_α mediante

$$D_\alpha = \{\, x \in \mathbb{R}^3 \,:\, \alpha_v(x) = \alpha \,\}, \qquad \text{donde} \qquad \alpha_v(x) = \sup\{\alpha \,:\, v \in C^\alpha(x)\},$$

y las funciones de estructura por

$$S_p(l) = \|f(\cdot + l) - f(\cdot)\|_{L^p}^p. \tag{11}$$

En este contexto, Jaffard [55] demostró la validez del formalismo multifractal en el caso de la función de Riemann. Este resultado motiva también el análisis de otras propiedades provenientes del estudio de la turbulencia como la intermitencia. Veremos cómo este concepto puede ser adaptado al lenguaje de las funciones utilizando las funciones de estructura (11), o alternativamente ciertos filtros de Fourier de paso alto, y basándonos en las conceptos probabilísticos como el de kurtosis.

Del cuerpo de la tesis. Capítulos 2, 3, 4 y 5

En los capítulos 2, 3 y 4, trabajaremos en las propiedades geométricas de la función de Riemann.

En el capítulo 2, primero determinaremos la notación y las herramientas que utilizaremos durante todo el estudio geométrico, y después calcularemos el comportamiento asintótico de ϕ alrededor de múltiplos racionales su periodo. Estas fórmulas, que constituirán la base para demostrar los resultados principales de los capítulos posteriores, ya fueron dadas por Duistermaat [29] para la función

$$\phi_D(x) = \sum_{n=1}^{\infty} \frac{e^{i\pi n^2 x}}{i\pi n^2},$$

otra generalización de la función no diferenciable de Riemann original que está trivialmente relacionada con ϕ. En principio, no habría inconveniente en adaptar sus resultados a nuestro entorno, salvo quizás porque los cálculos, aun básicos, podrían ser pesados. Sin embargo, he decidido calcular el comportamiento asintótico de ϕ directamente esenciamente por dos razones. La primera es para que esta tesis sea lo más autocontenida posible. La segunda es que seguiremos un camino que me parece más intuitivo, aunque es en esencia el mismo que el de Duistermaat, y por ello compararemos los dos caminos continuamente para resaltar las ventajas y desventajas de cada uno de ellos. La demostración se basa en la profunda relación entre la función de Riemann y la función θ de Jacobi que, a su vez, interactúa con el grupo modular. Los resultados de este capítulo son demasiado largos y técnicos para incluirlos aquí, por lo que el lector los podrá consultar en las proposiciones 2.12 y 2.15.

En el capítulo 3, retomamos la función ϕ y su imagen $\phi(\mathbb{R})$ como representante de la trayectoria del experimento de los filamentos de vórtice poligonales y analizamos su dimensión de Hausdorff. Entre otros factores, este estudio viene motivado por la imagen 1.5 en la que se puede observar cierta estructura autosemejante, dado que se sabe que la autosemejanza es habitualmente un indicador de fractalidad. El resultado principal es el siguiente teorema, que corresponde al teorema 3.1 en el texto principal.

Teorema. *Sea ϕ la función no diferenciable de Riemann definida en (9). Entonces,*

$$1 \leq \dim_{\mathcal{H}} \phi(\mathbb{R}) \leq 4/3.$$

La falta de una autosemejanza exacta hace que el cálculo de una buena cota inferior sea una tarea complicada que sin duda será objeto de futuras investigaciones.

Este teorema puede ser generalizado al contexto de la multifractalidad arriba mencionado. De hecho, cuando Jaffard demostró que el formalismo multifractal se cumple en el caso de la función de Riemann, probó que

$$d(\alpha) = \dim_{\mathcal{H}} D_\alpha = 4\alpha - 2, \qquad \forall \alpha \in [1/2, 3/4].$$

Podríamos preguntarnos si sería posible calcular la dimensión de Hausdorff de los conjuntos imagen $\phi(D_\alpha)$. El siguiente teorema, que corresponde al teorema 3.2, es una respuesta parcial a esta cuestión.

Teorema. *Sea ϕ la función no diferenciable de Riemann definida en (9). Entonces,*

$$\dim_{\mathcal{H}} \phi(D_\alpha) \leq \dim_{\mathcal{H}} \phi\Big(\bigcup_{\beta \leq \alpha} D_\beta \Big) \leq \frac{4\alpha - 2}{\alpha}, \qquad \forall \alpha \in [1/2, 3/4].$$

Las demostraciones de ambos teoremas se basan en el comportamiento asintótico de ϕ alrededor de múltiplos racionales de su periodo, así como en la aproximación de los números irracionales por medio de las fracciones continuas.

Sin dejar de lado la interpretación de ϕ como trayectoria, y pensando en una partícula que la sigue, podríamos preguntarnos por la velocidad en la que esta se mueve. Parece claro que podremos calcular algún tipo de velocidad media, ya que la función ϕ viene dada por una expresión explícita, y bastaría con tomar dos puntos cualesquiera y hacer el cociente de la distancia entre los dos con la diferencia entre los valores correspondientes del parámetro de la curva. Pero ¿podemos hacer esto infinitesimalmente? Es decir, ¿podemos determinar la velocidad y, en particular, la dirección de la partícula en un momento preciso? Esta pregunta, es decir, la diferenciabilidad geométrica de ϕ, es a la que intentaremos responder a lo largo del capítulo 4. El resultado principal es el siguiente.

Teorema. *Sea ϕ la función no diferenciable de Riemann definida en (9). No existe ningún punto $x \in \mathbb{R}$ para el cual $\phi(\mathbb{R})$ tenga una tangente en $\phi(x)$.*

En este punto, es importante hacer dos comentarios. El primero es que el resultado es relevante porque no hay una conexión clara entre la regularidad analítica y la geométrica de ϕ. Podemos comprobarlo en las imágenes de $\phi(\mathbb{R})$ producidas por ordenador, que muestran que en los puntos racionales donde ϕ no tiene derivada, el conjunto $\phi(\mathbb{R})$ tiene dos tangentes laterales, que no coinciden porque son perpendiculares. Por otro lado, en los puntos donde ϕ tiene derivada, se observa en $\phi(\mathbb{R})$ un patrón en espiral que impide que exista tangente ninguna. En cuanto a los irracionales, hacer un análisis preliminar parecido es más complicado. El segundo comentario es que necesitamos encontrar una buena definición de tangente, dado que las definiciones habituales de la geometría diferencial no nos sirven porque ϕ no es diferenciable en ningún intervalo abierto. Parece razonable utilizar una definición puramente geométrica, pero por otro lado, como el conjunto viene parametrizado por una función, una definición paramétrica facilitaría los cálculos. Así pues, daremos dos definiciones, una geométrica y otra paramétrica, y estudiaremos la relación entre ellas. En concreto, demostraremos que el resultado para la definición paramétrica lo implica para la geométrica, y entonces será suficiente trabajar desde la primera perspectiva. El lector puede consultar todos los detalles, así como los teoremas precisos de los que se deduce el teorema anterior, en la sección 4.3.

En el capítulo 5 cambiaremos de tema para trabajar en la intermitencia de la función de Riemann. Para ello, y siguiendo la motivación dada en la introducción, adaptaremos las definiciones de las funciones de estructura, filtros de paso alto, kurtosis e intermitencia al lenguaje de las funciones y demostraremos el siguiente teorema.

Teorema. *La función no diferenciable de Riemann es intermitente.*

El lector encontrará la definición precisa de intermitencia en el capítulo 5. Los resultados que corresponden a este teorema son los corolarios 5.7 y 5.11, que no son más que casos especiales de los más amplios corolarios 5.5 y 5.10.

De los apéndices

Como ya he mencionado, la expresión que se utiliza habitualmente para describir el efecto de Talbot se obtiene mediante razonamientos que, aunque puedan ser razonables desde un punto de vista físico, no son matemáticamente correctos. Analizar si estos cálculos se pueden formalizar rigurosamente es el objetivo del apéndice A. Para ello, primero repasaremos todos estos pasos y argumentos físicos y trataremos de entender por qué sirven como aproximaciones para los experimentos en un laboratorio. Después, necesitaremos encontrar el contexto matemático adecuado en el que poder trabajar, que por la propia naturaleza de las expresiones que manejaremos deberá ser el de las distribuciones. Así pues, los resultados que probaremos serán en convergencia muy débil.

En el apéndice B, repasaremos los conocimientos básicos de la teoría de fracciones continuas que utilizaremos asiduamente. Las definiremos y motivaremos su existencia para después enunciar y demostrar algunas propiedades elementales pero extremadamente útiles e importantes.

Finalmente, en el apéndice C, daremos una muy breve descripción de algunas simetrías de la ecuación de Schrödinger como la simetría galileana o la pseudoconforme, que utilizaremos en algunos puntos de la tesis.

CHAPTER 1

Introduction

1.1 The history of Riemann's non-differentiable function

1.1.1 Are continuous functions differentiable?

The concept of function, by which an element in a set is assigned another element in another set, is a very natural one. Indeed, any kind of change, movement or interaction, specially when it is with respect to time, is subject to be registered. That is why it must have been, in some way or another, in the minds of thinkers and mathematicians since many centuries, even millenniums ago. However, the formalisation of mathematical concepts is not a trivial task, and requires many trials and failures, the participation of many people and usually a long period of time.

Functions are no exception to this rule, and many definitions have been given for them along the history. A number of them, specially the first ones, followed the intuition of the practical use, since a function was nothing but a tool to describe natural phenomena. During the 18th century, even when mathematicians were far from reaching a consensus about a proper definition, the first differential equations were proposed. For instance, the very famous Euler equations in fluid dynamics were proposed by Leonhard Euler in 1757 [36]. From the perspective of the topic of this dissertation, at least one thing can be deduced at once: that whatever a function was considered to be at the time, it could be differentiated. Concerns about regularity of functions came later.

Euler's definitions are considered to have beem essential in the development of analysis. Following John Bernoulli's ideas, he first proposed [35] the following in 1748:

> *A function of a variable quantity is an analytic expression composed in any way of the variable quantity and numbers or constant quantities.*

From the modern perspective, these functions are indeed regular and, in general, smooth functions. However, the problem of the vibrating string showed movements that could not be described using such an *analytic expression*, so this turned out to be too restrictive. Thus, with the passing of the years, the need of an analytic expression based on basic operations was slowly left behind and more abstract definitions, similar

to the modern one, gained popularity. The following, which many times is referred to as the Dirichlet definition, is due to Fourier [39, s. 417], in 1822:

> *In general, the function $f(x)$ represents a succession of values or ordinates each of which is arbitrary. An infinity of values being given of the abscissa x, there are an equal number of ordinates $f(x)$. All have actual numerical values, either positive or negative or null. We do not suppose these ordinates to be subject to a common law; they succeed each other in any manner whatever, and each of them is given as it were a single quantity.*

This definition is very close to the modern one and implies nothing about regularity, but when it came to actual research, most functions were assumed to be regular enough for the objectives set. Also, probably based in practical experiences, it became the general thinking at the time that a continuous function must be differentiable, except maybe at isolated points. It is usual to cite Ampère, who supoosedly wrote a proof of this [1] in 1806. In his words,

> *I first propose to demonstrate that the function on x and i,*
>
> $$\frac{f(x+i)-f(x)}{i},$$
>
> *which expresses the relationship between the difference of two values x and $x+i$ of a variable and of the difference of the corresponding two values of any function $f(x)$, cannot become null nor infinite for all values of x when $i=0$, supposition by which the expression becomes $0/0$; it will necessarily follow from this proof that*
>
> $$\frac{f(x+i)-f(x)}{i}$$
>
> *reduces to a function of x.*

However, the proof relied in properties that a continuous function "should satisfy", but that actually cannot be deduced from the definition [1]. No one was aware of the mistake at the time, again because probably all available functions indeed had those properties. In words of Darboux [21] in 1875,

> *Excellent, renowned geometers, among whom Ampère must be counted, had tried to give rigorous proofs of the existence of the derivative [of a continuous function]. This attempts were undoubtedly far from being satisfactory; but, I repeat, no doubt about the existence of a derivative for continuous functions had ever been formulated.*

Indeed, in a speech in the Royal Academy of Sciences in Berlin in 1872 [95], Weierstrass had described the situation as follows:

> *Up to the present time, it has been generally assumed that a well-defined and continuous function of a real variable always has a first derivative, the value of which can only become indefinite or infinitely large at individual points. As far as I know, even in the writings of Gauss, Cauchy*

[1] It should be noted that there is no concluding evidence that Ampère intended to prove the existence of a derivative for *all continuous* functions. It is suggested in [74] that Ampère must have given that proof thinking of all functions indeed, but only all functions that were considered at the time, which following the teachings of Lagrange would correspond to the analytic functions of nowadays.

> *or Dirichlet there is no statement that would undoubtedly show that these mathematicians, who were used to the strictest criticism in their science, were of a different opinion.*

In the same speech, however, he shed some light on the matter, showing that Ampère's result, widely accepted to be correct, was indeed not so:

> *It was only Riemann, as I learned from some of his listeners, who stated with certainty (in 1861, or perhaps earlier) that this assumption was inadmissible and that for example it is not true in the function represented by the infinite series*
>
> $$\sum_{n=1}^{\infty} \frac{\sin(n^2 x)}{n^2}.$$
>
> *Unfortunately, the proof of this has not been published by Riemann and does not appear to have survived in his papers or by oral transmission. This is all the more regrettable since I do not know with certainty how Riemann expressed himself to his listeners. The mathematicians who, after Riemann's claim had become known in wider circles, dealt with the subject, seem (at least in their majority) to have been of the opinion that it was sufficient to prove the existence of functions which cannot be differentiated in any interval as small as desired. It is very easy to prove that there are functions of this kind, and I therefore believe that Riemann only considered functions that have no derivative for any value of their argument. However, it seems to me somewhat difficult to prove that the specified trigonometric series represents a function of this kind; but one can easily build continuous functions of a real argument x, for which the simplest means can be used to show that they have no derivative for any value of x.*

In any case, Weierstrass' account of

$$f(x) = \sum_{n=1}^{\infty} \frac{\sin\left(n^2 x\right)}{n^2} \tag{1.1}$$

seems to have been the first time a function was publicly proposed to be continuous function and yet nowhere differentiable. However, Weierstrass had to find an alternative example because, as he admitted, he had not succeeded in proving such a claim. This function is

$$W_{a,b}(x) = \sum_{n=1}^{\infty} b^n \cos(a^n x\pi), \qquad 0 < b < 1, \quad a \text{ an odd integer}, \quad ab > 1 + \frac{3}{2}\pi, \tag{1.2}$$

and is nowadays known as the Weierstrass funcition, published in written form by Du Bois-Reymond in [28]. It is, no doubt, the first function in history who was rigorously proven and published to be continuous and nowhere differentiable, which lead the way for many new examples that were designed and published by many authors in the following years.

It is only fair to mention that many years after, in the 1920s, previously unpublished works of Bolzano were brought to light by the Czech Academy of Sciences and published in 1930. In the first volume [11], corresponding to notes entitled *Functionenlehre* and dated in 1834, Bolzano thought of a sequence of geometrically defined, piecewise linear functions which converge to a continuous function having a dense set

of points where it has no derivative. The example, although correct, was rigorously proven only when it was rediscovered a century later. In any case, up to what is known to date, it is the oldest example of a function of the kind we are discussing. Also, a manuscript of Cellérier was found and published in 1890 [15], one year after his death, in which the proof of the non-differentiability of a function very similar to Weiesrtrass' (1.2) is given. The note lacks a date, and although its discoverers describe it as *un papier jauni par le temps*, a paper yellowed by time, they considered impossible to determine when it was written. There is no guess whether Cellérier's results are previous or posterior to those of Weierstrass and Du Bois-Reymond, though by the fashion in which it is written, there seems to be no doubt that he obtained the results independently.

The discovery of these functions shook the foundations of analysis. Many mathematicians heavily criticised these works, claiming that they were unnatural, artificial and absolutely unnecessary creations. Among the severest was Poincaré with his strong criticism to the loss of intuition in the teaching of mathematics [83], where in particular he wrote that *it seems that these strange functions try to resemble the least possible to the honourable functions that are useful for something*, and that *once, when a new function was invented, it was with a practical objective; these days, they are invented on purpose to show that our ancestors' reasoning was incorrect, and we shall never get anything more out of them.*

But one thing was clear: serious flaws in the way mathematics were being produced and validated became evident. Rigour of mathematics was at stake, and whatever some said, intuition had to be banished from proofs since the price to pay, the prospective of having more *theorems* like Ampère's, was definitely unreasonable. In this sense, very clarifying are the following words by Cellérier, who justified his work cited above by saying that

> *It is clear that the examination of these special cases follows a sole objective: to discern the principles that are essential to every function from those which are not, since for the latter the easiest way to prove that they are not general is to produce an exception.*

The criticism lost support in the beginning of the new century, when natural phenomena which followed such an irregular behaviour, such as the Brownian motion, were discovered. In words of Perrin [82], honoured with the Nobel Prize for Physics in 1926,

> *At first side the consideration of such cases seems merely an intellectual exercise, certainly ingenious but artificial and sterile in application, the desire for absolute accuracy carried to a ridiculous pitch. And often, those who hear of curves without tangents, or functions without derivatives, think at first that evidently nature presents no such complications, nor even offers any suggestion of them. The contrary, however, is true, and the logic of mathematicians has kept them nearer to reality than the practical representations employed by physicists.*

This way, continuous and non-differentiable functions, and similar irregular objects, became progressively accepted, well-established and widely studied.

Meanwhile, the differentiability of the function (1.1) in Weierstrass' speech, which for evident reasons became known as Riemann's non-differentiable function, remained unsolved for almost one century. This contributed to its fame as a first groundbreaking example of pathological mathematics. However, from the historic account above related one can get a funny *a posteriori* conclusion. Indeed, Riemann's non-differentiable

function is neither the first example of a continuous and nowhere differentiable function, nor is nowhere differentiable, as we are to see in Subsection 1.1.2. What is more, according to [14], there are genuine doubts nowadays whether the definition of (1.1) is due to Riemann, since apparently, *the so-called 'Riemann example' cannot be brought in recorded connection with either Riemann or his students*. From this point of view, and in the strictest sense, it should maybe be called just "a function". Nevertheless, we should not do so, for that would be an unfair treatment for such a complex function. And we shall not do so, also for the sake of preserving the myth of the function which can undoubtedly be made responsible of opening Pandora's box of *monsters*, as continuous non-differentiable functions are often called, and of the consequent enrichment of mathematical analysis. Itself, an imperfect monster that is still alive and friendly enough to produce, after so many years, enough material to write a PhD dissertation.

1.1.2 The analytic study of Riemann's non-differentiable function

Riemann's non-differentiable function was devised as a counterexample to the belief of the mid 19th century that continuous functions always had a derivative except maybe at some isolated points. Even if no one was able to prove the non-differentiability of Riemann's example, the existence of these kind of functions seemed reasonable to the majority, and many looked for and found alternative counterexamples like (1.2) and gave the corresponding proofs in the following years.

However, the first answer to the problem regarding Riemann's function did not come until 1916. That year, Hardy [47] published a less elemental but more powerful method to work with the Weierstrass function and similar ones, by which he removed the artificial restrictions in (1.2) and established the validity of the result under the condition $ab > 1$. But most importantly for us, he was able to combine this method with some other results which he obtained together with Littlewood [48] to show that Riemann's function (1.1) was not differentiable in points πx if x is irrational or else if $x = (2m+1)/(2n)$ or $x = 2m/(4n+1)$ for some $m, n \in \mathbb{Z}$. Therefore, only points πx with x a rational of the kind $(2m+1)/(2n+1)$ and $2m/(4m+3)$ were left out of the result. More than 50 years later, in 1970, Gerver [42] published the proof that the function was indeed differentiable at points πx with $x = (2m+1)/(2n+1)$, with derivative equal to $-1/2$, showing this way that the very celebrated conjecture was false. Moreover, in [43] he proved that for the remaining rational values of x Riemann's function does not have a derivative, therefore closing the problem that had been open for around 100 years. A very nice historic discussion on the differentiability of Riemann's function can be found in [75, 89]. Alternative and simpler proofs were published in the following years [54, 69, 90].

In the same works, some generalisations of Riemann's function (1.1) were also studied. For instance, Hardy [47] proved that no function

$$\sum_{n=1}^{\infty} \frac{\sin(n^2 x)}{n^\alpha}, \qquad \alpha < 5/2, \tag{1.3}$$

is differentiable in points πx with x irrational, and Gerver [43] suggested that his method could be used for more general functions $\sum_{n=1}^{\infty} \sin(f(n)x)/f(n)$ where f is a polynomial of degree at least 2. This was done by Queffelec [84] for such polynomials with integer coefficients.

Later, Holschneider and Tchamitchian [51] reproved the results for Riemann's function by Hardy and Gerver by using the wavelet transform, and saw that there are infinitely many points where Riemann's function is differentiable on the left, but not

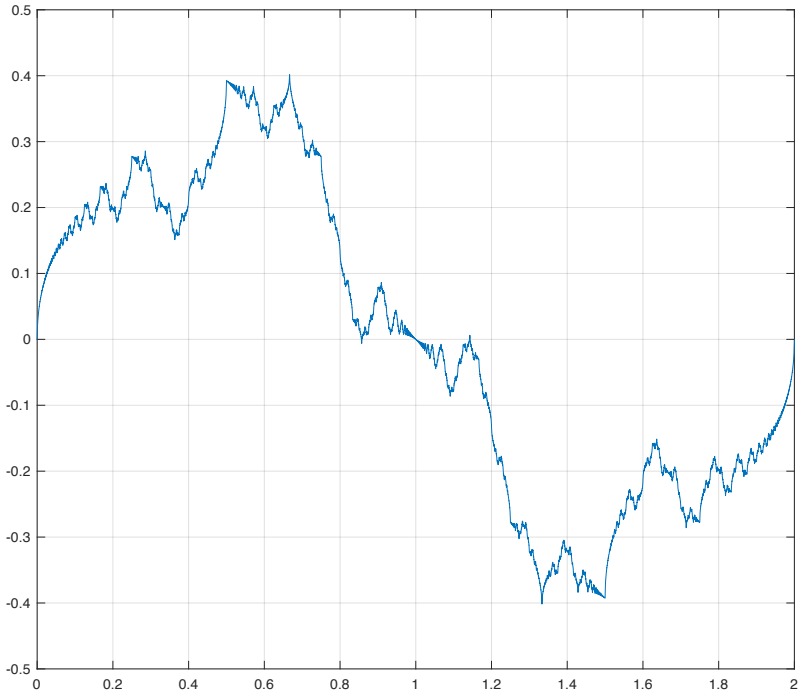

FIGURE 1.1: The graph of Riemann's non-differentiable function rescaled as $R(\pi x)$, for $x \in [0, 2]$.

on the right, or vice versa, such that the graph of the function has a cusp, which can now be seen in Figure 1.1. Moreover, they went deeper in the study of the regularity of Riemann's function in which was the natural step forward: in the points where the function is known to be non-differentiable, can something be said about its local Hölder regularity? In this direction, the wavelet transform had been established as a tool to answer this question by Jaffard in [58].

In [51] and in subsequent works, it has been usual to work with complex generalisations of Riemann's function f like

$$\phi_D(t) = \sum_{n=1}^{\infty} \frac{e^{i\pi n^2 t}}{i\pi n^2}, \tag{1.4}$$

which satisfies $\operatorname{Re} \phi_D(t) = f(\pi t)/\pi$. Using it, Duistermaat[2]made in [29] a big contribution in understanding the behaviour of Riemann's function near a particular point. He computed the asymptotic behaviour of ϕ_D near rational points, this is, an expansion for $\phi_D(x_0 + h) - \phi_D(x_0)$ for every rational number x_0 and small values of h. This turned useful to describe properties of the graph of f; indeed, computer-made plots of it like that in Figure 1.1, which of course did not exist in the times of Weierstrass and Hardy, had apparently been available for some years. He noticed that the existence of the derivative in the corresponding rational points could be quite clearly deduced, at least for those with small denominator, but he specially remarked the impressive repetition of similar patters in decreasing sizes, for f and also for ϕ_D shown in Figure 1.2. Moreover, he was able to explain this, since he established an approximate functional equation for ϕ_D from which he deduced the asymptotic behaviour above mentioned and described the graph of f and the image $\phi_D(\mathbb{R})$ with more detail. He did this by using the Jacobi θ function and its relationship with the modular group.

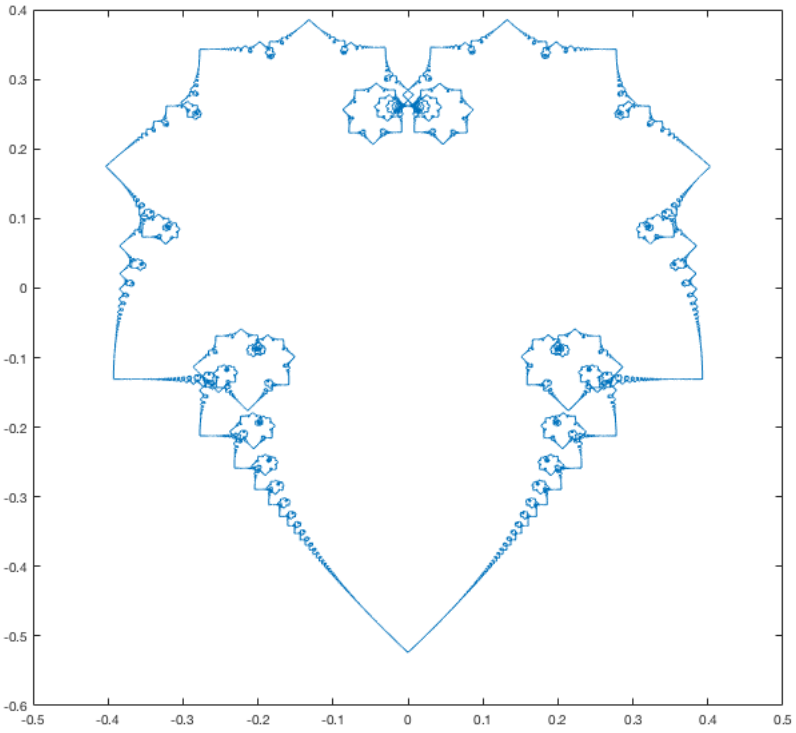

FIGURE 1.2: The image of ϕ_D defined in (1.4).

Joining the modular approach by Duistermaat and wavelet and chirp expansion techniques, Jaffard and Meyer in [61] but specially Jaffard [2] [55] carried on a thorough analysis of the Hölder regularity of the function. He showed that if α is the supreme Hölder regularity of f in some point where it is not differentiable, then $\alpha \in [1/2, 3/4]$ must hold. What is more, he related this with the diophantine properties of irrationals ρ, showing that $\alpha(\rho) = 1/2 + 1/(2\tau(\rho))$, where $\tau(\rho)$ is the supremum of the values $\tau > 0$ such that $|\rho - p_n/q_n| < q_n^{-\tau}$ holds for infinitely many convergents p_n/q_n of the continued fraction of ρ. This result, together with a variation of the classical Jarnik-Besicovitch theorem [38, Theorem 10.3], allowed him to prove that

$$d(\alpha) = 4\alpha - 2, \qquad \text{for } \alpha \in [1/2, 3/4], \tag{1.5}$$

where $d(\alpha)$ is the Hausdorff dimension of the set of points where the supremum Hölder regularity of f is α, called the spectrum of singularities of f. This way, he established a relationship with turbulence, where computing the spectrum of singularities of the velocity of a fluid undergoing fully developed turbulence is an important task, and checked the validity of the multifractal formalism proposed by Frisch and Parisi in [41]. We will review this connection with turbulence in more detail in Section 1.4.

Jaffard also computed in the same publication the spectrum of singularities of the functions (1.3) for $\alpha > 1$, and later, the analysis was extended to

$$\sum_{n=1}^{\infty} \frac{e^{2\pi i P(n)x}}{n^{\alpha}}, \qquad \alpha > 1, \tag{1.6}$$

[2] The works of Duistermaat and Jaffard have been a great inspiration and a source of techniques for the development of this thesis as will become evident in Chapters 2 and 3. Indeed, the D in the subindex of ϕ_D stands for Duistermaat.

where P is a polynomial. This was done first by Chamizo and Córdoba in [16], where differentiability properties were studied in the case of monomials $P(n) = n^k$ and for some combinations between α and k, and later by Chamizo and Ubis [17], who analysed the Hölder regularity and the spectrum of singularities for $P(n) = n^k$ for any $k \in \mathbb{N}$ and for any α. Later, they extended this analysis to general polynomials P in [18]. Very recently, digging into the relationship that these functions have with Jabobi's θ function, this analysis was extended to modular forms by Pastor [81].

Also in the last decades, one more generalisation of Riemann's non-differentiable function

$$\sum_{n\in\mathbb{Z}\setminus\{0\}} \frac{e^{i\pi n^2 t+2\pi i n x}}{\pi i n^2}, \tag{1.7}$$

has been studied in the setting of the Schrödinger equation. Indeed, (1.7) is a solution to the free Schrödinger equation, from which (1.4) is recovered if $x = 0$. In many works, among which are [64, 77–80, 87], regularity properties of such solutions have been studied. Sometimes, time is fixed to analyse the function in space, in horizontal lines of $\mathbb{R}^2$, while some other times space is fixed and the solution analysed vertically. Contributions have been given also in oblique lines of $\mathbb{R}^2$, motivated by the conjectures by Berry and Klein in [7, 9]. Indeed, solutions like (1.7) are related to Riemann's non-differentiable function as indicated, but they are also related to the optical Talbot effect which we will discuss in Section 1.3, since some solution to the Schrödinger equation, obtained by approximation from the Helmholtz equation, has been used by physicists to model this phenomenon.

More recently, generalisations of (1.7) to solutions to dispersive partial differential equations have been studied, for instance, in [19, 33, 34]. Moreover, in [19] this was related to the vortex filament equation, an important part for the motivation of this dissertation and which we address in Section 1.2.

1.1.3 The geometric study of Riemann's non-differentiable function

Riemann's non-differentiable function was designed as an example showing regularity pathologies and defined in a completely analytic way, so one should not be surprised by the fact that it has traditionally been studied from an analytic point of view. However, it is apparent after the few last results in the previous subsection that geometric flavoured results concerning the graph of Riemann's function started to complement its classical analytic study. Along these lines, even more geometric results have been obtained during the last decades. For instance, the box-counting or Minkowski dimension of the graphs of the real and imaginary parts of (1.6) with $P(n) = n^k$ for $k \in \mathbb{N}$ was computed in [16, 17]. In particular, with the help of number theory, it was established in [16] that the Minkowski dimension of the graph of Riemann's function (1.1) is $4/3$.

In the setting of the generalisation (1.7), Berry and Klein [7, 9] also conjectured fractal dimensions for the graphs of their real and imaginary parts along lines in $\mathbb{R}^2$. According to them, this dimension would depend on the direction of the line considered. This problem has been extensively tackled in the works referred to above, in the end of the previous subsection.

It is undeniable that the study of geometric properties of the graph of these functions is of interest and, in view of the research done, a deep topic. But, for a moment, dressing up as Poincaré, we may wonder, is there any reason apart from the mathematical curiosity by which we should study this function from a geometric perspective? It is the objective of this introduction to convince the reader that there is such a

reason, at least for the case of Riemann's non differentiable function. Indeed, we will see that it plays a surprising role as a temporal trajectory in the context of the evolution of vortex filaments following the binormal flow. In this sense, one could define Riemann's function as the parametrisation of this trajectory, and then deduce an analytic expression for it, so that it can be regarded as a purely geometric object. We proceed to present and explain this setting in Section 1.2.

1.2 Riemann's non-differentiable function from a physical perspective

In spite of the classical work concerning Riemann's non-differentiable function was fully analytic, a surprising connection with a physical experiment was brought to light in [26], where Riemann's function was shown to be extremely similar to temporal trajectories of certain vortex filaments following the binormal flow. This discovery motivates a geometric, and also a physical, analysis of the function. We devote this section to present this connection.

1.2.1 The binormal flow, the vortex filament equation and Riemann's function

The vortex filament equation is an evolution model for one vortex filament dynamics, proposed in 1906 [20] and rediscovered in 1965 [3]. More precisely, it is the evolution equation for a curve in space $\boldsymbol{X} : \mathbb{R}^2 \to \mathbb{R}^3$ parametrised in arclength s and in time t given by

$$\boldsymbol{X}_t = \boldsymbol{X}_s \times \boldsymbol{X}_{ss}. \tag{1.8}$$

Of course, it is endowed with an initial datum $\boldsymbol{X}(s, 0)$. This equation can be alternatively written in terms of the binormal vector of the curve. To see that, let us first recall the Frenet-Serret formulas

$$\begin{pmatrix} \boldsymbol{T}_s \\ \boldsymbol{N}_s \\ \boldsymbol{B}_s \end{pmatrix} = \begin{pmatrix} 0 & \kappa & 0 \\ -\kappa & 0 & \tau \\ 0 & -\tau & 0 \end{pmatrix} \begin{pmatrix} \boldsymbol{T} \\ \boldsymbol{N} \\ \boldsymbol{B} \end{pmatrix}, \tag{1.9}$$

where $\boldsymbol{T} = \boldsymbol{X}_s$ is the tangent vector, $\boldsymbol{N} = \boldsymbol{T}_s/\|\boldsymbol{T}_s\|$ is the normal vector and $\boldsymbol{B} = \boldsymbol{T} \times \boldsymbol{N}$ is the binormal vector. Also, $\kappa = \kappa(s, t)$ and $\tau = \tau(s, t)$ are the curvature and the torsion of the curve, respectively. Writing the right hand side of (1.8) in terms of the tangent $\boldsymbol{T}$, one deduces at once that

$$\boldsymbol{X}_t = \boldsymbol{T} \times \boldsymbol{T}_s = \boldsymbol{T} \times \kappa\, \boldsymbol{N} = \kappa\, \boldsymbol{B},$$

so that the curve evolves in the direction indicated by the binormal vector at each time. For this reason, the flow that evolves according to the vortex filament equation is often referred to as the binormal flow, and the equation written as

$$\boldsymbol{X}_t = \kappa\, \boldsymbol{B}$$

accordingly.

Data with corners have been analysed in a series of papers and seem to grasp the main features of real experiments. In [45], self-similar solutions to the equation are studied and shown to be regular for any time $t > 0$. These solutions develop a singularity in the shape of a corner at $t = 0$, showing that they correspond to

a V-shaped initial datum formed by the union of two non-parallel half-lines. This is precisely the behaviour of the air in a delta wing during a flight [23]. Also, the reconnection of two different filaments, as the ones left behind by a flying plane, may create two new cornered filaments that evolve in a similar way as predicted by the equation. This behaviour has also been observed in the study of superfluid helium [88]. In [4], the V-shaped initial datum is generalised to any curve which is smooth except at a point where it has a corner, and in [5] polygonal lines are considered, translating the problem from a single corner to multiple cornered data.

One may also analyse the evolution of a closed curve, a situation which most of us are familiar with. Think, for instance, of a ring produced by smokers with their mouth. We all know that the ring does not lose its shape when it travels, at least for a short period of time, until at some points it starts to disperse. However, one may think that under ideal conditions, with a more faithful source as a circular smoke cannon and without the interference of the movement of the air, the ring would travel in space keeping its shape unaltered. But what would happen if the ring were not a circular ring, but rather, let us say, a triangular *ring*? This question is directly related to the evolution of vortex filaments produced by nozzles with corners. Very nice laboratory experiments were performed in [66], where they produced, among many others, a vortex filament of a clover-like shape. Even if this is not an exact triangle, it lets us make an idea of what we can expect. What is clear is that, compared to the circular ring, we face a completely different behaviour.

With this physical background in mind, and following the program of studying the vortex filament equation (1.8) for initial data with corners, in [26] the evolution of a planar and regular polygon of $M \in \mathbb{N}$ sides is studied. In the case of the circle, the datum is a smooth and planar curve with a constant, non-vanishing curvature, so the binormal points in the direction which is perpendicular to the starting plane. It is therefore not surprising that the binormal flow makes the circle translate in space in the direction perpendicular to the plane where it lies. However, the evolution of regular polygons is nothing of the kind. It is proved that this evolution is periodic in time, but also that the filament has a polygonal shape in every rational multiple of the period, with a number of sides proportional to the denominator of the fraction considered. This phenomenon, which strikingly is the same as the Talbot effect in optics that we will discuss in Section 1.3, was suggested in [63], at least for some of these rational times, by numeric simulations for the evolution of a square. We will later give details on these computations. Also, these computations give mathematical support to the axis-switching phenomenon that is observed in several experiments with jets from triangular or squared nozzles (see, for instance, [46]).

In [26], they also do numeric simulations to visualise the trajectory given by $\boldsymbol{X}_M(0,t)$, which represents the movement of a corner of the initial polygon. The ones corresponding to $M = 3, 4, 5$ are shown in Figure 1.3, which is taken from [26, Figure 2]. If a correction is applied to these trajectories by removing the displacement in the direction perpendicular to the original plane (the vertical displacement in Figure 1.3), one can see a striking similarity between them and the image of ϕ_D defined in (1.4). Moreover, the differences become imperceptible when the number of sides increases. For the sake of completeness, Figure 3 from [26] is reproduced in Figure 1.4, where the trajectories for $M = 3, 10$ are shown next to the image of ϕ_D.

It is then expectable that the correct version of Riemann's non-differentiable function that matches the trajectories should be ϕ_D with a vertical displacement. Indeed,

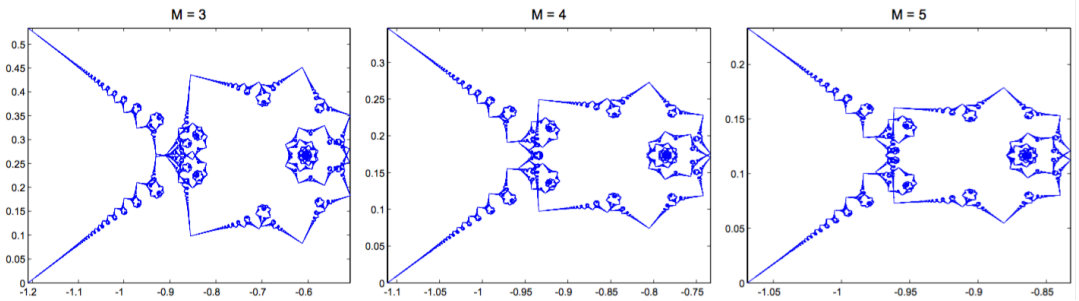

FIGURE 1.3: This is [26, Figure 2]. These three plots are numeric simulations of $\boldsymbol{X}_M(0,t)$ for the values $M = 3, 4, 5$, which being plane trajectories in the three-dimensional space, have been projected onto the complex plane.

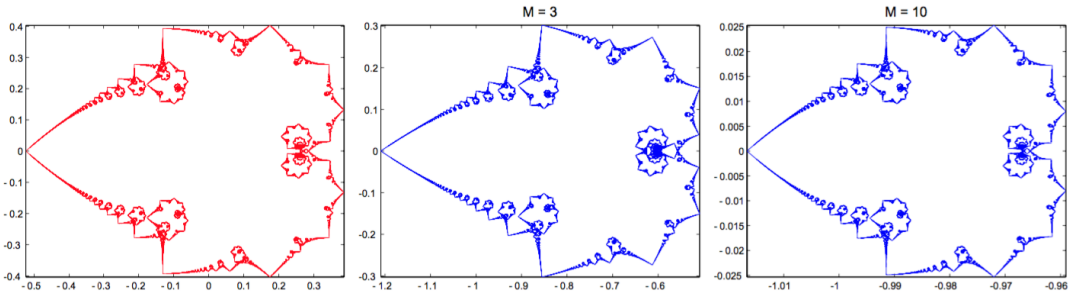

FIGURE 1.4: On the left, the image of $i\,\phi_D$, see Figure 1.2 for comparison. On the center and on the right, $\boldsymbol{X}_M(0,t) - i\,t$, where $\boldsymbol{X}_M(0,t)$ are the numeric simulations for the trajectories of a corner of the initial polygon of $M = 3$ and $M = 10$ sides, respectively. These trajectories lie on a plane, and have been projected onto the complex plane. These plots have been taken from [26, Figure 3].

we will see that the function we seek is

$$\phi(t) = \sum_{k\in\mathbb{Z}} \frac{e^{-4\pi^2 i k^2 t} - 1}{-4\pi^2 k^2}. \tag{1.10}$$

The similarity between the image of ϕ shown in Figure 1.5 and the numeric trajectories in Figure 1.3 is evident.

There is no much need to explain that this function is indeed a version of Riemann's non-differentiable function, since it is a sum of exponentials with quadratic phases, whose inverse amplitudes are also quadratic. However, for clearness, one can easily check that the relationship with ϕ_D (1.4) is

$$\phi(t) = -\frac{i}{2\pi}\phi_D(-4\pi t) + it + \frac{1}{12}, \qquad \forall t \in \mathbb{R}, \tag{1.11}$$

which as said before is essentially nothing but ϕ_D with a linear vertical displacement. It is not the first time this alternative function appears, since in [90] Smith used this function in his very short proof of the differentiability properties of the original function (1.1).

At this point, the appearance of Riemann's non-differentiable function in the evolution of regular polygons by the binormal flow might seem, at least, mysterious. In the next section, we will review the arguments of [26] and show heuristically that the

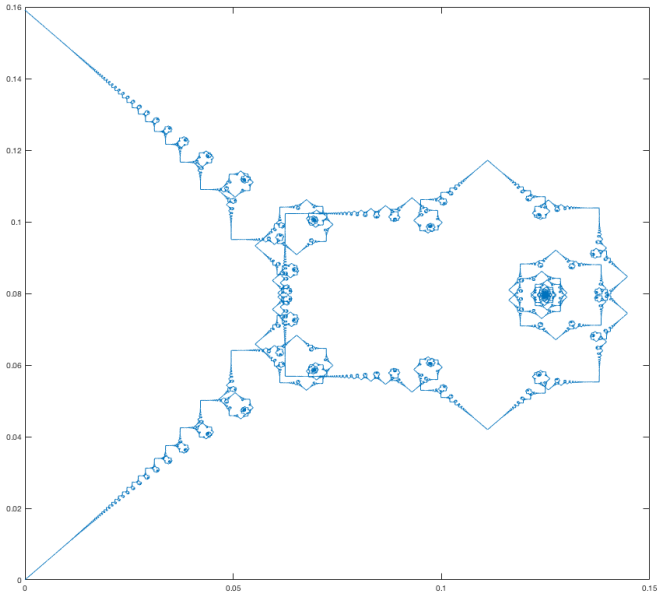

FIGURE 1.5: The image of ϕ corresponding to the interval $[0, 1/(2\pi)]$. When interpreted as the image of a parametric curve, it resembles the trajectories of the corners of a polygonal nozzle in the vortex filament experiment, shown in Figure 1.3.

analytic expression (1.10) is a little bit more than a simple guess.

1.2.2 The evolution of a regular polygon

The objective in this subsection is to mathematically express the problem of the evolution of a planar regular polygon discussed in the previous subsection, to obtain a solution and to understand why the version ϕ of Riemann's non-differentiable function defined in (1.10) appears related to the trajectories of the corners of the polygon.

A remarkable result concerning the analysis of the vortex filament equation (1.8) was proved by Hasimoto in [49], where he established a direct relationship between the binormal flow and the Schrödinger equation. Indeed, if κ and τ are the curvature and the torsion of the curve $\boldsymbol{X}$ respectively, define the filament function

$$\Psi(s,t) = \kappa(s,t)\, e^{i \int_0^s \tau(\sigma,t)\, d\sigma}. \tag{1.12}$$

Hasimoto proved that Ψ is a solution to the nonlinear Schrödinger equation

$$\Psi_t = i\Psi_{ss} + i\,\frac{\Psi}{2}\left(|\Psi|^2 + A(t)\right), \tag{1.13}$$

where $A(t)$ is some real function of time. Since then, many authors including those cited in the previous subsection have used this transformation to translate the problem from the vortex filament equation to the nonlinear Schrödinger equation (1.13). Indeed, if one were able to model the initial datum $\boldsymbol{X}_M(s,0)$ in the setting of the Hasimoto transformation (1.12), then solving (1.13) amounts to knowing the curvature and the torsion of the curve. Assuming the curve is regular enough and that the curvature does not vanish so that the Frenet-Serret frame $\{\boldsymbol{T}, \boldsymbol{N}, \boldsymbol{B}\}$ is well defined,

at least theoretically one may now integrate the differential system (1.9) to get it. Finally, the curve $\boldsymbol{X}$ would be recovered integrating the tangent vector.

Hence, the first step is to model the initial datum in the setting of Ψ (1.12). Since the initial polygon is planar, it should have no torsion, so $\Psi_M(s,0) = \kappa_M(s,0)$. The challenge is then to model the curvature of a regular polygon. It is clear that the curvature will be zero along the sides, while there is a sudden change of direction in each of the corners. Hence, if we let the arclength parameter s be in $[0, 2\pi)$, a reasonable option is to uniformly distribute M Dirac deltas in the interval. After establishing the corresponding coefficients according to the Gauss-Bonnet theorem, we extend to the whole real line periodically so that we set

$$\Psi_M(s,0) = \kappa_M(s,0) = \frac{2\pi}{M} \sum_{k\in\mathbb{Z}} \delta\left(s - \frac{2\pi}{M}k\right). \tag{1.14}$$

While it seems reasonable to define the initial datum this way, the conditions required to eventually integrate the Frenet-Serret system do not hold any longer, since the curvature is zero almost everywhere. This implies that the normal and binormal vectors are not well-defined. To overcome this difficulty, the parallel frame is used instead, where the normal plane usually defined by the basis $\{\boldsymbol{N}, \boldsymbol{B}\}$ is given an alternative basis $\{\boldsymbol{e_1}, \boldsymbol{e_2}\}$ such that the derivatives of these vectors do not depend on themselves but only on the tangent. Thus, since $\boldsymbol{T}$ is well-defined along the sides of the polygon, hence almost everywhere, the evolution of the frame is well-defined. The equations analogue to the Frenet-Serret system for this frame are

$$\begin{pmatrix} \boldsymbol{T}_s \\ (\boldsymbol{e_1})_s \\ (\boldsymbol{e_2})_s \end{pmatrix} = \begin{pmatrix} 0 & \alpha & \beta \\ -\alpha & 0 & 0 \\ -\beta & 0 & 0 \end{pmatrix} \begin{pmatrix} \boldsymbol{T} \\ \boldsymbol{e_1} \\ \boldsymbol{e_2} \end{pmatrix}. \tag{1.15}$$

Here, α and β are functions of s and t that adapt perfectly to the setting of the Hasimoto transformation (1.12), since one can check that $\Psi = \alpha + i\beta$. Therefore, first solving the NLS (1.13) with the datum (1.14) and then integrating the system (1.15), one should be able to recover $\boldsymbol{T}$ and $\boldsymbol{X}$. Eventually, we seek the trajectory $\boldsymbol{X}_M(0,t)$ because $s = 0$ corresponds to a corner in the initial datum (1.14).

In any case, the first problem consists in solving the nonlinear Schrödinger equation (1.13) with the initial datum (1.14). Let us explore first a heuristic approach which is, in principle, far from being rigorous. We may try to approximate the solution by removing the nonlinear terms from the equation and therefore working with the free Schrödinger equation

$$\psi_t(s,t) = i\,\psi_{ss}(s,t) \tag{1.16}$$

and keeping the initial datum (1.14). It is easy to see that the linear solution is

$$\psi_M(s,t) = e^{it\partial_s^2}\left(\frac{2\pi}{M}\sum_{k\in\mathbb{Z}} \delta\left(\cdot - \tfrac{2\pi}{M}k\right)\right)(s) = \sum_{k\in\mathbb{Z}} e^{iMks - iM^2k^2t}. \tag{1.17}$$

Then, one should integrate the differential system (1.15) in s first and then integrate the tangent vector in s again to obtain the solution $\boldsymbol{X}_M$. Following the heuristic reasoning, we might just integrate ψ twice in space. But since ψ is a solution to the free Schrödinger equation, integrating it twice in s is equivalent to integrating it once

in t and then multiplying by i, so

$$\begin{aligned} \boldsymbol{X}_M(0,t) &\approx i\int_0^t \psi_M(0,\tau)\,d\tau = i\int_0^t \sum_{k\in\mathbb{Z}} e^{-iM^2k^2\tau}\,d\tau = \sum_{k\in\mathbb{Z}} \frac{e^{-iM^2k^2t}-1}{-M^2k^2} \\ &= \frac{4\pi^2}{M^2}\,\phi\left(\frac{M^2}{4\pi^2}\,t\right), \end{aligned} \tag{1.18}$$

where our proposed version of Riemann's non-differentiable function ϕ appears.

This approach is nothing but a rough trial to get the trajectory of a corner, yet the numeric simulations in [26], and in particular Figures 1.3 and 1.4, show that they adapt very well to reality and seem to grasp the main features, especially for large values of M. What is more, the Fourier coefficients of $\boldsymbol{X}_M(0,t)-it$, let us call them a_n^M, were computed in [24] and it was shown that

$$na_n^M \approx \begin{cases} 1, & \text{when } n \text{ is a square,} \\ 0, & \text{otherwise,} \end{cases}$$

see [24, Figure 11]. Also, the larger the value of M, the better this approximation seems to be. Hence, in the setting of Figure 1.4, this is some evidence that there must be some convergence of $\boldsymbol{X}_M(0,t)-it$ to $\phi_D(t)$. A similar analysis was done in [25] for the case when the initial polygon is not planar, where the trajectories of corners were also shown to approach functions of the kind of Riemann's non-differentiable function.

All these experiments suggest that there must be some convergence from $\boldsymbol{X}_M(0,t)$ to $\phi(t)$ when $M\to\infty$ in a still undetermined sense. Could we expect, perhaps, something like

$$\lim_{M\to\infty} \frac{M^2}{4\pi^2}\,\boldsymbol{X}_M\left(0,\frac{4\pi^2}{M^2}\,t\right) = \phi(t),$$

which is naively motivated by the linearised simplification (1.18)? This is no claim nor conjecture that the limit above should precisely hold, but in view of the references above, it seems very reasonable to think that the effect of the nonlinear terms in (1.13) tends to vanish when $M\to\infty$.

When it comes just to the function ϕ, (1.18) shows that analytically it corresponds to the artificial choice of $M=2\pi$ so that

$$\phi(t) = i\int_0^t \psi_{2\pi}(0,\tau)\,d\tau \qquad \text{and} \qquad \psi_{2\pi}(s,t) = \sum_{n\in\mathbb{Z}} e^{2\pi ins-4\pi^2in^2t}. \tag{1.19}$$

The conclusion of this section is clear now. We have seen that Riemann's non-differentiable function appears naturally in the evolution of vortex filaments following the binormal flow. Since this model seems to describe several real phenomena that have been observed in experiments, we are in the position to claim that Riemann's non-differentiable function, in its adapted version ϕ (1.10), is an intrinsically physical object and locus that could be defined as the limit trajectory in the experiment of the regular polygons instead of by means of an analytic expression. This is a strong reason that motivates the geometric analysis of the function itself and of the subset of the complex plane constituted by its image, shown in Figure 1.5. For instance, in view of the irregularity of that set, it is natural to wonder whether it is a fractal or not, so the study of its Hausdorff dimension seems of interest. Also, being itself the representative of a physical trajectory, it represents the displacement of a point of a vortex filament. Picking two points in the trajectory, one can of course compute the average velocity of the point in that interval, but can this be done infinitesimally? In other words, can we

determine the velocity that the point has at each moment? Geometrically speaking, does the trajectory admit tangent vectors? We are wondering, thus, about what we may call the geometric differentiability of Riemann's function. These are only two among the possible geometric questions that can be posed about ϕ and its image.

These topics will be developed in the forthcoming chapters. In Chapter 2, the asymptotic behaviour of ϕ will be developed as a tool to answer the questions posed about the Hausdorff dimension and tangency properties of its image in Chapters 3 and 4, respectively.

1.3 The Talbot effect

The Talbot effect is a physical optical effect based on the diffraction of light that was discovered by Henry Fox Talbot in 1836. The ultimate objective of this section is to unravel the relationship between this effect and the evolution of polygonal vortex filaments governed by the binormal flow.

We begin in Subsection 1.3.1 with the physical description of the Talbot effect, with its historic development and with the research, past and present, concerning it. As we could have expected, its study has been mostly physically oriented, based sometimes in arguments of doubtful mathematical validity which we will highlight and address in Appendix A. Then, in Subsection 1.3.2, we will deduce an accurate mathematical expression that describes the effect, and we will explicitly relate it with the evolution of the polygons.

In what concerns the mathematical content of the dissertation, the mathematical description of the Talbot effect will play a role in the computation of the asymptotic behaviour of Riemann's non-differentiable function in Section 2.2. Also, as above mentioned, in Appendix A, we will investigate whether the usual physical reasoning can be rigorously established.

1.3.1 Description of the Talbot effect

What happens if in a dark room light is sent towards a diffraction grating, that is, a plate of opaque material with several vertical and equidistant narrow slits cut, and crosses it? In other words, if we place a screen on the other side of the grating to capture the light that has passed through, what will we see?

Henry Fox Talbot must have been wondering so when in the 1830s he carried out the experiment. Educated at the University of Cambridge and a member of the Royal Society, this English polymath left important contributions in many scientific disciplines such as mathematics, optics, chemistry and botany. As a curiosity and proof of the latter, two species of plants, *Sideritis purpurea Talbot* and *Talbotia elegans Balfour*, bear his name. He also worked in deciphering Egyptian end Assyrian inscriptions. Of noble family, he was elected Member of the Parliament between 1832 and 1835. He is, however, mostly known for his invention of one of the first methods of photography, the process of calotype, by which a negative copy of the desired image was obtained by direct exposure, and later used to produce by contact as many positive copies as needed. Even if patenting issues made him lose success in favour of the Daguerrotype, modern non-digital photography is based in Talbot's procedure.

Anyway, regarding the experiment, Talbot wrote in the fourth part [92] of a series of articles where he describes several experiments and findings about the behaviour of light and its interaction with different media, that

> *About ten or twenty feet from the radiant point, I placed in the path of the ray an equidistant grating (...), with its lines vertical.*

Talbot defined his grating as *"a plate of glass covered with gold-leaf, on which several hundred parallel lines are cut, in order to transmit light at equal intervals"*. Then, he wrote his observations in the following terms.

> *I then viewed the light which had passed through this grating with a lens of considerable magnifying power. The appearance was very curious, being a regular alternation of numerous lines or bands of red and green colour, having their direction parallel to to the lines of the grating. On removing the lens a little further from the grating, the bands gradually changed their colours, and became alternately blue and yellow. When the lens was a little more removed, the bands again became red and green. And this change continued to take place for an indefinite number of times, as the distance between the lens and the grating increased. In all cases the bands exhibited two complementary colours.*
>
> *It was very curious to observe that though the grating was greatly out of the focus of the lens, yet the appearance of the bands was perfectly distinct and well defined.*
>
> *This however only happens when the radiant point has a* very small *apparent diameter, in which case the distance of the lens may be increased even to one or two feet from the grating without much impairing the beauty and distinctness of the coloured bands. So that if the source of light were a mere mathematical point it appears possible that this distance might be increased without limit...*

From Talbot's description above, the second and shortest paragraph is the most meaningful one. As expected, when placing the lens close to the grating, he saw the focused illuminated slits. When removing the lens further from the grating, we would, and probably he did, expect to see the slits blurred. But on the contrary, he remarked the perfect distinction of the bands even if the lens could not focus the grating.

Talbot also describes the alternating of the color of the bands. This was due to his experiments being done with white light, but if a monochromatic ray was used instead, no such alternance happened, and moreover the appearence of the succesive bands was much more neat. The result of the experiment, known as the Talbot effect, can be simplified in the amazing picture shown in Figure 1.6. The Talbot carpet, called like that probably for its resemblance to an elegant rug, is a two dimensional schematic representation of the effect, and allows to visualise and explain what the screen will reflect. Indeed, one has to think of a plane version of the experiment as follows. In the three dimensional space, let the grating be on the plane OXY so that the slits are parallel to the axis Y and light travels in direction Z. Then, we must project everything onto the plane $Y = 0$. This way, the grating is on the line $Z = 0$ and the slits become points. In Figure 1.6, monochromatic light is represented in white, and any horizontal line $Z = z_0$ will represent a screen placed at a distance z_0 from the grating. A very nice simulation, which makes the understanding of this experiment very simple, can be found in the widget [94] in a virtual laboratory of the University of Vienna.

The top edge of the Talbot carpet shows white dots exactly at the same position as on the grating. This means that a screen placed at the distance z_T will be illuminated in the same places as the grating. In other words, the grating will be exactly represented in the screen. However, if the screen is placed in half the distance, $z_T/2$, points will have moved: they are exactly in the middle of the points of the original grating. We could say that the grating *has been translated half a period.* On the other

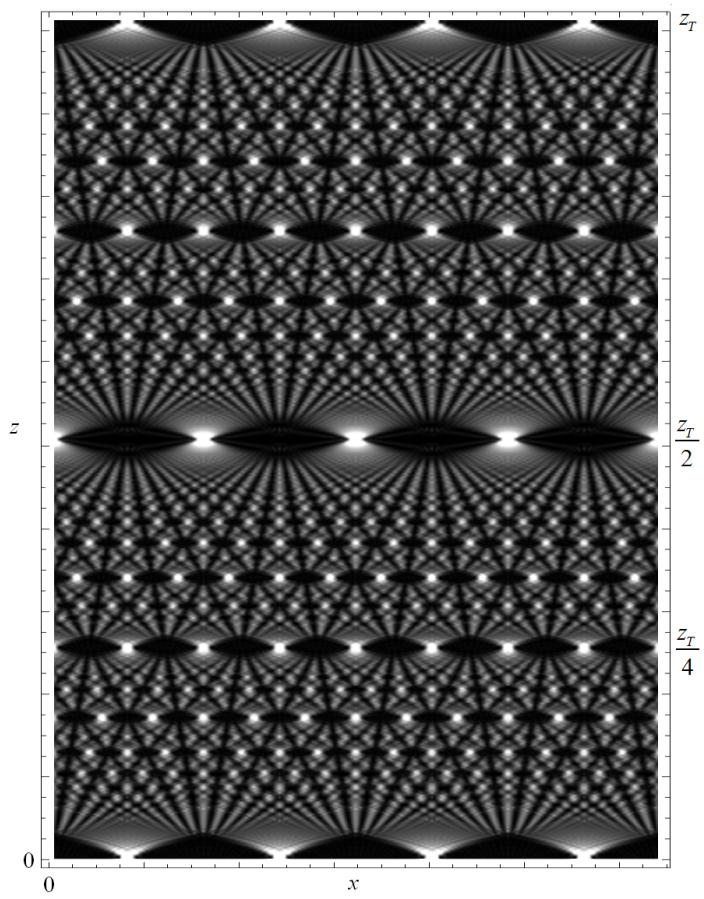

FIGURE 1.6: The Talbot carpet. Modified version of original image by Ben Goodman, available in https://commons.wikimedia.org/wiki/File:Optical_Talbot_Carpet.png

hand, in distances $z_T/4$ or $3z_T/4$, the number of points has doubled, so the screen will reflect a tighter copy of the grating, where the distance between slits has been halved. One can deduce the phenomenon of tightening and translating in any other fraction of the distance z_T, which is usually referred to as the Talbot distance. The reader is referred to [10] for a nice introduction on the experiment and its different applications.

The explanation of this phenomenon resides in the wavy nature of the light, and therefore, it is subject to the laws governing the propagation on waves. One of them, diffraction, indicates that any wave that encounters an obstacle or an aperture deviates, and since the Talbot effect is based on light passing through very narrow slits, one should not be surprised by the fact that diffraction has to be taken into account.

Diffraction can be described very accurately by the Huygens-Fresnel principle. In 1690, in his *Traité de la lumière* [53], Huygens proposed that every point in the wavefront of a certain wave behaves as a source of a spherical wave preserving the properties of the original, such as the wavelength and the velocity. According to it, a wave passing through a narrow hole behaves like in the sketch in Figure 1.7. Huygens also proposed that light travelled as a wave and that followed this principle. However, there was no agreement for a unique theory of light at the time. Indeed, in 1704, Newton proposed in his *Opticks* [76] one more theory for the behaviour of light, claiming that it was a stream of particles. The effects of the passing of light

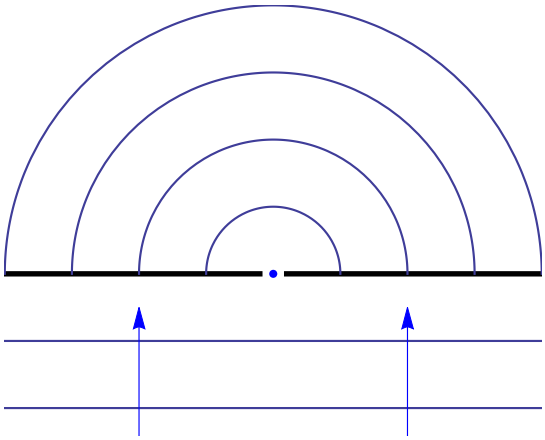

FIGURE 1.7: Schematic representation of the diffraction of a planar wave after passing through a small opening, according to the Huygens principle. Here, every blue line represents a wavefront, that is, a set of contiguous points that are in the same phase of oscillation.

though a narrow slit observed in experiments could be explained by both theories quite satisfactorily, so none could be unquestionably established.

Both theories coexisted, with a general tendency to accept Newton's over Huygens', until Young explained in 1804 in a lecture in the Royal Society of London [98] that from an experiment he had performed it could be deduced that light experimented interference in a similar way as water waves did:

> *I have found so simple and so demonstrative a proof of the general law of the interference of two portions of light, which I have already endeavoured to establish, that I think it right to lay before the Royal Society, a short statement of the facts which appear to me so decisive.*

He was speaking of the original version of the very celebrated double slit experiment, in which, by the way, he did not use a double slit but a slip of a card put in the middle of the solar beam so as to divide it into two. It is the modern version of the experiment that light passes through a plate with two parallel slits. The pattern received in a screen on the opposite side is not formed by two luminous bands, as might have been expected from Newton's corpuscular theory, but by a central white band and a sequence of less intense, parallel fringes (see Figure 1.8).

We can deduce from the manner in which Young expressed himself that he considered his proof absolutely irrefutable:

> *Those who are attached to the Newtonian theory of light, or to the hypotheses of modern opticians, founded on views still less enlarged, would do well to endeavour to imagine any thing like an explanation of these experiments, derived from their own doctrines; and, if they fail in the attempt, to refrain at least from idle declamation against a system which is founded on the accuracy of its application to all these facts, and to a thousand others of a similar nature.*
>
> *(...) we are fully authorised to conclude, that there must be some strong resemblance between the nature of sound and that of light.*

Indeed, Newton's *projectile hypothesis of light*, as Young denoted it, was almost completely discarded after this experiment, only to be recovered with the advent of the quantum theory of the wave-particle duality, in the beginning of the 20th century.

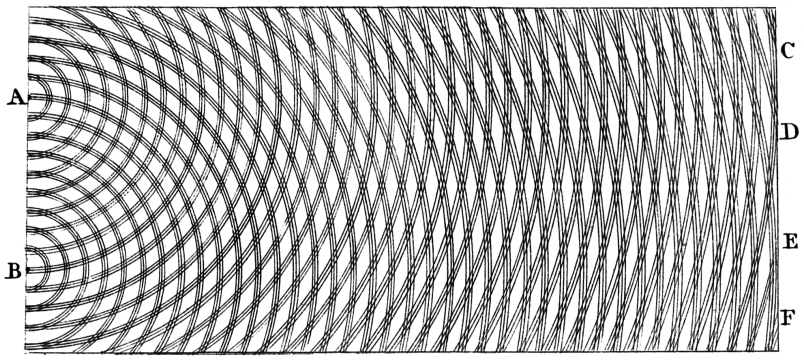

FIGURE 1.8: Young's sketch of the double slit experiment, which explains that the pattern observed is due to the wavy nature of light, the Huygens principle and the consequent interference. On the right hand side part of the figure, lighter and darker *lines* can be distinguished: the lighter ones represent constructive interference where luminous fringes form, while the darker ones stand for destructive interference and no light is visible there. The points C, D, E, F represent these dark fringes on the screen placed on the rightmost position of the sketch. This phenomenon cannot be deduced from Newton's corpuscular theory.

It seemed natural to repeat Young's experiment not with two slits, but with three, four, or any other number that would be considered of interest. Whether the motivations of Talbot to test this were related to Young's, or they were more related to his interest in photography and his experiments with the camera obscura, we do not know. But it seems clear that the first account of these experiments and therefore the first description of the Talbot effect is recorded in Talbot's work [92] discussed earlier. It is clear now, the effect was a consequence of the interference among all the circular waves created in each of the several hundred slits of the grating, which created those neat patterns of light bands. However, there is little doubt that an attempt to generalise the sketch in Figure 1.8 to scores of slits would have been fruitless.

Apparently, unlike Young's very celebrated contribution, Talbot's experiment went unnoticed for many years. The phenomenon was rescued by Lord Rayleigh [86] in 1881 while he aimed to produce copies of original diffraction gratings. Naive as it may seem to anyone who is not used to this kind of experiments, they will be convinced of the difficulty of the task when they read Rayleigh speak about *"a beautiful glass grating containing nearly 12,000 lines, ruled at a rate of 17,280 to the inch"*. He seems to have come into Talbot's work almost by accident in the process of confronting several technical problems to obtaining a satisfactory copy:

> *In the course of the last summer, however, I found accidentally that Fox Talbot had made, many years ago, some kindred observations; and the perusal of his account of them induced me to alter somewhat my proposed line of attack.*

By the time, Young's theory of light was already established, so Rayleigh, assuming that he could work with monochromatic light (he was able to remove the inconvenience of having to deal with several colours at the same time by placing a red or green crystal in front of the source of white light) and therefore with a single wave-length λ, could

compute analytically that the Talbot distance is given by

$$z_T = \frac{\lambda}{1 - \sqrt{1 - \lambda^2/d^2}}.$$

Here, d represents the common distance between two successive slits. If the wavelength is considerably smaller than the separation between slits, then the above expression can be simplified by truncating the Taylor expansion of $\sqrt{1 - \lambda^2/d^2}$ in the second term to obtain

$$z_T = \frac{2d^2}{\lambda}, \tag{1.20}$$

which is the usual and simplest expression for the Talbot distance. Following Young's quote regarding the resemblance of sound and light, Rayleigh based his computations in his book *The Theory of Sound* [85], where he treated the behaviour of a plane wave when travelling across a grating. From the perspective of his original objective, he turned the Talbot distance into a method to copy diffraction gratings, avoiding chemical procedures he had considered at first, since it would be enough to place a photosensitive plate at distance z_T from the original grating to produce a copy.

It is reasonable to think that Rayleigh must have observed the behaviour of light in intermediate distances, but from the point of view of having fulfilled his task, he seems not to have paid much attention to it, and he definitely did not publish anything. After another long period of inactivity, in the late 50s this intermediate behaviour was studied experimentally in [50] with gratings formed using ultrasonic waves, and tighter copies of the original gratings were observed in several rational multiples of z_T. Shortly after, in [97], this was explained with the help of the Fresnel-Kirchhoff diffraction theory and what they call *parabolic approximation*.

More recently, a more precise mathematical description has been given in [9] and [72], where the Talbot effect is analysed from the perspective of the Helmholtz equation. As we will see and analyse in Subsection 1.3.2, this approach is very related to the evolution of the polygon by the binormal flow, so let us give some preliminary details of their computations here.

We assume that light, of wavy nature, follows the wave equation. Let $\boldsymbol{x} \in \mathbb{R}^n$ stand for the space variable and $t \geq 0$ for the time, and let U be the solution to the wave equation

$$\partial_t^2 U(\boldsymbol{x}, t) = c^2 \, \Delta U(\boldsymbol{x}, t)$$

where $c > 0$ is the speed of propagation. If the solution is assumed to have separated variables, this is, if there exist two functions X and T such that $U(\boldsymbol{x}, t) = X(\boldsymbol{x})\, T(t)$, then the equation reads as

$$\frac{1}{c^2} \frac{T''(t)}{T(t)} = \frac{\Delta X(\boldsymbol{x})}{X(\boldsymbol{x})}, \tag{1.21}$$

both of which sides must be equal to a constant, let us say, $-\mu$. The solution $T(t)$ to the resulting equation depends on the sign of μ: if $\mu < 0$, then T has an exponential behaviour in time, and if $\mu = 0$, T grows linearly. Neither of these behaviours are expected in the propagation of waves. In contrast, $\mu > 0$ implies an oscillating $T(t)$. Assuming this case, it is usual to set $\mu = k^2$ for some $k > 0$, for this way k represents the wavenumber $k = 2\pi/\lambda$ where λ is the wavelength. The equation satisfied by $X(\boldsymbol{x})$,

$$\Delta X(\boldsymbol{x}) + k^2 \, X(\boldsymbol{x}) = 0,$$

is called the Helmholtz equation. Let us adapt $X(\boldsymbol{x})$ to the setting of the Talbot carpet, so let $\boldsymbol{x} = (x, z) \in \mathbb{R}^2$ and call $X(\boldsymbol{x}) = u(x, z)$ to the solution to the Helmholtz

equation

$$\Delta_{x,z}u + k^2 u = 0, \qquad x \in \mathbb{R}, \quad z > 0. \tag{1.22}$$

Then, in resemblance to Figure 1.6 and considering the slits of the grating to be infinitely narrow so that they behave as punctual sources of light, the boundary datum at $z = 0$ is modelled by means of Dirac deltas. But before that, it is convenient to rescale the variables according to the information already available. Indeed, the grating is periodic with a period given by the distance between slits $d > 0$, and according to Rayleigh's result, the solution should also be periodic in z, with a period given by the Talbot distance z_T. Then, let

$$\xi = \frac{x}{d}, \qquad \zeta = \frac{z}{z_T} = \frac{\lambda}{2d^2}\, z. \tag{1.23}$$

so that the boundary condition is

$$u(\xi, 0) = \sum_{n\in\mathbb{Z}} \delta(\xi - n) = \sum_{n\in\mathbb{Z}} e^{2\pi i n\xi} \tag{1.24}$$

This function is sometimes called a Dirac comb, or even a train of deltas, which is equal to the sum of exponentials as a consequence of the Poisson summation formula. Then, one may try to test (1.22) by separating variables so that

$$u(\xi, \zeta) = \sum_{n\in\mathbb{Z}} \eta(\zeta)\, e^{2\pi i n\xi}.$$

Now, the fact that $\Delta_{x,z}u(\xi,\zeta) = (\frac{1}{d^2}\, u_{\xi\xi} + \frac{1}{z_T^2}\, u_{\zeta\zeta})(\xi,\zeta)$ yields

$$\eta(\zeta) = \eta(\zeta, n) = e^{\pm i z_T k \zeta \sqrt{1 - \frac{4\pi^2 n^2}{k^2 d^2}}} = e^{\pm 4\pi i (\frac{d}{\lambda})^2 \zeta \sqrt{1 - (\frac{\lambda n}{d})^2}}.$$

The sign in the phase can be determined with the help of the Sommerfeld radiation condition. This principle states that the source of energy, in this case the slits, must indeed be a source, not a sink of energy for waves coming from infinity. In other words, the source must radiate energy and not receive it. In the above solutions, there are clearly two regimes depending on the value of n. When $|n| \geq \lambda/d$, the functions are exponential in ζ. The wave should not increase its amplitude when travelling forward because, according to Sommerfeld's principle, it spreads and loses energy. That suggests that the correct choice of the sign should be a plus. On the other hand, when $|n| < \lambda/d$ the solutions oscillate, and each of the signs represent the direction, forward or backward, of the travelling wave. To see this, observe that from (1.21) we can easily get $T(t) = e^{\pm ickt}$ which oscillates. Since $t > 0$, the sign in the phase does not play an important role, so choose it to be minus. Then, the phase of the n-th wave, in all variables ξ, ζ, t, recalling that $k = 2\pi/\lambda$, is

$$\text{phase}(\xi, \zeta, t) = -2\pi \frac{ct}{\lambda} + 2\pi n\xi \pm 4\pi \left(\frac{d}{\lambda}\right)^2 \zeta \sqrt{1 - \left(\frac{\lambda\, n}{d}\right)^2}.$$

Let $C \in \mathbb{R}$ be a constant, so that $\text{phase}(\xi, \zeta, t) = C$ represents a line where the phase is constant, that is, a wavefront. It can be sketched in the OXZ plane by the equation of the line

$$2\pi n\xi \pm 4\pi \left(\frac{d}{\lambda}\right)^2 \zeta \sqrt{1 - \left(\frac{\lambda\, n}{d}\right)^2} = C + 2\pi \frac{ct}{\lambda},$$

which crosses the vertical axis in the point

$$\left(0, \pm \frac{C + 2\pi \frac{ct}{\lambda}}{4\pi \left(\frac{d}{\lambda}\right)^2 \zeta \sqrt{1 - \left(\frac{\lambda n}{d}\right)^2}}\right).$$

If the chosen sign is negative, then this point travels downwards when t increases, and so does the wavefront, which travels towards the grating. On the contrary, if the sign is positive, then the point and therefore the wavefront travel upwards. The latter case is the correct behaviour according to the Sommerfeld condition, since the grating has to produce the wavefronts. Hence, we choose the plus sign, the same as in the exponential waves, so that

$$u(\xi, \zeta) = \sum_{n \in \mathbb{Z}} e^{4\pi i (\frac{d}{\lambda})^2 \zeta \sqrt{1 - (\frac{\lambda n}{d})^2}} \, e^{2\pi i n \xi} \tag{1.25}$$

At this point, the parabolic approximation mentioned above, consisting in

$$\sqrt{1 - x^2} \simeq 1 - \frac{x^2}{2} \qquad \text{for small enough } x, \tag{1.26}$$

is employed. It is usual to call (1.26) the *paraxial approximation* and we shall do so all along this dissertation. Hence,

$$u(\xi, \zeta) \approx e^{4\pi i (\frac{d}{\lambda})^2 \zeta} \sum_{n \in \mathbb{Z}} e^{2\pi i n \xi - 2\pi i n^2 \zeta}. \tag{1.27}$$

This expression, or rather

$$u(\xi, \zeta)\, e^{-4\pi i (\frac{d}{\lambda})^2 \zeta} \approx \sum_{n \in \mathbb{Z}} e^{2\pi i (n\xi - n^2 \zeta)} = v(\xi, \zeta), \tag{1.28}$$

is which will yield a very detailed description of the Talbot effect and the Talbot carpet, as we will see in the following subsection.

On the other hand, if the vertical variable ζ is identified with the time variable t, then v is a solution to the free Schrödinger equation with the datum proposed in (1.24). Moreover, compared to the solution in the setting of the regular polygon (1.17) and (1.19), we have

$$v(\xi, \zeta) = \psi_{2\pi}(\xi, \zeta/2\pi). \tag{1.29}$$

We devote the following Subsection 1.3.2 to develop all this, that is, to deduce the Talbot effect from (1.28) and explore its relationship with the evolution of the regular polygon by the binormal flow in view of (1.29).

However, before that, let us stop in (1.26) and (1.27) for one moment. The paraxial approximation works only when the variable is very small, close to zero, so it can be used to approximate the phase of u in (1.25) only for small values of n. However, the sum being in all the integers, it is clear that large values of n are completely out of the range of validity of the approximation, and hence that (1.27) is mathematically suspicious, or at least not immediate. On the other hand, the solution to the Schrödinger equation (1.28) matches very accurately the observations in physical experiments and the Talbot carpet in Figure 1.6, so there must be some truth in the approximation. Why is it, then, that the approximation seems to be physically correct while it makes no sense mathematically?

The answer comes from the examination of (1.25) from a physical perspective. Indeed, it can be justified physically that the larger values of n correspond to waves that contribute very little, and that therefore the main contribution to the solution in (1.25) come from small n that are subject to the paraxial approximation. Therefore, the conclusions obtained from the approximation (1.28) seem to be physically correct, at least from the perspective of experiments. But then the question is, is there any way that it can be given a rigorous mathematical sense?

We devote Appendix A to analyse all these questions. More particularly, in Section A.1 we explain the physical arguments that make the approximation (1.27) reasonable, and in Section A.2 we explore the possibilities of making it mathematically rigorous.

1.3.2 The mathematical description of the Talbot effect and its appearance in the evolution of the polygon

We devote this subsection to explain how a very accurate mathematical description of the Talbot effect can be obtained from the solution to the Schrödinger equation v (1.28) and also how it appears in the evolution of the regular M-sided polygon we studied in Subsection 1.2.2. For that, we review the arguments in [9, 72].

We just said that the relationship between v and ψ_M in the setting of the evolution of the M-sided polygon is given by (1.29). The Talbot carpet in Figure 1.6 shows a very clear behaviour in distances given by fractions of the Talbot distance z_T, so to see that both functions above show this behaviour mathematically, according to the rescaling (1.23) we evaluate them in $\zeta = p/q$. It is convenient to assume that the fractions considered are irreducible, so let $p, q \in \mathbb{N}$ such that $q > 0$ and $\gcd(p, q) = 1$. Also, since v is periodic in ζ with period 1, it will be enough to consider $0 < p < q$ so that $p/q \in [0, 1)$.

Since one of our goals is to relate the Talbot effect with the evolution of the M-sided regular polygons by the binormal flow described by ψ_M, let us do the computations with all generality for $M > 0$, so that the conclusions for v will be deduced, according to (1.29), by setting $M = 2\pi$. Since $\psi_M(s, t)$ is periodic in t of period $2\pi/M^2$, then let us analyse it in fractions of this period. Write

$$\psi_M(\xi, 2\pi/M^2(p/q)) = \sum_{n\in\mathbb{N}} e^{iMns - 2\pi i n^2 \frac{p}{q}}.$$

We split the sum in the integers modulo q, for which we let $n = mq + l$ where $m \in \mathbb{Z}$ and $l \in \{0, 1, \dots, q-1\}$ and write

$$\begin{aligned}\psi_M(\xi, 2\pi/M^2(p/q)) &= \sum_{m\in\mathbb{Z}} \sum_{l=0}^{q-1} e^{iM(mq+l)\xi - 2\pi i(mq+l)^2 \frac{p}{q}} \\ &= \sum_{m\in\mathbb{Z}} e^{iMmq\xi} \sum_{l=0}^{q-1} e^{iMl\xi - 2\pi i l^2 \frac{p}{q}}.\end{aligned}$$

The sum in m is now subject of application of the Poisson summation formula, so

$$\begin{aligned}\psi_M(\xi, 2\pi/M^2(p/q)) &= \frac{2\pi}{qM} \sum_{m\in\mathbb{Z}} \delta\left(\xi - \frac{2\pi}{qM}\, m\right) \sum_{l=0}^{q-1} e^{iMl\xi - 2\pi i l^2 \frac{p}{q}} \\ &= \frac{2\pi}{qM} \sum_{m\in\mathbb{Z}} \delta\left(\xi - \frac{2\pi}{qM}\, m\right) \sum_{l=0}^{q-1} e^{2\pi i \frac{ml}{q} - 2\pi i \frac{pl^2}{q}},\end{aligned}$$

where in the last equality we have used the property $\delta(\xi - a)\cdot f(\xi) = \delta(\xi - a) f(a)$ for any smooth function f and any $a \in \mathbb{R}$. Then, for each value $m \in \mathbb{Z}$, the inner sum in l is nothing but a generalised quadratic Gauss sum, defined as

$$G(a, b, c) = \sum_{m=0}^{c-1} e^{2\pi i \, \frac{a\, m^2 + b\, m}{c}}, \qquad a, b \in \mathbb{Z}, \quad c \in \mathbb{N}.$$

In other words,

$$\psi_M(\xi, 2\pi/M^2(p/q)) = \frac{2\pi}{qM} \sum_{m\in\mathbb{Z}} G(-p, m, q)\, \delta\left(\xi - \frac{2\pi}{qM}\, m\right). \tag{1.30}$$

Some features of the Talbot effect can already be deduced from (1.30): not only the solution at the rational multiple of the period $\frac{2\pi}{M^2}\frac{p}{q}$ is also a sum of deltas, but it has q times more deltas than the initial datum (1.14) that represents the polygon (or the Talbot grating (1.24) if $M = 2\pi$). They are equidistributed, and while the distance between them in the initial polygon was $2\pi/M$, now it is $(2\pi/M)/q$. Moreover, each of them has its own coefficient. What is more, (1.30) can be further simplified to show that these coefficients do not depend on m but on the residue $m \pmod q$, so that the solution at the fraction $\frac{2\pi}{M^2}\frac{p}{q}$ keeps on being $2\pi/M$-periodic in ξ. This is done by splitting the sum again modulo q, setting $m = kq + r$, so that we get

$$\psi_M(\xi, 2\pi/M^2(p/q)) = \frac{2\pi}{qM} \sum_{k\in\mathbb{Z}} \sum_{r=0}^{q-1} G(-p, r, q)\, \delta\left(\xi - \frac{2\pi}{M}\, k - \frac{2\pi}{qM}\, r\right). \tag{1.31}$$

Either (1.30) or (1.31) are what we call the mathematical description of the Talbot effect. For clarity in the connection with Subsection 1.3.1, we write the corresponding expression for v by substituting $M = 2\pi$ to get

$$v(\xi, p/q) = \frac{1}{q} \sum_{k\in\mathbb{Z}} \sum_{r=0}^{q-1} G(-p, r, q)\, \delta\left(\xi - k - \frac{r}{q}\right). \tag{1.32}$$

Gauss sums are very well-known and extensively studied. The determination of their exact value depends on many cases, but there is quite a simple formula for their modulus. Indeed, for any $a, b, c \in \mathbb{Z}$ with $c > 0$ and $\gcd(a, c) = 1$, we have

$$|G(a, b, c)| = \begin{cases} \sqrt{c}, & \text{if } c \text{ is odd,} \\ \sqrt{2c}, & \text{if } c \text{ is even and } c/2 \equiv b \pmod 2, \\ 0, & \text{if } c \text{ is even and } c/2 \not\equiv b \pmod 2, \end{cases} \tag{1.33}$$

see [26, Appendix A] for a brief description.

Therefore, two clearly different cases of rational numbers have to be distinguished in (1.31)

- If the irreducible fraction p/q is such that q is odd, the coefficients $G(-p, r, q) \neq 0$ for all $r \in \{0, 1, \ldots, q-1\}$. From the perspective of the M sided polygon, that means that $\psi_M(\xi, 2\pi/M^2(p/q))$ will have exactly Mq equidistributed deltas in $\xi \in [0, 2\pi)$, centred at every $\xi = 2\pi r/(qM)$, hence the polygon at the fraction p/q of the period will have Mq sides. In terms of the optical Talbot effect, $v(\xi, p/q)$ will have exactly q equidistributed deltas in $\xi \in [0, 1)$, centred in every $\xi = r/q$. In the language of the Talbot carpet in Figure 1.6, at a distance $z = \frac{p}{q} z_T$ exactly q times more luminous points are created. For instance, at distances $z_T/3$ and $2z_T/3$ there are three times more points than in the grating $z = 0$, and at a distances $z_T/5, 2z_T/5, 3z_T/5$ and $4z_T/5$ there are five times more points.

- When q is even, half of the Gauss sums $G(p, r, q)$ will be zero according to (1.33). Therefore, $\psi_M(\xi, 2\pi/M^2(p/q))$ will have $Mq/2$ equidistributed deltas and the polygon at the fraction p/q of the period will have $Mq/2$ sides, while $v(\xi, p/q)$ will have $q/2$ equidistributed deltas in $\xi \in [0, 1)$.

  - If $q \equiv 2 \pmod 4$, we have $G(p, r, q) = 0$ if and only if r is even. That means that the deltas will be centred in positions $\xi = r/q$ for odd r. This is the case, for instance, of the distance $z = z_T/2$ in the Talbot carpet: no slit can be found in the positions of the original slits; instead, they are exactly in the middle of them. The same phenomenon can be seen in $z = z_T/6$ and $z = 5z_T/6$.
  - If $q \equiv 0 \pmod 4$, then the situation is complementary: $G(p, r, q) = 0$ if and only if r is odd, and hence the deltas are centred in $\xi = r/q$ for even r. In the Talbot carpet, this is the case of $z = z_T/4$ and $z = 3z_T/4$, where we can see that the grating has been duplicated by having an extra slit in the middle of the original ones, which are still there.

In particular, when $q = 2$, the resulting polygon will have M sides, the same as in the initial moment. However, the Dirac deltas are now in the middle of the initial ones, which implies that the polygon has rotated, as can be seen in the last figure of the numeric simplation [63, p. 1512]. This is precisely the axis-switching phenomenon that was mentioned in Subsection 1.2.1.

So, we have shown that the solution v to the free Schrödinger equation with the Dirac comb as an initial datum is a faithful mathematical representation of the Talbot effect. Not only that, also that the solution ψ_M corresponding to the evolution of an M-sided regular polygon shows it. However, remember that ψ_M is a solution to the free Schrödinger equation (1.16), which was adopted as a simplification of the nonlinear Schrödinger equation (1.13) to approximate the solution Ψ_M to the problem. Therefore, ψ_M might be far from accurately representing the actual solution. Even if it is not evident that the Talbot effect will survive this passing from the linear to the nonlinear equation, in [26] it was shown that it is indeed the case, that the nonlinear evolution also follows the Talbot effect. Thanks to the Galilean transformation, which sends a solution of (1.13) to another solution of the same equation by means of

$$G_\lambda \psi(s, t) = e^{i\lambda s - i\lambda^2 t} \psi(s - 2\lambda t, t), \qquad \forall \lambda \in \mathbb{R},$$

they were able to show that the solution to the NLS (1.13) generated by the Dirac comb (1.14) satisfies

$$\Psi_M(s,t) = \widehat{\Psi_M}(0,t) \sum_{k\in\mathbb{Z}} e^{iMks - iM^2k^2t} = \widehat{\Psi_M}(0,t)\, \psi_M(s,t). \tag{1.34}$$

Here, $\widehat{\Psi_M}(0,t)$ is the 0-th Fourier coefficient of Ψ_M. The solution (1.34) is indeed $2\pi/M$-periodic in s because so is $\Psi_M(s,0)$, and because the NLS equation (1.13) is invariant with respect to space translations.

It is clear now why the Talbot effect is still present in the nonlinear evolution: for every fixed time $t = t_0 > 0$, the coefficient $\widehat{\Psi_M}(0,t_0)$ is nothing but a constant, so the solution $\Psi_M(s,t_0)$ is nothing but the linear solution $\psi_M(s,t_0)$ multiplied by a constant. Therefore, as ψ_M, Ψ_M will be a sum of Dirac deltas in every rational multiple of $2\pi/M^2$. Also, according to the Hasimoto transformation (1.12) the filament function Ψ_M and the curvature κ_M share the support, so the curvature $\kappa_M(s,(p/q)\,2\pi/M^2)$ will also have a discrete, equidistributed support. In other words, the curve $\boldsymbol{X}_M(s, \frac{p}{q}\,\frac{2\pi}{M^2})$ will also be a polygon, in this case Mq sided if q is odd and $Mq/2$-sided if q is even, and not necessarily planar (see [63, Section 5.3] for some numeric simulations of the evolution of the square).

As we said in the beginning of the section, the Talbot effect will play an important role when we compute the asymptotic behaviour of Riemann's non-differentiable function ϕ (1.10) in Chapter 2, which is fundamental to prove the main geometric results of the dissertation in Chapters 3 and 4. This is motivated by the fact that symmetries of the Schrödinger equation like (1.32), which we present in Appendix C, can be used to compute Gauss sums iteratively. We will explain all this in Section 2.2.

1.4 Topics in turbulence

Different settings motivate the relationship of Riemann's non-differentiable function with turbulence. On the one hand, the fact that it is related to a phenomenon of vortex filaments makes the study of this connection a subject of interest. On the other hand, the analysis of its analytic regularity, specially in the work of Jaffard [55] led naturally to study the validity of the multifractal formalism for Riemann's function, a question that has its roots in the research on fully developed turbulence.

It is the objective in this section to explain this relationship and to motivate the interest of some turbulence related properties for Riemann's function, such as intermittency. We begin by explaining the multifractal formalism in Subsection 1.4.1 and the work done with Riemann's function. Then, we relate all that with the concept of intermittency in Subsection 1.4.2 and motivate its study in the setting of Riemann's function.

1.4.1 Multifractality

Fractals, even if not with this name, can be traced back many centuries, but it is probably in the late 19th century when mathematicians started to handle rigorously objects that did not fit with the geometric theory of the time. Precisely, Weiertrass' account of Riemann's and Weierstrass' functions is the first rigorous study of what from the modern perspective we would call fractals. However, the analytic approach was not the only one; of the same time are the Cantor sets based on set theory, and of a few decades later the snowflake by Von Koch, who designed it with the objective of building such an irregular object geometrically. But it is probably Mandelbrot's the

most linked name to fractals, after his very representative report [70] on the length of the coast of Great Britain and specially after his seminal work *The fractal geometry of nature* [71], where indeed he coined the term *fractal* and defined them to be sets whose Hausdorff dimension exceed their topological dimension.

Mathematically speaking, the first fractals one usually thinks about are self-similar fractals. The Cantor set and the Von Koch snowflake are examples of these, which can be thought to be made of several smaller copies of themselves. In general, a self-similar fractal will be related to a reduction scale $0 < r < 1$ and to a number $m \in \mathbb{N}$, so that the whole set will be the union of m copies of the set itself, which are $1/r$ times smaller. Somehow, in the setting of the irregularity that is inherent to fractals, these are the most regular ones, since they admit a single scale. Self-similar fractals can also be built so that they have a finite number of scales, but no more.

Roughly speaking, the multifractal analysis is the study of objects that admit a wide range of different scalings, so that their structure is more irregular. In this setting, multifractal measures have been found to be useful in the description of several physical phenomena, and have been accordingly studied (see the introdocutions of [22, 56] and references therein). However, these irregular situations might sometimes come not in the shape of measures or sets, but of functions. One may think, for instance, of the trajectory of a Brownian motion, but the most characteristic example is probably the velocity field of a fluid undergoing motion in fully developed turbulence. In such a situation, the velocity of the fluid may strongly depend on the position observed and may erratically change from place to place, a phenomenon which is called **intermittency**. It is generally assumed that the relevant quantity to study in these situations is the so called spectrum of singularities, which already appeared briefly in (1.5) and which, roughly speaking, associates to each value $\alpha \geq 0$ the Hausdorff dimension of the set of points where the function v in question behaves approximately as $|v(x) - v(y)| \approx |x - y|^\alpha$. If the velocity is so irregular, one expects its regularity to change from point to point, and therefore its spectrum of singularities to be a non-trivial, at least non-constant function.

However, the spectrum of singularities is usually difficult to measure experimentally. In this setting, Frisch and Parisi proposed in [41] an alternative method based on the measurement of averages of the velocity, which is nowadays called either the Frisch-Parisi conjecture or the multifractal formalism. The starting point is to measure averages of small increments $v(x + l, t) - v(x, t)$ of the velocity $v(x, t)$, where $x \in \mathbb{R}^n$ is the space variable, $l \in \mathbb{R}^n$ is a small spacial variation and $t > 0$ is the time variable. This is done by means of the p-th moments

$$\langle |v(x + l, t) - v(x, t)|^p \rangle , \qquad p > 0, \tag{1.35}$$

where $\langle \cdot \rangle$ stands for some average for which there seems to be no general agreement in the literature. It can be an ensemble average, consisting in a mean of the velocities corresponding to several realisations of the experiment, which would yield a function of x, l and t. It can also be a long-time average, that is, an average of the increment $|v(x + l, t) - v(x, t)|^p$ over two times $1 \ll T_1 < T_2$, which would yield a function of x and l. We refer to [40] and the introduction in [13] for further discussions on the meaning of $\langle \cdot \rangle$. In any case, it is usual to consider the turbulence to be homogeneous, such that these averages do not depend on x, and also isotropic, so that they do not depend on the direction of $l \in \mathbb{R}^3$ but only on its length $\ell = |l|$. In case (1.35) is understood like an ensemble average, it is common to do so for large times and to assume that the velocity is stationary in that range, so that the dependence on t can be dropped. Under all these assumptions, the averages (1.35) are called structure

functions and denoted by

$$S_p(\ell) = \langle |v(x+l) - v(x)|^p \rangle \,, \tag{1.36}$$

where $\ell = |l|$ and $l \in \mathbb{R}^n$.

To deduce the multifractal formalism, Frisch and Parisi work with a theoretical probabilistic description of the velocity, giving it a probability density. Let us denote the probability density function of the increments $w(x,l,t) = v(x+l,t) - v(x,t)$ by $q(x,l,t) = q(x,\ell)$, which is independent of time. Then, they interpret the structure functions as the probabilistic moments. Assume that the structure functions behave like a power law when ℓ is very small. Then, we can write

$$\ell^{\zeta(p)} \simeq S_p(\ell) = \langle |w(x,l)|^p \rangle = \int_{\mathbb{R}^3} |x|^p \, q(x,\ell)\, dx, \qquad \text{when } |\ell| \ll 1, \tag{1.37}$$

for some function $\zeta(p)$. On the other hand, denote the spectrum of singularities by $d(\alpha)$, and the set of points x where $w(x,l) \simeq \ell^\alpha$ as D_α. Then, by the definition of the spectrum of singularities, D_α has Hausdorff dimension $d(\alpha)$. Let us measure in the integral in (1.37) only the contribution of the set $\{|x| \simeq \ell^\alpha\}$, which is

$$\begin{aligned} \int_{|x|\simeq\ell^\alpha} |x|^p \, q(x,\ell)\, dx \simeq \ell^{\alpha p} \int_{|x|\simeq\ell^\alpha} q(x,\ell)\, dx = \ell^{\alpha p} \operatorname{Prob}(w(x,l) \simeq \ell^\alpha) \\ = \ell^{\alpha p} \operatorname{Prob}(x \in D_\alpha). \end{aligned} \tag{1.38}$$

Now, when $\ell \to 0$, the set D_α scales in size ℓ into approximately $\ell^{-d(\alpha)}$ copies of itself. If we suppose that at scale $\ell = 1$ the set has volume $\simeq 1$, then the copies at scale $\ell \ll 1$ have volume $\simeq \ell^3$, and therefore, the probability of being in the set D_α with respect to the domain of the experiment scales like $\ell^{3-d(\alpha)}$. Thus, according to (1.38), the contribution of D_α to $S_p(\ell)$ is approximately of the order $\ell^{\alpha p+3-d(\alpha)}$. Now, $S_p(\ell)$ will be of the order of the biggest contribution, which by $\ell \to 0$ is given by the smallest of the exponents obtained. One could therefore expect that

$$\zeta(p) = \inf_\alpha \{\alpha p + 3 - d(\alpha)\}. \tag{1.39}$$

This is a Legendre transform that can be inverted under certain conditions. For instance, if $d(\alpha)$ is concave, then

$$d(\alpha) = \inf_p \{\alpha\, p - \zeta(p) + 3\}. \tag{1.40}$$

Any of the forms (1.39) or (1.40) are what we called the multifractal formalism, while the Frisch-Parisi conjecture claims their validity.

Many physically oriented works have been done in the sense explained above, relying in suppositions like (1.38) and heuristic reasoning as the above, which seem to be physically acceptable. Nevertheless, these arguments are not mathematically rigorous and the range of validity of the multifractal formalism is unclear. Hence, to determine rigorous conditions under which it holds is an important and interesting goal. An effort to shed some light in this direction was done in [22, 37, 55–57, 60], where precise conditions were given for functions to satisfy the formalism. In this setting, the functions considered need not come from an experiment governed by a statistical law, at least directly, so the structure functions (1.36) have to be given a new meaning. It is usual to replace the statistical p moments by the usual L^p norms

so that

$$S_p(\ell) = \int |f(x+\ell) - f(x)|^p \, dx. \tag{1.41}$$

At this point, let us be more precise with the definitions given above. Let $\alpha \geq 0$. A function f is said to be α-Hölder in $x_0 \in \mathbb{R}^n$, and denoted $f \in C^\alpha(x_0)$, if there exists a polynomial P with $\deg P \leq \alpha$ such that

$$|f(x_0 + h) - P(h)| \leq C|h|^\alpha, \qquad \text{when } |h| \text{ is small.}$$

Then, the Hölder exponent of f at a given point x_0 is the maximal Hölder regularity of f at x_0, defined as

$$\alpha_f(x_0) = \sup\{\alpha \geq 0 \mid f \in C^\alpha(x_0)\}, \tag{1.42}$$

Calling the set of points with exponent α

$$D_{f,\alpha} = \{x \mid \alpha_f(x) = \alpha\}, \tag{1.43}$$

the spectrum of singularities of f is defined to be the Hausdorff dimension of this set,

$$d_f(\alpha) = \dim_{\mathcal{H}} D_{f,\alpha} = \dim_{\mathcal{H}}\{x \in \mathbb{R} \mid \alpha_f(x) = \alpha\}, \qquad \forall \alpha \geq 0.$$

It is usual to extend this definition to values of α yielding an empty set by setting their image to be $-\infty$. In this setting, a function is said to be multifractal if its spectrum of singularities is non trivial, in the sense that it is defined at least on an open interval of Hölder exponents α. If there is no risk of confusion with the function f, we will simply denote $D_{f,\alpha}$ as D_α and $d_f(\alpha)$ as $d(\alpha)$.

Also, the assumption (1.37) that $S_p(\ell)$ behaves as $\ell^{\zeta(p)}$ need not hold. In this deterministic setting, the exponent $\zeta(p)$ can be defined as the closest power to such a law when $\ell \to 0$,

$$\zeta(p) = \liminf_{\ell \to 0} \frac{\log S_p(\ell)}{\log \ell}, \tag{1.44}$$

though it can also be defined by many other several means, like

$$\sup\{s \mid f \in B^{s/p}_{p,\infty}\}, \qquad \sup\{s \mid f \in W^{s/p,p}\}, \qquad \sup\{s \mid f \in H^{s/p,p}\}, \tag{1.45}$$

where $B^s_{p,q}$ are Besov spaces, $W^{s,p}$ are Sobolev-Slobodeckij spaces and $H^{s,p}$ are Bessel potential spaces. All these definitions, though apparently different, were shown to be equivalent if $p > 1$, see [56].

In this sense, partial results concerning functions in Sobolev spaces were given by Jaffard in [59], and extended to Besov spaces by Eyink in [37], while Daubechies and Lagarias [22] checked the multifractal formalism in its form (1.39) for several one dimensional examples. In [56], Jaffard showed for general functions that the multifractal formalism in (1.40) gives an upper bound for the spectrum of singularities, but that the reverse need not be true. In the same spirit, he checked it to be valid for self-similar functions in [57]. Also, in [60] he proved its validity for several classical functions. Many of these contribution are based in the wavelet analysis, see [62, Chapter 9] for an overview on the use of wavelet methods in the multifractal analysis.

In what concerns Riemann's non-differentiable function, the analysis of the Hölder regularity led Duistermaat [29] to study the regularity of the function in irrational points by means of their diophantine properties, and he was able to establish a partial connection between $\alpha_{\phi_D}(x)$ and a variant of the irrationality exponent of x computed

by means of its continued fraction convergents p_n/q_n,

$$\tau(x) = \sup\left\{\tau \mid \left|x - \frac{p_n}{q_n}\right| < \frac{1}{q_n^\tau}, \text{ for infinitely many } \frac{p_n}{q_n} \text{ not both odd}\right\}, \quad (1.46)$$

establishing $\alpha_{\phi_D}(x) \leq 1/2 + 1/(2\tau(x))$. In [55], Jaffard proved that the equality holds,

$$\alpha_{\phi_D}(x) = \frac{1}{2} + \frac{1}{2\tau(x)}, \quad (1.47)$$

and together with the spectrum of singularities of Riemann's function

$$d_R(\alpha) = \begin{cases} 4\alpha - 2, & \text{if } \alpha \in [1/2, 3/4], \\ 0, & \text{if } \alpha = 3/2, \\ -\infty, & \text{otherwise,} \end{cases} \quad (1.48)$$

he proved that R satisfies the multifractal formalism.

In the following subsection, we will comment on the relationship between multifractality and the concept of intermittency that has appeared in the beginning of the section, with a special stress on the computations for Riemann's non-differentiable function.

1.4.2 Intermittency

In the previous subsection, we made the first reference to the concept of intermittency in the setting of fully developed turbulence, when we referred to the very irregular behaviour of the velocity field which shows a high, uncontrolled variability and strongly depends on the observed point. It is, therefore, related to the behaviour in small scales of the object or phenomenon under consideration. In the same way that the multifractal formalism was adapted from that context to the environment of functions, the objective in the following lines is to do so with the concept of intermittency. For that, we will essentially follow Tennekes and Lumley [93] and Frisch [40], where a statistical approach is explained in parallelism with the first definition we gave for the structure functions (1.36). Then, as done in (1.41), we will adapt these definitions to a more deterministic setting.

In the following lines, we work in one dimension for clarity. For $t \geq 0$, let $X(t)$ be a stochastic process, a random function of time. This means that for every value of time t_0, $X(t_0)$ is a random variable that takes its values according to a probability distribution determined by the corresponding probability density function $p_{t_0}(x)$. Let us assume that the process is stationary, that is, that these probability distributions do not depend on time, so that $p_{t_0}(x) = p(x)$ for all $t_0 \geq 0$. For each realisation of the process, $X(t)$ produces a sample real function of time $x(t)$ which will accordingly have a graph with time t in the abscissa and x in the ordinate. A double graph which represents together a sample function $x(t)$ and the density function $p(x)$ is shown in Figure 1.9. According to the motivation, intermittency should represent a high variability of the values of the sample in a very small distance. How can that phenomenon be captured in Figure 1.9? Assume that $p(x)$ has very thin tails, so that the bulk of the distribution is close to the mean value. Assume also for simplicity that the mean is zero. Then, a random sample $x(t)$ will likely be concentrated along the abscissa with very little chance of gaining some meaningful height, see Figure 1.10. On the contrary, if $p(x)$ has fat tails, even if the bulk of $x(t)$ will still lie around the horizontal axis, the chances of spreading far from it are higher and what are called *outlier values* will likely occur, see Figure 1.11. This shows that, somehow, the fatter

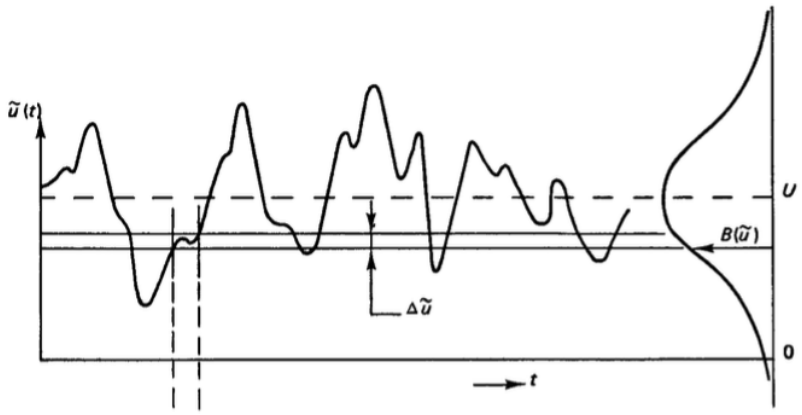

FIGURE 1.9: A sample path of the stochastic process $X(t)$ on the left, where the abscissa is t and the ordinate is x. On the right, the graph of the probability density function $p(x)$ rotated, with an independent ordinate p but whose its abscissa is the same axis x as the ordinate for $X(t)$. This is [93, Figure 6.1], reproduced here with permission of the MIT Press.

the tails of the probability distribution are, the wilder the variability of will be and the more outsider values there will be; in other words, the more intermittent $x(t)$ will be.

As defended in [96], the fatness of the tails of the probability distribution of a random variable X is effectively measured by its **kurtosis** or **flatness**

$$\mathrm{Kurt}[X] = \mathbb{E}\left[\left(\frac{X-\mu}{\sigma}\right)^4\right] = \frac{\mathbb{E}[(x-\mu)^4]}{\mathbb{E}[(x-\mu)^2]^2}. \tag{1.49}$$

Here, $\mu = \mathbb{E}[X]$ stands for the mean and $\sigma = \mathbb{E}[(X-\mu)^2]^{1/2}$ for the standard deviation. According to this definition, the values lying within the distance given by the standard deviation from the mean contribute very little to the kurtosis, so a distribution with a large kurtosis must have a fatter tail than one with a small kurtosis. Hence, large kurtosis indicates the propensity of creating outliers. This agrees with the sketches in Figures 1.10 and 1.11.

Following Frisch [40], let now $V(t) = V(x,t)$ stand for the stochastic velocity of a fluid following a stationary probability distribution, and we assume as before that the it is homogeneous and isotropic. We have seen that the kurtosis accounts for the abundance of outlier values, but we are still missing the part involving the analysis only in small scales. It is clear that this behaviour can be measured in terms of the increments $V(x+l,t) - V(x,t)$ used in (1.35), where the scale in consideration depends on the smallness of the modulus $\ell = |l|$ of the space displacement $l \in \mathbb{R}^3$. Then, according to (1.49),

$$\frac{\left\langle |V(x+l,t) - V(x,t)|^4 \right\rangle}{\left\langle |V(x+l,t) - V(x,t)|^2 \right\rangle^2} = \frac{S_4(\ell)}{S_2(\ell)^2},$$

which depends only on $\ell = |l|$, should be a good measure of the intermittency of V. Observe that this is nothing but a quotient between the structure functions that were

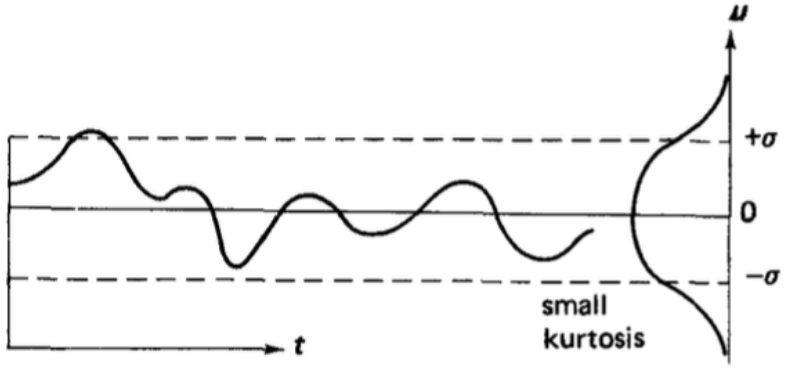

FIGURE 1.10: A probability distribution $p(x)$ with thin tails. The typical sample path will create very few values far from the mean. This is part of [93, Figure 6.4], reproduced here with permission of the MIT Press.

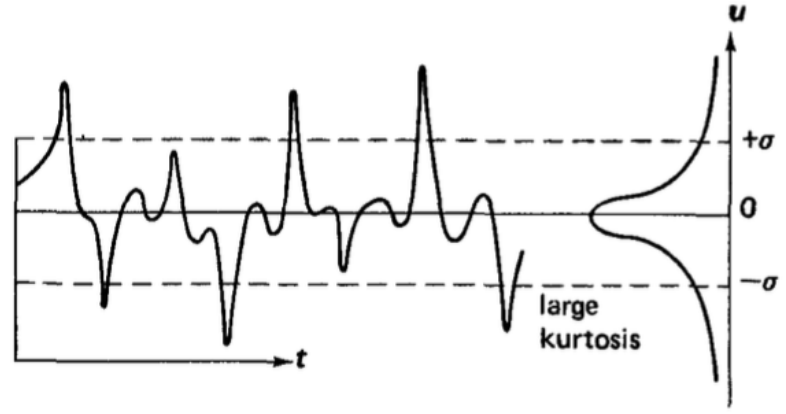

FIGURE 1.11: A probability distribution $p(x)$ with fat tails. Values far from the mean are somewhat common in a typical path. This is part of [93, Figure 6.4], reproduced here with permission of the MIT Press.

defined in (1.36). Motivated by this, we define the **flatness** of V as the function

$$G(\ell) = \frac{S_4(\ell)}{S_2(\ell)^2}. \tag{1.50}$$

The larger $G(\ell)$, the higher the kurtosis of the increments of V will be and the more intermittent V will be. In this setting, V is said to be **intermittent** in case $G(\ell)$ grows without bound when ℓ tends to zero.

However, this is not the only way to deal with the small scale behaviour. Frisch also proposes to work with the Fourier transform of the velocity and to remove the low frequencies. Indeed, since those low frequencies represent large oscillations, they will not be noticed when looking at small enough scales. In case the Fourier transform

of V can be defined, then V can be written as

$$V(x,t) = \int_{\mathbb{R}} \widehat{V}(x,\omega)\, e^{i\omega\, t}\, d\omega,$$

so a way to remove the low frequencies is to define

$$V_{>\Omega}(x,t) = \int_{|\omega|>\Omega} \widehat{V}(x,\omega)\, e^{i\omega\, t}\, d\omega, \tag{1.51}$$

which is called the **high-pass filter** of V. Then, the kurtosis of the high-pass filtered velocity should be a good indicator of its intermittent behaviour, so we define an alternative **flatness** by

$$F(\Omega) = \frac{\left\langle |V_{>\Omega}(x,t)|^4 \right\rangle}{\left\langle |V_{>\Omega}(x,t)|^2 \right\rangle^2}, \tag{1.52}$$

which again, since we are assuming that the process V is homogeneous and stationary, does not depend on x nor on t, but only on Ω.

Apart from the motivation of the high variability of the velocity field of a fluid in fully developed turbulence, it is common to find the notion of intermittency related to self-similarity, which is very present in the theory of turbulence. Indeed, Kolmogorov assumed in his seminal theory of 1941 that turbulent flows are self-similar in different scales. Despite the success of this theory, there is experimental evidence that the behaviour of these flows does not agree with many conclusions that are deduced from this assumption of self-similarity. In this setting, intermittency can be understood as a measure of the lack of self-similarity.

That turbulence is self-similar in different scales can be interpreted as the fact that the increments of the velocity of the fluid obey a unique statistical scaling law, this is, that

$$V(x+\lambda l,t) - V(x,t) \qquad \text{and} \qquad \lambda^\beta \Big(V(x+l,t) - V(x,t) \Big)$$

share statistical distribution for some $\beta > 0$ and all arbitrary $\lambda > 0$. In terms of structure functions (1.36), this means that

$$S_p(\lambda \ell) = \lambda^{p\beta}\, S_p(\ell), \qquad \text{for all } \lambda > 0,$$

and the flatness of such a flow would be constant because

$$G(\lambda\ell) = \frac{S_4(\lambda\ell)}{S_2(\lambda\ell)^2} = \frac{\lambda^{4\beta}\, S_4(\ell)}{\left(\lambda^{2\beta}\, S_2(\ell)\right)^2} = \frac{S_4(\ell)}{S_2(\ell)^2} = G(\ell), \qquad \text{for all } \lambda > 0.$$

In other words, self-similar flows have a constant flatness. A similar reasoning may be performed for the flatness F (1.52) defined by means of high-pass filters. Thus, a flow that is intermittent in small scales cannot be self-similar.

Consequently, a reasonable, physically flavoured definition of intermittency, albeit not very precise, may be the following.

Definition 1.1. A turbulent flow is said to be **intermittent** if its velocity changes very much from point to point, even if the distance between two points is very small. Alternatively, intermittency is in some sense a measure of the lack of self-similarity of the flow in small scales. These concepts can be concentrated in the flatness, either in G (1.50) or in F (1.52), in the sense that the flow is intermittent in small-scales if

either

$$\lim_{\ell \to 0} G(\ell) = +\infty \qquad \text{or} \qquad \lim_{\Omega \to \infty} F(\Omega) = +\infty.$$

As in Subsection 1.4.1, the determination of the mathematical validity and applicability of these concepts is an interesting problem. However, while in the case of the multifractal formalism there was a clear conjecture to test, here we have only a couple of definitions to work with. From here to the end of the section, we will motivate the study of the flatness for functions in general, and for Riemann's non-differentiable function in particular, in connection to the multifractal formalism.

As we said, Riemann's non-differentiable function satisfies the multifractal formalism, which has to be adapted from (1.40) to

$$d(\alpha) = \inf_p \{\alpha\, p - \zeta(p) + 1\}.$$

because the analysis must be performed in $\mathbb{R}$ now. For that, the spectrum of singularities (1.48) was computed on the one hand, and on the other hand the exponent $\zeta(p)$ was determined using the characterisation of Besov spaces in (1.45). Then, according to the definition of $\zeta(p)$ in (1.44), $S_p(\ell)$ defined in (1.41) must be close to $\ell^{\zeta(p)}$ when $\ell \to 0$. However, in principle we cannot conclude that such a power law holds since there might be lower order corrections, say logarithmic. Hence, the exact asymptotic behaviour of $S_p(\ell)$ when $\ell \to 0$, which is critical in Definition 1.1, cannot be directly deduced only from the knowledge of $\zeta(p)$.

One may wonder what the role of high-pass filters (1.51) is in this setting. To see that, we first need to adapt it to the deterministic setting of functions. In the case of periodic functions $f : [0, 1] \to \mathbb{C}$ given by their Fourier series

$$f(x) = \sum_{n \in \mathbb{Z}} a_n\, e^{2\pi i n x}, \tag{1.53}$$

which is precisely the case of Riemann's function, the high-pass filter is defined by removing the low Fourier modes that represent large oscillations, leaving

$$f_{\geq N}(x) = \sum_{|n| \geq N} a_n\, e^{2\pi i n x}, \qquad N \in \mathbb{N}. \tag{1.54}$$

Then, as in (1.41), the statistical p-moments are replaced by the usual L^p norm, so that the flatness F will be

$$F(N) = \frac{\|f_{\geq N}\|_4^4}{\|f_{\geq N}\|_2^4}. \tag{1.55}$$

The objective is then to know the behaviour of $\|f_{\geq N}\|_p^p$ for large values of N.

It is well known that Besov spaces are intrinsically related to Littlewood-Paley decompositions of the Fourier series (1.53). Indeed, if $\zeta(p)$ is interpreted from the point of view of Besov spaces as in the second option in (1.45), then it can be shown that $\|f_{\geq N}\|_p^p$ must be close to $N^{-\zeta(p)}$. But as for $S_p(\ell)$, there might be lower order terms whose determination is critical in the definition of the flatness F.

To determine the existence and the nature of these deviations in the flatness, both for the structure functions and for the high-pass filters, and hence to decide whether Riemann's non-differentiable function is intermittent, has been part of the thesis project and of this dissertation, and will be discussed in more detail in Chapter 5.

1.5 Conclusion

Throughout the previous introductory sections, we have gone through the historic development of Riemann's non-differentiable function and have given an overview of related concepts such as the vortex filament equation, the evolution of a polygon according to the binormal flow, the Talbot effect and some topics related to turbulence. We have also seen and explained how Riemann's function appears, or has been studied in one way or another, in each of them. Hoping that a satisfactory motivation has been given for a geometrically and physically oriented mathematical study of Riemann's non-differentiable function, let us proceed to present and prove the mathematical results that make up this dissertation in Chapters 2, 3, 4, 5 and Appendix A.

CHAPTER 2

Preliminaries on the geometry of Riemann's non-differentiable function

In the setting of the experiment of the vortex filaments explained in Section 1.2, the generalisation of Riemann's function (1.10), which we display here again for convenience,

$$\phi(t) = \sum_{k\in\mathbb{Z}} \frac{e^{-4\pi^2 ik^2 t} - 1}{-4\pi^2 k^2}, \tag{2.1}$$

was shown to be a very precise representative of a physical trajectory. This suggests, on the one hand, that it is natural to undergo a rigorous mathematical analysis of the set $\phi(\mathbb{R})$, shown in Figure 1.5, from a geometric point of view. On the other hand, ϕ seems to be the most natural version of the original function (1.1) to analyse geometrically, rather than the original function itself or other previously studied generalisations like ϕ_D, which are probably more natural analytically. Indeed, in view of (1.11), qualitative analytic results for ϕ_D are valid for ϕ and vice versa, but both functions describe substantially different geometric objects, the linear term on the right hand side of (1.11) playing an important role (See Figures 2.1A and 2.1B, where the latter corresponds to $\phi(x) - ix$). Moreover, both functions being non-injective, it is difficult to measure its effect in the images.

The contents of chapter correspond to the introductory and preliminary results needed for the geometric analysis of Riemann's non-differentiable function in Chapters 3 and 4. More precisely, in Section 2.1 we set the basic setting and notation we will use, and in Section 2.2 we will establish the asymptotic behaviour of ϕ near points that are in direct correspondence with rational numbers. All this will be of great importance in Chapter 3, where we state and prove results about the Hausdorff dimension of the trajectory $\phi(\mathbb{R})$ when regarded as a subset of $\mathbb{R}^2$, and also in Chapter 4, where we develop the study of the existence of geometric tangents to the same set.

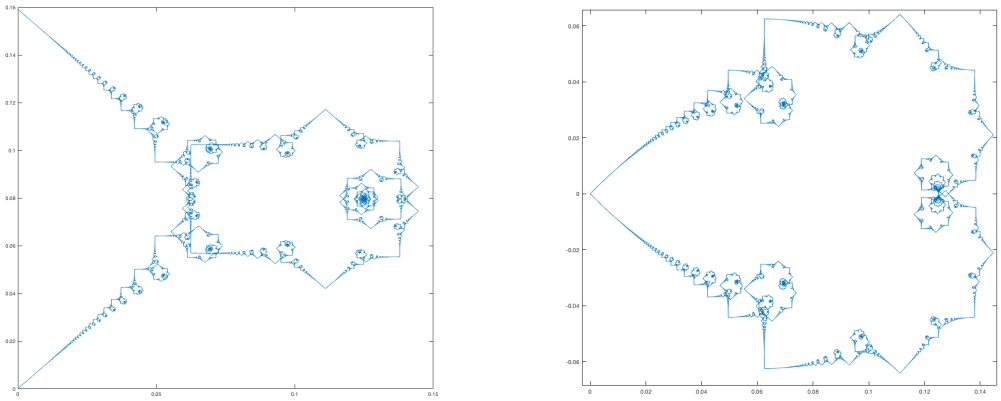

(A) $\phi(x)$ (B) $-\frac{i}{2\pi}\phi_D(-4\pi x)+\frac{1}{12}$

FIGURE 2.1: Comparison between the images of the curves in the period $x \in [0, 1/2\pi]$ as subsets of the complex plane.

The contents of this chapter are based in the note [31][1] and the main article [30][2].

2.1 Mathematical setting

Let ϕ be the geometric version of Riemann's non-differentiable function (2.1). It is very easy to check, either directly, or else by (1.11) and noting that ϕ_D (1.4) has period 2, that ϕ has the periodic property given by

$$\phi\left(t+\frac{1}{2\pi}\right)=\phi(t)+\frac{i}{2\pi}, \qquad \forall t\in\mathbb{R}. \tag{2.2}$$

Thus, we can consider that ϕ has period $1/(2\pi)$. Indeed, if we call $F=\phi([0,1/(2\pi)])$, the above periodicity property implies that

$$\phi(\mathbb{R})=\bigcup_{k\in\mathbb{Z}}\left(F+\frac{ik}{2\pi}\right), \tag{2.3}$$

so $\phi(\mathbb{R})$ is a countable union of translations of F. In other words, $\phi(\mathbb{R})$ is made up of countably many copies of the basic set F. The direct consequence of this is that whichever geometric property we want to prove for the trajectory $\phi(\mathbb{R})$, it will be enough to prove it only for this basic set.

Following this, in the same way that in Subsection 1.1.2 it was convenient to rescale the original Riemann function (1.1) as $R(\pi x)$, it will be convenient for us to rescale the interval $[0,1/(2\pi)]$ to $[0,1]$. For that, send

$$t\in[0,1/(2\pi)]\mapsto x=2\pi t\in[0,1]$$

and identify

$$t=t_x=x/2\pi, \qquad x\in[0,1]. \tag{2.4}$$

[1] Eceizabarrena, D. "Some geometric properties of Riemann's non-differentiable function". In: *C. R. Math. Acad. Sci. Paris* 357.11-12 (2019), pp. 846–850. DOI: 10.1016/j.crma.2019.10.007.

[2] Eceizabarrena, D. "Asymptotic behaviour and Hausdorff dimension of Riemann's non-differentiable function". In: (2019). Preprint: http://arxiv.org/abs/1910.02530v1.

Then,

- If $x = p/q \in [0,1)$ with p and q non-negative and coprime integers, we call $t_{p/q} = t_{p,q}$ a rational point.
- If $x = \rho \in [0,1)$ is irrational, we call t_ρ an irrational point.

According to (1.11), which can be rewritten as

$$\phi(t_x) = -\frac{i}{2\pi}\,\phi_D(-2x) + i\,t_x + \frac{1}{12}, \tag{2.5}$$

and to the differentiability properties of $R(\pi x)$ or equivalently of ϕ_D, we have

$$\phi \text{ is differentiable in } t_x \quad \Leftrightarrow \quad \phi_D \text{ is differentiable in } 2x. \tag{2.6}$$

The result of Gerver [42, 43] implies that ϕ_D is differentiable in $2x$ if $2x$ is a rational of the form $(2m+1)/(2n+1)$ for some $m, n \in \mathbb{N}$, which means that $x = (2m+1)/(4n+2)$, or equivalently $x = p/q$ with p and q coprime and $q \equiv 2 \pmod 4$. Hence,

$$\phi \text{ is differentiable in } t_x \quad \Leftrightarrow \quad x = \frac{p}{q}, \quad \gcd(p,q) = 1, \quad q \equiv 2 \pmod 4.$$

We will see in the coming sections that this analytic distinction between rational points is also of great importance in the geometric analysis of ϕ.

2.2 Asymptotic behaviour near rational points

As we have already suggested, the asymptotic behaviour of ϕ around rational points plays a key role in the proofs of the geometric results concerning the Hausdorff dimension and the tangents of $\phi(\mathbb{R})$. When we speak of the asymptotic behaviour of ϕ around a point t_x, we mean an expression for

$$\phi(t_x + h) - \phi(t_x) \qquad \text{when } h \text{ is small,}$$

so that a very precise analytic behaviour of the function around the point can be obtained. One could think, for instance, of the Taylor series of a general function, but much more general expansions can happen in this case.

The objective of this section is to compute the asymptotic behaviour of ϕ near rational points $t_{p,q}$. We will be able to compute the behaviour around 0 and 1/2 directly in Subsections 2.2.4 and 2.2.5, and later extend them to the rest of rationals in Subsections 2.2.6 and 2.2.7. But before that, we devote Subsections 2.2.1, 2.2.2 and 2.2.3 to explain heuristically the ideas on how we do that.

2.2.1 Preliminaries

As we said in Subsection 1.1.2, Duistermaat already gave in [29] the asymptotic behaviour of ϕ_D near rational points. He first realised that the derivative of ϕ_D is directly related to the Jacobi θ function

$$\theta(z) = \sum_{k\in\mathbb{Z}} e^{\pi i k^2 z}, \qquad z \in \mathbb{H}, \tag{2.7}$$

where $\mathbb{H} = \{z \in \mathbb{C} \mid \mathrm{Im}(z) > 0\}$ is the upper complex half-plane, because

$$\phi_D'(z) = \frac{1}{2}\left(\theta(z) - 1\right), \qquad \forall z \in \mathbb{H}. \tag{2.8}$$

The θ function has a well-known interaction with the modular group Γ of fractional linear transformations with integer coefficients, or Möbius transformations that satisfy

$$\gamma(z) = \frac{az+b}{cz+d}, \qquad a,b,c,d \in \mathbb{Z}, \qquad ad - bc = 1.$$

This group, which is so under the operation of composition, is generated by the transformations

$$S(x) = \frac{1}{z} \qquad \text{and} \qquad T(z) = z + 1.$$

It is well-known that the Jacobi θ function interacts very well with S, since the inversion identity

$$\theta\left(\frac{-1}{z}\right) = \sqrt{\frac{z}{i}}\,\theta(z), \qquad \forall z \in \mathbb{H}, \tag{2.9}$$

holds with the principal branch of the square root, but the trivial relationship that θ has with transformations of the kind of T is not with T itself, but with $T^2(z) = z+2$, since

$$\theta(z+2) = \theta(z), \qquad \forall z \in \mathbb{H}. \tag{2.10}$$

Therefore, rather than with the whole group $\Gamma = \langle S, T\rangle$, Jacobi's θ function interacts with the subgroup $\Gamma_\theta = \langle S, T^2\rangle$, the so called θ-modular group, which alternatively can be proved to be

$$\Gamma_\theta = \left\{ \gamma(x) = \frac{ax+b}{cx+d} \quad | \quad a,b,c,d \in \mathbb{Z},\ ad-bc = 1,\ a \equiv d \not\equiv b \equiv c \,(\mathrm{mod}\ 2) \right\}. \tag{2.11}$$

Properties (2.9) and (2.10) and the fact that Γ_θ is a group imply that there exists an identity relating $\theta(\gamma(z))$ with $\theta(z)$ for every $\gamma \in \Gamma_\theta$, which indeed is

$$\theta(\gamma(z)) = e_\gamma \sqrt{cz+d}\,\theta(z), \qquad \forall \gamma \in \Gamma_\theta. \tag{2.12}$$

Here, e_γ is an eighth root of the unity depending only on c and d. More details on the properties of the Jacobi θ function, of the modular group and in general of modular forms can be found in [2, 91].

Duistermaat used the transformation (2.12) in (2.8) and integrated the identity to obtain an asymptotic expansion for $\phi_D(x) - \phi_D(r)$, where r is the rational pole of the $\gamma \in \Gamma_\theta$ chosen. Then, one may use (1.11) to translate the asymptotic behaviour for ϕ_D to ϕ. In this dissertation, however, we will compute the asymptotic behaviour of ϕ directly. One of the reasons to do this is to have a complete, self-contained account of the whole program regarding the geometric analysis of ϕ. On the other hand, this procedure tackles the problem from a slightly different perspective, even if the underlying idea in the proof is exactly the same as Duistermaat's, strongly inspired on it and also based on the interaction (2.12). But this alternative approach is more deductive and brings to light the connections and interactions with several symmetries of the Schrödinger equation, the Gauss sums and the Talbot effect.

Let us sketch this difference between the two perspectives here. Duistermaat chooses first $\gamma \in \Gamma_\theta$, then combines (2.12) with (2.8) and integrates the latter to arrive to the asymptotic expression for the pole of γ. Then, determines the subset

of rationals that can be found as poles of $\gamma \in \Gamma_\theta$ in this way, and checks that the remaining rationals can be managed by a translation of ϕ_D over 1.

In our case, according to (1.19) the role of θ is played by $\psi_{2\pi}$, which we saw to be the mathematical representation of the Talbot effect in (1.31) in Subsection 1.3.2. On the other hand, $\psi_{2\pi}$ being a solution to the free Schrödinger equation, some of the symmetries of the equation yield invariances of $\psi_{2\pi}$. Evaluating the invariance coming from the pseudoconformal symmetry in rationals $t_{p,q}$ and comparing the coefficients of the Dirac deltas obtained, we can deduce an iterative algorithm to reduce a general quadratic Gauss sum $G(p,r,q)$ with arbitrarily large q to another one with either $q=1$ or $q=2$, which can be easily computed. The same algorithm can be used to iterate the invariances at the level of $\psi_{2\pi}$ to eventually obtain a transformation which we should be able to translate to ϕ because, as suggested, from (1.19) we have

$$\phi(t_{p,q}+h)-\phi(t_{p,q}) = i\int_{t_{p,q}}^{t_{p,q}+h} \psi_{2\pi}(0,\tau)\,d\tau = i\int_{t_{p,q}}^{t_{p,q}+h} \theta(-4\pi\tau)\,d\tau. \tag{2.13}$$

Therefore, we deduce that there exists a transformation which makes it possible to reduce $\phi(t_{p,q}+h)-\phi(t_{p,q})$ with arbitrary $q\in\mathbb{N}$ to either $q=1$ or $q=2$, this is, to either $\phi(h)-\phi(0)=\phi(h)$ or $\phi(t_{1,2}+h)-\phi(t_{1,2})$.

In view of (2.13), it is only the transformation in the time variable that we care about, and since $\psi_{2\pi}(0,t)=\theta(-4\pi t)$, it is trivially translated to θ. Moreover, from the perspective of θ it turns out to be precisely a transformation in Γ_θ, and therefore its interaction with θ is precisely (2.12). Thus, the reduction consists in plugging (2.12) into (2.13) and changing variables. The algorithm, alas, does not provide with an explicit expression for the transformation, so once the rational p/q fixed, the task is to find the proper $\gamma\in\Gamma_\theta$ that sends p/q to either 0 or $1/2$.

In Subsection 2.2.2 we will deduce the iterative algorithm that gives these reductions; as already said, it is based on the Talbot effect. Then, in Subsection 2.2.3 we will find the transformations $\gamma\in\Gamma_\theta$ that are necessary to bring p/q to either 0 or $1/2$, and we will also explain how the computations for the reduction work by formal means. But even if we were able to rigorously establish this reduction process, it will be necessary to know the asymptotic behaviour of ϕ around 0 and $t_{1,2}$. We compute both rigorously in Subsections 2.2.4 and 2.2.5. Finally, in Subsections 2.2.6 and 2.2.7 we will make the previous formal computations rigorous and therefore compute the asymptotic behaviour around any rational $t_{p,q}$.

Before starting, for simplicity and during the rest of this chapter, the function $\psi_{2\pi}$ will be denoted just by

$$\psi(s,t)=\psi_{2\pi}(s,t)=\sum_{n\in\mathbb{Z}} e^{2\pi i n s-4\pi^2 i n^2 t}, \qquad \psi(s,0)=\psi_{2\pi}(s,0)=\sum_{n\in\mathbb{N}}\delta(s-n). \tag{2.14}$$

Also, an important remark needs to be done. Indeed, the expressions (1.19) and (2.13) are formal expressions in the classical functional sense because the Jacobi θ function (2.7) is only defined in the upper complex half-plane $\mathbb{H}$, and not on the real line $\mathbb{R}$. However, for the sake of simplicity, work with these formal expressions along Subsections 2.2.2 and 2.2.3, where computations will be formal anyway. As we said, the arguments will be made rigorous starting in Subsection 2.2.4.

2.2.2 Heuristic reduction: an iterative algorithm to compute Gauss sums using the Talbot effect

We begin this subsection by recalling the expression of the Talbot effect from Subsection 1.3.2. Replacing $M = 2\pi$ in (1.31),

$$\psi\left(s, \frac{p/q}{2\pi}\right) = \psi(s, t_{p,q}) = \frac{1}{q} \sum_{k\in\mathbb{Z}} \sum_{r=0}^{q-1} G(-p, r, q)\, \delta\left(s - k - \frac{r}{q}\right). \tag{2.15}$$

From this expression and the pseudoconformal symmetry of the Schrödinger equation we will deduce the so-called reciprocity formula for quadratic Gauss sums. Then, we will use this formula to deduce the existence of an iterative algorithm by which we will be able to reduce any Gauss sums $G(p, r, q)$ to a different $G(p', r', q')$ with $q' < q$, and eventually to either $q' = 1$ or $q' = 2$.

The main idea is that symmetries together with an invariant initial datum yields an invariance for the corresponding solution, in case uniqueness of solutions is granted. Let us exemplify this with a very easy case. The free Schrödinger equation is translation invariant: if $u(s, t)$ is a solution, then so is $u(s + 1, t)$. This symmetry takes the initial condition $u(s, 0)$ to $u(s + 1, 0)$. In (2.14), $\psi(s, 0) = \psi(s + 1, 0)$, so assuming uniqueness, the two generated solutions must also coincide, and consequently space periodicity $\psi(s, t) = \psi(s + 1, t)$ is deduced for any time.

This procedure was applied in [26] with the Galilean symmetry of the Schrödinger equation to deduce the Talbot effect also in the non-linear evolution of the polygon as we explained in Subsection 1.3.2. In this case, we use the pseudoconformal symmetry of the Schrödinger equation defined by

$$\begin{aligned} \mathcal{P}u(s, t) &= \frac{1}{\sqrt{4\pi i t}}\, \overline{u}\left(\frac{s}{t}, \frac{1}{t}\right) e^{is^2/(4t)}, \\ \mathcal{P}u(s, 0) &= \mathcal{F}^{-1}\left(\overline{u}(4\pi\cdot, 0)\right)(s) = \frac{1}{4\pi}\mathcal{F}^{-1}\overline{u}\left(\frac{s}{4\pi}, 0\right). \end{aligned} \tag{2.16}$$

where the bar represents complex conjugation and the choices $\sqrt{i} = (1 + i)/\sqrt{2}$ and $\sqrt{-1} = i$ are determined by the fundamental solution of the Schrödinger equation, see Remark C.1 in Appendix C. In the case of the initial condition $\psi_0(s) = \psi(s, 0)$ in (2.14), the Poisson summation formula implies that $\widehat{\psi_0} = \psi_0$, and $\overline{\psi_0} = \psi_0(s)$ also holds. Hence,

$$\mathcal{P}\psi_0(s) = \frac{1}{4\pi}\psi_0\left(\frac{s}{4\pi}\right).$$

Now, the datum of the left hand-side generates the solution $\mathcal{P}\psi(s, t)$, while the right hand-side datum generates the solution $(1/(4\pi))\,\psi(s/(4\pi), t/(4\pi)^2)$. If uniqueness of solutions is assumed, then

$$\mathcal{P}\psi(s, t) = \frac{1}{4\pi}\psi\left(\frac{s}{4\pi}, \frac{t}{(4\pi)^2}\right),$$

which after rearrangement leads to the pseudoconformal invariance for ψ,

$$\psi(s, t) = \frac{1}{(4\pi i t)^{1/2}}\, e^{is^2/(4t)}\, \overline{\psi}\left(\frac{s}{4\pi t}, \frac{1}{(4\pi)^2 t}\right). \tag{2.17}$$

The key here is that (2.17) allows the time reduction

$$t_{p,q} \to \frac{1}{(4\pi)^2}\,\frac{1}{t_{p,q}} = \frac{1}{2\pi}\,\frac{q}{4p} = t_{q,4p}. \tag{2.18}$$

To see this effect at the level of Gauss sums, evaluate (2.17) in $t_{p,q}$ and use the Talbot effect (2.15) to get

$$\begin{aligned} &\frac{1}{q}\sum_{k\in\mathbb{Z}}\sum_{r=0}^{q-1} G(-p,r,q)\,\delta\left(s-k-\frac{r}{q}\right) \\ &\qquad = \frac{e^{\frac{i\pi}{2}\frac{q}{p}s^2}}{2\sqrt{2ipq}}\sum_{k\in\mathbb{Z}}\sum_{r=0}^{4p-1}\overline{G(-q,r,4p)}\,\delta\left(s-\frac{2p}{q}k-\frac{r}{2q}\right), \end{aligned} \tag{2.19}$$

and equating the coefficients of the respective Dirac deltas at $s=0$, one gets a very nice proof for the well-known reciprocity formula for Gauss sums,

$$G(p,0,q) = \sqrt{\frac{q}{p}}\,\frac{1+i}{4}\,G(-q,0,4p), \tag{2.20}$$

which can be found written in a slightly different but equivalent way, for instance, in [6, Theorem 1.2.2].

Remark 2.1. Strictly speaking, (2.20) is valid only when $\gcd(q,4p)=1$, or equivalently since we are already assuming that p and q are coprime, when q is odd. This is because it is convenient to work with reduced fractions when we use the Talbot effect in the reduction (2.18). Thus, when q is even, the formula has to be adapted as follows: if $q/(4p) = a/b$ as a reduced fraction, then on the right hand side of (2.19) q and $4p$ should be replaced by a and c respectively, and equating the Dirac deltas at $s=0$ as before,

$$\frac{1}{q}\,G(p,0,q) = \frac{1+i}{4}\,\frac{2}{\sqrt{ac}}\,G(-a,0,c),$$

which of course reduces to (2.20) when q is odd. Moreover, this shows that (2.20) can be given a sense when q is even if we interpret

$$G(da,0,dc) = d\,G(a,0,c), \qquad \forall a,c \text{ coprime and } d\in\mathbb{N}.$$

Formula (2.20) is a powerful one, from which one can deduce at once the non-trivial sum

$$G(1,0,q) = \sqrt{q}\,\frac{1+i}{4}\,G(-q,0,4) = \sqrt{q}\,(1+i)(1+(-i)^q)/2 \qquad \text{for all } q\in\mathbb{N}.$$

Indeed, Gauss sums are easy to compute by hand when q is small, so this suggests an iterative method to compute any $G(p,0,q)$. For that, to be able to reduce the value of q, we need to combine (2.20) with the trivial modular property

$$G(p,0,q) = G(p(\mathrm{mod}\ q),0,q). \tag{2.21}$$

We gather the iterations needed in the following Algorithm 2.2. Let us not take care of the multiplying factors coming from each time we use the reciprocity formula (2.20), but just control the reduction of the inner variables p and q of the Gauss sums.

Algorithm 2.2. *Let $p,q\in\mathbb{N}$ coprime integers such that $q\neq 1,2,4$ and $p<q$. Denote by R the reciprocity formula (2.20) and by M the modularity formula (2.21).*

- *If* $p < q/2$, *do* $(p,q) \xrightarrow{R} (-q,4p) \xrightarrow{M} (4p-q,4p)$.
  - *If* $p < q/4$, *then* $4p < q$. *The denominator has been reduced.*
  - *If* $q/4 < p < q/2$, *iterate again* $(4p-q,4p) \xrightarrow{R} (-p,4p-q) \xrightarrow{M} (3p-q,4p-q)$. *And* $0 < 4p-q < q$. *The denominator has been reduced.*
- *If* $q/2 < p < q$, *do* $(p,q) \xrightarrow{M} (p-q,q) \xrightarrow{R} (q,4(q-p))$.
  - *If* $p > 3q/4$, *then* $4(q-p) < q$. *The denominator has been reduced.*
  - *If* $q/2 < p < 3q/4$, *iterate again* $(q,4(q-p)) \xrightarrow{M} (4p-3q,4(q-p)) \xrightarrow{R} (q-p,3q-4p)$, *where* $3q-4p < q$. *The denominator has been reduced.*

If $q = 4$, *then* $(p,4) \xrightarrow{R} (-4,4p) = (-1,p) \xrightarrow{M} (p-1,p)$, *where* $p = 1$ *or* $p = 3$. *Therefore, the denominator* q *can always be reduced to* $q = 1$ *or* $q = 2$. *When* $q = 2$, *then* $(1,2) \xrightarrow{R} (-2,4) = (-1,2) \xrightarrow{M} (1,2)$, *so the algorithm takes* $q = 2$ *to itself.*

Following Algorithm 2.2 we can compute no matter which Gauss sum $G(p,0,q)$ in finitely many steps.

The idea now is to translate this algorithm from the Gauss sums to the function ψ. Recall that the reciprocity formula (2.20) comes from the pseudoconformal invariance (2.17), so each time that we use it for the Gauss sums amounts to using the pseudoconformal invariance at the level of ψ. Is there a transformation corresponding to the modular property (2.21)? Indeed, one can easily check that it is a consequence of the time periodicity of ψ,

$$\psi(s,t+1/2\pi) = \psi(s,t), \tag{2.22}$$

which is evident in (2.14), and that corresponds to the reduction

$$t_{p,q} \to t_{p,q} + \frac{k}{2\pi} = \frac{1}{2\pi}\left(\frac{p}{q} + k\right) = t_{p+kq,q}, \qquad \forall k \in \mathbb{Z}. \tag{2.23}$$

In short, what Algorithm 2.2 shows is that for every irreducible rational number p/q there exists a transformation μ, formed by several combinations of (2.18) and (2.23), and which has attached two other transformations a_μ and b_μ, such that

$$\psi(s,t) = a_\mu(s,t)\,\psi\left(b_\mu(s,t),\mu(t)\right)$$

and either $\mu(t_{p,q}) = t_{0,1} = 0$ or $\mu(t_{p,q}) = t_{1,2}$. This identity could therefore be plugged into (2.13) and a change of variables $\mu(t) = \tau$ should lead to the result. However, we do not know an explicit expression for μ, so we still cannot do these computations.

But we may be able to get some properties of μ. Let us rewrite (2.13) by changing variables $r = 2\pi\tau$ as

$$\phi(t_x+h) - \phi(t_x) = i\int_x^{x+2\pi h} \psi(0,r/2\pi)\,dr = \frac{i}{2\pi}\int_x^{x+2\pi h} \theta(-2r)\,dr, \tag{2.24}$$

only to adapt it to the setting of Algorithm 2.2 so that the integrating variable r is in the same scale as p/q. In terms of θ, the time transformations coming from (2.17) and (2.22) are applied to $\eta(r) = \theta(-2r)$. According to (2.18), reciprocity changes $\eta(r) \to \eta(-1/4r)$, which translates as $\theta(r) \to \theta(-1/r)$, while in view of (2.23) with $k = 1$, modularity changes $\eta(r) \to \eta(r+1)$ which translates as $\theta(r) \to \theta(r+2)$. These

two transformations,

$$r \to 1/r \qquad \text{and} \qquad r \to r+2,$$

are precisely the generators of the θ-modular group Γ_θ (2.11). Since the transformation whose existence we have deduced is a combination of both, then it must be a θ-modular transformation $\gamma \in \Gamma_\theta$. Observe that we have changed the scale in (2.24) again, with a change of variables $2r = \sigma$. The proper setting is now

$$\phi(t_x + h) - \phi(t_x) = \frac{i}{4\pi} \int_{2x}^{2x+4\pi h} \theta(-\sigma)\, d\sigma, \tag{2.25}$$

and if $x = p/q$, then since the reduction will yield asymptotics at 0 or $t_{1,2}$, then either $\gamma(2p/q) = 0$ or $\gamma(2p/q) = 1$ will hold. From now on, we will denote as $\tilde{p}/\tilde{q}$ the irreducible fraction coming from $2p/q$, so that

$$\begin{array}{lll} \tilde{p} = 2p, & \tilde{q} = q, & \text{if } q \text{ is odd,} \\ \tilde{p} = p, & \tilde{q} = q/2, & \text{if } q \text{ is even.} \end{array} \tag{2.26}$$

At this point, we can guess which rational numbers can be sent to 0 and which cannot. Assume both $\tilde{p}, \tilde{q}$ are odd and that $\gamma \in \Gamma_\theta$ is such that $\gamma(\tilde{p}/\tilde{q}) = 0$. The coefficients in the numerator of γ, a and b, are coprime, so either $a = \tilde{q}$ and $b = -\tilde{p}$ or $a = -\tilde{q}$ and $b = \tilde{p}$ must hold. But then the parity condition in (2.11) is not kept, hence γ does not exist. These points are precisely corresponding to p/q with $q \equiv 2 \,(\mathrm{mod}\ 4)$, because then p is odd and $\tilde{p}/\tilde{q} = p/(q/2)$, where $q/2$ is odd. On the other hand, if $q \equiv 0 \,(\mathrm{mod}\ 4)$, then $\tilde{p}/\tilde{q} = p/(q/2)$ with p odd and $q/2$ even, and if $q \equiv 1, 3 \,(\mathrm{mod}\ 4)$, then $\tilde{p}/\tilde{q} = 2p/q$ with $2p$ even and q odd.

In Subsection 2.2.3, we prove that the general scheme for the θ-modular transformations corresponding to $t_{p,q}$ is

$$\begin{array}{lllll} q \text{ odd} & \Longrightarrow & \tilde{p} = 2p, & \tilde{q} = q, & \exists \gamma \in \Gamma_\theta \text{ such that } \gamma(\tilde{p}/\tilde{q}) = 0. \\ q \equiv 0 \,(\mathrm{mod}\ 4) & \Longrightarrow & \tilde{p} = p, & \tilde{q} = q/2, & \exists \gamma \in \Gamma_\theta \text{ such that } \gamma(\tilde{p}/\tilde{q}) = 0. \\ q \equiv 2 \,(\mathrm{mod}\ 4) & \Longrightarrow & \tilde{p} = p, & \tilde{q} = q/2, & \exists \gamma \in \Gamma_\theta \text{ such that } \gamma(\tilde{p}/\tilde{q}) = 1. \end{array} \tag{2.27}$$

We will also compute these transformations.

2.2.3 Formal reduction: the modular group

The objective in this subsection is to give the formal arguments starting from (2.25) that allow to reduce the asymptotic behaviour around a rational $t_{p,q}$ to either 0 ot $t_{1,2}$. Even if the computations are formal (because, as we said in the end of Subsection 2.2.1, neither (2.13) nor (2.25) makes sense rigorously), the heuristic conclusions are very enlightening. For that, we need to compute the θ-modular transformations that follow the classification (2.27) explicitly. This was essentially done by Jaffard [55], whose steps we follow here.

We will use continued fractions to determine the coefficients a, b, c, d of the transformations

$$\gamma \in \Gamma_\theta, \qquad \gamma(x) = \frac{ax+b}{cx+d}$$

that were defined in (2.11). For the basics about the theory of continued fractions, we refer the reader to the Appendix B. In the case of $\tilde{p}/\tilde{q}$, its continued fraction is finite because it is a rational number, so there exists $N \in \mathbb{N}$ such that $\tilde{p}/\tilde{q} = [a_0; a_1, \ldots, a_N]$, where $a_n \in \mathbb{N}$ for all $n \in \mathbb{N}$. As usual, the n-th convergent $\tilde{p}_n/\tilde{q}_n = [a_0; a_1, \ldots, a_n]$

satisfies $|\tilde{p}/\tilde{q} - \tilde{p}_n/\tilde{q}_n| < \tilde{q}_n^{-2}$ and

$$\tilde{p}_n\,\tilde{q}_{n-1} - \tilde{q}_n\,\tilde{p}_{n-1} = (-1)^{n-1} \tag{2.28}$$

for every $n \leq N$.

2.2.3.1 Transformation for rationals p/q such that $\tilde{p}$ and $\tilde{q}$ are not both odd

According to the classification (2.27), these are the rationals whose asymptotic behaviour can be reduced to that around 0. Choose

$$a = \tilde{q}, \qquad b = -\tilde{p}, \tag{2.29}$$

which satisfy the parity conditions necessary for $\gamma \in \Gamma_\theta$ and make $\gamma(\tilde{p}/\tilde{q}) = 0$. Since $\tilde{p} = \tilde{p}_N$ and $\tilde{q} = \tilde{q}_N$, in view of (2.28), we use $\tilde{p}_{N-1}$ and $\tilde{q}_{N-1}$ for the coefficients in the denominator.

- If $\tilde{p}_{N-1}$ and $\tilde{q}_{N-1}$ are not both odd, we choose

  $$c = (-1)^{N-1}\,\tilde{q}_{N-1}, \qquad d = (-1)^N\,\tilde{p}_{N-1},$$

  so that $ad - bc = (-1)^N\,(\tilde{q}\,\tilde{p}_{N-1} - \tilde{p}\,\tilde{q}_{N-1}) = (-1)^{2N} = 1$. Moreover, if $\tilde{p}$ is even, then by (2.28) $\tilde{p}_{N-1}$ must be odd, and thus, $\tilde{q}_{N-1}$ must be even. Otherwise, if $\tilde{q}$ is even, then $\tilde{q}_{N-1}$ is odd and $\tilde{p}_{N-1}$ is even. In both cases, the parity conditions are satisfied.

- If $\tilde{p}_{N-1}$ and $\tilde{q}_{N-1}$ are both odd, the choice above does not satisfy the parity conditions, so choose instead

  $$c = (-1)^{N-1}\,\tilde{q}_{N-1} + \tilde{q}, \qquad d = (-1)^N\,\tilde{p}_{N-1} - \tilde{p}.$$

  In the same way as above, both the determinant condition and the parity condition are satisfied.

Remark 2.3. The choice of c and d is not unique. Indeed, parity and the determinant are preserved if we choose $c' = c + 2k\tilde{q}$ and $d' = d - 2k\tilde{p}$, for no matter which $k \in \mathbb{Z}$. If $k = 1$, we may work with $\tilde{q} < c < 4\tilde{q}$ in both cases. If $k = -1$ in the first case and $k = -2$ in the second one, we may also work with $-4\tilde{q} < c < -\tilde{q}$.

2.2.3.2 Transformation for rationals p/q such that $\tilde{p}$ and $\tilde{q}$ are both odd

We saw in (2.27) that these rationals cannot be sent to 0 because for that (2.29) would be required, but it does not satisfy the parity conditions. We choose instead

$$a = (-1)^{N-1}\,\tilde{q}_{N-1} + \tilde{q}, \quad b = (-1)^N\tilde{p}_{N-1} - \tilde{p},$$

$$c = (-1)^{N-1}\tilde{q}_{N-1}, \qquad d = (-1)^N\,\tilde{p}_{N-1}.$$

Indeed, by (2.28) $\tilde{p}_{N-1}$ and $\tilde{q}_{N-1}$ cannot both be odd, so parity conditions are preserved, and also $ad - bc = 1$. One can easily check that $\gamma(\tilde{p}/\tilde{q}) = 1$.

Remark 2.4. As in the previous case, the choice of a, b, c, d is not unique, since all properties are preserved if

$$\begin{aligned} a &= (-1)^{N-1}\,\tilde{q}_{N-1} + (2k+1)\tilde{q}, & b &= (-1)^N\tilde{p}_{N-1} - (2k+1)\tilde{p}, \\ c &= (-1)^{N-1}\tilde{q}_{N-1} + 2k\tilde{q}, & d &= (-1)^N\,p_{N-1} - 2k\tilde{p}, \end{aligned}$$

for any $k \in \mathbb{Z}$. With $k = 1$, we may assume $\tilde{q} < c < 3\tilde{q}$, and with $k = -1$, we may work with $-3\tilde{q} < c < -\tilde{q}$.

2.2.3.3 Formal argument for the reduction

Once the transformations have been found, let us use them to do the computations for the reduction from $t_{p,q}$ to either 0 or $t_{1,2}$.

We start with the case of a rational p/q with $0 < p \le q$ coprime and such that $q \equiv 0, 1, 3 \pmod 4$. We just saw that there exists $\gamma \in \Gamma_\theta$ such that $\gamma(\tilde{p}/\tilde{q}) = 0$. According to (2.25), for $h \in \mathbb{R}$ we have

$$\phi(t_{p,q} + h) - \phi(t_{p,q}) = \frac{i}{4\pi} \int_{\tilde{p}/\tilde{q}}^{\tilde{p}/\tilde{q}+4\pi h} \theta(-\sigma)\, d\sigma. \tag{2.30}$$

Conjugate and use the transformation (2.12) with the γ above so that

$$\overline{\phi(t_{p,q} + h) - \phi(t_{p,q})} = \frac{\overline{i\, e_\gamma}}{4\pi} \int_{\tilde{p}/\tilde{q}}^{\tilde{p}/\tilde{q}+4\pi h} \frac{\theta(\gamma(\sigma))}{\sqrt{c\sigma + d}}\, d\sigma. \tag{2.31}$$

Now, we change variables $\gamma(\sigma) = r$. Taking into account that $a = \tilde{q}$, $b = -\tilde{p}$ and $ad - bc = 1$, it is easy to see check that

$$\gamma(x) = \frac{ax + b}{cx + d} \qquad \Longrightarrow \qquad \gamma^{-1}(x) = \frac{dx - b}{-cx + a}, \quad \gamma'(x) = \frac{1}{(cx + d)^2}.$$

Then, the boundaries of the integral become $\gamma(\tilde{p}/\tilde{q}) = 0$ and

$$\gamma(\tilde{p}/\tilde{q} + 4\pi h) = \frac{4\pi\tilde{q}^2 h}{1 + 4\pi c\tilde{q}h}. \tag{2.32}$$

At this point, the cases $h > 0$ and $h < 0$ have to be considered separately. To avoid a null denominator, if $h \ge 0$, following Subsections 2.2.3.1 and 2.2.3.2 we let $c = c_+$ be such that $\tilde{q} < c_+ < 4\tilde{q}$. On the other hand, if $h < 0$, choose $c = c_-$ such that $-4\tilde{q} < c_- < -\tilde{q}$. This way, we have $4\pi c\tilde{q}h \ge 0$ in both cases. With (2.32) in mind, define

$$b(h) = \frac{\tilde{q}^2 h}{1 + 4\pi c_\pm \tilde{q}h} = \begin{cases} \frac{\tilde{q}^2 h}{1+4\pi c_+ \tilde{q}h}, & \text{when } h \ge 0, \\ \frac{\tilde{q}^2 h}{1+4\pi c_- \tilde{q}h}, & \text{when } h < 0. \end{cases} \tag{2.33}$$

Then, (2.31) turns into

$$\overline{\phi(t_{p,q} + h) - \phi(t_{p,q})} = \frac{\overline{i\, e_\gamma}}{4\pi} \int_0^{4\pi b(h)} \frac{\theta(r)}{(\tilde{q} - c_\pm r)^{3/2}}\, dr, \qquad \forall h > 0.$$

When $|h|$ is small, $b(h)$ behaves like $\tilde{q}^2 h$, so the variable r of the integral is small and $\tilde{q} - cr$ is similar to $\tilde{q}$. In view of this heuristic reasoning and (2.30), the asymptotic around $t_{p,q}$ will behave approximately as

$$\phi(t_{p,q} + h) - \phi(t_{p,q}) \approx \frac{e_\gamma}{\tilde{q}^{3/2}} \frac{i}{4\pi} \int_0^{4\pi\tilde{q}^2 h} \theta(-r)\, dr = \frac{e_\gamma}{\tilde{q}^{3/2}}\, \phi(\tilde{q}^2\, h). \tag{2.34}$$

This means that when $h \to 0$, the behaviour of ϕ around $t_{p,q}$ is essentially the same as around 0, except that we need to rescale by $\tilde{q}^2$ in the variable and by $\tilde{q}^{-3/2}$ in the image.

On the other hand, if $q \equiv 2 \pmod 4$, there exists $\gamma \in \Gamma_\theta$ such that $\gamma(\tilde{p}/\tilde{q}) = 1$. The same steps as before lead to

$$\overline{\phi(t_{p,q}+h) - \phi(t_{p,q})} = \frac{\overline{i\, e_\gamma}}{4\pi} \int_1^{1+4\pi b(h)} \frac{\theta(r)}{(\tilde{q} - c_\pm(r-1))^{3/2}}\, dr.$$

Again, when $|h|$ is small enough then $b(h) \approx \pm\tilde{q}^2|h|$ and thus the denominator inside the integral is essentially $\tilde{q}^{3/2}$. Consequently,

$$\begin{aligned} \phi(t_{p,q}+h) - \phi(t_{p,q}) &\approx \frac{e_\gamma}{\tilde{q}^{3/2}} \frac{i}{4\pi} \int_1^{1+4\pi\tilde{q}^2 h} \theta(-r)\, dr \\ &= \frac{e_\gamma}{\tilde{q}^{3/2}} \left(\phi(t_{1,2} + \tilde{q}^2\, h) - \phi(t_{1,2})\right). \end{aligned} \tag{2.35}$$

As with the other rationals, the behaviour of ϕ around $t_{p,q}$ is essentially the same as around $t_{1,2}$ when $h \to 0$, taking into account the same scalings as in the previous case.

It seems clear that the arguments of approximation used to obtain the reductions (2.34) and (2.35) will work in the limit $h \to 0$. However, the formal expression (2.30) still needs to be given a rigorous sense. That can be done if we work with the limit

$$\phi\left(t_{p,q}+h\right) - \phi(t_{p,q}) = \frac{i}{4\pi} \lim_{\epsilon\to 0^+} \int_{\tilde{p}/\tilde{q}}^{\tilde{p}/\tilde{q}+4\pi h} \theta(-\tau + i\epsilon)\, d\tau. \tag{2.36}$$

We elaborate on the details and obtain the precise asymptotic behaviour in Subsections 2.2.6 and 2.2.7.

We have established the path to compute the asymptotic behaviour around every rational $t_{p,q}$ based on the behaviour around 0 and $t_{1,2}$. However, we still do not know how ϕ behaves near these basic points. Hence, before getting into making the reasoning of the present section rigorous, let us compute the asymptotic behaviour around 0 and $t_{1,2}$ in Subsections 2.2.4 and 2.2.5 respectively. We do this directly.

2.2.4 Asymptotic behaviour around 0

Taking into account that $\phi(0) = 0$, as can be readily deduced from the definition (2.1), to compute the asymptotic behaviour of ϕ around 0 means to compute an expression for $\phi(h)$. We base our computation on the Poisson summation formula, as suggested by Duistermaat [29], even if the idea can clearly be traced back to Smith [90]. We will avoid approximations in order to eventually get a complete asymptotic series.

We begin assuming $h > 0$. Let us write the function as

$$\phi(h) = -h \sum_{k\in\mathbb{Z}} g(2\pi k\sqrt{h}), \qquad \text{where} \qquad g(x) = \frac{e^{-ix^2} - 1}{x^2}. \tag{2.37}$$

The Poisson summation formula then implies

$$\phi(h) = -\frac{\sqrt{h}}{2\pi} \sum_{k\in\mathbb{Z}} \widehat{g}\left(\frac{k}{2\pi\sqrt{h}}\right) \tag{2.38}$$

in case $|g(x)| + |\widehat{g}(x)| \le C(1+|x|)^{-1-\delta}$ for some $C, \delta > 0$ (see, for instance, [44, Theorem 3.1.17]). The function g is bounded in any compact set because it is analytic, and it decreases as $|x|^{-2}$ when $|x| \to \infty$. Hence, it satisfies the hypothesis. Concerning $\widehat{g}$, we prove the following lemma, very similar to [79, Lemma 1].

Lemma 2.5. *The Fourier transform of g defined in (2.37) is*

$$\widehat{g}(\xi) = 2\pi^2 |\xi| \operatorname{erfc}\left(\frac{1-i}{\sqrt{2}}\,\pi\,|\xi|\right) - \sqrt{2\pi}\,(1+i)\,e^{i\pi^2\xi^2}, \qquad \forall \xi \in \mathbb{R},$$

where $\operatorname{erfc}(z) = 1 - \operatorname{erf}(z)$ *stands for the complementary error function and* $\operatorname{erf}(z) = \frac{2}{\sqrt{\pi}} \int_0^z e^{-w^2}\,dw$ *is the error function, for* $z \in \mathbb{C}$. *Its asymptotic expansion for* $x \in \mathbb{R}$ *at infinity is*

$$\operatorname{erfc}(x) = \frac{e^{-x^2}}{\sqrt{\pi}} \left(\frac{1}{x} + \sum_{n=1}^{N} (-1)^n \frac{(2n-1)!!}{2^n\, x^{2n+1}}\right) + O\left(\frac{1}{x^{2N+3}}\right), \qquad \forall N \in \mathbb{N}. \quad (2.39)$$

Remark 2.6. The integral of the holomorphic function e^{-w^2}, $w \in \mathbb{C}$ in the definition of the error function can be computed along any path connecting 0 and z.

Proof. Integrating by parts, we may write

$$\widehat{g}(\xi) = -2i \int_{\mathbb{R}} e^{-ix^2} e^{-2\pi i\xi x}\,dx + 2\pi i\xi \int_{\mathbb{R}} \frac{e^{-2\pi i\xi x}}{x}\,dx - 2\pi i\xi \int_{\mathbb{R}} \frac{e^{-ix^2}}{x} e^{-2\pi i\xi x}\,dx.$$

The first two integrals are the very well-known Fourier transforms of the Gaussian function and of $1/x$, which are given by

$$\mathcal{F}_x\left(e^{-ix^2}\right)(\xi) = \sqrt{\pi}\,\frac{1-i}{\sqrt{2}}\,e^{i\pi^2\xi^2}, \qquad \mathcal{F}_x\left(1/x\right)(\xi) = -\pi i \operatorname{sign}(\xi),$$

while the third one is the convolution of both of them which, except the constants outside the integral, is

$$\int_{\mathbb{R}} e^{i\pi^2 x^2} \operatorname{sign}(\xi - x)\,dx = \int_{-\infty}^{\xi} e^{i\pi^2 x^2}\,dx - \int_{\xi}^{\infty} e^{i\pi^2 x^2}\,dx = \operatorname{sign}(\xi) \int_{-|\xi|}^{|\xi|} e^{i\pi^2 x^2}\,dx.$$

Hence,

$$\widehat{g}(\xi) = -\sqrt{2\pi}\,(1+i)\,e^{i\pi^2\xi^2} + 2\pi^2|\xi| - 4\pi^2\sqrt{\pi}\,\frac{1-i}{\sqrt{2}}|\xi| \int_0^{|\xi|} e^{i\pi^2 y^2}\,dy.$$

The last integral is essentially $\operatorname{erf}(\frac{1-i}{\sqrt{2}}\,\pi|\xi|)$, since by taking the path $\eta(t) = \frac{1-i}{\sqrt{2}}\,\pi t$, $t \in (0, |\xi|)$, we get

$$\operatorname{erf}(\tfrac{1-i}{\sqrt{2}}\,\pi|\xi|) = \tfrac{2}{\sqrt{\pi}} \int_0^{|\xi|} e^{-\eta(t)^2}\,\eta'(t)\,dt = 2\sqrt{\pi}\,\tfrac{1-i}{\sqrt{2}} \int_0^{|\xi|} e^{i\pi^2 t^2}\,dt,$$

and thus,

$$\widehat{g}(\xi) = -\sqrt{2\pi}\,(1+i)\,e^{i\pi^2\xi^2} + 2\pi^2|\xi| \left(1 - \operatorname{erf}\left(\frac{1-i}{\sqrt{2}}\pi|\xi|\right)\right).$$

The asymptotic expansion of $\operatorname{erfc}(x)$, $x \in \mathbb{R}$ is obtained from the definition after integrating by parts N times. □

Since the error function is analytic, so is $\widehat{g}$. Also, truncating the asymptotic expansion (2.39) in the first term, we have $\operatorname{erfc}(x) = \pi^{-1/2} e^{-x^2}\left(x^{-1} + O(x^{-3})\right)$, so

we get

$$\widehat{g}(\xi) = -\sqrt{2\pi}\,(1+i)\,e^{i\pi^2\xi^2} + 2\pi^2\,|\xi|\,\frac{e^{i\pi^2\xi^2}}{\sqrt{\pi}}\left(\frac{1+i}{\sqrt{2}}\frac{1}{\pi\,|\xi|} + O(|\xi|^{-3})\right) = O(|\xi|^{-2}), \tag{2.40}$$

when $|\xi| > 1$. Thus, the conditions required to use the Poisson summation formula in (2.38) are satisfied. Given that $\widehat{g}(0) = \int_{\mathbb{R}} g(x)\,dx = -\sqrt{2\pi}\,(1+i)$ on the one hand, and that g being even implies that $\widehat{g}$ is even as well on the other hand, (2.38) can be rewritten as

$$\phi(h) = \frac{1+i}{\sqrt{2\pi}}\,\sqrt{h} - \frac{\sqrt{h}}{\pi}\sum_{k=1}^{\infty}\left(\frac{\pi k}{\sqrt{h}}\,\operatorname{erfc}\left(\frac{1-i}{2\sqrt{2}}\,\frac{k}{\sqrt{h}}\right) - \sqrt{2\pi}\,(1+i)\,e^{ik^2/(4h)}\right).$$

Replace now the asymptotic expression for the complementary error function (2.39) so that for each $k \in \mathbb{N}$, and for every $N \in \mathbb{N}$,

$$\begin{aligned}\frac{\pi k}{\sqrt{h}}\,\operatorname{erfc}\left(\frac{1-i}{2\sqrt{2}}\,\frac{k}{\sqrt{h}}\right) - \sqrt{2\pi}\,e^{ik^2/(4h)}\,(1+i)& \\ = \sqrt{\pi}\frac{1+i}{\sqrt{2}}e^{\frac{ik^2}{4h}}\sum_{n=1}^{N}\frac{(2n-1)!!\,2^{n+1}\,h^n}{i^n\,k^{2n}} + O\left(\frac{\sqrt{h}}{k}\right)^{2N+2}&.\end{aligned}$$

Hence, summing in $k \in \mathbb{N}$ and changing the order of summation, for every $N \in \mathbb{N}$ we get

$$\phi(h) = \frac{1+i}{\sqrt{2\pi}}\,\sqrt{h} - \frac{1-i}{\sqrt{2\pi}}\sum_{n=1}^{N}\frac{2^{n+1}\,(2n-1)!!}{i^{n-1}}\left(\sum_{k=1}^{\infty}\frac{e^{ik^2/(4h)}}{k^{2n}}\right)h^{n+\frac{1}{2}} + O\left(h^{N+\frac{3}{2}}\right). \tag{2.41}$$

This expression accurately describes the asymptotic behaviour of ϕ around 0.

For negative values $h < 0$, uncertainty might come when taking $\sqrt{h}$. However, the asymptotic expression (2.41) can easily be shown to be correct also in this case using the natural symmetry

$$\phi(-h) = \overline{\phi(h)}.$$

Indeed, writing $h = -|h| < 0$, conjugation of (2.41) implies

$$\phi(-|h|) = \frac{1-i}{\sqrt{2\pi}}\,\sqrt{|h|} - \frac{1+i}{\sqrt{2\pi}}\sum_{n=1}^{N}2^{n+1}\,i^{n-1}\,(2n-1)!!\left(\sum_{k=1}^{\infty}\frac{e^{\frac{-ik^2}{4|h|}}}{k^{2n}}\right)|h|^{n+\frac{1}{2}} + O\left(h^{N+\frac{3}{2}}\right),$$

while direct substitution in (2.41) leads to

$$\phi(-|h|) = \frac{1+i}{\sqrt{2\pi}}\,\sqrt{-|h|} - \frac{1-i}{\sqrt{2\pi}}\sum_{n=1}^{N}\frac{2^{n+1}\,(2n-1)!!}{i^{n-1}}\left(\sum_{k=1}^{\infty}\frac{e^{\frac{ik^2}{-4|h|}}}{k^{2n}}\right)(-|h|)^{n+\frac{1}{2}} + O\left(h^{N+\frac{3}{2}}\right).$$

These two expressions coincide if $\sqrt{-1} = -i$. Therefore, the asymptotic expression (2.41) works also for $h < 0$ if the branch of the complex square root is chosen so that

$\sqrt{-1} = -i$.

In short, we have been able to prove the asymptotic behaviour of ϕ around zero, an asymptotic expansion for $\phi(h)$ when $|h|$ is small enough. We gather this result in the following proposition.

Proposition 2.7. *Let*

$$Y_n(h) = \sum_{k=1}^{\infty} \frac{e^{ik^2/(4h)}}{k^{2n}}, \qquad n \in \mathbb{N}, \tag{2.42}$$

and $N \in \mathbb{N}$. Then,

$$\phi(h) = \frac{1+i}{\sqrt{2\pi}}\sqrt{h} - \frac{1-i}{\sqrt{2\pi}} \sum_{n=1}^{N} \frac{2^{n+1}\,(2n-1)!!}{i^{n-1}}\, Y_n(h)\, h^{n+\frac{1}{2}} + O\left(h^{N+\frac{3}{2}}\right) \tag{2.43}$$

for every $h \in \mathbb{R}$, where $\sqrt{-1} = -i$ if $h < 0$. In particular, when $N = 1$,

$$\phi(h) = \frac{1+i}{\sqrt{2\pi}}\sqrt{h} - 4\frac{1-i}{\sqrt{2\pi}}\, Y_1(h)\, h^{3/2} + O\left(h^{5/2}\right). \tag{2.44}$$

The above, together with (2.47), allows to deduce a self-similar expression for ϕ with an error term of lower order,

$$\phi(h) = \frac{3}{2}\frac{1+i}{\sqrt{2\pi}}\sqrt{h} - 4\pi^2\frac{1-i}{\sqrt{2\pi}}\left[\frac{1}{6} - 2\phi\left(\frac{-1}{16\pi^2 h}\right)\right] h^{3/2} + O\left(h^{5/2}\right). \tag{2.45}$$

Expressions (2.43) and (2.44) come directly from (2.41), but let us explain the third expression (2.45), which is probably the most significant one. For that, let us comment on some properties of Y_n defined in (2.42).

For every $n \in \mathbb{N}$, it is easy to see that all $Y_n(1/\cdot)$ is 8π-periodic, and that both Y_n and $Y_n(1/\cdot)$ follow a circular pattern, since

$$Y_n(h) = e^{i/(4h)} + O\left(\sum_{k=2}^{\infty}\frac{1}{k^{2n}}\right) \in B\left(e^{i/(4h)}, \frac{\pi^2}{6} - 1\right) \subset A\left(2 - \frac{\pi^2}{6}, \frac{\pi^2}{6}\right), \tag{2.46}$$

where $B(x,r)$ denotes the ball with center x and radius r and $A(r_1,r_2)$ is the annulus centred in the origin and of radii $r_1 < r_2$. As a consequence, $Y_n(1/\cdot)$ does not have a limit when $h \to 0$. But more interestingly, the function Y_1 is the cause of the selfsimilarity of ϕ that we already noticed when looking at Figure 2.1. This self-similarity is even more evident in Figure 2.2, where $\phi(\mathbb{R})$ has been zoomed around the origin. This is happening because $Y_1(1/\cdot)$ is similar to Riemann's function in the sense that it is an infinite sum of quadratic phases with quadratic amplitudes, with the particularity that the variable is inverted. We can be more precise about this, since combining the definition (2.42) with the definition of ϕ_D (1.4) and then with (1.11) to translate it to ϕ, we see that

$$Y_1(h) = \frac{\pi^2}{6} - \frac{i}{8h} - 2\pi^2\,\phi\left(\frac{-1}{16\pi^2 h}\right). \tag{2.47}$$

Substituting this into (2.44) leads to the self-similar asymptotic (2.45).

When $h \to 0$, the variable of the self-similar term $\phi(-1/(16\pi^2 h))$ tends to infinity, so by the periodic property (2.2) of ϕ infinitely many copies of $\phi([0, 1/(2\pi)])$ are being produced. However, these copies are generated at the level of the lower order term

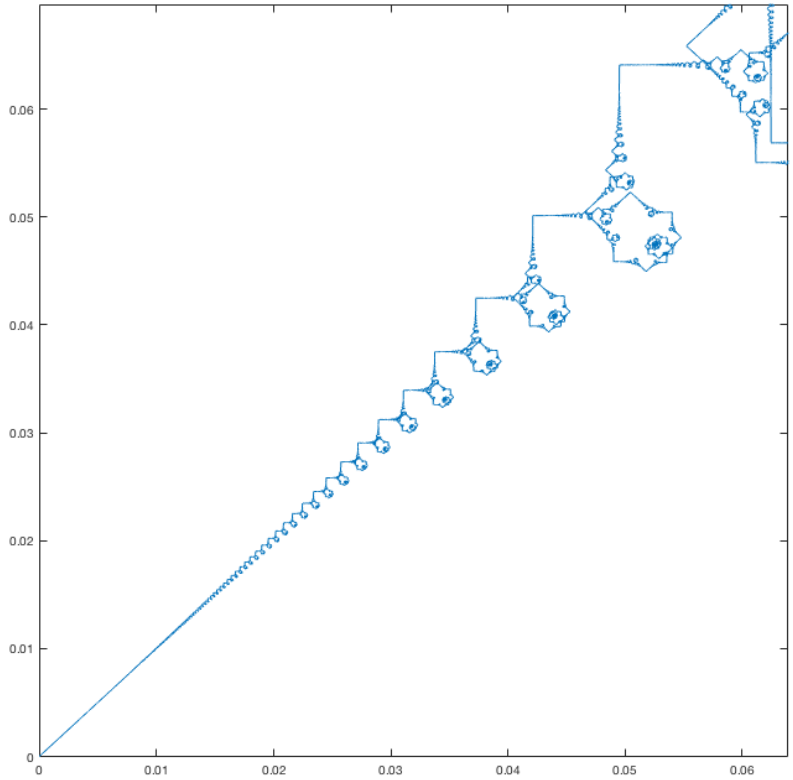

FIGURE 2.2: Zoom of $\phi([0, 1/(2\pi)])$ around $\phi(0) = 0$.

$h^{3/2}$, so when $h \to 0$ they are negligible with respect to the leading $\sqrt{h}$ term. That is why in Figure 2.2 we see that the more the function approaches the origin $\phi(0) = 0$, the more it resembles a straight line in the direction determined by the coefficient $(1+i)/\sqrt{2} = e^{i\pi/4}$. However, when h is a bit larger so that the $h^{3/2}$ term ceases to be negligible, but still small enough so that the lower order term $O(h^{5/2})$ is comparatively small, the effect of the self-similar term is noticeable: one can see those copies , which get smaller and smaller until at some point they are too small to be noticed with the eye.

2.2.5 Asymptotic behaviour around $t_{1,2}$

To compute the asymptotic behaviour of ϕ around $t_{1,2}$, one may follow the procedure of Section 2.2.4, first writing

$$\phi(t_{1,2} + h) - \phi(t_{1,2}) = -h \sum_{k\in\mathbb{Z}} (-1)^k \, g(2\pi k\sqrt{h}).$$

The situation is a bit more technical now, but the Poisson summation formula can still be used combined with distribution theory. Writing $(-1)^x = e^{-i\pi x}$ and taking into account that $\mathcal{F}(e^{-i\pi(\cdot)}) = \delta_{-1/2}$, we get

$$\mathcal{F}_x\left(e^{-i\pi x} g(2\pi x\sqrt{h})\right)(\xi) = \frac{1}{2\pi\sqrt{h}}\left[\delta_{-1/2} * \widehat{g}\left(\frac{\cdot}{2\pi\sqrt{h}}\right)\right](\xi) = \frac{1}{2\pi\sqrt{h}}\,\widehat{g}\left(\frac{1-2\xi}{4\pi\sqrt{h}}\right).$$

Therefore, since $\widehat{g}$ is even, we get

$$\phi(t_{1,2}+h)-\phi(t_{1,2})=-\frac{\sqrt{h}}{2\pi}\sum_{k\in\mathbb{Z}}\widehat{g}\left(\frac{2k-1}{4\pi\sqrt{h}}\right).$$

In this sum, $\widehat{g}$ is never evaluated in 0, so the bound (2.40) can be used to get

$$|\phi(t_{1,2}+h)-\phi(t_{1,2})|\le C_1\sqrt{h}\sum_{k\in\mathbb{Z}}\frac{h}{(2k-1)^2}=C_2\,h^{3/2} \tag{2.48}$$

for $h<1$, where $C_1,C_2>0$. This is enough to conclude that ϕ is differentiable in $t_{1,2}$ with $\phi'(t_{1,2})=0$, also that $\phi\in C^{3/2}(t_{1,2})$. This result is equivalent to $\phi'_D(1)=-1/2$, proved by Duistermaat [29] and representative of Gerver's original result [42] concerning the existence of the derivative of the original Riemann's function at certain rational points. The different values are, of course, a consequence of (1.11). Using the expression for $\widehat{g}$ that we got in Lemma 2.5 and the asymptotic expansion of the error function in (2.39), we would be able to get an asymptotic expansion for $\phi(t_{1,2}+h)-\phi(t_{1,2})$. However, there is a simpler way to proceed, taking advantage of the computations we did for $\phi(h)$.

First, it is not difficult to prove that

$$\phi(h+t_{1,2})=\frac{1}{8}+\frac{i}{4\pi}+\frac{\phi(4h)}{2}-\phi(h). \tag{2.49}$$

This can be done by splitting the sum into the even and odd indices. Maybe more easily, one can first prove $\phi_D(h+1)=\phi_D(4h)/2-\phi_D(h)$ by splitting the corresponding sum into the even and odd indices, and then translate the identity to ϕ using (1.11). For completeness, we sketch the splitting of the sum for ϕ_D,

$$\begin{aligned}\phi_D(h+1)&=\sum_{n=1}^{\infty}\frac{e^{i\pi n^2(h+1)}}{i\pi n^2}=\sum_{n=1}^{\infty}(-1)^{n^2}\frac{e^{i\pi n^2h}}{i\pi n^2}=\sum_{\substack{n=1\\ n\text{ even}}}^{\infty}\frac{e^{i\pi n^2h}}{i\pi n^2}-\sum_{\substack{n=1\\ n\text{ odd}}}^{\infty}\frac{e^{i\pi n^2h}}{i\pi n^2}\\ &=2\sum_{\substack{n=1\\ n\text{ even}}}^{\infty}\frac{e^{i\pi n^2h}}{i\pi n^2}-\phi_D(h)=2\sum_{n=1}^{\infty}\frac{e^{i\pi 4n^2h}}{i\pi 4n^2}-\phi_D(h)\\ &=\frac{1}{2}\phi_D(4h)-\phi_D(h),\end{aligned}$$

where the key element is that $(-1)^{n^2}=1$ when n is even and $(-1)^{n^2}=-1$ when n is odd. In any case, evaluating (2.49) at $h=0$ we get

$$\phi(t_{1,2})=\frac{1}{8}+\frac{i}{4\pi}, \tag{2.50}$$

which implies that (2.49) can be rewritten as

$$\phi(t_{1,2}+h)-\phi(t_{1,2})=\frac{\phi(4h)}{2}-\phi(h).$$

It is now evident that we can use the asymptotic behaviour of ϕ around 0 that we proved in Proposition 2.7. The main, most evident feature is that, according to (2.43),

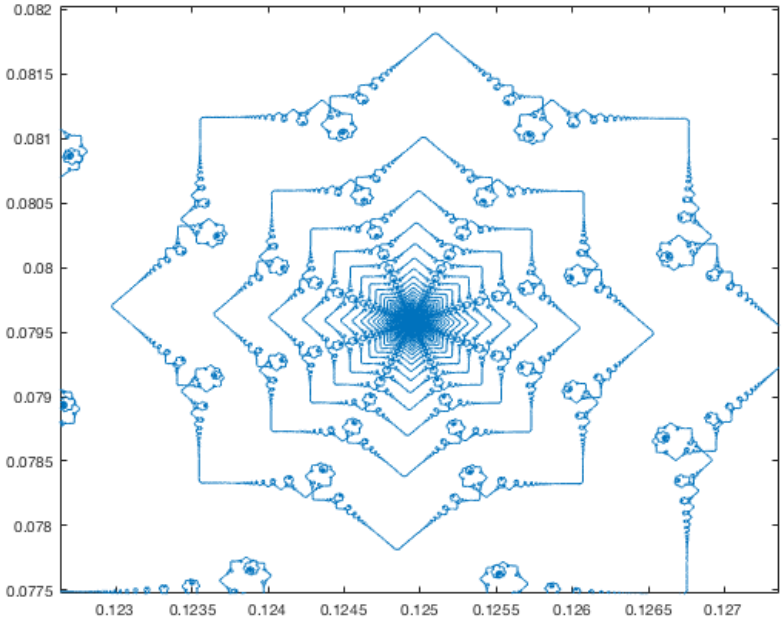

FIGURE 2.3: Zoom of $\phi([0, 1/(2\pi)]$ around $\phi(t_{1,2})$.

what should be the principal term of the new asymptotic is

$$\frac{1+i}{\sqrt{2\pi}}\left(\frac{\sqrt{4h}}{2}-\sqrt{h}\right)=0$$

and vanishes, so that the principal order is really $O(h^{3/2})$, hence the differentiability and the bound we got in (2.48). In the higher order terms, the subtraction generates

$$4^n\,Y_n(4h)-Y_n(h)=4^n\sum_{\substack{k=1\\ k\text{ odd}}}^{\infty}\frac{e^{ik^2/(16h)}}{k^{2n}},$$

so define

$$Z_n(h)=\sum_{\substack{k=1\\ k\text{ odd}}}^{\infty}\frac{e^{ik^2/(16h)}}{k^{2n}},$$

which are analogous to Y_n and satisfy similar properties, such as periodicity and the circular pattern. As a consequence of all this, the asymptotic behaviour around $t_{1,2}$ can be written as follows.

Proposition 2.8. *Let $N\in\mathbb{N}$. Then,*

$$\phi(t_{1,2}+h)-\phi(t_{1,2})=-\frac{1-i}{\sqrt{2\pi}}\sum_{n=1}^{N}\frac{2^{3n+1}\,(2n-1)!!}{i^{n-1}}\,Z_n(h)\,h^{n+\frac{1}{2}}+O\left(h^{N+\frac{3}{2}}\right)$$

for every $h\in\mathbb{R}$, where $\sqrt{-1}=-i$ when $h<0$. In particular, when $N=1$,

$$\phi(t_{1,2}+h)-\phi(t_{1,2})=-16\,\frac{1-i}{\sqrt{2}}\,Z_1(h)\,h^{3/2}+O\left(h^{5/2}\right). \tag{2.51}$$

Figure 2.3 shows a zoom of Riemann's function around $\phi(t_{1,2})$, a situation that is

very well described by this proposition. Indeed, as we said, Z_1 is of the same kind as Y_1, and therefore satisfies properties very similar to (2.46). That means that $Z_1(h)$ turns around the origin in a circular pattern, and the more h approaches to zero, the faster it does it. Since in (2.51) this is multiplied by the leading order term $h^{3/2}$, which tends to zero when $h \to 0$, this circular pattern turns into a spiral that concentrates in $\phi(t_{1,2})$.

Remark 2.9. Identities similar to (2.49) can be obtained for other rationals using the same trick of splitting the sum. For instance, one can prove

$$\phi(h + t_{1,4}) = \frac{1}{16} + \frac{i}{8}\left(\frac{1}{\pi} + \frac{1}{2}\right) + \frac{1+i}{4}\,\phi(4h) - i\phi(h),$$

and hence

$$\phi(t_{1,4}) = \frac{1}{16} + \frac{i}{8}\left(\frac{1}{\pi} + \frac{1}{2}\right), \qquad \phi(t_{1,4} + h) - \phi(t_{1,4}) = \frac{1+i}{4}\,\phi(4h) - i\phi(h).$$

The complete asymptotic expansion around $\phi(t_{1,4})$ can thus be computed using that of $\phi(h)$ in the same way as above. As a curiosity, from (2.50) one can deduce

$$\frac{1}{8} = \sum_{k\in\mathbb{Z}\setminus\{0\}} \frac{e^{-i\pi k^2} - 1}{k^2} \quad \Longrightarrow \quad \sum_{n=1}^{\infty} \frac{(-1)^n}{n^2} = -\frac{\pi^2}{12},$$

and from the value of $\phi(t_{1,4})$ above, one can similarly prove

$$\sum_{k=1}^{\infty} \frac{i^{k^2}}{k^2} = \frac{\pi^2}{24}(1 + 3i).$$

Analogous computations can be done for $t_{1,3}$, $t_{1,6}$ and $t_{1,8}$, for which an explicit complete asymptotic expansion could be obtained if needed and which, in a similar way as above, yield the sums

$$\sum_{n=1}^{\infty} \frac{(e^{2\pi i/3})^{n^2}}{n^2} = \frac{\pi^2}{9}\left(-\frac{1}{2} + \frac{2\sqrt{3}}{3}i\right), \quad \sum_{n=1}^{\infty} \frac{(e^{\pi i/3})^{n^2}}{n^2} = \frac{\pi^2}{108}\left(3 + 4\sqrt{3}i\right),$$

$$\sum_{n=1}^{\infty} \frac{(e^{\pi i/4})^{n^2}}{n^2} = \frac{\pi^2}{16}\left(-\frac{3\sqrt{2}-1}{3} + \sqrt{2}i\right).$$

2.2.6 Asymptotic behaviour around $t_{p,q}$ such that q ≡ 0, 1, 3 (mod 4)

Once the asymptotic behaviour has been established around 0 and $t_{1,2}$, let us face the case of a general rational $t_{p,q}$. For that, we make the reduction process explained in Subsection 2.2.3.3 rigorous.

First of all, the identity (2.13), in which the reduction is based, can be given a precise sense in the form of

$$\phi(t) = i \lim_{\epsilon\to 0} \int_0^t \theta(-4\pi\tau + i\epsilon)\, d\tau.$$

This identity can be checked by using Fubini's theorem first and the dominated convergence theorem afterwards. Consequently, the asymptotic behaviour of ϕ around

$t_{p,q}$ can be written as

$$\phi\left(t_{p,q}+h\right)-\phi(t_{p,q})=\frac{i}{4\pi}\lim_{\epsilon\to 0^+}\int_{\tilde{p}/\tilde{q}}^{\tilde{p}/\tilde{q}+4\pi h}\theta(-\tau+i\epsilon)\,d\tau. \tag{2.52}$$

as was already suggested in (2.36).

Let p/q be an irreducible fraction such that $q\equiv 0,1,3 \pmod 4$. Remember that in this case, the irreducible fraction $\tilde{p}/\tilde{q}=2p/q$ is such that $\tilde{p}$ and $\tilde{q}$ are not both odd and that there exists $\gamma\in\Gamma_\theta$ satisfying $\gamma(\tilde{p}/\tilde{q})=0$. The idea is to use the transformation law for the Jacobi θ function (2.12) so that, after conjugating, (2.52) can be rewritten as

$$\overline{\phi(t_{p,q}+h)-\phi(t_{p,q})}=\frac{1}{4\pi i e_\gamma}\lim_{\epsilon\to 0}\int_{\tilde{p}/\tilde{q}}^{\tilde{p}/\tilde{q}+4\pi h}\frac{\theta(\gamma(\tau+i\epsilon))}{\sqrt{c(\tau+i\epsilon)+d}}\,d\tau. \tag{2.53}$$

Observing that $\phi'(z)=i\theta(-4\pi z)$ whenever $\operatorname{Im} z>0$, integrate by parts choosing

$$\begin{aligned} u&=\tfrac{1}{\gamma'(\tau+i\epsilon)\sqrt{c(\tau+i\epsilon)+d}}=(c(\tau+i\epsilon)+d)^{3/2}, & du&=\tfrac{3c}{2}\sqrt{c(\tau+i\epsilon)+d}\,d\tau,\\ dv&=\theta(\gamma(\tau+i\epsilon))\,\gamma'(\tau+i\epsilon)\,d\tau, & v&=4\pi i\,\phi\left(-\tfrac{\gamma(\tau+i\epsilon)}{4\pi}\right), \end{aligned}$$

which yields

$$\frac{1}{e_\gamma}\lim_{\epsilon\to 0}\left[\phi\left(-\frac{\gamma(\tau+i\epsilon)}{4\pi}\right)(c(\tau+i\epsilon)+d)^{3/2}\Big|_{\tilde{p}/\tilde{q}}^{\tilde{p}/\tilde{q}+4\pi h}-\frac{3c}{2}\int_{\tilde{p}/\tilde{q}}^{\tilde{p}/\tilde{q}+4\pi h}\phi\left(-\frac{\gamma(\tau+i\epsilon)}{4\pi}\right)\sqrt{c(\tau+i\epsilon)+d}\,d\tau\right].$$

We have passed from managing θ to ϕ, which is already well-defined on the real line. We can now take the limit $\epsilon\to 0$ clearly in the first term. On the other hand, due to the finiteness of the integrating interval, all the terms inside the integral can be shown to be bounded independently of ϵ, so the limit can be taken inside by the theorem of dominated convergence to get

$$\begin{aligned}&\phi(t_{p,q}+h)-\phi(t_{p,q})\\ &\quad=e_\gamma\left[\phi\left(\frac{\gamma(\tau)}{4\pi}\right)(c\tau+d)^{3/2}\Big|_{\frac{\tilde{p}}{\tilde{q}}}^{\frac{\tilde{p}}{\tilde{q}}+4\pi h}-\frac{3c}{2}\int_{\frac{\tilde{p}}{\tilde{q}}}^{\frac{\tilde{p}}{\tilde{q}}+4\pi h}\phi\left(\frac{\gamma(\tau)}{4\pi}\right)\sqrt{c\tau+d}\,d\tau\right].\end{aligned} \tag{2.54}$$

Remark 2.10. We remark here that identity (2.54) is valid for every $\gamma\in\Gamma_\theta$, since we still have not used any particular property of the transformation that $\gamma(\tilde{p}/\tilde{q})=0$.

Coming back to $\gamma\in\Gamma_\theta$ such that $\gamma(\tilde{p}/\tilde{q})=0$, according to (2.32) and the definition of the function $b(h)$ in (2.33), and recalling that the coefficients satisfy $ad-bc=1$ and that, in this case, $a=\tilde{q}$, $b=-\tilde{p}$ and $c=c_\pm$, the first boundary term is

$$\begin{aligned}\phi\left(-\frac{\gamma(\tilde{p}/\tilde{q}+4\pi h)}{4\pi}\right)\left(c_\pm(\tilde{p}/\tilde{q}+4\pi h)+d\right)^{3/2}&=\phi(-b(h))\,\frac{(1+4\pi c_\pm\tilde{q}h)^{3/2}}{\tilde{q}^{3/2}}\\ &=\frac{\phi(-b(h))}{(\tilde{q}-4\pi c_\pm b(h))^{3/2}}\end{aligned}$$

The second boundary term corresponds to evaluating the first one in $h = 0$. Of course, it is null because $\gamma(\tilde{p}/\tilde{q}) = 0$. Hence,

$$\phi(t_{p,q}+h) - \phi(t_{p,q}) = e_\gamma \left[\frac{(1+4\pi c_\pm \tilde{q} h)^{\frac{3}{2}}}{\tilde{q}^{3/2}} \, \phi\left(b(h)\right) \right. \\ \left. - \frac{3}{2} c_\pm \int_{\frac{\tilde{p}}{\tilde{q}}}^{\frac{\tilde{p}}{\tilde{q}}+4\pi h} \phi\left(\frac{\gamma(\tau)}{4\pi}\right) \sqrt{c_\pm \tau + d} \, d\tau \right]$$

Next step consists in changing variables $\gamma(\tau) = r$ in the integral, in a similar way as in (2.31), so that we get

$$\phi(t_{p,q}+h) - \phi(t_{p,q}) = e_\gamma \left[\frac{\phi\left(b(h)\right)}{\left(\tilde{q} - 4\pi c_\pm b(h)\right)^{3/2}} - 6\pi c_\pm \int_0^{b(h)} \frac{\phi(r)}{(\tilde{q} - 4\pi c_\pm r)^{5/2}} \, dr \right]. \tag{2.55}$$

We already see the possibility of using the asymptotic behaviour around 0 in the $\phi(b(h))$ and $\phi(r)$ inside the integral, since $b(h)$ behaves like $\tilde{q}^2 h$ when h is small. For the following lines, call $b = b(h)$ for simplicity and develop $\phi(b)$ following Proposition 2.7. Use also the Taylor series

$$(1-x)^{-\alpha} = \sum_{n=0}^{\infty} \binom{n+\alpha-1}{n} x^n, \qquad |x| < 1 \tag{2.56}$$

to develop $(\tilde{q} - 4\pi c_\pm b)^{-3/2}$ and $(\tilde{q} - 4\pi c_\pm r)^{-5/2}$.

Remark 2.11. This Taylor expansion can be used now because $4\pi c_\pm b/\tilde{q} < 1$ for all $h \in \mathbb{R}$ and also $4\pi c_\pm r/\tilde{q} \leq 1$ for every $0 < r < b$. However, the result will eventually not be valid for all $h \in \mathbb{R}$ because $\lim_{h\to\infty} 4\pi c_\pm b(h)/\tilde{q} = 1$. Indeed, requiring $4\pi c_\pm b(h)/\tilde{q} < \delta$ for some fixed $0 < \delta < 1$ means that $h < (\frac{\delta}{4\pi \frac{c}{\tilde{q}}(1-\delta)})/\tilde{q}^2$. Consequently, the final asymptotic expansion we get will be valid in any bounded set of the form $|h| < M/\tilde{q}^2$, for any fixed $M > 0$. This is not important if q is fixed, but it will be vital when we work with tangents around irrationals in Subsection 4.6, because the approximations we will use there will be rationals p_n/q_n with varying q_n and everything that depends on q will need to be taken into account.

In any case,

$$\phi(t_{p,q}+h) - \phi(t_{p,q}) = \frac{e_\gamma}{\tilde{q}^{3/2}} \left[\frac{1+i}{\sqrt{2\pi}} \, b^{\frac{1}{2}} + \left(2\pi \, \frac{1+i}{\sqrt{2\pi}} \, \frac{c_\pm}{\tilde{q}} - 4 \, \frac{1-i}{\sqrt{2\pi}} \, Y_1(b) \right) b^{\frac{3}{2}} \right. \\ \left. + O\left(b^{\frac{5}{2}}\right) \right]. \tag{2.57}$$

Using (2.56) again, expand $b^{1/2}$ and $b^{3/2}$ to obtain

$$\begin{aligned} b(h)^{1/2} &= \tilde{q}\, h^{1/2} \left(1 - 2\pi \, c_\pm \tilde{q} h + O\left(c_\pm^2 \, \tilde{q}^2 \, h^2\right)\right), \\ b(h)^{3/2} &= \tilde{q}^3 \, h^{3/2} \left(1 + O\left(\tilde{q} \, c_\pm h\right)\right), \\ b(h)^{5/2} &= O\left(\tilde{q}^5 h^{5/2}\right). \end{aligned} \tag{2.58}$$

These expansions are only valid when $4\pi|c_\pm \tilde{q} h| < 1$. We use them to expand (2.57) in terms of h and obtain

$$\phi(t_{p,q}+h)-\phi(t_{p,q}) = e_\gamma \left(\frac{1+i}{\sqrt{2\pi}} \frac{h^{1/2}}{\tilde{q}^{1/2}} - 4\,\frac{1-i}{\sqrt{2\pi}}\, Y_1(b(h))\, \tilde{q}^{3/2}\, t^{3/2} + O\left(\tilde{q}^{\frac{7}{2}}\, h^{\frac{5}{2}}\right)\right),$$

the asymptotic behaviour of ϕ around $t_{p,q}$ which, according to the restrictions from the Taylor expansions, is valid for $\tilde{q}^2\, h < 1/(4\pi \frac{c_+}{\tilde{q}})$ when $h > 0$ and for $\tilde{q}^2\, |h| < 1/(4\pi \frac{|c_-|}{\tilde{q}})$ when $h < 0$. We have therefore proved the following proposition.

Proposition 2.12. *Let $p, q \in \mathbb{N}$ such that $q \equiv 0, 1, 3\ (mod\ 4)$, $p < q$ and $\gcd(p,q) = 1$. Define $\tilde{p}$ and $\tilde{q}$ so that $\tilde{p}/\tilde{q} = 2p/q$ is an irreducible fraction, and set*

$$Y_1(h) = \sum_{k=1}^{\infty} \frac{e^{ik^2/(4h)}}{k^2} \qquad \text{and} \qquad b(h) = \begin{cases} \frac{\tilde{q}^2 h}{1+4\pi c_+ \tilde{q} h}, & \text{when } h \geq 0, \\ \frac{\tilde{q}^2 h}{1+4\pi c_- \tilde{q} h}, & \text{when } h < 0, \end{cases}$$

where $\tilde{q} \leq c_+, |c_-| \leq 4\tilde{q}$ as in Subsection 2.2.3. Then, there exists a complex eighth root of unity $e_{p,q}$ depending only on p and q such that

$$\phi(t_{p,q}+h)-\phi(t_{p,q}) = \frac{e_{p,q}}{\sqrt{\pi}} \frac{1+i}{\sqrt{2}} \left(\frac{h^{1/2}}{\tilde{q}^{1/2}} + 4\, i\, Y_1(b(h))\, \tilde{q}^{3/2}\, h^{3/2} + O\left(\tilde{q}^{7/2}\, h^{5/2}\right)\right), \quad \text{when } |h| \leq \frac{1}{4\pi \frac{|c_\pm|}{\tilde{q}}} \frac{1}{\tilde{q}^2}, \tag{2.59}$$

where $c_\pm = c_+$ when $h > 0$ and $c_\pm = c_-$ when $h < 0$. Also, $\sqrt{-1} = -i$ when $h < 0$. The corresponding the self-similar form is

$$\begin{aligned} &\phi(t_{p,q}+h)-\phi(t_{p,q}) \\ &\quad = \frac{3}{2} \frac{e_{p,q}}{\sqrt{\pi}} \frac{1+i}{\sqrt{2}} \left(\frac{h^{1/2}}{\tilde{q}^{1/2}} + \frac{8\pi^2}{3} i \left(\frac{1}{6} - \frac{i}{2\pi} \frac{c_\pm}{\tilde{q}} - 2\phi\left(\frac{-1}{16\pi^2 b(h)}\right)\right) \tilde{q}^{\frac{3}{2}}\, h^{\frac{3}{2}} \right. \\ &\qquad \left. + O\left(\tilde{q}^{\frac{7}{2}}\, h^{\frac{5}{2}}\right)\right) \end{aligned} \tag{2.60}$$

for the same values $|h| \leq 1/(4\pi \frac{|c_\pm|}{\tilde{q}} \tilde{q}^2)$ as above. Also equivalently, rescaling the variable in the two previous expressions, a third form of the asymptotic is

$$\begin{aligned} &\phi\left(t_{p,q} + \frac{h}{\tilde{q}^2}\right) - \phi(t_{p,q}) \\ &\quad = \frac{1}{\sqrt{\pi}} \frac{1+i}{\sqrt{2}} \frac{e_{p,q}}{\tilde{q}^{3/2}} \left(h^{1/2} + 4\, i\, Y_1(\beta(h))\, h^{3/2} + O\left(h^{5/2}\right)\right) \\ &\quad = \frac{3}{2\sqrt{\pi}} \frac{1+i}{\sqrt{2}} \frac{e_{p,q}}{\tilde{q}^{3/2}} \left(h^{\frac{1}{2}} + \frac{8\pi^2}{3} i \left(\frac{1}{6} - \frac{i}{2\pi} \frac{c_\pm}{\tilde{q}} - 2\phi\left(\frac{-1}{16\pi^2 \beta(h)}\right)\right) h^{\frac{3}{2}} \right. \\ &\qquad \left. + O\left(h^{\frac{5}{2}}\right)\right) \end{aligned} \tag{2.61}$$

for all $|h| \leq 1/(4\pi\frac{|c_\pm|}{\tilde{q}})$*, where* $\beta(h) = b(h/\tilde{q}^2)$.

Remark 2.13. Even if enough for our purposes in Chapters 3 and 4, the condition $|h| \leq 1/(4\pi\frac{|c_\pm|}{\tilde{q}}\tilde{q}^2)$ seems very artificial. Something more reasonable would be a condition of the kind

$$|h| \leq \frac{M}{q^2}, \qquad \text{for any fixed } M > 0, \tag{2.62}$$

as in Remark 2.11 when we analysed the first Taylor expansion we used. This is also what we could expect from the heuristic computations in Subsection 2.2.2, where we predicted that $\phi(t_{p,q} + h) - \phi(t_{p,q}) \simeq \phi(q^2 h)$. For if the asymptotic around 0 can be truncated when $h < M$ whenever $M > 0$ is fixed, then it is expectable that the asymptotic around $t_{p,q}$ can be truncated when $q^2 h < M$ whenever $M > 0$ is fixed. Indeed, this condition we get is a consequence of our proof and not a real range for the asymptotics, which can be proved to be valid in any interval like (2.62). The problem is that our proof lies in several Taylor expansions, among which most problematic are (2.58), which are not valid when h is over the condition. However, when plugging these expansions in (2.57), the higher order terms seem to simplify. For instance, the second term from $b^{1/2}$ cancels with one of the first terms of $b^{3/2}$. It is expectable that this happens in successive powers of b, but it is not within our grasp.

But then, how to prove that we can really extend the range of validity? This is a very good point to see the actual difference between our approach and Duistermaat's, since it is his which gives the whole range. As we said, everything is essentially the same until (2.54), a point where the intuitive path we took heuristically in Subsection 2.2.3, even if most intuitive, is not the most effective one. There, instead of using the transformation γ that sends $\tilde{p}/\tilde{q}$ to zero, he used $S\gamma \in \Gamma_\theta$, where we recall that $S(z) = -1/z$. Indeed,

$$\gamma(x) = \frac{\tilde{q}x - \tilde{p}}{cx + d} \qquad \Longrightarrow \qquad S\gamma(x) = -\frac{cx + d}{\tilde{q}x - \tilde{p}},$$

which, as we said in the preliminaries, has its pole in $\tilde{p}/\tilde{q}$. Hence using (2.54) with $S\gamma$ we get

$$\begin{aligned}
&\phi(t_{p,q} + h) - \phi(t_{p,q}) \\
&\quad = e_\gamma \left[\phi\left(\frac{-1}{4\pi\gamma(\frac{\tilde{p}}{\tilde{q}} + 4\pi h)} \right) (4\pi\tilde{q}h)^{\frac{3}{2}} - \frac{3c}{2} \int_{\frac{\tilde{p}}{\tilde{q}}}^{\frac{\tilde{p}}{\tilde{q}}+4\pi h} \phi\left(\frac{S\gamma(\tau)}{4\pi} \right) \sqrt{\tilde{q}\tau + \tilde{p}}\, d\tau \right] \\
&\quad = e_\gamma \left[\phi\left(\frac{-1}{16\pi^2 b(h)} \right) (4\pi\tilde{q}h)^{\frac{3}{2}} - \frac{3c}{2} \int_{\frac{\tilde{p}}{\tilde{q}}}^{\frac{\tilde{p}}{\tilde{q}}+4\pi h} \phi\left(\frac{S\gamma(\tau)}{4\pi} \right) \sqrt{\tilde{q}\tau + \tilde{p}}\, d\tau \right],
\end{aligned}$$

directly obtaining powers of h. The first term is precisely that appearing in (2.60). The main term of order $h^{1/2}$ is hidden inside the integral, because writing $\phi(t)$ in relationship with ϕ_D as in (1.11), it comes from integrating the linear term $S\gamma(\tau)\sqrt{\tilde{q}\tau - \tilde{p}} = \frac{cx+d}{\sqrt{\tilde{q}\tau - \tilde{p}}}$. This way one gets exactly the self-similar asymptotic (2.60) without any restriction for the variable h, and moreover, the error term is explicitly given by

$$\frac{\tilde{q}}{2\sqrt{\pi}} \int_{\tilde{p}/\tilde{q}}^{\tilde{p}/\tilde{q}+4\pi h} \phi_D(-\gamma(r))\sqrt{\tilde{q}r - \tilde{p}}\, dr.$$

Once we clarified the details about the range of validity, let us comment on the very rich asymptotic expansion itself. As in the behaviour around 0 in (2.45), the

second form (2.60) describes the self-similar behaviour of ϕ by means of the term

$$\phi(-1/(16\pi^2 b(h))), \tag{2.63}$$

and the same reasoning about the infinitely many copies of $\phi([0,1/(2\pi)])$ applies here too (see, for instance, Figure 4.1B in Chapter 4, where a zoom around $\phi(t_{1,8})$ is shown). Also, the third expression (2.61) rigorously confirms what was anticipated in (2.34): that when $h \to 0$, the behaviour of ϕ around $t_{p,q}$ is essentially the same as the behaviour around 0 presented in Proposition 2.7, except a rescaling by $\tilde{q}^{-2}$ in the variable and $\tilde{q}^{3/2}$ in the image, and the substitution of h by $\beta(h)$ in the self-similarity generating term (2.63).

On the other hand, the leading square root term is the cause of every right-angled corner in Figure 1.5, because when $h > 0$ and $h \to 0$,

$$\begin{aligned}\phi(t_{p,q}-h)-\phi(t_{p,q}) &\sim \frac{e_{p,q}}{\sqrt{\pi}}\,\frac{1+i}{\sqrt{2}}\,\frac{h^{1/2}}{\tilde{q}^{1/2}} = -i\,\frac{e_{p,q}}{\sqrt{\pi}}\,\frac{1+i}{\sqrt{2}}\,\frac{|h|^{1/2}}{\tilde{q}^{1/2}}\\ &\sim -i\,\left(\phi(t_{p,q}+|h|)-\phi(t_{p,q})\right),\end{aligned}$$

where i represents a rotation of 90 degrees in the complex plane. Above, $\sim$ stands for equivalent infinitesimals and $\sqrt{-1} = -i$, as was stated in the statement of Proposition 2.12 in the same way as in the asymptotic expansion around 0. As we did there, one way to determine this choice is to use symmetric properties of ϕ, except that there is no such symmetry around $\phi(t_{p,q})$ for $q > 2$. However, a similar argument yields the result if we work with the limit $h \to 0$ in the asymptotic expression of $\phi(t_{p,q}+h)-\phi(t_{p,q})$. Let us see this.

Let $|h| \ll 1$. We start with (2.55), where the leading term when $h \to 0$ is the first one. Indeed, $\lim_{h\to 0} b(h) = 0$, so by Proposition 2.7, we have

$$\frac{\phi(b(h))}{(\tilde{q}-4\pi c_{\pm} b(h))^{3/2}} \sim \frac{\frac{1+i}{\sqrt{2\pi}}\,b^{1/2}+O(b^{3/2})}{\tilde{q}^{3/2}}$$

and

$$\int_0^b \frac{\phi(r)}{(\tilde{q}-4\pi c_{\pm} r)^{5/2}}\,dr \sim \frac{1+i}{\sqrt{2\pi}}\int_0^b \frac{r^{1/2}+O(r^{3/2})}{\tilde{q}^{5/2}}\,dr = \frac{1+i}{\sqrt{2\pi}}\,\frac{b^{3/2}+O(b^{5/2})}{\tilde{q}^{5/2}}.$$

Consequently, from (2.55) we get

$$1 = \lim_{h\to 0} \frac{\phi(t_{p,q}+h)-\phi(t_{p,q})}{e_{p,q}\,\tilde{q}^{-3/2}\,\phi(b(h))}. \tag{2.64}$$

Let now $h > 0$ and define $b_-(h)$ by

$$b(-h) = -\frac{\tilde{q}^2 h}{1+4\pi c_- \tilde{q} h} = -b_-(h),$$

so that $\phi(b(-h)) = \overline{\phi(b_-(h)}$. Therefore, evaluate (2.64) in $-h$ and conjugate it so that

$$\begin{aligned}
1 &= e_{p,q} \lim_{h\to 0} \frac{\overline{\phi(t_{p,q}-h)-\phi(t_{p,q})}}{\tilde{q}^{-3/2}\,\overline{\phi(b(-h))}} = e_{p,q} \lim_{h\to 0} \frac{\overline{\phi(t_{p,q}-h)-\phi(t_{p,q})}}{\tilde{q}^{-3/2}\,\phi(b_-(h))} \\
&= e_{p,q} \lim_{h\to 0} \frac{\overline{\phi(t_{p,q}-h)-\phi(t_{p,q})}}{\tilde{q}^{-3/2}\,\phi(b(h))} \frac{\phi(b(h))}{\phi(b_-(h))} = e_{p,q} \lim_{h\to 0} \frac{\overline{\phi(t_{p,q}-h)-\phi(t_{p,q})}}{\tilde{q}^{-3/2}\,\phi(b(h))} \\
&= e_{p,q}^2 \lim_{h\to 0} \frac{\overline{\phi(t_{p,q}-h)-\phi(t_{p,q})}}{\phi(t_{p,q}+h)-\phi(t_{p,q})}.
\end{aligned}$$

We used (2.64) in the last equality, and

$$\lim_{h\to 0} \frac{\phi(b(h))}{\phi(b_-(h))} = \lim_{h\to 0} \frac{b(h)^{1/2}}{b_-(h)^{1/2}} = 1.$$

in the previous one. Finally, using the asymptotic behaviour in Proposition 2.12, we get

$$1 = e_{p,q}^2 \lim_{h\to 0} \frac{\overline{e_{p,q}(1+i)(-h)^{1/2}}}{e_{p,q}(1+i)h^{1/2}} = e_{p,q}^2 \frac{\overline{e_{p,q}}}{e_{p,q}} \frac{1-i}{1+i} \overline{\sqrt{-1}} = -i\overline{\sqrt{-1}},$$

which implies that $\sqrt{-1} = -i$ must hold so that Proposition 2.12 works also for $h < 0$.

To finish this section, in the spirit of Remark 2.13, the bound given by the truncation of the asymptotic behaviour around $t_{p,q}$ in its first term works in general when $|h| \lesssim 1/q^2$. We make it explicit here because we will use it in following sections.

Corollary 2.14. *Let $p, q \in \mathbb{N}$ such that $q \equiv 0, 1, 3 \pmod 4$ and $\gcd(p, q) = 1$. Let $M > 0$. Then, there exists $C_M > 0$ independent of p and q such that*

$$|\phi(t_{p,q}+h) - \phi(t_{p,q})| \le C_M \frac{|h|^{1/2}}{q^{1/2}}, \qquad \forall |h| < \frac{M}{q^2}.$$

Proof. The conclusion is immediate under the conditions of Proposition 2.12, since in view of (2.59),

$$\tilde{q}^{7/2}h^{5/2} < \tilde{q}^{3/2}h^{3/2} < \tilde{q}^{-1/2}h^{1/2} \qquad \text{holds if} \quad h < \frac{1}{\tilde{q}^2}.$$

Assume then that h is out of the range in Proposition 2.12, that is, $4\pi|c_\pm \tilde{q} h| \ge 1$. According to Remark 2.11, under the condition $4\pi c_\pm b(h)/\tilde{q} < \delta < 1$, there exists a constant $C_\delta > 0$ such that (2.57) is

$$|\phi(t_{p,q}+h) - \phi(t_{p,q})| \le C_\delta \frac{b(h)^{1/2}}{q^{3/2}}. \tag{2.65}$$

The condition for $b(h)$ above means that

$$h < \frac{\delta}{4\pi \frac{c_\pm}{\tilde{q}}(1-\delta)} \frac{1}{q^2}.$$

Since $\delta/(1-\delta)$ covers the whole positive real line for $\delta \in (0, 1)$, there exists a δ_M such that $M = \frac{\delta}{4\pi \frac{c_\pm}{\tilde{q}}(1-\delta)}$. That means that (2.65) holds for $|h| \le M/\tilde{q}^2$. Then, $4\pi|c_\pm \tilde{q} h| \ge 1$ directly implies $|b(h)| \le \tilde{q}^2|h|/2$ so that since C_δ really depends on M,

we get

$$|\phi(t_{p,q}+h)-\phi(t_{p,q})| \le \frac{C_\delta}{2}\frac{h^{1/2}}{q^{1/2}}, \qquad \forall |h| < \frac{M}{q^2}.$$

□

2.2.7 Asymptotic behaviour around $t_{p,q}$ such that $q \equiv 2 \pmod 4$

Let p/q be an irreducible fraction such that $q \equiv 2 \pmod 4$. Then, both $\tilde{p}$ and $\tilde{q}$ in the irreducible fraction $\tilde{p}/\tilde{q} = 2p/q$ are odd and there exists $\gamma \in \Gamma_\theta$ such that $\gamma(\tilde{p}/\tilde{q}) = 1$. The strategy we use is exactly the same as in Subsection 2.2.6, so we only point out the main changes with respect to it.

Arguing the same way with the extension to the complex plane (2.52), when integrating by parts in (2.53) we choose

$$v = 4\pi i \left[\phi\left(-\frac{\gamma(\tau+i\epsilon)}{4\pi}\right) - \phi\left(-\frac{\gamma(\tilde{p}/\tilde{q}+i\epsilon)}{4\pi}\right)\right]$$

instead. Then, after taking the limit $\epsilon \to 0$ and changing variables $\gamma(\tau) = r$ as before, we get

$$\phi(t_{p,q}+h)-\phi(t_{p,q}) = e_\gamma \left[\frac{\phi(t_{1,2}+b(h))-\phi(t_{1,2})}{(\tilde{q}-4\pi c_\pm b(h)^{3/2}} - 6\pi\, c_\pm \int_0^{b(h)} \frac{\phi(t_{1,2}+r)-\phi(t_{1,2})}{(\tilde{q}-4\pi c_\pm r)^{5/2}}\, dr\right]$$

for all $h \in \mathbb{R}$. Now we can develop $\phi(t_{1,2}+b(h))-\phi(t_{1,2})$ using Proposition 2.8, and use Taylor expansions (2.56) to get a series in terms of $b = b(h)$, which is

$$\phi(t_{p,q}+h)-\phi(t_{p,q}) = e_\gamma \left[-16\,\frac{1-i}{\sqrt{2\pi}}\, Z_1(b)\,\frac{b^{3/2}}{\tilde{q}^{3/2}} + \frac{1}{\tilde{q}^{3/2}}\, O\left(b^{5/2}\right)\right].$$

Finally, expanding the Taylor series for powers of $b(h)$ as in (2.58), we get the wanted asymptotic behaviour, which we reproduce directly in the following proposition.

Proposition 2.15. *Let $p, q \in \mathbb{N}$ such that $q \equiv 2 \pmod 4$, $p < q$ and $\gcd(p,q) = 1$. Define $\tilde{p}$ and $\tilde{q}$ so that $\tilde{p}/\tilde{q} = 2p/q$ is an irreducible fraction, and set*

$$Z_1(h) = \sum_{\substack{k=1\\ k\ odd}}^{\infty} \frac{e^{ik^2/(16h)}}{k^2} \qquad \text{and} \qquad b(h) = \begin{cases} \frac{\tilde{q}^2 h}{1+4\pi c_+ \tilde{q} h}, & \text{when } h \ge 0,\\ \frac{\tilde{q}^2 h}{1+4\pi c_- \tilde{q} h}, & \text{when } h < 0, \end{cases}$$

where $\tilde{q} \le c_+, |c_-| \le 3\tilde{q}$ as in Subsection 2.2.3. Then, there exists a complex eighth root of unity $e_{p,q}$ depending only on p and q such that

$$\phi(t_{p,q}+h)-\phi(t_{p,q}) = e_{p,q}\left(-16\,\frac{1-i}{\sqrt{2\pi}}\, Z_1(b(h))\,\tilde{q}^{3/2}\,h^{3/2} + O\left(\tilde{q}^{7/2}h^{5/2}\right)\right), \quad \text{whenever } |h| < \frac{1}{4\pi\frac{|c_\pm|}{\tilde{q}}}\,\frac{1}{\tilde{q}^2}, \tag{2.66}$$

where $c_\pm = c_+$ *when* $h > 0$ *and* $c_\pm = c_-$ *when* $h < 0$. *Rescaling the variable, an alternative form of the asymptotic behaviour is*

$$\phi\left(t_{p,q} + \frac{h}{\tilde{q}^2}\right) - \phi(t_{p,q}) = \frac{e_{p,q}}{\tilde{q}^{3/2}} \left(-16\,\frac{1-i}{\sqrt{2\pi}}\, Z_1(\beta(h))\, h^{3/2} + O\left(h^{5/2}\right)\right), \qquad \text{whenever } |h| < \frac{1}{4\pi \frac{|c_\pm|}{\tilde{q}}},$$

where $\beta(h) = b(h/\tilde{q}^2)$.

The same reasons as in the previous subsection show that $\sqrt{-1} = -i$ is the correct branch of the square root for $h < 0$ here too.

Proposition 2.15 rigorously confirms (2.35), this is, that ϕ behaves around $t_{p,q}$ with $q \equiv 2 \pmod 4$ the same as around $t_{1,2}$, except the already familiar scalings and the substitution of τ by $\beta(\tau)$ in the argument of Z_1. As in $t_{1,2}$ the circular pattern of Z_1 makes the leading term form a spiral-like behaviour, showing that the situation in all these rationals is like in Figure 2.3.

The analogous result of Corollary 2.14 is also satisfied, with an equally analogous proof.

Corollary 2.16. *Let* $p, q \in \mathbb{N}$ *such that* $q \equiv 2 \pmod 4$ *and* $\gcd(p,q) = 1$. *Let* $M > 0$. *Then, there exists* $C_M > 0$ *independent of* p *and* q *such that*

$$|\phi(t_{p,q} + h) - \phi(t_{p,q})| \leq C_M q^{3/2}\, h^{3/2}, \qquad \forall |h| \leq \frac{M}{q^2}.$$

CHAPTER 3

The Hausdorff dimension of Riemann's non-differentiable function

In Figure 1.5, apart from the spikiness we could expect from the non-differentiability of the function, the fact that smaller and smaller copies of the set $\phi([0, 1/(2\pi)])$ appear inside itself specially call the attention. In this sense, the set has certain self-similar features, which have been explained by the asymptotic behaviour of ϕ around rational points in Subsection 2.2. It is known that self-similarity is usually an indicator of fractality, so it is natural to ask what the Hausdorff dimension of the set, when regarded as a subset of the complex plane $\mathbb{C}$ or of the Euclidean plane $\mathbb{R}^2$, could be. We present a partial answer to this question, an upper estimate for the Hausdorff dimension of $\phi(\mathbb{R})$.

Theorem 3.1. *Let ϕ be Riemann's non-differentiable function (2.1). The Hausdorff dimension of its image satisfies*

$$1 \leq \dim_{\mathcal{H}} \phi(\mathbb{R}) \leq 4/3.$$

The upper bound in this theorem is a consequence of the asymptotic expansion of ϕ around its rational points; indeed, thanks to the bounds implied in Corollaries 2.14 and 2.16, the whole set can be covered by balls centred at these rational points. On the other hand, the asymptotic behaviour in Proposition 2.12 shows that ϕ is, in a manner of speaking, *continuously self-similar*, in the sense that it does not have discrete scaling factors and that the copies generated are not exact. This makes it tougher to exploit self-similarity to get a good lower bound, and thus, the optimality of the upper bound is unclear. However, the lower bound in the theorem is just a consequence of ϕ being continuous, so the structure of the function is not being taken into account. It seems reasonable that the dimension should be strictly greater than one.

Theorem 3.1 can be generalised to the context of multifractality treated in Subsection 1.4.1. Recalling (1.43), let $D_\alpha = \{t \mid \alpha_\phi(t) = \alpha\}$ be the set of points where

ϕ has supremum Hölder regularity α. We already saw in (1.48) that the spectrum of singularities of Riemann's function is

$$d(\alpha) = \dim_{\mathcal{H}} D_\alpha = 4\alpha - 2, \qquad \forall \alpha \in [1/2, 3/4], \tag{3.1}$$

which is completed with $d(3/2) = 0$. For the remaining α, the sets D_α are empty and by convention, $d(\alpha) = -\infty$. A natural question is whether the multifractal nature of the function ϕ is translated from its domain to its image $\phi(\mathbb{R})$. In this sense, we prove one more partial result.

Theorem 3.2. *Let ϕ be Riemann's non-differentiable function (2.1) and $D_\alpha = \{t \in \mathbb{R} \mid \alpha_\phi(t) = \alpha\}$. Then,*

$$\dim_{\mathcal{H}} \phi(D_\alpha) \leq \dim_{\mathcal{H}} \phi\Big(\bigcup_{\sigma \leq \alpha} D_\sigma \Big) \leq \frac{4\alpha - 2}{\alpha}, \qquad \forall \alpha \in [1/2, 3/4].$$

Theorem 3.2 generalises Theorem 3.1 in the following sense. In view of (3.1), the set $D_{3/2}$ consists of the points where ϕ is differentiable, and we know that these points, up to the rescaling (2.4), are rational points. Indeed, $2\pi D_{3/2} \subset \mathbb{Q}$. Therefore, the union $\cup_{\sigma \leq 3/4} D_\sigma$ covers the whole real line except a countable number of points, and $\dim_{\mathcal{H}} \phi(\mathbb{R}) = \dim_{\mathcal{H}} \phi(\cup_{\sigma \leq 3/4} D_\sigma) \leq 4/3$.

Theorem 3.2 is also a consequence of the asymptotic behaviour of ϕ around rational points computed in Section 2.2. Also, since the setting is the same as that of the spectrum of singularities computed by Jaffard, it is not surprising that its proof also lies on the Diophantine properties of irrational numbers, and particularly on the rate of convergence of their continued fraction approximations.

Before going into details and proofs, let us recall the definition of the Hausdorff dimension of a set $A \subset \mathbb{R}^n$. Let $d \geq 0$. The d-Hausdorff content of diameter $\delta > 0$ of the set A is

$$\mathcal{H}^d_\delta(A) = \inf \left\{ \sum_{i \in I} (\operatorname{diam} U_i)^d \mid A \subset \bigcup_{i \in I} U_i, \quad \operatorname{diam} U_i < \delta \quad \forall i \in I, \quad I \text{ countable} \right\}, \tag{3.2}$$

where the sets U_i can be chosen to be open sets if needed. The smaller the diameter δ is allowed to be, the larger the content $\mathcal{H}^d_\delta(A)$ is, since the choice for coverings is smaller and therefore the infimum is taken over a smaller set. Taking the limit $\delta \to 0$ yields to the the d-Hausdorff measure of A

$$\mathcal{H}^d(A) = \lim_{\delta \to 0} \mathcal{H}^d_\delta(A) = \sup_{\delta > 0} \mathcal{H}^d_\delta(A).$$

Finally, the Hausdorff dimension of A is

$$\dim_{\mathcal{H}} A = \inf\{ d \mid \mathcal{H}^d(A) = 0\} = \sup\{ d \mid \mathcal{H}^d(A) = \infty\}. \tag{3.3}$$

These definitions and many basic and well-known properties that we might use along this section, may be found, for instance, in [38, 73].

We prove Theorem 3.1 in Section 3.1, and then Theorem 3.2 in Section 3.2. Finally, in Section 3.3 we prove an auxiliary result needed in the multifractal case.

The contents of this chapter are based in the note [31][1] and the main article [30][2].

[1] Eceizabarrena, D. "Some geometric properties of Riemann's non-differentiable function". In: *C. R. Math. Acad. Sci. Paris* 357.11-12 (2019), pp. 846–850. DOI: 10.1016/j.crma.2019.10.007.

[2] Eceizabarrena, D. "Asymptotic behaviour and Hausdorff dimension of Riemann's non-differentiable function". In: (2019). Preprint: http://arxiv.org/abs/1910.02530v1.

3.1 The dimension of $\phi(\mathbb{R})$

The objective of this chapter is to prove Theorem 3.1. As suggested in Section 2.1, it will be enough to prove the corresponding result for the set $\phi([0, 1/(2\pi)])$:

Theorem 3.3. *Let ϕ be Riemann's non-differentiable function (2.1). Then,*

$$1 \leq \dim_{\mathcal{H}} \phi([0, 1/(2\pi)]) \leq 4/3.$$

Indeed, this implies Theorem 3.1 for the whole set $\phi(\mathbb{R})$ because according to (2.3),

$$\phi(\mathbb{R}) = \bigcup_{k\in\mathbb{Z}} \left(\phi([0, 1/(2\pi)]) + \frac{i}{2\pi}\, k \right),$$

which is a countable union. The Hausdorff dimension of a countable union of sets is the supremum among the Hausdorff dimensions of each of the sets (see, for instance, [73, Chapter 4]), so

$$\dim_{\mathcal{H}} \phi(\mathbb{R}) = \sup_{k\in\mathbb{Z}} \dim_{\mathcal{H}} \left(\phi([0, 1/2\pi]) + \frac{i}{2\pi}\, k \right).$$

But of course, all such translated sets have the same Hausdorff dimension, so it is enough to work with the one corresponding to $k = 0$.

Proof of Theorem 3.3. We start with the lower bound. Since ϕ is a continuous and non-constant curve, there exist $0 \leq s < t \leq 1/(2\pi)$ such that $\phi(s) \neq \phi(t)$. Let $[\phi(s), \phi(t)] \subset \mathbb{R}^2$ denote the line segment connecting $\phi(s)$ and $\phi(t)$, and L its infinite extension. Then, the orthogonal projection $P_\perp : \phi([s, t]) \to L$ is a Lipschitz map, so

$$\dim_{\mathcal{H}} P_\perp \phi([s, t]) \leq \dim_{\mathcal{H}} \phi([s, t]),$$

see, for instance, [38, Proposition 3.3]. Since the continuity of ϕ implies $[\phi(s), \phi(t)] \subset P_\perp(\phi([s, t]))$, we get

$$\dim_{\mathcal{H}} \phi([0, 1/(2\pi)]) \geq \dim_{\mathcal{H}} \phi([s, t]) \geq \dim_{\mathcal{H}} P_\perp \phi([s, t]) \geq \dim_{\mathcal{H}} [\phi(s), \phi(t)] = 1.$$

Let us prove the upper bound. The first remark is that we may work only with t_ρ with irrational $\rho \in \mathbb{R} \setminus \mathbb{Q}$ because the set of rational points is countable, therefore zero dimensional. If we call the set of irrationals

$$\mathcal{I} = \{\, t_\rho \mid \rho \in [0, 1] \setminus \mathbb{Q} \,\},$$

then by the property regarding the dimension of the union of sets above,

$$\dim_{\mathcal{H}} \phi([0, 1/(2\pi)]) = \dim_{\mathcal{H}} \phi(\mathcal{I})$$

and thus it suffices to work with $\phi(\mathcal{I})$.

It is enough to find a proper countable cover of the set $\phi(\mathcal{I})$. First, observe that

$$(0, 1) \setminus \mathbb{Q} \subset \bigcup_{\substack{1\leq p<q \\ \gcd(p,q)=1 \\ q\geq Q_0}} B\left(\frac{p}{q}, \frac{1}{q^2}\right), \qquad \forall Q_0 \in \mathbb{N}. \tag{3.4}$$

This cover is a direct consequence of the theory of continued fractions, which we treat in Appendix B. For $\rho \in (0,1) \setminus \mathbb{Q}$, let p_n/q_n be its convergents by continued fractions for all $n \in \mathbb{N}$. These convergents are irreducible rationals such that

$$\lim_{n\to\infty} q_n = +\infty \qquad \text{and} \qquad |\rho - p_n/q_n| < q_n^{-2}, \qquad \forall n \in \mathbb{N}.$$

Consequently, for no matter how large $Q_0 \in \mathbb{N}$, we can find $N_0 \in \mathbb{N}$ such that $q_n \geq Q_0$ and $|\rho - p_n/q_n| < q_n^{-2}$ for every $n > N_0$, hence (3.4).

Let us tranlate this cover to $\phi(\mathcal{I})$ by using the asymptotic behaviour around t_{p_n,q_n} obtained in the previous subsections. Call $h_n = t_\rho - t_{p_n,q_n}$ so that $\phi(t_{p_n,q_n} + h_n) = \phi(t_\rho)$. Moreover, $|h_n| < 1/(2\pi q_n^2)$. If $q_n \equiv 0, 1, 3 \pmod 4$, then choose any $M \geq 1/(2\pi)$ in Corollary 2.14 so that there exists a constant $C > 0$ such that

$$|\phi(t_\rho) - \phi(t_{p_n,q_n})| \leq C\,\frac{|h_n|^{1/2}}{q_n^{1/2}} \leq \frac{C}{q_n^{3/2}}, \qquad \forall n \in \mathbb{N}. \tag{3.5}$$

In case $q_n \equiv 2 \pmod 4$, the bound given in Corollary 2.16 is better than the one in Corollary 2.14 because $|h_n| \leq q_n^{-2}$ implies $q_n^{3/2}\,|h_n|^{3/2} \leq |h_n|^{1/2}/q_n^{1/2}$, so (3.5) holds too. Thanks to this bound, (3.4) can be translated to the image of ϕ because there exists $C > 0$ such that

$$\phi(\mathcal{I}) \subset \bigcup_{\substack{1\leq p<q \\ \gcd(p,q)=1 \\ q\geq Q_0}} B\left(\phi\left(t_{p,q}\right), \frac{C}{q^{3/2}}\right), \qquad \forall Q_0 \in \mathbb{N}, \tag{3.6}$$

which represents a cover of $\phi(\mathcal{I})$. Now, let $d > 0$. This cover can be used to give an upper bound of the d-Hausdorff content (3.2) of diameter $\delta < C/Q_0^{3/2}$, since we have

$$\begin{aligned} \mathcal{H}^d_{C/Q_0^{3/2}}(\phi(\mathcal{I})) &\leq \sum_{\substack{1\leq p<q \\ \gcd(p,q)=1 \\ q\geq Q_0}} \left(\operatorname{diam} B\left(\phi\left(t_{p,q}\right), \frac{C}{q^{3/2}}\right)\right)^d = C^d \sum_{q=Q_0}^{\infty} \frac{\varphi(q)}{q^{3d/2}} \\ &\leq C^d \sum_{q=Q_0}^{\infty} \frac{1}{q^{3d/2-1}} \end{aligned} \tag{3.7}$$

for every $Q_0 \in \mathbb{N}$. Here, φ is Euler's totient function, whose trivial but in general best bound $\varphi(q) < q$ we used above. Then, we take the limit $Q_0 \to \infty$ so that

$$\mathcal{H}^d(\phi(\mathcal{I})) = \lim_{Q_0\to\infty} \mathcal{H}^d_{C/Q_0^{3/2}}(\phi(\mathcal{I})) \leq C^d \lim_{Q_0\to\infty} \sum_{q=Q_0}^{\infty} \frac{1}{q^{3d/2-1}}.$$

The sum inside the limit converges if and only if $3d/2 - 1 > 1$, or equivalently $d > 4/3$, in which case

$$\mathcal{H}^d(\phi(\mathcal{I})) = 0.$$

According to the definition of the Hausdorff dimension (3.3), $\dim_{\mathcal{H}}(\phi(\mathcal{I})) \leq 4/3$ as we wanted. □

Remark 3.4. The proof above gives no information about $\mathcal{H}^{4/3}(\phi(\mathcal{I}))$, but we can learn something more if we use the Dirichlet approximation theorem instead of the continued fraction theory to obtain a cover like (3.4). Dirichlet's theorem states that given a natural number $N \in \mathbb{N}$ and any irrational ρ, there exist $p, q \in \mathbb{Z}$, such that

$1 \le q \le N$ and $|\rho - p/q| < 1/(qN)$. This implies that

$$[0,1] \setminus \mathbb{Q} \subset \bigcup_{\substack{1\le q\le N\\ 1\le p\le q}} B\left(\frac{p}{q}, \frac{1}{qN}\right), \qquad \forall N \in \mathbb{N}.$$

Fix $N \in \mathbb{N}$ and let $p_N(\rho)/q_N(\rho)$ be the approximation of ρ corresponding to N. Plug this in (3.5) so that we get

$$\left|\phi(t_\rho) - \phi(t_{p_N(\rho),q_N(\rho)})\right| \le C\,\frac{|\rho - p_N(\rho)/q_N(\rho)|^{1/2}}{q_N(\rho)^{1/2}} \le \frac{C}{q_N(\rho)\,N^{1/2}},$$

which means that

$$\phi(\mathcal{I}) \subset \bigcup_{\substack{1\le q\le N\\ 1\le p\le q}} B\left(\phi(t_{p,q}), \frac{C}{qN^{1/2}}\right), \qquad \forall N \in \mathbb{N}.$$

Observe, moreover, that the diameters of the balls satisfy $1/(qN^{1/2}) \le N^{-1/2}$. Thus, for $1 \le d < 2$,

$$\mathcal{H}^d_{N^{-1/2}}(\phi(\mathcal{I})) \le \sum_{\substack{1\le q\le N\\ 1\le p\le q}} \frac{1}{(qN^{1/2})^d} = \sum_{q=1}^{N} \frac{1}{q^{d-1}\,N^{d/2}} \le \frac{N^{2-3d/2}}{(2-d)},$$

which shows as before that $\mathcal{H}^d(\phi(\mathcal{I})) = \lim_{N\to\infty} \mathcal{H}^d_{N^{-1/2}}(\phi(\mathcal{I})) = 0$ for every $d > 4/3$, but also and more interestingly,

$$\mathcal{H}^{4/3}(\phi(\mathcal{I})) = \lim_{N\to\infty} \mathcal{H}^{4/3}_{N^{-1/2}}(\phi(\mathcal{I})) \le \frac{1}{2-4/3} = 3/2.$$

3.2 A generalisation to the multifractal setting

In this section, we prove Theorem 3.2. We follow the structure of the proof of Theorem 3.3; here too, it is enough to prove the results for the sets restricted to the basic interval $[0, 1/(2\pi)]$. However, we use deeper results connecting the rate of convergence of the approximations by continued fractions with the Hölder regularity coefficient α_ϕ defined in (1.42).

Proof Of Theorem 3.2. For an irrational $\rho \in (0,1) \setminus \mathbb{Q}$, let p_n/q_n be its n-th covergent by continued fractions. We said that $|\rho - p_n/q_n| < 1/q_n^2$, but let us quantify how much smaller than q_n^{-2} this error is by defining the sequence $(\gamma_n)_{n\in\mathbb{N}}$ as

$$\left|\rho - \frac{p_n}{q_n}\right| = \frac{1}{q_n^{\gamma_n}}, \qquad \forall n \in \mathbb{N}.$$

It is clear that $\gamma_n > 2$ for every $n \in \mathbb{N}$. Of all the convergents, let us work only with those satisfying $q_n \equiv 0, 1, 3 \pmod 4$, which are always infinitely many (see Proposition B.12), and define

$$\begin{aligned}\gamma(\rho) &= \sup\{\tau \mid \gamma_n \ge \tau \text{ for infinitely many } n \in \mathbb{N} \text{ such that } q_n \equiv 0,1,3 \,(\mathrm{mod}\ 4)\}\\ &= \limsup_{\substack{n\to\infty\\ q_n\equiv 0,1,3\,(\mathrm{mod}\ 4)}} \gamma_n.\end{aligned} \tag{3.8}$$

There is a direct connection between this coefficient and the Hölder exponent α_ϕ given by

$$\alpha_\phi(t_\rho) = \frac{1}{2} + \frac{1}{2\gamma(\rho)}. \tag{3.9}$$

This identity is an adaptation of the original result for ϕ_D we saw in (1.47), which was shown by Jaffard in [55]. It is the expectable analogous result for ϕ because, according to the identity (1.11), ϕ and ϕ_D share regularity properties. We give the details and proof of this adaptation in Section 3.3.

The idea of the proof is that the definition of γ_n allows to improve the bound in (3.5) because now, if $h_n = t_\rho - t_{p_n,q_n}$,

$$|\phi(t_\rho) - \phi(t_{p_n,q_n})| \leq C\,\frac{|h_n|^{1/2}}{q_n^{1/2}} = \frac{C}{q_n^{(1+\gamma_n)/2}}, \qquad \forall n \in \mathbb{N}, \tag{3.10}$$

and then $\gamma(\rho)$ can be used to control the exponent of the bound. Thus, we take the set of points with fixed $\gamma(\rho) = \gamma$ and we cover it like in (3.6) but with balls of smaller diameter. Therefore we will get a better estimation for the Hausdorff dimension. Finally, the correspondence (3.9) connects these sets with the sets where ϕ has a given regularity.

Define the sets of points of a determinate coefficient $\beta \geq 2$,

$$R_\beta = \{t_\rho \in \mathcal{I} \mid \gamma(\rho) = \beta\} = D_{\frac{1}{2}+\frac{1}{2\beta}} \cap \mathcal{I}, \tag{3.11}$$

where the last equality holds because of (3.9). Let $\beta > 2$ and $t_\rho \in \cup_{\sigma\geq\beta} R_\sigma$, so that $\gamma(\rho) \geq \beta$, and choose $\epsilon > 0$ such that $\gamma(\rho) - \epsilon \geq \beta - \epsilon > 2$. By definition of $\gamma(\rho)$, the set of indices

$$A_{\rho,\epsilon} = \{n \in \mathbb{N} \mid q_n \equiv 0, 1, 3 \,(\mathrm{mod}\ 4) \text{ and } \gamma_n > \beta - \epsilon\}$$

is infinite for all $\epsilon > 0$ as above, and moreover, from (3.10) we get

$$|\phi(t_\rho) - \phi(t_{p_n,q_n})| < \frac{C}{q_n^{(1+\beta-\epsilon)/2}}, \qquad \forall n \in A_{\rho,\epsilon}.$$

As in (3.6), this shows that

$$\phi\Big(\bigcup_{\sigma\geq\beta} R_\sigma\Big) \subset \bigcup_{\substack{1\leq p<q \\ \gcd(p,q)=1 \\ q\geq Q_0}} B\left(\phi(t_{p,q}), \frac{C}{q^{(1+\beta-\epsilon)/2}}\right), \qquad \forall Q_0 \in \mathbb{N}.$$

Repeating the same procedure as in (3.7), we get

$$\mathcal{H}^d\left(\phi\Big(\bigcup_{\sigma\geq\beta} R_\sigma\Big)\right) \leq C^d \lim_{Q_0\to\infty} \sum_{q=Q_0}^{\infty} \frac{1}{q^{\frac{1+\beta-\epsilon}{2}d-1}} = 0, \qquad \forall d > \frac{4}{1+\beta-\epsilon}.$$

This means that

$$\dim_{\mathcal{H}} \phi\Big(\bigcup_{\sigma\geq\beta} R_\sigma\Big) \leq \frac{4}{1+\beta-\epsilon},$$

which is valid for every $0 < \epsilon\beta - 2$. Hence, taking the limit $\epsilon \to 0$ we get

$$\dim_{\mathcal{H}} \phi\Big(\bigcup_{\sigma \geq \beta} R_\sigma \Big) \leq \frac{4}{1+\beta}, \qquad \forall \beta > 2.$$

By the correspondence (3.11), can be rewritten in terms of D_α as

$$\dim_{\mathcal{H}} \phi\Big(\mathcal{I} \cap \bigcup_{\sigma \leq \alpha} D_\sigma \Big) \leq \frac{4\alpha - 2}{\alpha}, \qquad \text{for every} \quad \frac{1}{2} \leq \alpha < \frac{3}{4}.$$

This conclusion is also valid for $\alpha = 3/4$. Indeed, every irrational ρ satisfies $\gamma(\rho) \geq 2$, which according to (3.9) means that $\alpha(t_\rho) \leq 3/4$. This means that all the irrational t_ρ are in $\mathcal{I} \cap \bigcup_{\sigma \leq 3/4} D_\sigma$, so that the difference with the whole interval $[0, 1/(2\pi)]$ is a subset of the rationals $\{t_x \mid x \in \mathbb{Q} \cap [0,1]\}$, at most a countable set which has Hausdorff dimension 0. Hence, according to Theorem 3.3,

$$\dim_{\mathcal{H}} \phi\Big(\mathcal{I} \cap \bigcup_{\sigma \leq 3/4} D_\sigma \Big) = \dim_{\mathcal{H}} \phi(\mathcal{I}) = \dim_{\mathcal{H}} \phi([0, 1/(2\pi)]) = 4/3.$$

The rational points in $\bigcup_{\sigma \leq \alpha} D_\sigma$, which according to their asymptotic behaviour are all in $D_{1/2}$, can of course be included because they form a zero dimensional set. Finally, to conclude the result for $\bigcup_{\sigma \leq \alpha} D_\sigma$ it is enough to note, as in the previous subsection, that it is a countable union of translates of $[0, 1/(2\pi)] \cap \bigcup_{\sigma \leq \alpha} D_\sigma$, all of which have, of course, the same Hausdorff dimension. Hence,

$$\dim_{\mathcal{H}} \phi\left(D_\alpha\right) \leq \dim_{\mathcal{H}} \phi\Big(\bigcup_{\sigma \leq \alpha} D_\sigma \Big) \leq \frac{4\alpha - 2}{\alpha}, \qquad \text{for every} \quad \frac{1}{2} \leq \alpha \leq \frac{3}{4}$$

where the first inequality is just a consequence of the inclusion $D_\alpha \subset \bigcup_{\sigma \leq \alpha} D_\sigma$. □

3.3 An auxiliary result

The objective in this subsection is to deduce (3.9) from the known identity (1.47). As we commented in the end of Subsection 1.4.1, the latter corresponds to a very precise connection between the Hölder regularity of ϕ_D at an irrational point ρ and some kind of irrationality exponent [3] of ρ, which was proved by Jaffard in [55] and which reads as

$$\alpha_{\phi_D}(\rho) = \frac{1}{2} + \frac{1}{2\tau(\rho)}. \tag{3.12}$$

We recall that $\alpha_{\phi_D}(\rho)$ was defined in (1.42) as the local Hölder exponent

$$\alpha_{\phi_D}(\rho) = \sup\left\{\alpha \geq 0 \mid \phi_D \in C^\alpha(\rho)\right\},$$

[3] The irrationality exponent of an irrational ρ is defined as

$$\mu(\rho) = \sup\left\{ \mu > 0 \,:\, \left|\rho - \frac{p}{q}\right| < \frac{1}{q^\mu} \text{ for infinitely many rationals } \frac{p}{q} \right\},$$

and it can be checked (as in Lemma 3.6) that it is equivalent to use only the convegrents by continued fractions; if p_n/q_n are the convergents of ρ, then

$$\mu(\rho) = \sup\left\{ \mu > 0 \,:\, \left|\rho - \frac{p_n}{q_n}\right| < \frac{1}{q^\mu} \text{ for infinitely many } n \in \mathbb{N} \right\}.$$

and τ in (1.46) as

$$\tau(x) = \sup\left\{\tau \,:\, \left|x - \frac{p_n}{q_n}\right| < \frac{1}{q_n^\tau}, \text{ for infinitely many } \frac{p_n}{q_n} \text{ not both odd}\right\},$$

where p_n/q_n are continued fraction convergents of ρ and by p/q not both odd we mean that p and q are not both odd at the same time. We recall that the convergents p_n/q_n are always irreducible fractions (see Appendix B).

From the relationship between ϕ_D and ϕ in (2.5), both functions share regularity properties. As in (2.6), ϕ has at t_ρ the regularity of ϕ_D at 2ρ, so

$$\alpha_\phi(t_\rho) = \alpha_{\phi_D}(2\rho).$$

Therefore, from (3.12) we immediately get

$$\alpha_\phi(t_\rho) = \frac{1}{2} + \frac{1}{2\tau(2\rho)}.$$

However, it would be interesting to relate $\alpha_\phi(t_\rho)$ directly with some irrationality exponent of ρ, and not of 2ρ. Observe that this multiplication by 2 is the same as we experienced in (2.26) and (2.27); there, we passed from classifying a rational p/q according to whether p and q were both odd or not to classifying it according to whether $q \equiv 0, 1, 3 \pmod 4$ or not. It is expectable that the same will happen here, since τ is defined using only convergents p_n/q_n such that not both p_n and q_n are odd. In this sense, we expect that defining

$$\gamma(\rho) = \sup\left\{\gamma \,:\, \left|x - \frac{p_n}{q_n}\right| < \frac{1}{q_n^\gamma} \text{ for infinitely many } n \in \mathbb{N} \text{ with } q_n \equiv 0, 1, 3 \,(\mathrm{mod}\ 4)\right\}$$

as in (3.8), we will have

$$\alpha_\phi(t_\rho) = \frac{1}{2} + \frac{1}{2\gamma(\rho)},$$

which is precisely (3.9). To check that this is the case, we prove the following.

Lemma 3.5. *Let $\rho \in \mathbb{R} \setminus \mathbb{Q}$. Then, $\gamma(\rho) = \tau(2\rho)$.*

Although this lemma can be proved directly with the definitions of γ and τ above and using the convergents of ρ and 2ρ, let us split the proof in two steps. First, we prove in Lemma 3.6 that γ and τ can be defined also using any rational. Then, once the restriction of needing convergents has been removed, we will prove the equality in Lemma 3.7. Define, thus,

$$\tau_R(x) = \sup\left\{\tau \,:\, \left|x - \frac{p}{q}\right| < \frac{1}{q^\tau}, \text{ for infinitely many rationals } \frac{p}{q} \text{ not both odd}\right\},$$

where the fractions must be irreducible. Define, analogously,

$$\gamma_R(\rho) = \sup\left\{\gamma : \left|x - \frac{p}{q}\right| < \frac{1}{q^\gamma} \text{ for inf. many rationals } \frac{p}{q} \text{ with } q \equiv 0, 1, 3 \,(\mathrm{mod}\ 4)\right\}. \tag{3.13}$$

Lemma 3.6. *Let $\rho \in \mathbb{R} \setminus \mathbb{Q}$. Then, $\tau_R(\rho) = \tau(\rho)$ and $\gamma_R(\rho) = \gamma(\rho)$.*

Proof. We prove $\tau_R(\rho) = \tau(\rho)$, the proof for γ is analogous. First, it is clear that

$$\left\{\tau : \left|x - \frac{p_n}{q_n}\right| < \frac{1}{q_n^\tau} \text{ for infinitely many convergents } \frac{p_n}{q_n} \text{ not both odd}\right\}$$
$$\subset \left\{\tau : \left|x - \frac{p}{q}\right| < \frac{1}{q^\tau} \text{ for infinitely many rationals } \frac{p}{q} \text{ not both odd}\right\},$$

so taking the supremum we get $\tau(\rho) \leq \tau_R(\rho)$. Take now τ such that there are infinitely many rationals p/q not both odd such that $|x - p/q| < q^{-\tau}$. Assume that $\tau > 2$, so that

$$\left|x - \frac{p}{q}\right| < \frac{1}{q^\tau} \leq \frac{1}{2q^2} \quad \Longrightarrow \quad 2 \leq q^{\tau-2}$$

holds whenever $q > 2^{1/(\tau-2)}$. Since there are infinitely many rationals, in particular there are infinitely many satisfying that last property. According to Theorem B.11, every such rational is a convergent of ρ, so there are infinitely many continued fraction convergents p_n/q_n such that $|\rho - p_n/q_n| < q_n^{-\tau}$. Thus,

$$\left\{\tau > 2 : \left|x - \frac{p}{q}\right| < \frac{1}{q^\tau} \text{ for infinitely many rationals } \frac{p}{q} \text{ not both odd}\right\}$$
$$\subset \left\{\tau > 2 : \left|x - \frac{p_n}{q_n}\right| < \frac{1}{q_n^\tau} \text{ for infinitely many convergents } \frac{p_n}{q_n} \text{ not both odd}\right\}. \tag{3.14}$$

Once this is established, recall from Proposition B.10 that the convergents satisfy $|\rho - p_n/q_n| < q_n^{-2}$ for every $n \in \mathbb{N}$. Also, Proposition B.6 implies that two consecutive convergents p_n/q_n and p_{n-1}/q_{n-1} can not be both of the form odd/odd. As a consequence, $\tau(\rho) \geq 2$, and by the trivial inequality we proved in the beginning of the proof, $2 \leq \tau(\rho) \leq \tau_R(\rho)$. Thus, we separate two cases. If $\tau_R(\rho) = 2$, then $2 \leq \tau(\rho) \leq \tau_R(\rho) = 2$ and hence $\tau(\rho) = \tau_R(\rho)$. Otherwise, $\tau_R(\gamma) > 2$, and by the definition of the supremum and by (3.14),

$$\begin{aligned}
\tau_R(\rho) &= \sup\left\{\tau > 2 : \left|x - \frac{p}{q}\right| < \frac{1}{q^\tau} \text{ for infinitely many rationals } \frac{p}{q} \text{ not both odd}\right\} \\
&\leq \sup\left\{\tau > 2 : \left|x - \frac{p_n}{q_n}\right| < \frac{1}{q_n^\tau} \text{ for inf. many convergents } \frac{p_n}{q_n} \text{ not both odd}\right\} \\
&\leq \sup\left\{\tau \geq 2 : \left|x - \frac{p_n}{q_n}\right| < \frac{1}{q_n^\tau} \text{ for inf. many convergents } \frac{p_n}{q_n} \text{ not both odd}\right\} \\
&= \tau(\rho),
\end{aligned}$$

and the proof is complete. □

Thanks to Lemma 3.6, proving Lemma 3.5 amounts to proving the analogue result for τ_R and γ_R.

Lemma 3.7. *Let $\rho \in \mathbb{R} \setminus \mathbb{Q}$. Then, $\gamma_R(\rho) = \tau_R(2\rho)$.*

Proof. Let us rewrite $\tau_R(2\rho)$ as

$$\begin{aligned}
\tau_R(2\rho) &= \sup\left\{\tau : \left|2\rho - \frac{p}{q}\right| < \frac{1}{q^\tau}, \text{ for infinitely many } \frac{p}{q} \text{ not both odd}\right\} \\
&= \sup\left\{\tau : \left|\rho - \frac{1}{2}\frac{p}{q}\right| < \frac{1}{2q^\tau}, \text{ for infinitely many } \frac{p}{q} \text{ not both odd}\right\}.
\end{aligned}$$

We want to write the bound $1/(2q^\tau)$ in terms of the denominator of the new fraction $(p/q)/2$, and there are two different cases:

1. If p is even and q is odd, then $p/(2q) = (p/2)/q$, and the denominator is q. We let the condition as $|\rho - (p/2)/q| < 1/(2q^\tau)$.
2. If p is odd and q is even, then $p/(2q)$, and the denominator is $2q$. We rewrite the condition as $|\rho - p/(2q)| < 2^{\tau-1}/(2q)^\tau$.

Since the condition must hold for infinitely many rationals, we relabel the fractions and let the conditions

$$\left|\rho - \frac{p}{q}\right| < \frac{1}{2q^\tau} \qquad \text{if } q \text{ odd} \tag{$P1_\tau$}$$

and

$$\left|\rho - \frac{p}{q}\right| < \frac{2^{\tau-1}}{q^\tau} \qquad \text{if } q \equiv 0 \pmod 4 \tag{$P2_\tau$}$$

so that $\tau_R(2\rho)$ is equivalently given by

$$\tau_R(2\rho) = \sup\left\{\tau \ : \ \text{infinitely many } \frac{p}{q} \text{ satisfy their corresponding } (P1_\tau) \text{ or } (P2_\tau)\right\},$$

where the rationals have to be, of course, such that $q \equiv 0, 1, 3 \pmod 4$.

By Lemma 3.6, we know that $\tau_R(2\rho), \gamma_R(\rho) \geq 2$, so we may work only with $\tau, \gamma \geq 2$ all along the proof. Fix $\epsilon > 0$.

With the definition (3.13) of $\gamma_R(\rho)$ in mind, assume that $\gamma \geq 2$ is such that $|\rho - p/q| < 1/q^{\gamma+\epsilon}$ for infinitely many rationals with $q \equiv 0, 1, 3 \pmod 4$. For such $q \equiv 0 \pmod 4$,

$$\frac{1}{q^{\gamma+\epsilon}} < \frac{2}{q^\gamma} \leq \frac{2^{\gamma-1}}{q^\gamma}$$

always holds, so $(P2_\gamma)$ holds. Also, for those $q \equiv 1, 3 \pmod 4$,

$$\frac{1}{q^{\gamma+\epsilon}} < \frac{1}{2q^\gamma} \implies 2 < q^\epsilon,$$

which holds for $q > 2^{1/\epsilon}$, so $(P1_\gamma)$ holds. In short, all rationals that satisfy $q > 2^{1/\epsilon}$, which are infinitely many, satisfy the corresponding $(P1_\gamma)$ or $(P2_\gamma)$, so

$$\begin{aligned}\left\{\gamma \geq 2 \mid \left|x - \frac{p}{q}\right| < \frac{1}{q^{\gamma+\epsilon}} \text{ for inf. many } \frac{p}{q} \text{ with } q \equiv 0, 1, 3 \,(\mathrm{mod}\ 4)\right\} \\ \subset \left\{\tau \geq 2 \ : \ \text{infinitely many } \frac{p}{q} \text{ satisfy } (P1_\tau) \text{ or } (P2_\tau)\right\},\end{aligned}$$

or equivalently,

$$\begin{aligned}\left\{\sigma \geq 2 + \epsilon \mid \left|x - \frac{p}{q}\right| < \frac{1}{q^{\sigma}} \text{ for inf. many } \frac{p}{q} \text{ with } q \equiv 0, 1, 3 \,(\mathrm{mod}\ 4)\right\} - \epsilon \\ \subset \left\{\tau \geq 2 \ : \ \text{infinitely many } \frac{p}{q} \text{ satisfy } (P1_\tau) \text{ or } (P2_\tau)\right\},\end{aligned}$$

Then, if we assume that $\gamma_R(\rho) > 2$ and choose $\epsilon < \gamma_R(\rho) - 2$, then $\gamma_R(\rho) > 2 + \epsilon$, and thus the supremum of the left hand side set is $\gamma_R(\rho) - \epsilon$. This shows that

$$\gamma_R(\rho) > 2 \quad \implies \quad \gamma_R(\rho) - \epsilon \leq \tau_R(2\rho), \qquad \forall \epsilon < \gamma_R(\rho) - 2. \tag{3.15}$$

In particular, $2 < \gamma_R(\rho) - \epsilon \leq \tau_R(2\rho)$, so

$$\gamma_R(\rho) > 2 \quad \Longrightarrow \quad \tau_R(2\rho) > 2. \tag{3.16}$$

Let us now look for the reverse inequality. Let $\tau \geq 2$ and assume that there are infinitely many rationals satisfying the corresponding $(P1_{\tau+\epsilon})$ or $(P2_{\tau+\epsilon})$. For the rationals satisfying $(P1_{\tau+\epsilon})$, then

$$\left|\rho - \frac{p}{q}\right| < \frac{1}{2q^{\tau+\epsilon}} < \frac{1}{q^{\tau}},$$

always, and for those satisfying $(P2_{\tau+\epsilon})$,

$$\left|\rho - \frac{p}{q}\right| < \frac{2^{\tau+\epsilon-1}}{q^{\tau+\epsilon}} < \frac{1}{q^{\tau}} \quad \Longrightarrow \quad 2^{\tau+\epsilon-1} < q^{\epsilon},$$

which holds for all that satisfy $q > 2^{(\tau+\epsilon-1)/\epsilon}$. Since the set of these rationals is infinite, there are infinitely many of them such that $q > 2^{(\tau+\epsilon-1)/\epsilon}$, so there are infinitely many of them, all with $q \equiv 0, 1, 3 \pmod 4$, that satisfy $|\rho - p/q| < 1/q^{\tau}$. Hence,

$$\left\{\tau \geq 2 \,:\, \text{infinitely many } \frac{p}{q} \text{ satisfy } (P1_{\tau+\epsilon}) \text{ or } (P2_{\tau+\epsilon})\right\}$$
$$\subset \left\{\gamma \geq 2 \,:\, \left|x - \frac{p}{q}\right| < \frac{1}{q^{\gamma}} \text{ for inf. many } \frac{p}{q} \text{ with } q \equiv 0, 1, 3 \,(\text{mod } 4)\right\},$$

or equivalently,

$$\left\{\sigma \geq 2 + \epsilon \,:\, \text{infinitely many } \frac{p}{q} \text{ satisfy } (P1_{\sigma}) \text{ or } (P2_{\sigma})\right\} - \epsilon$$
$$\subset \left\{\gamma \geq 2 \,:\, \left|x - \frac{p}{q}\right| < \frac{1}{q^{\gamma}} \text{ for inf. many } \frac{p}{q} \text{ with } q \equiv 0, 1, 3 \,(\text{mod } 4)\right\},$$

Now, as before, if we assume $\tau_R(2\rho) > 2$, then choose $\epsilon < \tau_R(2\rho) - 2$ so that $2 + \epsilon < \tau_R(2\rho)$. This implies that the supremum of the set on the left hand side is precisely $\tau_R(2\rho) - \epsilon$, so we get

$$\tau_R(2\rho) > 2 \quad \Longrightarrow \quad \tau_R(2\rho) - \epsilon \leq \gamma_R(\rho), \qquad \forall \epsilon < \tau_R(2\rho) - 2. \tag{3.17}$$

In particular, $2 < \tau_R(2\rho) - \epsilon \leq \gamma_R(\rho)$, so we also get

$$\tau_R(2\rho) > 2 \quad \Longrightarrow \quad \gamma_R(\rho) > 2. \tag{3.18}$$

To conclude, join (3.16) and (3.18) to get

$$\gamma_R(\rho) = 2 \quad \Longleftrightarrow \quad \tau_R(2\rho) = 2,$$

and on the other hand, when $\gamma_R(\rho), \tau_R(2\rho) > 2$, from (3.15) and (3.17) we get

$$\gamma_R(\rho) - \epsilon \leq \tau_R(2\rho) \leq \gamma_R(\rho) + \epsilon, \qquad \forall \epsilon < \min\{\gamma_R(\rho) - 2, \tau_R(2\rho) - 2\}.$$

Consequently,

$$\gamma_R(\rho) = \tau_R(2\rho),$$

and the proof is complete. □

CHAPTER 4

Geometric differentiability of Riemann's non-differentiable function

We continue discussing the fact that Riemann's non-differentiable function ϕ defined in (2.1) describes a physical trajectory in the context of the binormal flow. More precisely, we saw in Subsection 1.2.2 that if the initial vortex filament is a regular and planar polygon of $M \in \mathbb{N}$ sides and if M is large, then the image of ϕ in Figure 1.5 resembles much to the temporal trajectory of any of the corners of the polygon.

Assume that the initial polygon is formed by particles. As the time goes on, we know from the experience (for instance, from the experiment in [66]) and numeric simulations (for example in [63]) that the polygon evolves and moves in space periodically. Therefore, we can speak about the velocity of the polygon, which can be estimated, for instance, by the distance travelled divided over one period. On the other hand, it was shown in [26] that the particle corresponding to a corner translates in space according to the trajectory in Figure 1.5. We can also compute an average velocity of this particle by picking the position at any moment and comparing it to the initial point, measuring the distance travelled in a straight line and dividing it over the time. But can we say something about the velocity that the particle has at each moment? In other words, if we select a time and detect the position of the particle, can we determine the direction and the speed it will take from there? And can we do this at any time, or at least, at some time?

Strictly speaking, the filament itself is not made of particles; it is rather the locus along which the fluid under consideration has null curl. That is, it rotates around the filament. But this also makes the evolution of this curve interesting to analyse. So, even if we can we determine the movement of the corners of the filament, can we measure its velocity point by point?

This question can be easily translated to a mathematical language using the definition of ϕ and its image set. Does the trajectory determined by the image of the geometric Riemann's non-differentiable function ϕ admit a tangent somewhere? Regarding it as a parametric curve, do tangents exist? The main result in this section

is the following answer to the question, stated here with no technicalities.

Theorem 4.1. *Let ϕ be Riemann's non-differentiable function (2.1). There does not exist a point in which $\phi(\mathbb{R})$ has a tangent.*

This result is meaningful because there is not a clear connection between analytic regularity of ϕ and geometric tangency to $\phi(\mathbb{R})$. First, the direct analytic approach to tangency is very restricted by the fact that the derivative of ϕ exists almost nowhere. One could think of checking, at least, the points where the derivative exists, but the results of Gerver [42, 43] we commented in Subsection 1.1.2 together with (1.11), or alternatively and more directly, the asymptotic behaviour in Proposition 2.15, show that the derivative of ϕ is 0 at those points, which is useless to determine a tangent. What is more, if we zoom Figure 1.5 around one of such points like $\phi(t_{1,2})$ as in Figure 2.3 (for convenience, also in Figure 4.1A), we see that a spiralling pattern is generated. On the other hand, the derivative in the rest of rationals does not exist, which could make us think that a tangent does not exist, but nevertheless a similar zoom in Figure 4.1B shows the existence of two different geometric tangents at each side. It is the non-matching of both side-tangents which prevents a single tangent to exist. These guesses, based in computer-made plots, are fully supported by the asymptotic behaviour of ϕ around rational points that was given in Subsection 2.2.

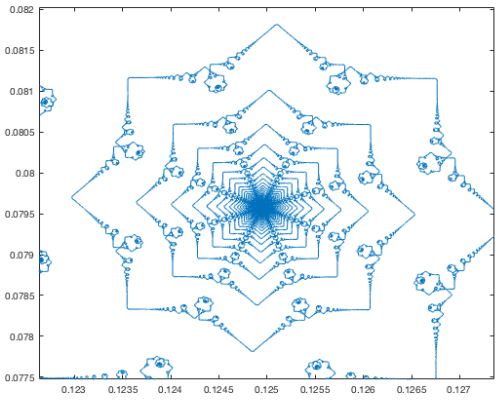

(A) Around $\phi(t_{1/2})$, placed in the centre of the spiral, where precisely the spiral pattern prevents a tangent from forming.

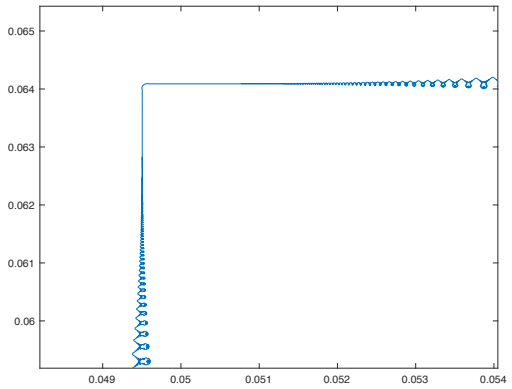

(B) Around $\phi(t_{1/8})$, placed on the corner, where two different side tangents can be distinguished.

FIGURE 4.1: Zooms of Figure 1.5 around the two different types of rational points.

Last, even if ϕ is not differentiable in irrational points, in view of Figure 4.1B one cannot directly conclude that there is no geometric tangent there. Also, contrary to the situation with rational points, no asymptotic behaviour around irrationals is available. In an attempt to visualise the situation, in Figure 4.2 we plot the image of $(t_\rho - \epsilon, t_\rho + \epsilon)$ for an irrational $\rho \in \mathbb{R} \setminus \mathbb{Q}$ and some $\epsilon > 0$. However, instead of seeing a precise behaviour of the function around t_ρ, we observe a pattern like in Figure 4.1 which corresponds to the rational approximation of ρ with smallest denominator in that interval. However, the fact this pattern changes very much when ϵ decreases suggests that the behaviour of ϕ around t_ρ highly depends on the scale under consideration and that therefore a tangent may not exist.

As already suggested, the main ingredient in the proof of Theorem 4.1 is the asymptotic behaviour of ϕ around every rational $t_{p/q}$ to which we devoted Section 2.2. Tangency around a rational is easy to manage, but a more subtle analysis is required

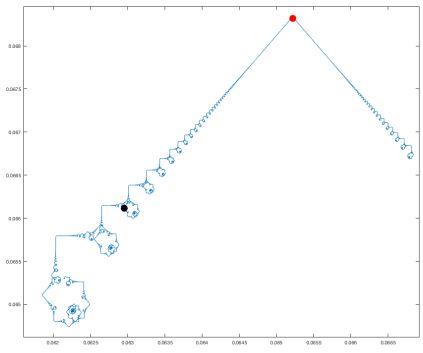

(A) $\epsilon = 0.002$ and the approximation is $\phi(t_{1/7})$. The first approximation to π by continued fractions is $22/7$, which for $\pi - 3$ turns into $1/7$.

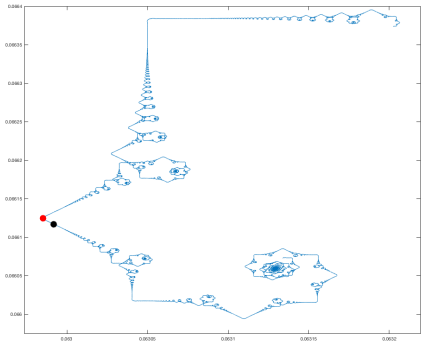

(B) $\epsilon = 0.0001$ and the approximation is $\phi(t_{16/113})$. The third approximation to π by continued fractions is the very famous $355/113$, which for $\pi - 3$ turns into $16/113$. The spiral on the right corresponds to the second approximation, $333/106$, or $15/106$ for $\pi - 3$.

FIGURE 4.2: Plots of $\phi((t_{\pi-3} - \epsilon, t_{\pi-3} + \epsilon))$. The black point corresponds to $\phi(t_{\pi-3})$, while the red points correspond to rational approximations which show either a corner or a spiral. Having changed the scale, the behaviour of ϕ is completely different.

around an irrational, since as we said above no asymptotic behaviour is available around it. A way to know how the function approaches it is to work with rational approximations, among which the approximations by continued fractions are the most effective ones. The proof will then depend on how fast they approach the irrational. This classification was remarked to be important by Duistermaat [29] and by Jaffard [55] in his multifractal analysis when computing the spectrum of singularities (1.48).

As importantly, in this non-canonical setting it is crucial to choose the concept of tangent carefully. Even if ϕ is a curve, the classic theory of differential geometry is of no use because Riemann's function is not differentiable in any open set. For this reason, we work with a purely geometric definition coming from geometric measure theory, as well as with one using the parametrisation ϕ. The first one is convenient in terms of the irregularity of the set, while the second one allows to perform computations using the asymptotic behaviour.

We begin discussing the geometric definition for a tangent in Section 4.1, and in Section 4.2 we define an alternative, parametric approach and work on the relationship between the two concepts. Once we stablish what a tangent means in this geometric context and given a precise sense to the result in Theorem 4.1, we will present the main Theorem 4.18 in Section 4.3. This result implies Theorem 4.1 but says more, since it describes the geometric behaviour of the curve around every point. Then, Sections 4.4, 4.5 and 4.6 are devoted to proving the several cases in Theorem 4.18.

Following the notation of previous chapters, along this chapter we denote by $\mathcal{H}^s$ the s-Hausdorff measure, by $\dim_{\mathcal{H}}$ the Hausdorff dimension and by $B(x, r)$ the open ball with center at x and radius r.

These results in this section were announced in the note [31][1] and are based on the article [32][2].

4.1 A geometric approach

When treating irregular objects in $\mathbb{R}^n$, especially curve-like objects, the question whether it has a tangent is natural. However, a general set need not be the image of a function, let alone be parametrised by a continuous function. A general definition should therefore have a geometric flavour.

Any definition of a tangent at a point should reflect the fact that close to the point, the set is concentrated in a particular direction. Many different approaches to measure this concentration have been proposed. Here, we reproduce the definition given by Falconer for s-sets in [38]. Let $0 \leq s \leq n$. A Borel set $F \subset \mathbb{R}^n$ is said to be an s-set if $\dim_{\mathcal{H}} F = s$ and if $0 < \mathcal{H}^s(F) < \infty$. For $x \in \mathbb{R}^n$, $\mathbb{V} \in \mathbb{S}^{n-1}$ and $\varphi > 0$, we define $S_D(x, \mathbb{V}, \varphi)$ to be the closed double cone with vertex x, direction $\mathbb{V}$ and opening $\varphi > 0$. More precisely, it is the closure of the set consisting of those $y \in \mathbb{R}^n$ such that the vector $y - x$ forms an angle at most $\varphi/2$ with $\mathbb{V}$ or $-\mathbb{V}$ (see figure 4.3A).

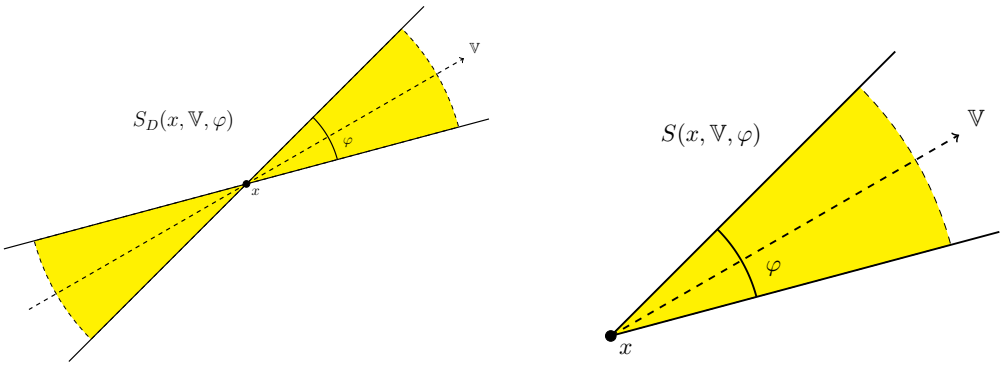

(A) The double cone $S_D(x, \mathbb{V}, \varphi)$.

(B) The single cone $S(x, \mathbb{V}, \varphi)$.

FIGURE 4.3: Cones.

Definition 4.2. Let $0 \leq s \leq n$ and $F \subset \mathbb{R}^n$ be an s-set. We say that $\mathbb{V} \in \mathbb{S}^{n-1}$ is a tangent of F at $x \in F$ if

$$\overline{D}^s(F, x) = \limsup_{r \to 0} \frac{\mathcal{H}^s(F \cap B(x, r))}{(2r)^s} > 0 \tag{4.1}$$

and if for every $\varphi > 0$,

$$\lim_{r \to 0} \frac{\mathcal{H}^s(F \cap (B(x, r) \setminus S_D(x, \mathbb{V}, \varphi)))}{(2r)^s} = 0. \tag{4.2}$$

Condition (4.1) means that there is some concentration of the set F around x, no matter how close we are from it. Since the cones in condition (4.2) can be as narrow as we wish, we also ask that this concentration only happens in direction $\mathbb{V}$.

[1] Eceizabarrena, D. "Some geometric properties of Riemann's non-differentiable function". In: *C. R. Math. Acad. Sci. Paris* 357.11-12 (2019), pp. 846–850. DOI: 10.1016/j.crma.2019.10.007.

[2] Eceizabarrena, D. "Geometric differentiability of Riemann's non-differentiable function". In: *Adv. Math.* 366 (2020), p. 107091. DOI: 10.1016/j.aim.2020.107091.

However, this definition requires the knowledge of the Hausdorff dimension of the set. If $F = \phi(\mathbb{R})$, we only know that $1 \leq \dim_{\mathcal{H}} F \leq 4/3$, so there is no obvious choice of s to use in Definition 4.2. On the other hand, when working with a curve, it is natural to use some one dimensional measure such as the length, even if there are curves with infinite length and even some whose images have Hausdorff dimension greater than 1. Therefore, we propose an alternative one-dimensional approach by means of the 1-Hausdorff content,

$$\mathcal{H}^1_\infty(F) = \inf\left\{ \sum_{i\in I} \operatorname{diam} U_i : F \subset \bigcup_{i\in I} U_i, \;\; I \text{ countable} \right\},$$

where we recall that the sets U_i can be chosen to be open sets.

Definition 4.3. Let $F \subset \mathbb{R}^n$ be the image of some continuous curve. We say that $\mathbb{V} \in \mathbb{S}^{n-1}$ is a tangent of F at $x \in F$ if

$$\limsup_{r\to 0} \frac{\mathcal{H}^1_\infty(F \cap B(x,r))}{2r} > 0$$

and if

$$\lim_{r\to 0} \frac{\mathcal{H}^1_\infty\left((F \cap B(x,r)) \setminus S_D(x,\mathbb{V},\varphi)\right)}{2r} = 0, \qquad \forall \varphi > 0. \tag{4.3}$$

Remark 4.4. Since $\mathcal{H}^1(F) \geq \mathcal{H}^1_\infty(F)$ for any set $F \subset \mathbb{R}^n$, condition (4.2) for $s = 1$ implies (4.3). Thus, if for a given $x \in F$ no vector satisfies (4.3) so that no tangent exists in the sense of Definition 4.3, then no tangent exists in the sense of Definition 4.2 for $s = 1$.

The advantage of using the 1-Hausdorff content is that it is particularly easy to manage in the case of curves, as shown in the following lemma.

Lemma 4.5. *Let $f : \mathbb{R} \to \mathbb{R}^n$ be a continuous curve and $a, b \in \mathbb{R}$ such that $a < b$. Then,*

$$\mathcal{H}^1_\infty(f([a,b])) = \operatorname{diam}(f([a,b])).$$

Also, let $x \in \mathbb{R}$, $r > 0$ and assume there exists $\epsilon > 0$ such that either $f(x+\epsilon) \notin B(f(x),r)$ or $f(x-\epsilon) \notin B(f(x),r)$. Then,

$$r \leq \mathcal{H}^1_\infty\left(f(\mathbb{R}) \cap B(f(x),r)\right) \leq 2r.$$

Proof. We postpone the proof to the end of the subsection. □

An immediate consequence of Lemma 4.5 is that condition (4.3) is redundant.

Lemma 4.6. *Let $f : \mathbb{R} \to \mathbb{R}^n$ be a continuous, non-constant curve and $F = f(\mathbb{R})$. Then, for every $x \in \mathbb{R}$ and for small enough $r > 0$,*

$$\frac{1}{2} \leq \frac{\mathcal{H}^1_\infty(F \cap B(f(x),r))}{2r} \leq 1.$$

Proof. Let $x \in \mathbb{R}$. Since f is not a constant, the exists $y \in \mathbb{R}$ such that $f(x) \neq f(y)$. Call $r_x = |f(y) - f(x)| > 0$, so $f(y) \notin B(f(x),r)$ for every $r < r_x$. By the second part of Lemma 4.5 we get

$$r \leq \mathcal{H}^1_\infty\left(f(\mathbb{R}) \cap B(f(x),r)\right) \leq 2r, \qquad \forall r < r_x.$$

□

Remark 4.7. One could also state Definition 4.3 with the s-Hausdorff content

$$\mathcal{H}^s_\infty(F) = \inf\left\{ \sum_{i\in I} (\operatorname{diam} U_i)^s : F \subset \bigcup_{i\in I} U_i, \;\; I \text{ countable} \right\}$$

instead of $\mathcal{H}^1_\infty$, and ask whether $\phi(\mathbb{R})$ has a tangent for the cases of interest $1 \leq s \leq 4/3$. Then, the arguments in Remark 4.4 would also apply here so that we could obtain results in the sense of Definition 4.2 for every $1 \leq s \leq 4/3$. However, complications arise due to the lack of an analogue to the very useful Lemma 4.5. In any case, as we will see, the proof for the non-existence of tangents in the $\mathcal{H}^1_\infty$ setting is based on a parametric approach (see Section 4.2) independent of the measure chosen and the dimension of the set, which suggests that no tangent should exist in the $\mathcal{H}^s_\infty$ setting. To clarify this and to prove it rigorously is a future work deeply related to the computation of the Hausdorff dimension of $\phi(\mathbb{R})$.

To finish this subsection, let us prove Lemma 4.5, which is based in the following two auxiliary lemmas

Lemma 4.8. *Let $A, B \subset \mathbb{R}^n$. If $\overline{A} \cap \overline{B} \neq \emptyset$, then*

$$\operatorname{diam}(A \cup B) \leq \operatorname{diam} A + \operatorname{diam} B.$$

Proof. Let $x, y \in A \cup B$. If $x, y \in A$, then $|x - y| \leq \operatorname{diam} A$, and if $x, y \in B$, then $|x - y| \leq \operatorname{diam} B$. In any other case, let $z \in \overline{A} \cap \overline{B}$ so that $|x - y| \leq |x - z| + |z - y| \leq \operatorname{diam} A + \operatorname{diam} B$. □

Lemma 4.9. *Let $f : \mathbb{R} \to \mathbb{R}^n$ be a continuous function and $a, b \in \mathbb{R}$ such that $a < b$. Let $N \in \mathbb{N}$ and $U_1, \ldots, U_N \subset \mathbb{R}^n$ a minimal covering by open sets of $f([a, b])$. Then, the sets $U_1, \ldots, U_N$ can be reordered so that*

$$U_{k+1} \cap \bigcup_{i=1}^{k} U_i \neq \emptyset, \qquad \forall k \in \{1, \ldots, N-1\}.$$

Proof. Define $g(x) = f(a + (b - a)x)$ to rescale the interval $[a, b]$ to $[0, 1]$. We prove it by induction on k. For $k = 1$, choose U_1 such that $g(0) \in U_1$, and define

$$\epsilon_1 = \sup\{\, \epsilon \in [0, 1] \quad : \quad g([0, \epsilon]) \subset U_1 \,\}.$$

If $\epsilon_1 = 1$, then $N = 1$ and we are done. If not, $g(\epsilon_1) \in \partial U_1$. In particular, $g(\epsilon_1) \notin U_1$ because U_1 is open, so $\exists U_2 \neq U_1$ such that $g(\epsilon_1) \in U_2$. Moreover, since U_2 is also open, $U_1 \cap U_2 \neq \emptyset$.

Assume now that $U_1, \ldots, U_k$ are ordered according to the statement and define

$$\epsilon_k = \sup\{\, \epsilon \in [0, 1] \quad : \quad g([0, \epsilon]) \subset \bigcup_{i=1}^{k} U_i \,\}.$$

If $\epsilon_k = 1$, then $N = k$ and we are done. If not, $g(\epsilon_k) \in \partial\left(\bigcup_{i=1}^{k} U_i\right)$, and since all $U_1, \ldots, U_k$ are open, $g(\epsilon_k) \notin \bigcup_{i=1}^{k} U_i$. Then, there exists U_{k+1} different from the previous ones such that $g(\epsilon_k) \in U_{k+1}$. Moreover, U_{k+1} is also open, so $U_{k+1} \cap \bigcup_{i=1}^{k} U_i \neq \emptyset$. □

Proof of Lemma 4.5. For the first part, $f([a,b])$ covers itself, so

$$\mathcal{H}^1_\infty(f([a,b])) \leq \operatorname{diam} f([a,b]).$$

Let $\{U_i\}_{i\in I}$ be a covering by open sets of $f([a,b])$. By compactness, we may extract a finite subcovering $\{U_i\}_{i=1}^N$, where $N \in \mathbb{N}$. Then,

$$\operatorname{diam}(f([a,b])) \leq \operatorname{diam}\left(\bigcup_{i=1}^N U_i\right) \leq \sum_{i=1}^N \operatorname{diam} U_i \leq \sum_{i\in I} \operatorname{diam} U_i,$$

where the second inequality holds by Lemma 4.9 and induction on Lemma 4.8. As a consequence, $\operatorname{diam} f([a,b]) \leq \mathcal{H}^1_\infty(f([a,b]))$.

For the second part, the upper bound is trivial if we choose $B(f(x),r)$ as a covering. Assume there exists $\epsilon > 0$ such that $f(x+\epsilon) \notin B(f(x),r)$ and define

$$\epsilon_0 = \sup\{\, \epsilon > 0 \quad : \quad f([x,x+\epsilon]) \subset B(f(x),r)\,\}.$$

Then, $f(x+\epsilon_0) \in \partial B(f(x),r)$, so $|f(x+\epsilon_0) - f(x)| = r$. By the first part,

$$\begin{aligned}\mathcal{H}^1_\infty(f(\mathbb{R}) \cap B(f(x),r)) &\geq \mathcal{H}^1_\infty(f((x,x+\epsilon_0)) \cap B(f(x),r)) \\ &= \mathcal{H}^1_\infty(f((x,x+\epsilon_0))) \\ &= \operatorname{diam}(f((x,x+\epsilon_0))) \\ &\geq |f(x+\epsilon_0) - f(x)| = r.\end{aligned}$$

The case where an $\epsilon > 0$ exists such that $f(x-\epsilon) \notin B(f(x),r)$ is analogous. □

4.2 A parametric approach

Definition 4.3 suits the characteristics of $F = \phi(\mathbb{R})$, but it does not suggest any direct method to work with the parametrisation ϕ. In the rest of this subsection, we look for an alternative definition using some parametrisation of the curve and relate it to the geometric approach.

When looking for a tangent at $\phi(x)$, since ϕ is not injective, we propose to work only with points which are close to $\phi(x)$ in parameter; in other words, to consider only $\phi((x-\delta, x+\delta))$ for some convenient $\delta > 0$. Also, in Figure 4.1B we see that Riemann's function may approach a given point from different directions on the right and on the left. To describe this behaviour, we propose to define tangents on the right, looking only at $\phi((x,x+\delta))$, and on the left, looking only at $\phi((x-\delta,x))$, for some $\delta > 0$. Thus, instead of using double cones S_D, we use single cones $S(x,\mathbb{V},\varphi)$ consisting on the closure of the set of points $y \in \mathbb{R}^n$ such that $y - x$ forms with $\mathbb{V}$ an angle of at most $\varphi/2$ (see figure 4.3B). Following the idea of condition (4.3), we propose the following definition.

Definition 4.10. Let $f : \mathbb{R} \to \mathbb{R}^n$ be a continuous curve and $x \in \mathbb{R}$. We say that f has a **tangent on the right** at x in direction $\mathbb{V} \in \mathbb{S}^{n-1}$ if

$$\forall \varphi > 0, \qquad \exists \delta_\varphi > 0 \qquad \text{such that} \qquad f((x,x+\delta_\varphi)) \subset S(f(x),\mathbb{V},\varphi).$$

We say that f has a **tangent on the left** at x in direction $\mathbb{V}$ if

$$\forall \varphi > 0, \qquad \exists \delta_\varphi > 0 \qquad \text{such that} \qquad f((x-\delta_\varphi,x)) \subset S(f(x),\mathbb{V},\varphi).$$

We say that f has a **tangent** at x if it has both tangents on the right and on the left and if their directions are diametrically opposite.

Remark 4.11. Using Definition 4.10, we might want to derive tangency properties for a set $F \subset \mathbb{R}^n$ which is parametrised by a continuous function $f : \mathbb{R} \to \mathbb{R}^n$ satisfying $f(\mathbb{R}) = F$. The obvious choice is saying that F has a tangent in $f(x)$ if f has a tangent in x. However, this definition depends on the chosen parametrisation f and may yield many undesirable results. For example, if we parametrise the real axis in $\mathbb{R}^2 \simeq \mathbb{C}$, which should have tangent $1 \in \mathbb{S}^1$ everywhere, using the function

$$x \mapsto (f(x), 0), \qquad \text{where} \qquad f(x) = \begin{cases} x, & x < 0, \\ 0, & 0 < x < 1, \\ x - 1, & x \geq 1, \end{cases}$$

then every $\mathbb{V} \in \mathbb{S}^1$ is a tangent of f in $1/2$, which would mean that every direction is a tangent to the real axis at the origin.

Remark 4.11 shows that Definition 4.10 is too weak to determine a geometric tangent. Nevertheless, we focus on the reverse direction of the reasoning, since according to the following proposition, Definition 4.3 implies Definition 4.10.

Proposition 4.12. *Let $f : \mathbb{R} \to \mathbb{R}^n$ be a continuous function, $F = f(\mathbb{R})$, $x \in \mathbb{R}$ and $\mathbb{V} \in \mathbb{S}^{n-1}$. Then, condition (4.3) rewritten as*

$$\lim_{r \to 0} \frac{\mathcal{H}^1_\infty \left((F \cap B(f(x), r)) \setminus S_D(f(x), \mathbb{V}, \varphi) \right)}{r} = 0, \qquad \forall \varphi > 0,$$

implies that

$$\forall \varphi > 0, \quad \exists \delta_\varphi > 0 \quad : \quad f((x - \delta_\varphi, x + \delta_\varphi)) \subset S_D(f(x), \mathbb{V}, \varphi).$$

Proof. By contradiction, assume there exists $\varphi_0 > 0$ such that for every $\delta > 0$ we have

$$f((x - \delta, x + \delta)) \not\subset S_D(f(x), \mathbb{V}, \varphi_0).$$

Then, there exists a sequence of real numbers $(\delta_n)_{n \in \mathbb{N}}$, which we can assume to be positive (after extracting the subsequence of all positive or all negative terms, and if they are negative the proof is analogous), with $\lim_{n \to \infty} \delta_n = 0$ such that $f(x + \delta_n) \notin S_D(f(x), \mathbb{V}, \varphi_0)$. This property also holds for any cone with an angle $\varphi < \varphi_0$. Define

$$\sigma_n = \sup\{\sigma > 0 \quad : \quad f((x + \delta_n - \sigma, x + \delta_n)) \cap S_D(f(x), \mathbb{V}, \varphi/2) = \emptyset\}.$$

By continuity of f, $0 < \sigma_n \leq \delta_n$, and also $f(x + \delta_n - \sigma_n) \in \partial S_D(f(x), \mathbb{V}, \varphi/2)$. Call

$$F_n = f((x + \delta_n - \sigma_n, x + \delta_n)),$$

so that $F_n \cap S_D(f(x), \mathbb{V}, \varphi/2) = \emptyset$. Define

$$r_n = \sup\{|y - f(x)| \quad : \quad y \in F_n\},$$

so $\lim_{n \to \infty} r_n = 0$ because $0 < \sigma_n \leq \delta_n \to 0$. Now, since $F_n \subset F$ and $F_n \subset B(f(x), r_n)$, by Lemma 4.5 we may write

$$\begin{aligned} &\mathcal{H}^1_\infty \left((F \cap B(f(x), r_n)) \setminus S_D(f(x), \mathbb{V}, \varphi/2) \right) \\ &\quad \geq \mathcal{H}^1_\infty \left((F_n \cap B(f(x), r_n)) \setminus S_D(f(x), \mathbb{V}, \varphi/2) \right) \\ &\quad = \mathcal{H}^1_\infty (F_n) = \operatorname{diam} F_n. \end{aligned}$$

We analyse two cases now.

- If $\operatorname{dist}(f(x), f(x+\delta_n)) \leq r_n/2$, then

$$\operatorname{dist}(f(x+\delta_n), \partial B(f(x), r_n)) \geq r_n/2.$$

  Hence, by the definition of r_n, we get $\operatorname{diam} F_n \geq r_n/2$.

- Else, if $\operatorname{dist}(f(x), f(x+\delta_n)) > r_n/2$, we have

$$f(x+\delta_n) \in A(f(x), r_n/2, r_n) \setminus S_D(f(x), \mathbb{V}, \varphi).$$

  Also, since $f(x+\delta_n-\sigma_n) \in \partial S_D(f(x), \mathbb{V}, \varphi/2)$, we have

$$\begin{aligned}\operatorname{diam} F_n &\geq \operatorname{dist}\left(f(x+\delta_n), f(x+\delta_n-\sigma_n)\right)\\ &\geq \operatorname{dist}\left(f(x+\delta_n), S_D(f(x), \mathbb{V}, \varphi/2)\right)\end{aligned}$$

  and also

$$\begin{aligned}&\operatorname{dist}\left(f(x+\delta_n), S_D(f(x), \mathbb{V}, \varphi/2)\right)\\ &\qquad \geq \operatorname{dist}\left(A(f(x), r_n/2, r_n) \setminus S_D(f(x), \mathbb{V}, \varphi), S_D(f(x), \mathbb{V}, \varphi/2)\right)\\ &\qquad = \frac{r_n}{2}\sin\left(\varphi/4\right).\end{aligned}$$

In short, we always get

$$\operatorname{diam} F_n \geq \frac{r_n}{2}\min\left(1, \sin\left(\varphi/4\right)\right),$$

so

$$\frac{\mathcal{H}^1_\infty\left(\left(F \cap B(f(x), r_n)\right) \setminus S_D(f(x), \mathbb{V}, \varphi/2)\right)}{r_n} \geq \frac{\min\left(1, \sin\left(\varphi/4\right)\right)}{2} > 0, \qquad \forall n \in \mathbb{N},$$

holds for every $0 < \varphi < \varphi_0$. Since $\lim_{n\to\infty} r_n = 0$, the limit in the statement cannot hold. □

Corollary 4.13. *Let $f : \mathbb{R} \to \mathbb{R}^n$ be a continuous and non-constant function, $F = f(\mathbb{R})$, $x \in \mathbb{R}$ and $\mathbb{V} \in \mathbb{S}^{n-1}$. If $\mathbb{V}$ is a tangent of F at $f(x)$ in the sense of Definition 4.3, then it is a tangent of f at x in the sense of Definition 4.10.*

In other words, if $\mathbb{V}$ is not a tangent of f at x, then it is not a tangent of F in $f(x)$.

Remark 4.14. Condition (4.3) is independent of f, so the conclusion in Proposition 4.12 holds for **every** parametrisation f of F. Thus, according to Corollary 4.13, given a curve-like set $F \subset \mathbb{R}^n$ and $y \in F$, in order to conclude that $\mathbb{V} \in \mathbb{S}^{n-1}$ is not a tangent of F at y, it is enough to find an appropriate parametrisation f and $x \in \mathbb{R}$ with $f(x) = y$ not allowing $\mathbb{V}$ as a tangent in x. For instance, in the example of Remark 4.11, f allowed $i \in \mathbb{S}^1 \subset \mathbb{C}$ as a tangent in $1/2$, but i is not a tangent of the parametrisation $g(x) = x$ at 0. Corollary 4.13 implies that, as expected, i is not a tangent of the real line at the origin.

Definition 4.10 makes the vector $f(x+r) - f(x)$ converge to the direction $\mathbb{V}$ when $r \to 0$. In the following lemma, we give a more direct way to work with the parametrisation in case $f(x+r) - f(x) \neq 0$.

Lemma 4.15. *Let $f : \mathbb{R} \to \mathbb{R}^n$ be a continuous curve and $x \in \mathbb{R}$. Then, f has a tangent on the right at x in direction $\mathbb{V} \in \mathbb{S}^{n-1}$ if and only if for every sequence $(r_n)_{n\in\mathbb{N}}$ satisfying $r_n > 0$, $f(x + r_n) - f(x) \neq 0$ for all $n \in \mathbb{N}$ and $\lim_{n\to\infty} r_n = 0$ we have*

$$\lim_{n\to\infty} \frac{f(x + r_n) - f(x)}{|f(x + r_n) - f(x)|} = \mathbb{V}.$$

Moreover, if one of such sequences exists, then the tangent is unique.

The same result applies for tangents on the left by changing $f(x+r_n)$ for $f(x-r_n)$.

Proof. The proof consists in writing the cone condition in Definition 4.10 in terms of the vector $f(x + r) - f(x)$ for $r > 0$. The formulation in terms of sequences comes from the need to take care of the cases $f(x + r) = f(x)$, where the direction of $f(x + r) - f(x) = 0$ is not well-defined.

On the other hand, if f has tangents $\mathbb{V}_1$ and $\mathbb{V}_2$ in x and if there exists a sequence $(r_n)_n$ as above, then

$$\mathbb{V}_1 = \lim_{n\to\infty} \frac{f(x + r_n) - f(x)}{|f(x + r_n) - f(x)|} = \mathbb{V}_2,$$

so the tangent, if it exists, is unique. □

Remark 4.16. Lemma 4.15 shows that the situation of Remark 4.11 is the only one in which we may have problems to compute tangents. Indeed, ambiguity will only arise in case the parametrisation is constant in a neighbourhood of x.

4.3 Main result

Once the definition of a tangent has been settled, let us rewrite Theorem 4.1 according to it.

Theorem 4.17. *Let ϕ be Riemann's non-differentiable function (2.1), $t \in \mathbb{R}$ and $\mathbb{V} \in \mathbb{S}^1$. Then, $\mathbb{V}$ is not a tangent of $\phi(\mathbb{R})$ in $\phi(t)$ in the sense of Definition 4.3.*

As we said in Section 2.1, by the periodic property of ϕ (2.2), the set $\phi(\mathbb{R})$ can be seen as a countable union of translates of $\phi([0, 1/(2\pi)])$ as in (2.3), so tangency properties will be determined by what happens in this latter set. Hence, it suffices to prove Theorem 4.17 for $\phi([0, 1/(2\pi)])$. Also, by Corollary 4.13, it is enough to prove that for any given $x \in [0, 1]$, no $\mathbb{V} \in \mathbb{S}^1$ is a tangent of ϕ in t_x in the sense of Definition 4.10. Last, to prove this we will use the characterisation given in Lemma 4.15.

The main result in this section is the upcoming Theorem 4.18. When $x \in [0, 1]\cap\mathbb{Q}$, two different cases were predicted in Figure 4.1. In the rationals corresponding to the corner in Figure 4.1B, we will see that both side limits of the limit in Lemma 4.15 exist, but that they are perpendicular and hence they do not coincide. On the other hand, in the rest of rationals corresponding to the spiral in Figure 4.1A, the limit in Lemma 4.15 can take any value in $\mathbb{S}^1$. Finally, if $x \in [0, 1] \setminus \mathbb{Q}$, we will show that the limit in Lemma 4.15 can take any value in an open set of $\mathbb{S}^1$. In the three cases, Lemma 4.15 shows that ϕ has no tangent in the corresponding point, hence Theorem 4.17.

Theorem 4.18. *Let ϕ be Riemann's non-differentiable function (2.1) and $x = p/q \in [0, 1] \cap \mathbb{Q}$ an irreducible fraction with $q > 0$.*

(a) If $q \equiv 0, 1, 3 \pmod 4$, there exists $e_{p,q} \in \mathbb{S}^1$ an eighth root of unity such that

$$\lim_{r\to 0^+} \frac{\phi(t_{p,q}+r)-\phi(t_{p,q})}{|\phi(t_{p,q}+r)-\phi(t_{p,q})|} = e_{p,q}\frac{1+i}{\sqrt{2}}$$

and

$$\lim_{r\to 0^+} \frac{\phi(t_{p,q}-r)-\phi(t_{p,q})}{|\phi(t_{p,q}-r)-\phi(t_{p,q})|} = e_{p,q}\frac{1-i}{\sqrt{2}}.$$

(b) If $q \equiv 2 \pmod 4$, then for any $\mathbb{V} \in \mathbb{S}^1$, there exist sequences $r_n, s_n \to 0^+$ (when $n \to \infty$) such that

$$\lim_{n\to\infty} \frac{\phi(t_{p,q}+r_n)-\phi(t_{p,q})}{|\phi(t_{p,q}+r_n)-\phi(t_{p,q})|} = \mathbb{V} = \lim_{n\to\infty} \frac{\phi(t_{p,q}-s_n)-\phi(t_{p,q})}{|\phi(t_{p,q}-s_n)-\phi(t_{p,q})|}$$

Let $x = \rho \in [0,1] \setminus \mathbb{Q}$.

(c) There exists an open set $V \subset \mathbb{S}^1$ such that for any $\mathbb{V} \in V$, there exists a sequence $r_n \to 0$ (when $n \to \infty$) such that

$$\lim_{n\to\infty} \frac{\phi(t_{\rho}+r_n)-\phi(t_{\rho})}{|\phi(t_{\rho}+r_n)-\phi(t_{\rho})|} = \mathbb{V}.$$

The cases (a) and (b) will easily follow from the asymptotic behaviour of ϕ around rationals that was computed in Section 2.2, in Propositions 2.12 and 2.15. However, the lack of the asymptotic behaviour around irrationals makes the case (c) more complicated. The proof will be based in the continued fraction approximations and the asymptotic behaviour around them. We prove each part of Theorem 4.18 separately in the upcoming subsections in the form of Propositions 4.19, 4.20 and 4.21.

4.4 Lack of tangents in $t_{p,q}$ such that $q \equiv 0, 1, 3 \pmod 4$

In this section, we prove part (a) of Theorem 4.18 in the form of Proposition 4.19. As we already suggested, we will use the asymptotic behaviour of ϕ around $t_{p,q}$ that we proved in Proposition 2.12 in Subsection 2.2.6. Among the three versions of the asymptotic behaviour we gave there, we will use the first one (2.59), from which we directly deduce

$$\lim_{h\to 0^+} \frac{\phi(t_{p,q}+h)-\phi(t_{p,q})}{e_{p,q}\frac{1+i}{\sqrt{2\pi}}\frac{h^{1/2}}{\tilde{q}^{1/2}}} = 1.$$

The term in the denominator is the parametrisation of a straight line with direction $e_{p,q}(1+i)/\sqrt{2}$, so we expect that $\phi([0, 1/(2\pi)])$ has a tangent to the right of $t_{p,q}$ given by $e_{p,q}(1+i)/\sqrt{2}$.

Proposition 4.19. *Let $p, q \in \mathbb{N}$ be such that $q > 0$, $\gcd(p,q) = 1$ and $q \equiv 0, 1, 3 \pmod 4$. Then,*

$$\lim_{h\to 0^+} \frac{\phi(t_{p,q}+h)-\phi(t_{p,q})}{|\phi(t_{p,q}+h)-\phi(t_{p,q})|} = e_{p,q}\frac{1+i}{\sqrt{2}},$$

so ϕ has a tangent on the right at $t_{p,q}$ in direction $e_{p,q}(1+i)/\sqrt{2}$. Also,

$$\lim_{h\to 0^+} \frac{\phi(t_{p,q}-h)-\phi(t_{p,q})}{|\phi(t_{p,q}-h)-\phi(t_{p,q})|} = e_{p,q}\frac{1-i}{\sqrt{2}},$$

so it has a tangent on the left in direction $e_{p,q}\,(1-i)/\sqrt{2}$.

Proof. It is enough to work with the shortened version of the asymptotic (2.59)

$$\phi(t_{p,q}+h)-\phi(t_{p,q}) = e_{p,q}\,\frac{1+i}{\sqrt{2\pi}}\,\frac{h^{1/2}}{\tilde{q}^{1/2}} + O\left(q^{3/2}h^{3/2}\right),$$

which we can do because we will take the limit $h\to 0$ eventually. Let $h>0$. Then,

$$\frac{\phi(t_{p,q}+h)-\phi(t_{p,q})}{|\phi(t_{p,q}+h)-\phi(t_{p,q})|} = \frac{e_{p,q}\frac{1+i}{\sqrt{2\pi}}\frac{h^{1/2}}{\tilde{q}^{1/2}}\left(1+O(q^2h)\right)}{\frac{1}{\sqrt{\pi}}\frac{h^{1/2}}{\tilde{q}^{1/2}}\,|1+O(q^2h)|} = e_{p,q}\frac{1+i}{\sqrt{2}}\frac{1+O(q^2h)}{|1+O(q^2h)|},$$

so

$$\lim_{h\to 0^+}\frac{\phi(t_{p,q}+h)-\phi(t_{p,q})}{|\phi(t_{p,q}+h)-\phi(t_{p,q})|} = e_{p,q}\frac{1+i}{\sqrt{2}}.$$

On the other hand, with the branch $\sqrt{-1}=-i$,

$$\phi(t_{p,q}-h)-\phi(t_{p,q}) = e_{p,q}\,\frac{1-i}{\sqrt{2\pi}}\,\frac{h^{1/2}}{\tilde{q}^{1/2}} + O\left(q^{3/2}h^{3/2}\right).$$

The same procedure as above shows that

$$\lim_{t\to 0}\frac{\phi(t_{p,q}-h)-\phi(t_{p,q})}{|\phi(t_{p,q}-h)-\phi(t_{p,q})|} = e_{p,q}\frac{1-i}{\sqrt{2}}.$$

□

4.5 Lack of tangents in $t_{p,q}$ such that $q \equiv 2 \pmod 4$

We now prove part (b) of Theorem 4.18, which we state again in Proposition 4.20. In this case, we will use the asymptotic behaviour (2.66) that we gave in Proposition 2.15 of Subsection 2.2.7. The reason for which ϕ does not have a tangent in these points is that it follows a spiralling pattern generated by Z_1, as we said in the end of Subsection 2.2.5. Therefore, there will be parts of the curve in every direction arbitrarily close to the point.

Proposition 4.20. *Let* $p,q\in\mathbb{N}$ *be such that* $q>0$, $\gcd(p,q)=1$ *and* $q\equiv 2 \pmod 4$. *For any* $\mathbb{V}\in\mathbb{S}^1$, *there exist sequences* $r_n, s_n\to 0^+$ *(when* $n\to\infty$*) such that*

$$\lim_{n\to\infty}\frac{\phi(t_{p,q}+r_n)-\phi(t_{p,q})}{|\phi(t_{p,q}+r_n)-\phi(t_{p,q})|} = \mathbb{V} = \lim_{n\to\infty}\frac{\phi(t_{p,q}-s_n)-\phi(t_{p,q})}{|\phi(t_{p,q}-s_n)-\phi(t_{p,q})|}$$

Proof. Let $h>0$, so

$$\begin{aligned}\frac{\phi(t_{p,q}+h)-\phi(t_{p,q})}{|\phi(t_{p,q}+h)-\phi(t_{p,q})|} &= \frac{-16\,e_{p,q}\,\frac{1-i}{\sqrt{2\pi}}\,\tilde{q}^{3/2}\,h^{3/2}\,\left(Z_1(b(h))+O(q^2h)\right)}{16\,\frac{1}{\sqrt{\pi}}\,\tilde{q}^{3/2}\,h^{3/2}\,|Z_1(b(h))+O(q^2h)|}\\ &= -e_{p,q}\,\frac{1-i}{\sqrt{2}}\,\frac{Z_1(b(h))+O(q^2h)}{|Z_1(b(h))+O(q^2h)|}.\end{aligned}$$

To take the limit when $h\to 0$, we need to understand $\lim_{h\to 0} Z_1(b(h))$ which, by continuity of Z_1 and since $b(h)\sim\tilde{q}^2h$ are equivalent infinitesimals, can be written as

$$\lim_{h\to 0} Z_1(b(h)) = \lim_{h\to 0} Z_1(\tilde{q}^2h) = \lim_{t\to+\infty} Z_1\left(\tilde{q}^2t^{-1}\right).$$

The function $Z_1(\tilde{q}^2/\cdot)$ has period $32\pi\tilde{q}^2$. Moreover,

$$Z_1(\tilde{q}^2 t^{-1}) = e^{-i\frac{t}{16\tilde{q}^2}} + \sum_{\substack{k=3\\ k \text{ odd}}}^{\infty} \frac{e^{-i\frac{k^2}{16\tilde{q}^2}t}}{k^2} \in B\left(e^{-i\frac{t}{16\tilde{q}^2}}, 1/4\right)$$

because $\sum_{\substack{k=3\\ k \text{ odd}}}^{\infty} k^{-2} = \pi^2/8 - 1 \leq 1/4$, so

$$\arg Z_1(\tilde{q}^2 t^{-1}) = -\frac{t}{16\tilde{q}^2} + \eta(t) \qquad \text{such that} \qquad |\eta(t)| \leq \frac{\pi}{4}.$$

From the fact that $\arg Z_1(\tilde{q}^2/(-48\pi\tilde{q}^2)) \geq 2\pi$ and $\arg Z_1(\tilde{q}^2/(16\pi\tilde{q}^2)) \leq 0$, by continuity and periodicity, the function $\arg Z_1(\tilde{q}^2 t^{-1})$ takes all possible values when $t \in [0, 32\pi\tilde{q}^2]$. In other words, for any $\zeta \in [0, 2\pi]$, there exists $t_\zeta \in [0, 32\pi\tilde{q}^2]$ such that $\arg Z_1(\tilde{q}^2 t_\zeta^{-1}) = \zeta$. Equivalently, for any $\mathbb{V} \in \mathbb{S}^1$, there exists $t_{\mathbb{V}} \in [0, 32\pi\tilde{q}^2]$ such that $Z_1(\tilde{q}^2 t_{\mathbb{V}}^{-1})/|Z_1(\tilde{q}^2 t_{\mathbb{V}}^{-1})| = \mathbb{V}$. Choose $\tau_n = 32\pi\tilde{q}^2 n + t_{\mathbb{V}}$ so that $Z_1(\tilde{q}^2\tau_n^{-1})/|Z_1(\tilde{q}^2\tau_n^{-1})| = \mathbb{V}$ for all $n \in \mathbb{N}$. This way,

$$\lim_{n\to\infty} \frac{\phi(t_{p,q} + \tau_n^{-1}) - \phi(t_{p,q})}{|\phi(t_{p,q} + \tau_n^{-1}) - \phi(t_{p,q})|} = -e_{p,q}\frac{1-i}{\sqrt{2}} \lim_{n\to\infty} \frac{Z_1(\tilde{q}^2\tau_n^{-1})}{|Z_1(\tilde{q}^2\tau_n^{-1})|} = -e_{p,q}\frac{1-i}{\sqrt{2}}\mathbb{V}.$$

In the same way, choosing $\sigma_n = 32\pi\tilde{q}^2 n - t_{\mathbb{V}}$ for every $n \in \mathbb{N}$, recalling that $\sqrt{-1} = -i$, we get

$$\begin{aligned}
\lim_{n\to\infty} \frac{\phi(t_{p,q} - \sigma_n^{-1}) - \phi(t_{p,q})}{|\phi(t_{p,q} - \sigma_n^{-1}) - \phi(t_{p,q})|} &= -e_{p,q}\frac{1+i}{\sqrt{2}} \lim_{n\to\infty} \frac{Z_1(-\tilde{q}^2\sigma_n^{-1})}{|Z_1(-\tilde{q}^2\sigma_n^{-1})|} \\
&= -e_{p,q}\frac{1+i}{\sqrt{2}} \frac{Z_1(\tilde{q}^2 t_{\mathbb{V}}^{-1})}{|Z_1(\tilde{q}^2 t_{\mathbb{V}}^{-1})|} \\
&= -e_{p,q}\frac{1+i}{\sqrt{2}}\mathbb{V}.
\end{aligned}$$

□

4.6 Lack of tangents in t_x such that x is irrational

In this subsection we prove part (c) of Theorem 4.18 in the form of the following Proposition.

Proposition 4.21. *Let $\rho \in [0,1] \setminus \mathbb{Q}$. There exists an open set $V \subset \mathbb{S}^1$ such that for any $\mathbb{V} \in V$, there exists a sequence $r_n \to 0$ with $n \to \infty$ such that*

$$\lim_{n\to\infty} \frac{\phi(t_\rho + r_n) - \phi(t_\rho)}{|\phi(t_\rho + r_n) - \phi(t_\rho)|} = \mathbb{V}.$$

In the case of an irrational $\rho \in [0,1]$, we have no asymptotics to describe the behaviour of the curve around it. To overcome this difficulty, we will work with rational approximations p_n/q_n, $n \in \mathbb{N}$ and use the asymptotic behaviour $\phi(t_{p_n,q_n}+h) - \phi(t_{p_n,q_n})$ in Propositions 2.12 and 2.15 choosing $h = h_n = t_\rho - t_{p_n,q_n} = (\rho - p_n/q_n)/2\pi$. By letting $n \to \infty$ we will be able to analyse the behaviour of ϕ around t_ρ.

The asymptotic behaviour at a fixed point $t_{p,q}$ is precise when $h \to 0$. But even if $\lim_{n\to\infty} h_n = 0$, every value of $n \in \mathbb{N}$ corresponds to a different approximation

and therefore to a different asymptotic expression which depends on q_n. Therefore, $\phi(t_\rho)$ will enter the range of the asymptotic around $\phi(t_{p_n,q_n})$ only if $|h_n| \lesssim 1/q_n^2$ for every $n \in \mathbb{N}$, or at least for large values of $n \in \mathbb{N}$. Moreover, the asymptotic will be absolutely precise only if $|h_n| \ll 1/q_n^2$.

The approximations given by the continued fraction expression of ρ, which we call convergents, satisfy the conditions above stated, so we do an extensive use of them. In Appendix B, a review of the most basic yet most important properties concerning continued fractions is given, so we refer the reader there every time we mention such a property. One of those we have already used more than once, $|\rho - p_n/q_n| < q_n^{-2}$, which is satisfied for every $n \in \mathbb{N}$, see Proposition B.10. In order to work with a more precise measurement of this error, define $K_n = K_n(\rho)$ by

$$|\rho - p_n/q_n| = \frac{K_n}{q_n^2}\,, \qquad 0 < K_n < 1, \tag{4.4}$$

for all $n \in \mathbb{N}$, so that $h_n = (K_n/2\pi)/q_n^2$. According to the above, and also to the rescaled version (2.61) of the asymptotics, this is the correct scale to work with. Also, infinitely many convergents p_n/q_n are such that q_n is odd, see Proposition B.12. In that case, we can work only with (2.61), and moreover, according to (2.27), $\tilde{q} = q$ which simplifies notation. Hence, from now on, we work with the subsequence of these convergents, which for simplicity we rename again simply as p_n/q_n.

As we said, since $n \to \infty$, $q = q_n$ is no longer fixed and it has to be taken care of. Regarding this, the function $\beta(s)$ defined in (2.61) depends on q, so we write this explicitly as β_q so that

$$\beta_q(s) = \frac{s}{1 + 4\pi \frac{c_\pm}{q} s}.$$

In the case of the continued fraction approximations, for simplicity we denote

$$\beta_n(s) = \frac{s}{1 + 4\pi \frac{c_n}{q_n} s} \tag{4.5}$$

instead of $\beta_{q_n}(s)$, to express that the dependence is now on $n \in \mathbb{N}$. What is more, rather than on q_n, β_n depends on c_n/q_n, which is bounded by $1 \leq |c_n/q_n| \leq 4$.

According to the above, the position of t_ρ in the rescaled asymptotic (2.61) depends on the sequence $(K_n)_{n\in\mathbb{N}}$. Some properties concerning it are given in Appendix B.2. Since the approximation works when $n \to \infty$, a study of its limit, or at least of its behaviour when $n \to \infty$, is needed. However, it is easy to build examples in which $\lim_{n\to\infty} K_n$ does not exist, see Corollary B.14. In view of this, let

$$K = \liminf_{n\to\infty} K_n \tag{4.6}$$

and extract a second subsequence such that, after renaming it again as the original sequence, $\lim_{n\to\infty} K_n = K$. We see in Appendix B.2 that $K \in [0, 1/\sqrt{5}]$, and that there are numbers for which $K = 0$ and also for which $K = 1/\sqrt{5}$. Indeed, our approach depends very much on this value.

- $K > 0$ corresponds to the case $|h_n| \simeq 1/q_n^2$, and the rescaled asymptotic (2.61) will be somehow *stuck* away from the origin. We will first take a third subsequence to manage the effect of c_n/q_n so that the asymptotics in (2.61), which depend on c_n/q_n, tend to some *limit asymptotic*. The irrational point tends to stabilise somewhere far from the origin in this limit asymptotic. In this stable setting, we will be able to conclude.

- $K = 0$ corresponds to the case $|h_n| \ll 1/q_n^2$. In this case, the irrational point tends to the origin in the rescaled asymptotic (2.61). We need to rescale a second time to exploit the selfsimilar properties of F described in (2.60) and (2.61), which show that the better copies of itself are generated the closer we get to the origin. Once we detect the copy in which t_ρ is, we will be able to conclude and deduce that no tangent can exist.

Let us rewrite the asymptotic (2.61) at each of the approximations p_n/q_n evaluated in $h = h_n = K_n/2\pi$. For that, taking into account that the main parameter is now $n \in \mathbb{N}$ and thus writing $e_{p_n,q_n} = e_n$, define the rescaled asymptotic

$$\begin{aligned} H_n(s) &= \sqrt{s} + 4i\, Y_1(\beta_n(s))\, s^{3/2} + O(s^{5/2}) \\ &= \frac{3}{2}\left(\sqrt{s} + \frac{8\pi^2}{3} i \left(\frac{1}{6} - \frac{i}{2\pi}\frac{c_n}{q_n} - 2\phi\left(\frac{-1}{16\pi^2\beta_n(s)}\right)\right) s^{3/2} + O\left(s^{5/2}\right)\right). \end{aligned} \tag{4.7}$$

so that for every $n \in \mathbb{N}$ we have

$$\phi\left(t_{p_n,q_n} + s/q_n^2\right) - \phi(t_{p_n,q_n}) = \frac{1+i}{\sqrt{2\pi}} \frac{e_n}{q_n^{3/2}} H_n(s), \tag{4.8}$$

and

$$\phi\left(t_\rho\right) - \phi(t_{p_n,q_n}) = \frac{1+i}{\sqrt{2\pi}} \frac{e_n}{q_n^{3/2}} H_n\left(\frac{K_n}{2\pi}\right). \tag{4.9}$$

In the case $K > 0$, we will use the first expression in (4.7), while when $K = 0$ the second expression will prove itself more useful.

Before splitting the analysis into the cases $K = 0$ and $K > 0$, we remark that the convergents approach ρ alternately from the right and from the left (Proposition B.8), but after having extracted subsequences, this may no longer be true. However, either the convergents on the right or those on the left must be infinitely many. We extract this infinite subsequence so that every convergent is on the same side of ρ. Moreover, we may assume they are on the left, so $\rho - \rho_n > 0$, and therefore work with $s > 0$ and with $c_n = (c_\pm)_n = (c_+)_n > 0$ in (4.7). Indeed, if this was not the case, the asymptotics (4.7) are also valid with $s = -|s| < 0$ recalling that $\sqrt{-1} = -i$, and the proof is analogous.

Remark 4.22. Let us sum up the subsequences we have extracted from the original sequence of convergents p_n/q_n:

- q_n is odd, so $\tilde{q}_n = q_n$ and the corresponding asymptotic behaviour is (4.9).
- $\lim_{n\to\infty} K_n = K \in [0, 1/\sqrt{5}]$,
- All p_n/q_n approach ρ from the left, so we work with $s > 0$ in (4.7).

4.6.1 $K > 0$

In this case, in the setting of the asymptotic (4.7), the position of t_ρ tends to stabilise somewhere far from the origin. However, there are two drawbacks to be solved:

(i) The asymptotic (4.7) depends on $n \in \mathbb{N}$.

(ii) Since $s = K_n/2\pi \to K/2\pi > 0$, we lack control of the error term in (4.7).

To solve the second issue, from (2.55) in Subsection 2.2.6 we recover a closed expression for (4.7),

$$H_n(s) = \sqrt{\pi}\frac{1-i}{\sqrt{2}}\left(\frac{\phi(\beta_n(s))}{(1-4\pi\frac{c_n}{q_n}\beta_n(s))^{3/2}} - 6\pi\frac{c_n}{q_n}\int_0^{\beta_n(s)}\frac{\phi(r)}{(1-4\pi\frac{c_n}{q_n}r)^{5/2}}\,dr\right), \quad (4.10)$$

where there is no longer an error term. On the other hand, regarding problem (i), let

$$a = \liminf_{n\to\infty}\frac{c_n}{q_n} \in [1,4] \quad (4.11)$$

and take a subsequence of the approximations which, after relabelling, satisfies

$$\lim_{n\to\infty} c_n/q_n = a.$$

Since (4.10) depends only on c_n/q_n (because so does β_n), we expect it to converge to

$$\begin{aligned} H(s) &= \sqrt{\pi}\frac{1-i}{\sqrt{2}}\left(\frac{\phi(\beta(s))}{(1-4\pi a\beta(s))^{3/2}} - 6\pi a\int_0^{\beta(s)}\frac{\phi(r)}{(1-4\pi ar)^{5/2}}\,dr\right) \\ &= \sqrt{s} + 4i\,Y_1(\beta\,(s))\,s^{3/2} + O(s^{5/2}), \end{aligned} \quad (4.12)$$

where

$$\beta(s) = \lim_{n\to\infty}\beta_n(s) = \frac{s}{1+4\pi as}. \quad (4.13)$$

We remark a small overlap of notation here, since in Subsection 2.2.6 q was fixed and we denoted $\beta_q(s) = \beta(s)$, while here $q = q_n$ varies and $\beta(s) = \lim_{n\to\infty}\beta_{q_n}(s)$. However, in this context where we make the dependence on q_n explicit, this should not be problematic.

We show in Lemma 4.23 that H_n converges uniformly to H.

Lemma 4.23. *Let $M > 0$. The sequence of functions H_n converges uniformly to H in $[0, M]$. In other words,*

$$\lim_{n\to\infty}\|H_n - H\|_{L^\infty([0,M])} = 0.$$

Proof. See Subsection 4.6.3. □

To prove Proposition 4.21, we use the characterisation with limits in Lemma 4.15 with the convergents p_n/q_n. The idea is that, apart from $\phi(t_{p_n,q_n})$, we use alternative approximations lying between t_ρ and t_{p_n,q_n}, each of them leading to a different tangent (see Figure 4.4).

Following Lemma 4.15 and (4.9), we compute

$$\lim_{n\to\infty}\frac{\phi(t_{p_n,q_n}) - \phi(t_\rho)}{|\phi(t_{p_n,q_n}) - \phi(t_\rho)|} = -\frac{1+i}{\sqrt{2}}\lim_{n\to\infty} e_n\frac{H_n(K_n/2\pi)}{|H_n(K_n/2\pi)|}. \quad (4.14)$$

From Lemma 4.23 and $\lim_{n\to\infty} K_n = K > 0$, we deduce that $\lim_{n\to\infty} H_n(K_n/2\pi) = H(K/2\pi)$. The cases $H(K/2\pi) \neq 0$ and $H(K/2\pi) = 0$ will require different approaches.

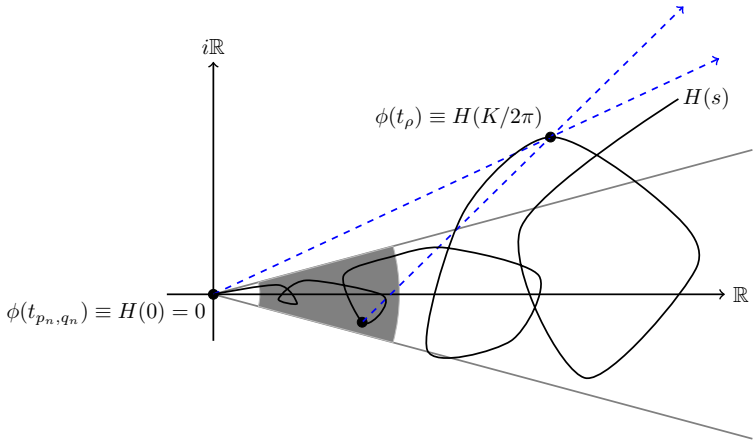

FIGURE 4.4: Schematic representation of the curve $H(s)$. According to Lemma 4.23 and to (4.9), the $q_n^{3/2}$-rescaled neighbourhood of $\phi(t_\rho)$ converges to this situation when $n \to \infty$. As approximations to $\phi(t_\rho)$, we use $\phi(t_{p_n,q_n})$ (the origin in the picture), but we might also use any other point between $\phi(t_{p_n,q_n})$ and $\phi(t_\rho)$, for instance one lying in the shaded region. Each approximation leads to different tangents, dashed in blue, and consequently, no tangent to $\phi(t_\rho)$ can exist.

4.6.1.1 $H(K/2\pi) \neq 0$

We write the limit (4.14) as

$$-\frac{1+i}{\sqrt{2}}\,\frac{H(K/2\pi)}{|H(K/2\pi)|}\lim_{n\to\infty} e_n.$$

This limit may or may not exist, but since we want to show that the curve approaches $\phi(t_\rho)$ from any direction in an open set of $\mathbb{S}^1$, taking into account that $e_n^8 = 1$ for all $n \in \mathbb{N}$, we take a subsequence of p_n/q_n such that, after relabelling, $e_n = e \in \mathbb{C}$ is constant. Thus, the limit and hence the candidate to be the tangent is

$$-\frac{1+i}{\sqrt{2}}\,e\,\frac{H(K/2\pi)}{|H(K/2\pi)|}. \tag{4.15}$$

Let us work with other approximations by letting $Q \in \mathbb{R}$ be such that

$$0 < Q < \frac{K}{2} < K_n$$

for big enough $n \in \mathbb{N}$. Then, the tangent can also be computed with the approximations $\phi(t_{p_n,q_n} + Q/(2\pi q_n^2))$, which by the choice of Q are always between $\phi(t_{p_n,q_n})$ and $\phi(t_\rho)$ in parameter. Consequently, by (4.9), the limit for the tangent as in Lemma 4.15

is

$$\begin{aligned}
&\lim_{n\to\infty} \frac{\phi(t_{p_n,q_n}+\frac{Q}{2\pi q_n^2})-\phi(t_\rho)}{|\phi(t_{p_n,q_n}+\frac{Q}{2\pi q_n^2})-\phi(t_\rho)|} \\
&\quad= \lim_{n\to\infty} \frac{\phi(t_{p_n,q_n}+\frac{Q}{2\pi q_n^2})-\phi(t_{p_n,q_n})+\phi(t_{p_n,q_n})-\phi(t_\rho)}{\left|\phi(t_{p_n,q_n}+\frac{Q}{2\pi q_n^2})-\phi(t_{p_n,q_n})+\phi(t_{p_n,q_n})-\phi(t_\rho)\right|} \\
&\quad= \lim_{n\to\infty} \frac{\frac{1+i}{\sqrt{2\pi}}\frac{e}{q_n^{3/2}}H_n\left(\frac{Q}{2\pi}\right)-\frac{1+i}{\sqrt{2\pi}}\frac{e}{q_n^{3/2}}H_n\left(\frac{K_n}{2\pi}\right)}{\left|\frac{1+i}{\sqrt{2\pi}}\frac{e}{q_n^{3/2}}H_n\left(\frac{Q}{2\pi}\right)-\frac{1+i}{\sqrt{2\pi}}\frac{e}{q_n^{3/2}}H_n\left(\frac{K_n}{2\pi}\right)\right|} \\
&\quad= \frac{1+i}{\sqrt{2}}\,e\,\frac{H\left(Q/2\pi\right)-H\left(K/2\pi\right)}{|H\left(Q/2\pi\right)-H\left(K/2\pi\right)|}.
\end{aligned} \tag{4.16}$$

Since $H(K/2\pi)\neq 0$ and $\lim_{s\to 0}H(s)=0$, by continuity of H we can choose $0<Q<K/2$ such that $H(K/2\pi)\neq H(Q/2\pi)\neq 0$. According to Lemma 4.15, a tangent will definitely not exist if

$$\frac{H(K/2\pi)}{|H(K/2\pi)|}\neq\frac{H\left(K/2\pi\right)-H\left(Q/2\pi\right)}{|H\left(K/2\pi\right)-H\left(Q/2\pi\right)|},$$

and in particular if $H(Q/2\pi)\notin H(K/2\pi)\mathbb{R}$.

With the definition of Y_1 (2.42) and the asymptotic (4.12) in mind, define for $m\in\mathbb{N}$ the sequences s_m as

$$\frac{1}{4\beta(s)}=2\pi m\Leftrightarrow s=s_m=\frac{1}{2\pi}\frac{1}{4m-2a} \tag{4.17}$$

and $\tilde{s}_m$ as

$$\frac{1}{4\beta(s)}=(2m+1)\pi\Leftrightarrow s=\tilde{s}_m=\frac{1}{4\pi}\frac{1}{2m+1-a}. \tag{4.18}$$

Then,

$$Y_1(\beta(s_m))=\sum_{k=1}^{\infty}\frac{e^{2\pi imk^2}}{k^2}=\sum_{k=1}^{\infty}\frac{1}{k^2}=\frac{\pi^2}{6}>0$$

and

$$Y_1(\beta(\tilde{s}_m))=\sum_{k=1}^{\infty}\frac{e^{(2m+1)\pi ik^2}}{k^2}=\sum_{k=1}^{\infty}\frac{e^{i\pi k^2}}{k^2}=\sum_{k=1}^{\infty}\frac{(-1)^k}{k^2}=-\frac{\pi^2}{12}<0.$$

Since $\lim_{m\to\infty}s_m=0=\lim_{m\to\infty}\tilde{s}_m$, the error terms $O(s_m^{5/2})$ and $O(\tilde{s}_m^{5/2})$ in (4.12) are negligible when $m\to\infty$. Also, the real part of $\sqrt{s_m}+4iY_1(\beta(s_m))\,s_m^{3/2}$ is $\sqrt{s_m}>0$, and the imaginary part is $4Y_1(\beta(s_m))\,s_m^{3/2}>0$, so for big enough $m\in\mathbb{N}$, $H(s_m)$ is in the first quadrant of the complex plane. On the other hand, the real part of $\sqrt{\tilde{s}_m}+4iY_1(\beta(\tilde{s}_m))\,\tilde{s}_m^{3/2}$ is $\sqrt{\tilde{s}_m}>0$ and the imaginary part is $4Y_1(\beta(\tilde{s}_m))\,\tilde{s}_m^{3/2}<0$, so $H(\tilde{s}_m)$ is in the fourth quadrant of $\mathbb{C}$ for big enough $m\in\mathbb{N}$.

Therefore, if $H(K/2\pi)$ is either in the first or the third quadrant, we can choose $Q=2\pi\tilde{s}_m$ for a big enough $m\in\mathbb{N}$ so that $H(Q/2\pi)$ is in the fourth quadrant, and thus $H(Q/2\pi)\notin H(K/2\pi)\mathbb{R}$. On the other hand, in case $H(K/2\pi)$ is in the second or the fourth quadrant, choose $Q=2\pi s_m$ for a sufficiently large $m\in\mathbb{N}$ such that $H(Q/2\pi)$ is in the first quadrant, and thus $H(Q/2\pi)\notin H(K/2\pi)\mathbb{R}$.

Moreover, define $f(x)=\arg(H(K/2\pi)-H(x/2\pi))$ for $0\leq x\leq Q$, which is a continuous function. Then, f takes every value between the two extremal arguments.

In other words, there exists an open set $V \subset \mathbb{S}^1$ such that for every $\mathbb{V} \in V$, there exists $Q_{\mathbb{V}} \in (0, Q)$ such that

$$\frac{H(K/2\pi) - H(Q_{\mathbb{V}}/2\pi)}{|H(K/2\pi) - H(Q_{\mathbb{V}}/2\pi)|} = \mathbb{V}.$$

Consequently, the method above shows that for every $V \in \mathbb{V}$ there is a sequence of approximations $\phi(t_{p_n,q_n} + Q_{\mathbb{V}}/(2\pi q_n^2))$ such that

$$\lim_{n\to\infty} \frac{\phi(t_{p_n,q_n} + \frac{Q_{\mathbb{V}}}{2\pi q_n^2}) - \phi(t_\rho)}{|\phi(t_{p_n,q_n} + \frac{Q_{\mathbb{V}}}{2\pi q_n^2}) - \phi(t_\rho)|} = -\frac{1+i}{\sqrt{2}}\, e\, \mathbb{V}.$$

4.6.1.2 $H(K/2\pi) = 0$

Like before, take the subsequence of the convergents p_n/q_n such that $e_n = e$ is constant. In this case, the limit is not (4.15), but on the other hand, from (4.9) we get

$$\frac{\sqrt{2\pi}}{1+i}\, e^{-1} \lim_{n\to\infty} q_n^{3/2} \left(\phi(t_\rho) - \phi(t_{p_n,q_n})\right) = \lim_{n\to\infty} H_n(K_n/2\pi) = 0. \tag{4.19}$$

Choose $0 < Q < K/2$ as in the previous case so that

$$\begin{aligned} &q_n^{3/2} \left(\phi(t_{p_n,q_n} + \tfrac{Q}{2\pi q_n^2}) - \phi(t_{p_n,q_n})\right) \\ &= q_n^{3/2} \left(\phi(t_{p_n,q_n} + \tfrac{Q}{2\pi q_n^2}) - \phi(t_\rho)\right) + q_n^{3/2} \left(\phi(t_\rho) - \phi(t_{p_n,q_n})\right) \end{aligned}$$

and hence, by (4.19) we get

$$\lim_{n\to\infty} q_n^{3/2} \left(\phi(t_{p_n,q_n} + \tfrac{Q}{2\pi q_n^2}) - \phi(t_\rho)\right) = \lim_{n\to\infty} q_n^{3/2} \left(\phi(t_{p_n,q_n} + \tfrac{Q}{2\pi q_n^2}) - \phi(t_{p_n,q_n}).\right)$$

Then, if the previous limit does not vanish, the limit corresponding to these new approximations is

$$\begin{aligned} \lim_{n\to\infty} \frac{\phi(t_{p_n,q_n} + \frac{Q}{2\pi q_n^2}) - \phi(t_\rho)}{\left|\phi(t_{p_n,q_n} + \frac{Q}{2\pi q_n^2}) - \phi(t_\rho)\right|} &= \lim_{n\to\infty} \frac{\phi(t_{p_n,q_n} + \frac{Q}{2\pi q_n^2}) - \phi(t_{p_n,q_n})}{\left|\phi(t_{p_n,q_n} + \frac{Q}{2\pi q_n^2}) - \phi(t_{p_n,q_n})\right|} \\ &= -\frac{1+i}{\sqrt{2}} e \lim_{n\to\infty} \frac{H_n(Q/2\pi)}{|H_n(Q/2\pi)|} \\ &= -\frac{1+i}{\sqrt{2}} e \frac{H(Q/2\pi)}{|H(Q/2\pi)|}. \end{aligned}$$

Then, since according to Lemma 4.15 the existence of a tangent requires that the limit above is the same for all approximations, it is enough to find two values of Q giving different values for it. For that, using the sequences $s_m, \tilde{s}_m$ in (4.17) and (4.18), choose $Q_1 = 2\pi s_m$ for big enough $m \in \mathbb{N}$ so that $H(Q_1/2\pi)$ is in the first quadrant and $Q_2 = 2\pi \tilde{s}_m$ so that $H(Q_2/2\pi)$ is in the fourth quadrant. Then,

$$\frac{H(Q_1/2\pi)}{|H(Q_1/2\pi)|} \neq \frac{H(Q_2/2\pi)}{|H(Q_2/2\pi)|}.$$

We can also make $0 < Q_1 < Q_2$. Moreover, defining $f(x) = \arg H(x/2\pi)$, because $f(Q_2) < 0 < f(Q_1)$ and by continuity of f, there exists an open set $V \subset \mathbb{S}^1$ (corresponding to arguments $(f(Q_2), f(Q_1)) \subset [-\pi, \pi)$) such that for any $\mathbb{V} \in V$, there

exists $Q_{\mathbb{V}} \in (Q_1, Q_2)$ such that

$$\frac{H(Q_{\mathbb{V}}/2\pi)}{|H(Q_{\mathbb{V}}/2\pi)|} = \mathbb{V}.$$

Consequently, for each $\mathbb{V} \in V$, there is a sequence of approximations $\phi(t_{p_n,q_n} + Q_{\mathbb{V}}/(2\pi q_n^2))$ so that

$$\lim_{n\to\infty} \frac{\phi(t_{p_n,q_n} + \frac{Q_{\mathbb{V}}}{2\pi q_n^2}) - \phi(t_\rho)}{|\phi(t_{p_n,q_n} + \frac{Q_{\mathbb{V}}}{2\pi q_n^2}) - \phi(t_\rho)|} = -\frac{1+i}{\sqrt{2}}\, e\, \mathbb{V}.$$

4.6.2 $K = 0$

In this case, $\lim_{n\to 0} H_n(K_n/2\pi) = H(0) = 0$. Thanks to the first expression in (4.7), we write

$$\lim_{n\to\infty} \frac{H_n(K_n/2\pi)}{(K_n/2\pi)^{1/2}} = \lim_{n\to\infty} \frac{\sqrt{K_n/2\pi} + 4i\, Y_1(\beta_n(K_n/2\pi))\,(K_n/2\pi)^{3/2} + O(K_n^{5/2})}{(K_n/2\pi)^{1/2}} = 1.$$

As a consequence,

$$\lim_{n\to\infty} \frac{H_n(K_n/2\pi)}{|H_n(K_n/2\pi)|} = \lim_{s\to 0} \frac{\frac{H_n(K_n/2\pi)}{(K_n/2\pi)^{1/2}}}{\frac{|H_n(K_n/2\pi)|}{(K_n/2\pi)^{1/2}}} = 1. \tag{4.20}$$

If, as before, to get the open set of directions we are looking for we take a subsequence of the convergents p_n/q_n such that $e_n = e$ is constant for every $n \in \mathbb{N}$, then proceeding as in (4.14), the limit for the tangent is

$$\lim_{n\to\infty} \frac{\phi(t_{p_n,q_n}) - \phi(t_\rho)}{|\phi(t_{p_n,q_n}) - \phi(t_\rho)|} = -\lim_{n\to\infty} e_n \frac{1+i}{\sqrt{2}} = -e\,\frac{1+i}{\sqrt{2}}.$$

But it is obvious that we cannot proceed as in the case $K > 0$, because every approximation taken at the scale of H_n as in (4.16) collapses to the same direction as in (4.20). In the setting of Figure 4.5, we approach more and more to the origin and *we see nothing* when $n \to \infty$.

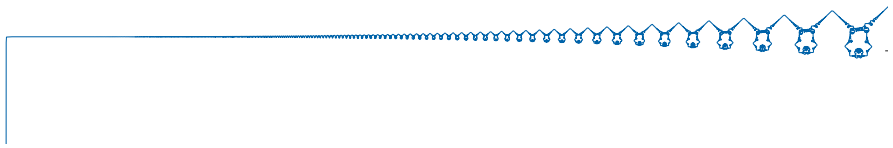

FIGURE 4.5: A picture of the rescaled asymptotic $H(s)$, where the corner represents $H(0)$ and corresponds to $\phi(t_{p_n,q_n})$. When $K = 0$, the irrational $\phi(t_\rho)$ approaches the corner. It is evident that at this scale any approximation to t_ρ lying between itself and t_{ρ_n} leads to the same horizontal tangent direction.

A way to solve this is using the self-similarity term in (4.7),

$$\frac{1}{6} - \frac{i}{2\pi}\frac{c_n}{q_n} - 2\phi\left(\frac{-1}{16\pi^2\beta_n(s)}\right). \tag{4.21}$$

As already explained in Subsection 2.2.4 after (2.47), and also in Subsection 2.2.6 after (2.63), by the periodic property $\phi(t+1/2\pi) = \phi(t)+i/2\pi$ for every $t \in \mathbb{R}$, (4.21) generates infinitely many copies of $\phi([0,1/(2\pi)])$ when $s \to 0$ because $1/\beta_n(s) \to \infty$. We will see that the more s approaches to zero, the more precise copies of $\phi([0,1/(2\pi)])$ we get. Yet, they are also smaller, so a second rescaling will be needed. Let us first identify the ranges in which copies are formed.

Lemma 4.24. *Let $n \in \mathbb{N}$. The self-similar expression (4.21) generates a copy of $\phi([0,1/(2\pi)])$ starting at each point*

$$s_{n,m} = \frac{1}{2\pi}\frac{1}{4m - 2\frac{c_n}{q_n}}, \qquad \text{for large enough } m \in \mathbb{N}. \tag{4.22}$$

Moreover, $s_{n,m} \to 0$ implies $m \to \infty$, and in this situation, $s_{n,m} \simeq 1/(8\pi m)$ are equivalent infinitesimals.

Proof. Copies of $\phi([0,1/(2\pi)])$ are generated by ϕ starting at $m/2\pi$ for every $m \in \mathbb{Z}$, so we look for points $s > 0$ such that

$$\frac{-1}{16\pi^2\beta_n(s)} = -\frac{m}{2\pi}, \qquad \forall m \in \mathbb{N}.$$

Solving, we find that those points, which we call $s = s_{n,m}$, satisfy

$$\frac{1}{8\pi m} = \beta_n(s) = \frac{s}{1 + 4\pi s\frac{c_n}{q_n}} \qquad \Leftrightarrow \qquad s = s_{n,m} = \frac{1}{2\pi}\frac{1}{4m - 2\frac{c_n}{q_n}}.$$

Moreover, since $1 \le c_n/q_n \le 4$, then $s_{n,m} \to 0$ if and only if $m \to \infty$, and it is immediate that $\lim_{m\to\infty} 8\pi m\, s_{n,m} = 1$. □

Now, we locate K_n in its corresponding range described by the points (4.22) in Lemma 4.24.

Lemma 4.25. *Let $n \in \mathbb{N}$ be large enough. Then, there exists a unique $m = m(n) \in \mathbb{N}$ such that*

$$s_{n,m(n)+1} < \frac{K_n}{2\pi} \le s_{n,m(n)}.$$

Moreover, $\lim_{n\to\infty} m(n) = +\infty$.

Proof. For fixed $n \in \mathbb{N}$, the sequence $s_{n,m}$ is strictly decreasing to zero in m. Also since $\lim_{n\to\infty} K_n = 0$, choose n big enough so that K_n is smaller than at least one value $s_{n,m}$. Then,

$$\exists! m = m(n) \qquad \text{such that} \qquad s_{n,m(n)+1} < \frac{K_n}{2\pi} \le s_{n,m(n)}.$$

As a consequence, since $\lim_{n\to\infty} K_n = 0$, we see that $\lim_{n\to\infty} s_{n,m(n)+1} = 0$. According to Lemma 4.24, this is equivalent to saying that $\lim_{n\to\infty} m(n) + 1 = +\infty$, which yields the result. □

Remark 4.26. Many times, we write just $s_{m(n)}$ instead of $s_{n,m(n)}$.

We proceed as follows: for fixed $n \in \mathbb{N}$, and once $\phi(t_{p_n,q_n} + s/q_n^2) - \phi(t_{p_n/q_n})$ has been rescaled to H_n by $q_n^{3/2}$, the point under analysis is in the interval $(s_{m(n)+1}, s_{m(n)})$, which corresponds to a copy of $\phi([0,1/(2\pi)])$. Then, we rescale the function again when the parameter is in a wider interval, $(s_{m(n)+2}, s_{m(n)})$, corresponding to two

successive copies of $\phi([0,1/(2\pi)])$ (see Figure 4.6). While $\phi(t_\rho)$ is in the first one, we take as approximations points in the second one, so that directions do not match to the ones of the convergents $\phi(t_{\rho_n})$.

FIGURE 4.6: Second rescaling of the asymptotic shown in Figure 4.5, where the corner $H(0)$ is on the left, out of the picture. Self-similarity is clearly visible in terms of copies of F, all very similar to each other. The parameter interval $(s_{m(n)+2}, s_{m(n)})$ represents two successive copies; the irrational $\phi(t_\rho)$ lies on the right hand-sided one.

4.6.2.1 Step 1 - First rescaling to get H_n

This step corresponds to (4.9).

4.6.2.2 Step 2 - Translate the copies of F in $(s_{n,m(n)+2}, s_{n,m(n)})$ to the origin

We translate a point on the left of $\phi(t_\rho)$ to the origin. Since $\phi(t_\rho)$ corresponds to $K_n/(2\pi) \in (s_{m(n)+1}, s_{m(n)})$, the approximation we use is $s_{m(n)+\mu}$ for some $1 \le \mu \le 2$, so we compute

$$H_n(s) - H_n(s_{m(n)+\mu}) \tag{4.23}$$

using the asymptotic (4.7). If $s \in (s_{m(n)+1}, s_{m(n)}]$, there exists $\alpha \in [0,1)$ such that

$$s = s_{m(n)+\alpha} = \frac{1}{2\pi}\frac{1}{4(m(n)+\alpha) - 2c_n/q_n}.$$

In particular, there exists $\alpha_n \in [0,1)$ such that $K_n/(2\pi) = s_{m(n)+\alpha_n}$, and $\phi(t_\rho)$ corresponds to $s_{m(n)+\alpha_n}$. Using (4.22) and Taylor's expansion $(1+x)^{-1/2} \simeq 1 - x/2$ when $x \to 0$, the first term in the asymptotic of (4.23) is

$$\begin{aligned}\sqrt{s} - \sqrt{s_{m+\mu}} &= \frac{1}{\sqrt{2\pi}}\left(\frac{1}{\sqrt{4m + 4\alpha - 2\frac{c_n}{q_n}}} - \frac{1}{\sqrt{4m + 4\mu - 2\frac{c_n}{q_n}}}\right) \\ &\simeq \frac{1}{\sqrt{2\pi}}\frac{1}{\sqrt{4m}}\left(1 - \frac{4\alpha - 2\frac{c_n}{q_n}}{8m} - 1 + \frac{4\mu - 2\frac{c_n}{q_n}}{8m}\right) = \frac{1}{\sqrt{2\pi}}\frac{\mu-\alpha}{4m^{3/2}}.\end{aligned} \tag{4.24}$$

when $m \to \infty$, where $\simeq$ stands for equivalent infinitesimals. The second term of (4.23) is

$$\begin{aligned}&\frac{8\pi^2}{3} i \left(\frac{1}{6} - \frac{i}{2\pi}\frac{c_n}{q_n} - 2\phi\left(\frac{-1}{16\pi^2\beta_n(s)}\right)\right) s^{3/2} \\ &\qquad - \frac{8\pi^2}{3} i \left(\frac{1}{6} - \frac{i}{2\pi}\frac{c_n}{q_n} - 2\phi\left(\frac{-1}{16\pi^2\beta_n(s_{m+\mu})}\right)\right) s_{m+\mu}^{3/2},\end{aligned}$$

which we split it into a sum $A+B$ such that

$$\begin{aligned}A &= \frac{8\pi^2}{3}i\Bigg[\left(\frac{1}{6}-\frac{i}{2\pi}\frac{c_n}{q_n}-2\phi\left(\frac{-1}{16\pi^2\beta_n(s)}\right)\right)\\ &\qquad\qquad -\left(\frac{1}{6}-\frac{i}{2\pi}\frac{c_n}{q_n}-2\phi\left(\frac{-1}{16\pi^2\beta_n(s_{m+\mu})}\right)\right)\Bigg]s^{3/2}\\ &= \frac{8\pi^2}{3}i\left[2\phi\left(\frac{-1}{16\pi^2\beta_n(s_{m+\mu})}\right)-2\phi\left(\frac{-1}{16\pi^2\beta_n(s)}\right)\right]s^{3/2}\end{aligned}$$

and

$$B = \frac{8\pi^2}{3}i\left(\frac{1}{6}-\frac{i}{2\pi}\frac{c_n}{q_n}-2\phi\left(\frac{-1}{16\pi^2\beta_n(s_{m+\mu})}\right)\right)\left(s^{3/2}-s_{m+\mu}^{3/2}\right).$$

From the proof of Lemma 4.24, the definition of $s_{m+\alpha}$ and the periodic property of ϕ, we have

$$\phi\left(\frac{-1}{16\pi^2\beta_n(s_{m+\alpha})}\right)=\phi\left(-\frac{m+\alpha}{2\pi}\right)=-i\frac{m+2}{2\pi}+\phi\left(\frac{2-\alpha}{2\pi}\right),$$

so

$$A=\frac{16\pi^2}{3}i\left(\phi\left(\frac{2-\mu}{2\pi}\right)-\phi\left(\frac{2-\alpha}{2\pi}\right)\right)s^{3/2}.$$

On the other hand, in the same spirit as before, since $(1+x)^{-3/2}\simeq 1-3x/2$ when $x\to 0$, we get

$$\begin{aligned}s^{3/2}-s_{m+\mu}^{3/2} &= \frac{1}{(2\pi)^{\frac{3}{2}}}\left(\frac{1}{(4m+4\alpha-2\frac{c_n}{q_n})^{3/2}}-\frac{1}{(4m+4\mu-2\frac{c_n}{q_n})^{3/2}}\right)\\ &\simeq \frac{1}{(2\pi)^{\frac{3}{2}}}\frac{1}{(4m)^{3/2}}\left(1-\frac{3}{2}\frac{4\alpha-2\frac{c_n}{q_n}}{4m}-1+\frac{3}{2}\frac{4\mu-2\frac{c_n}{q_n}}{4m}\right)\\ &= \frac{1}{(2\pi)^{\frac{3}{2}}}\frac{3(\mu-\alpha)}{16m^{5/2}}\end{aligned}$$

when $m\to\infty$. Hence,

$$\begin{aligned}B &\simeq \frac{8\pi^2}{3}i\left(\frac{1}{6}-\frac{i}{2\pi}\frac{c_n}{q_n}+i\frac{m+2}{\pi}-2\phi\left(\frac{2-\mu}{2\pi}\right)\right)\frac{3(\mu-\alpha)}{(2\pi)^{\frac{3}{2}}16m^{5/2}}\\ &= \frac{8\pi^2}{3}i\left(\frac{1}{6}-\frac{i}{2\pi}\frac{c_n}{q_n}+\frac{2i}{\pi}-2\phi\left(\frac{2-\mu}{2\pi}\right)\right)\frac{3(\mu-\alpha)}{(2\pi)^{\frac{3}{2}}16m^{5/2}}-\frac{\mu-\alpha}{4(2\pi)^{\frac{1}{2}}m^{3/2}}.\end{aligned}$$

The last term in B gets cancelled with (4.24), so

$$\begin{aligned}&H_n(s)-H_n(s_{m(n)+\mu})\\ &\quad= \frac{16\pi^2}{3}i\left(\phi\left(\frac{2-\mu}{2\pi}\right)-\phi\left(\frac{2-\alpha}{2\pi}\right)\right)s^{3/2}\\ &\qquad+\frac{8\pi^2}{3}i\left(\frac{1}{6}-\frac{i}{2\pi}\frac{c_n}{q_n}+\frac{2i}{\pi}-2\phi\left(\frac{2-\alpha}{2\pi}\right)\right)\frac{3(\mu-\alpha)}{(2\pi)^{\frac{3}{2}}16m^{5/2}}\\ &\qquad+O(s^{5/2})+O(s_{m+\mu}^{5/2}).\end{aligned}\tag{4.25}$$

The rescaling suggested by (4.25) to obtain the copies of $\phi([0,1/(2\pi)])$ is $s^{-3/2}$.

4.6.2.3 Step 3 - Rescale the $s^{3/2}$ term to identify the copy of F

Define

$$G_{n,\mu}(s) = s_{m+\mu}^{-3/2}\left[H_n(s) - H_n(s_{m+\mu})\right], \qquad \text{for } s \in (s_{m+1}, s_m), \tag{4.26}$$

which corresponds rescaling (4.25) with $s_{m+\mu}^{-3/2}$. First, we see that when $n \to \infty$ (and thus $m = m(n) \to \infty$), the higher order terms tend to zero independently of α because $\mu - \alpha \leq 2$ and

$$0 \leq \frac{\mu-\alpha}{m^{5/2}} s_{m+\mu}^{-3/2} \leq 2(2\pi)^{3/2}\frac{(4m+4\mu-2\frac{c_n}{q_n})^{3/2}}{m^{5/2}} \to 0.$$

Also

$$\frac{s_{m+\mu}^{5/2}}{s_{m+\mu}^{3/2}} = s_{m+\mu} \to 0 \qquad \text{and} \qquad \frac{s^{5/2}}{s_{m+\mu}^{3/2}} = \frac{1}{2\pi}\frac{(4m+4\mu-2\frac{c_n}{q_n})^{3/2}}{(4m+4\alpha-2\frac{c_n}{q_n})^{5/2}} \to 0.$$

Consequently,

$$\begin{aligned}
&\lim_{n\to\infty}\left|G_{n,\mu}(s) - \frac{16\pi^2}{3}i\left(\phi\left(\frac{2-\mu}{2\pi}\right) - \phi\left(\frac{2-\alpha}{2\pi}\right)\right)\right| \\
&\quad = \lim_{n\to\infty}\left|\frac{16\pi^2}{3}i\left(\phi\left(\frac{2-\mu}{2\pi}\right) - \phi\left(\frac{2-\alpha}{2\pi}\right)\right)\left(\frac{s^{3/2}}{s_{m+\mu}^{3/2}} - 1\right)\right| \\
&\quad \leq \lim_{n\to\infty} C\left|\frac{s^{3/2}}{s_{m+\mu}^{3/2}} - 1\right| = 0,
\end{aligned}$$

where $C > 0$ is independent of α and μ. The last equality holds because recalling that $s_{m+\mu} \leq s_{m+\alpha} = s$, we get

$$0 \leq \frac{s^{3/2}}{s_{m+\mu}^{3/2}} - 1 = \frac{4m+4\mu-2\frac{c_n}{q_n}}{4m+4\alpha-2\frac{c_n}{q_n}} - 1 = \frac{4(\mu-\alpha)}{4m+4\alpha-2\frac{c_n}{q_n}} \leq \frac{8}{4m+4\alpha-2\frac{c_n}{q_n}} \to 0.$$

Convergence is thus independent of α, so we have proved the following proposition.

Proposition 4.27. *Let $1 \leq \mu \leq 2$. Then,*

$$\lim_{n\to\infty}\sup_{\alpha\in(0,1)}\left|G_{n,\mu}\left(\frac{1}{4m(n)+4\alpha-2\frac{c_n}{q_n}}\right) - \frac{16\pi^2}{3}i\left(\phi\left(\frac{2-\mu}{2\pi}\right) - \phi\left(\frac{2-\alpha}{2\pi}\right)\right)\right| = 0.$$

4.6.2.4 Step 4 - Conclusion

Let us write $G_{n,\mu}$ in terms of ϕ using (4.8) and (4.26) so that

$$G_{n,\mu}(s) = \frac{\sqrt{2\pi}}{1+i}e^{-1}q_n^{3/2}s_{m(n)+\mu}^{-3/2}\left[\phi\left(t_{p_n,q_n} + \frac{s}{q_n^2}\right) - \phi\left(t_{p_n,q_n} + \frac{s_{m(n)+\mu}}{q_n^2}\right)\right].$$

Recall that $K_n/2\pi = s_{m(n)+\alpha_n}$, define $\alpha = \liminf_{n\to\infty}\alpha_n \in [0,1]$ and take the subsequence which, after being relabelled, satisfies $\lim_{n\to\infty}\alpha_n = \alpha$. From Proposition 4.27

and the continuity of ϕ, we can write

$$\lim_{n\to\infty} G_{n,\mu}(K_n/2\pi) = \frac{16\pi^2}{3} i \left(\phi\left(\frac{2-\mu}{2\pi}\right) - \phi\left(\frac{2-\alpha}{2\pi}\right)\right).$$

Then, since as long as $\alpha < \mu$ we have $0 < s_{m(n)+\mu} < s_{m(n)+\alpha}$, let us use the points $t_{\rho_n} + s_{m(n)+\mu}/q_n^2$ as approximations to t_ρ for the limit defining the tangent, which is

$$\begin{aligned}\lim_{n\to\infty} \frac{\phi(t_\rho) - \phi\left(t_{\rho_n} + \frac{s_{m(n)+\mu}}{q_n^2}\right)}{\left|\phi(t_\rho) - \phi\left(t_{\rho_n} + \frac{s_{m(n)+\mu}}{q_n^2}\right)\right|} &= \lim_{n\to\infty} \frac{\frac{1+i}{\sqrt{2\pi}}\, e\, q_n^{-3/2} s_{m(n)+\mu}^{3/2} G_{n,\mu}(K_n/2\pi)}{\left|\frac{1+i}{\sqrt{2\pi}}\, e\, q_n^{-3/2} s_{m(n)+\mu}^{3/2} G_{n,\mu}(K_n/2\pi)\right|} \\ &= \frac{1+i}{\sqrt{2}}\, e \lim_{n\to\infty} \frac{G_{n,\mu}(K_n/2\pi)}{|G_{n,\mu}(K_n/2\pi)|} \\ &= i\frac{1+i}{\sqrt{2}}\, e \frac{\phi\left(\frac{2-\mu}{2\pi}\right) - \phi\left(\frac{2-\alpha}{2\pi}\right)}{\left|\phi\left(\frac{2-\mu}{2\pi}\right) - \phi\left(\frac{2-\alpha}{2\pi}\right)\right|}.\end{aligned}$$

Define

$$f(x) = \arg\left(\phi\left(\frac{2-x}{2\pi}\right) - \phi\left(\frac{2-\alpha}{2\pi}\right)\right), \qquad \text{for } x \in (1,2),$$

which is continuous. Moreover,

$$f(1) = \arg\left(\frac{i}{2\pi} - \phi\left(\frac{2-\alpha}{2\pi}\right)\right) \qquad \text{and} \qquad f(2) = \arg\left(-\phi\left(\frac{2-\alpha}{2\pi}\right)\right).$$

If $\alpha \in (0,1)$, then $f(1) \neq f(2)$ and by continuity, f takes all values in $(f(1), f(2)) \in [0, 2\pi)$. If $\alpha = 0$ or $\alpha = 1$, we may choose the interval $(f(2), f(3/2))$. In both cases, these intervals correspond to an open set $V \subset \mathbb{S}^1$ such that for any $\mathbb{V} \in V$, there exists $\mu_{\mathbb{V}} \in (1,2)$ such that

$$\frac{\phi\left(\frac{2-\mu_{\mathbb{V}}}{2\pi}\right) - \phi\left(\frac{2-\alpha}{2\pi}\right)}{\left|\phi\left(\frac{2-\mu_{\mathbb{V}}}{2\pi}\right) - \phi\left(\frac{2-\alpha}{2\pi}\right)\right|} = \mathbb{V},$$

and therefore there is a sequence of approximations $\phi(t_{\rho_n} + s_{m(n)+\mu_{\mathbb{V}}}/q_n^2)$ such that

$$\lim_{n\to\infty} \frac{\phi(t_\rho) - \phi\left(t_{\rho_n} + s_{m(n)+\mu_{\mathbb{V}}}/q_n^2\right)}{\left|\phi(t_\rho) - \phi\left(t_{\rho_n} + s_{m(n)+\mu_{\mathbb{V}}}/q_n^2\right)\right|} = i\frac{1+i}{\sqrt{2}}\, e\, \mathbb{V}.$$

Proposition 4.21 is proved.

4.6.3 Proof of Lemma 4.23

To finish, we prove Lemma 4.23. To do so, we need some preliminary computations. Remember that we are working with an irrational $\rho \in [0,1] \setminus \mathbb{Q}$, with its continued fraction convergents p_n/q_n, which generate the sequence c_n corresponding to the values of $c_\pm$ appearing in the asymptotic behaviour of ϕ around t_{p_n,q_n} in Proposition 2.12 and that several subsequences were extracted from it so that $c_n > 0$ and $\lim_{n\to\infty} c_n/q_n = a$.

Lemma 4.28. *Let $\beta_n(s)$ and $\beta(s)$ be defined as in (4.5) and (4.13) and a as in (4.11). Let $M > 0$. Then, there exists a constant $C > 0$ such that the following hold for any $s > 0$ and for any $n \in \mathbb{N}$:*

(a) $0 \leq \beta_n(s) \leq 1/4\pi$ *and* $0 \leq \beta(s) \leq 1/4\pi$.

(b) *If* $s \le M$, *then* $1 \le (1 - 4\pi\frac{c_n}{q_n}\beta_n(s))^{-1} \le 1 + 16\pi M$ *and* $1 \le (1 - 4\pi a\beta(s))^{-1} \le 1 + 16\pi M$.

(c) $|\beta_n(s) - \beta(s)| \le C\ |a - c_n/q_n|$.

(d) $|\phi(\beta_n(s)) - \phi(\beta(s))| \le C\ |a - c_n/q_n|^{1/2}$.

(e) $\left|\beta_n(s)^2 - \beta(s)^2\right| \le C\ |a - c_n/q_n|$.

(f) $\left|\beta_n(s)^3 - \beta(s)^3\right| \le C\ |a - c_n/q_n|$.

(g) $\left|\frac{c_n}{q_n}\beta_n(s) - a\beta(s)\right| \le C\ |a - c_n/q_n|$.

(h) $\left|\left(\frac{c_n}{q_n}\beta_n(s)\right)^2 - (a\beta(s))^2\right| \le C\ |a - c_n/q_n|$.

(i) $\left|\left(\frac{c_n}{q_n}\beta_n(s)\right)^3 - (a\beta(s))^3\right| \le C\ |a - c_n/q_n|$.

Proof. For (a), using that $s \ge 0$ and $1 \le c_n/q_n \le 4$, we get

$$0 \le \beta_n(s) = \frac{s}{1 + 4\pi\frac{c_n}{q_n}s} \le \frac{s}{1 + 4\pi s} \le \frac{1}{4\pi}.$$

The same holds for $\beta(s)$ because $1 \le a \le 4$. For (b), by the definition of $\beta_n(s)$ and if $0 \le s \le M$, we write

$$1 - 4\pi\frac{c_n}{q_n}\beta_n(s) = \frac{1}{1 + 4\pi\frac{c_n}{q_n}s} \quad\Longrightarrow\quad 1 \le \frac{1}{1 - 4\pi\frac{c_n}{q_n}\beta_n(s)} = 1 + 4\pi\frac{c_n}{q_n}s \le 1 + 16\pi M.$$

The other inequality in (b) follows the same way. For (c), we write

$$\begin{aligned}\beta_n(s) - \beta(s) &= \frac{s}{1 + 4\pi\frac{c_n}{q_n}s} - \frac{s}{1 + 4\pi as} = \left(a - \frac{c_n}{q_n}\right)\frac{4\pi s^2}{(1 + 4\pi\frac{c_n}{q_n}s)(1 + 4\pi as)} \\ &= 4\pi\beta(s)\beta_n(s)\left(a - \frac{c_n}{q_n}\right),\end{aligned}$$

and using (a), we get

$$|\beta_n(s) - \beta(s)| \le \frac{1}{4\pi}\left|a - \frac{c_n}{q_n}\right|.$$

To prove (d), we need a result of Duistermaat [29, Lemma 4.1] stating that ϕ_D is globally $C^{1/2}$. From this, there exists $C > 0$ such that

$$|\phi(x) - \phi(y)| \le C\left(|x - y|^{1/2} + |x - y|\right), \quad \forall x, y \in \mathbb{R}.$$

This turns into $|\phi(x) - \phi(y)| \le C|x - y|^{1/2}$ in case $|x - y| \le 1$. Then, by (c), we have $|\beta_n(s) - \beta(s)| \le 1$, so

$$|\phi(\beta_n(s)) - \phi(\beta(s))| \le C\,|\beta_n(s) - \beta(s)|^{1/2} \le C\left|a - \frac{c_n}{q_n}\right|^{1/2}.$$

Properties (e) and (f) are proved like (c). Indeed,

$$\begin{aligned}\beta_n(s)^2-\beta(s)^2 &= s^2\,\frac{(1+4\pi as)^2-(1+4\pi\frac{c_n}{q_n}s)^2}{(1+4\pi\frac{c_n}{q_n}s)^2(1+4\pi as)^2}\\ &= 8\pi\frac{s^3\ (a-c_n/q_n)}{(1+4\pi as)^2(1+4\pi\frac{c_n}{q_n}s)^2}+16\pi^2\frac{s^4\ \left(a^2-(c_n/q_n)^2\right)}{(1+4\pi as)^2(1+4\pi\frac{c_n}{q_n}s)^2}.\end{aligned}$$

Since $a, c_n/q_n \le 4$ implies $a+c_n/q_n\le 8$, using (a) we get

$$\begin{aligned}&\left|\beta_n(s)^2-\beta(s)^2\right|\\ &\qquad\le 8\pi|\beta_n(s)|^2\frac{|\beta(s)|}{1+4\pi as}\left|a-\frac{c_n}{q_n}\right|+16\pi^2|\beta_n(s)|^2|\beta(s)|^2\left|a-\frac{c_n}{q_n}\right|\left|a+\frac{c_n}{q_n}\right|\\ &\qquad\le \frac{1}{8\pi^2}\left|a-\frac{c_n}{q_n}\right|+\frac{8}{16\pi^2}\left|a-\frac{c_n}{q_n}\right|=\frac{5}{8\pi^2}\left|a-\frac{c_n}{q_n}\right|.\end{aligned}$$

For (f), we write

$$\begin{aligned}\beta_n(s)^3-\beta(s)^3 &= s^3\frac{(1+4\pi as)^3-(1+4\pi\frac{c_n}{q_n}s)^3}{(1+4\pi\frac{c_n}{q_n}s)^3(1+4\pi as)^3}\\ &= 12\pi s^4\frac{a-c_n/q_n}{(1+4\pi\frac{c_n}{q_n}s)^3(1+4\pi as)^3}\\ &\qquad+48\pi^2 s^5\frac{a^2-(c_n/q_n)^2}{(1+4\pi\frac{c_n}{q_n}s)^3(1+4\pi as)^3}\\ &\qquad+(4\pi)^3 s^6\frac{a^3-(c_n/q_n)^3}{(1+4\pi\frac{c_n}{q_n}s)^3(1+4\pi as)^3},\end{aligned}$$

so since $|a^3-(c_n/q_n)^3\,|\le|a^2+ac_n/q_n+c_n^2/q_n^2|\le 3\cdot 4^2|a-c_n/q_n|$, we get

$$\begin{aligned}\left|\beta_n(s)^3-\beta(s)^3\right| &\le 12\pi|\beta_n(s)|^3|\beta(s)|\,|a-c_n/q_n|\\ &\qquad+48\pi^2\cdot 8|\beta_n(s)|^3|\beta(s)|^2\,|a-c_n/q_n|\\ &\qquad+(4\pi)^3|\beta_n(s)|^3|\beta(s)|^3 48\,|a-c_n/q_n|\\ &\le C\ |a-c_n/q_n|\,.\end{aligned}$$

The remaining properties are proved all by the same method. For (g), we use (a) and (c) to write

$$\begin{aligned}\left|\frac{c_n}{q_n}\beta_n(s)-a\beta(s)\right| &\le |\beta_n(s)|\left|\frac{c_n}{q_n}-a\right|+a|\beta_n(s)-\beta(s)|\\ &\le \frac{1+a}{4\pi}\left|a-\frac{c_n}{q_n}\right|\le\frac{5}{4\pi}\left|a-\frac{c_n}{q_n}\right|.\end{aligned}$$

For (h), we use (a) and (e) and write

$$\begin{aligned}\left|\left(\frac{c_n}{q_n}\beta_n(s)\right)^2-(a\beta(s))^2\right| &\le |\beta_n(s)|^2\left|\left(\frac{c_n}{q_n}\right)^2-a^2\right|+a^2\left|\beta_n(s)^2-\beta(s)^2\right|\\ &\le C\left|a-\frac{c_n}{q_n}\right|.\end{aligned}$$

Last, for (i), we use (a) and (f) to write

$$\left|\left(\frac{c_n}{q_n}\beta_n(s)\right)^3-(a\beta(s))^3\right|\le|\beta_n(s)|^3\left|\left(\frac{c_n}{q_n}\right)^3-a^3\right|+a^3\left|\beta_n(s)^3-\beta(s)^3\right|$$
$$\le C\left|a-\frac{c_n}{q_n}\right|.$$

□

Proof of Lemma 4.23. In this proof, we disregard constants not depending on M and on s. From (4.10) and (4.12) we write

$$H_n(s)-H(s)=A+B,$$

where

$$A=\frac{\phi(\beta_n(s))}{(1-4\pi\frac{c_n}{q_n}\beta_n(s))^{3/2}}-\frac{\phi(\beta(s))}{(1-4\pi a\beta(s))^{3/2}}$$

and

$$B=\frac{c_n}{q_n}\int_0^{\beta_n(s)}\frac{\phi(r)}{(1-4\pi\frac{c_n}{q_n}r)^{5/2}}\,dr-a\int_0^{\beta(s)}\frac{\phi(r)}{(1-4\pi ar)^{5/2}}\,dr.$$

Let us split $A=A_1+A_2$ such that

$$A_1=\phi(\beta_n(s))\left(\frac{1}{(1-4\pi\frac{c_n}{q_n}\beta_n(s))^{3/2}}-\frac{1}{(1-4\pi a\beta(s))^{3/2}}\right)$$

and

$$A_2=\frac{\phi(\beta_n(s))-\phi(\beta(s))}{(1-4\pi a\beta(s))^{3/2}}.$$

By Lemma 4.28-(b) and (d), we have

$$|A_2|\le(1+16\pi M)^{\frac{3}{2}}\left|a-\frac{c_n}{q_n}\right|^{\frac{1}{2}}.$$

For A_1, Lemma 4.28-(a) gives $|\phi(\beta_n(s))|\le\|\phi\|_{L^\infty([0,1/(4\pi)])}$, so if we use Lemma 4.28-(b) we write

$$|A_1|\le\frac{\left|(1-4\pi\frac{c_n}{q_n}\beta_n(s))^3-(1-4\pi a\beta(s))^3\right|}{(1-4\pi\frac{c_n}{q_n}\beta_n(s))^{\frac{3}{2}}(1-4\pi a\beta(s))^{\frac{3}{2}}\left((1-4\pi\frac{c_n}{q_n}\beta_n(s))^{\frac{3}{2}}+(1-4\pi a\beta(s))^{\frac{3}{2}}\right)}$$
$$\le C_M\left|(1-4\pi\frac{c_n}{q_n}\beta_n(s))^3-(1-4\pi a\beta(s))^3\right|$$
$$\le C_M\left(\left|\frac{c_n}{q_n}\beta_n(s)-a\beta(s)\right|+\left|\left(\frac{c_n}{q_n}\beta_n(s)\right)^2-(a\beta(s))^2\right|\right.$$
$$\left.+\left|\left(\frac{c_n}{q_n}\beta_n(s)\right)^3-(a\beta(s))^3\right|\right),$$

where $C_M = (1+16\pi M)^{9/2}$. Then, from Lemma 4.28-(g), (h) and (i) we get $|A_1| \leq C_M\,|a - c_n/q_n|$. Overall,

$$|A| \leq C_M \left(\left| a - \frac{c_n}{q_n} \right|^{1/2} + \left| a - \frac{c_n}{q_n} \right| \right). \tag{4.27}$$

For B, we write

$$\begin{aligned} |B| \leq & \left| a - \frac{c_n}{q_n} \right| \left| \int_0^{\beta_n(s)} \frac{\phi(r)}{(1-4\pi\frac{c_n}{q_n}r)^{5/2}}\,dr \right| \\ & + a \left| \int_0^{\beta_n(s)} \left(\frac{\phi(r)}{(1-4\pi\frac{c_n}{q_n}r)^{5/2}} - \frac{\phi(r)}{(1-4\pi ar)^{5/2}} \right) dr \right| \\ & + a \left| \int_{\beta(s)}^{\beta_n(s)} \frac{\phi(r)}{(1-4\pi ar)^{5/2}}\,dr \right| \\ = & \, |B_1| + |B_2| + |B_3|. \end{aligned}$$

From Lemma 4.28-(b), we deduce that if $0 \leq r \leq \beta_n(s)$, then

$$1 \leq \frac{1}{1-4\pi\frac{c_n}{q_n}r} \leq 1 + 16\pi M. \tag{4.28}$$

Hence,

$$|B_1| \leq |\beta_n(s)| \|\phi\|_{L^\infty([0,1/(4\pi)])} (1+16\pi M)^{\frac{5}{2}} \left| a - \frac{c_n}{q_n} \right| \leq C_M \left| a - \frac{c_n}{q_n} \right|.$$

Also from Lemma 4.28-(b), if r is between $\beta_n(s)$ and $\beta(s)$, then $r \leq \max\{\beta_n(s), \beta(s)\}$, so

$$1 \leq \frac{1}{1-4\pi ar} \leq 1 + 16\pi M \tag{4.29}$$

is also satisfied. Thus, by Lemma 4.28-(c) we get

$$|B_3| \leq a|\beta_n(s) - \beta(s)| \|\phi\|_{L^\infty([0,1/(4\pi)])} (1+16\pi M)^{\frac{5}{2}} \leq C_M \left| a - \frac{c_n}{q_n} \right|.$$

For B_2, we need to compute

$$\begin{aligned} & \frac{1}{(1-4\pi\frac{c_n}{q_n}r)^{\frac{5}{2}}} - \frac{1}{(1-4\pi ar)^{\frac{5}{2}}} \\ & \qquad = \frac{(1-4\pi ar)^5 - (1-4\pi\frac{c_n}{q_n}r)^5}{(1-4\pi\frac{c_n}{q_n}r)^{\frac{5}{2}}(1-4\pi ar)^{\frac{5}{2}} \left((1-4\pi\frac{c_n}{q_n}r)^{\frac{5}{2}} + (1-4\pi ar)^{\frac{5}{2}} \right)}, \end{aligned}$$

and from (4.28) and (4.29), we get

$$\begin{aligned} |B_2| & \leq a|\beta_n(s)| \|\phi\|_{L^\infty([0,1/(4\pi)])} (1+16\pi M)^{\frac{15}{2}} \left| (1-4\pi ar)^5 - (1-4\pi\frac{c_n}{q_n}r)^5 \right| \\ & \leq C_M \sum_{k=1}^{5} r^k \left| a^k - (c_n/q_n)^k \right| \end{aligned}$$

maybe renaming C_M. Here, $0 \leq r \leq \beta_n(s) \leq 1/(4\pi)$, and also there exists $C > 0$

such that $|a^k - (c_n/q_n)^k| \leq C\,|a - c_n/q_n|$ for every $k = 1, 2, 3, 4, 5$. Consequently, $|B_2| \leq C_M\ |a - c_n/q_n|$, so

$$|B| \leq C_M \left| a - \frac{c_n}{q_n} \right|.$$

Joining it with (4.27), we get

$$|H_n(s) - H(s)| \leq C_M \left(\left| a - \frac{c_n}{q_n} \right|^{1/2} + \left| a - \frac{c_n}{q_n} \right| \right), \qquad \forall s \in [0, M].$$

Therefore, we get the result

$$\lim_{n\to\infty} \|H_n - H\|_{L^\infty([0,M])} \leq C_M \lim_{n\to\infty} \left(\left| a - \frac{c_n}{q_n} \right|^{1/2} + \left| a - \frac{c_n}{q_n} \right| \right) = 0.$$

□

CHAPTER 5

Intermittency of Riemann's non-differentiable function

In Section 1.4, and in particular in Subsection 1.4.2, we put in context and justified the analysis of Riemann's non-differentiable function in the setting of turbulence and multifractality. We saw that these concepts are strongly related to intermittency and explained how the latter can be studied by means of either the structure functions or the high-pass filters. In this sense, we are interested in knowing whether Riemann's non-differentiable function is intermittent or not. Thus, we will adapt Definition 1.1 for intermittency and we will compute its flatness both from the perspective of structure functions and high-pass filtering.

Riemann's non-differentiable function ϕ has been shown to possess a periodic property, so it is reasonable to tackle the problem of intermittency from a periodic point of view. This is the setting of Jaffard's analysis [55] on the spectrum of singularities of Riemann's function, and also the one proposed in the definition of the high-pass filters in (1.54). Thus, instead of working with the natural geometric version of Riemann's function ϕ as defined in (1.10), it will be more convenient to work with the periodic version of the function,

$$R(x) = \sum_{n=1}^{\infty} \frac{e^{2\pi i n^2 x}}{n^2}, \quad x \in [0,1], \tag{5.1}$$

which is very similar to both the original (1.1) and Duistermaat's version (1.4).

In this setting, we will prove that Riemann's function (5.1) is intermittent. However, first we need to rigorously settle the definitions of high-pass filters and structure functions so that we can give a precise meaning to the concepts of flatness and intermittency. We do that in Section 5.1 following the concepts that were sketched in Section 1.4. We also set notation. Then, in Section 5.2 we state the main results of this chapter. Afterwards, in Sections 5.3 and 5.4 we will prove the results for high-pass filters and for structure functions respectively. Several auxiliary results and technical lemmas will be needed for that purpose, but in the interest of clarity, we gather them in the final Section 5.5.

The results of this chapter are a work in collaboration with Alexandre Boritchev, Maître de Conférences at Insititut Camille Jordan, Université Lyon 1 (Lyon, France), and Victor Vilaça da Rocha, Visiting Assistant Professor at Georgia Tech (Atlanta, Georgia, USA). More precisely, Corollaries 5.7 and 5.11 are the main result in the article [12][1], while Theorems 5.4 and 5.9 in all their generality and Corollaries 5.5 and 5.10 are part of the work in progress inside our ongoing project.

5.1 Preliminaries

Our choice of Riemann's function (5.1) being a periodic function of period 1, let us work in the torus $\mathbb{T} = \mathbb{R}/\mathbb{Z}$. For simplicity, we denote by $e_n(x) = e^{2\pi i n x}$ the functions which make up the orthonormal basis for $L^2(\mathbb{T})$, and for clearness when working with the structure functions and specially with the high-pass filters, we define

$$\sigma_k = \begin{cases} 1, & \text{if } k \text{ is the square of an integer,} \\ 0, & \text{otherwise.} \end{cases}$$

Thus, R can be written as a Fourier series very clearly as

$$R(x) = \sum_{n=1}^{\infty} \frac{e_{n^2}(x)}{n^2} = \sum_{k=1}^{\infty} \frac{\sigma_k}{k}\, e_k(x). \tag{5.2}$$

As is usual for two positive functions f and g, we write $f \lesssim g$ to denote that there exists a constant $C > 0$ such that $f \leq Cg$. We also write $f \simeq g$ to denote that $f \lesssim g$ and $g \lesssim f$ at the same time. If the constants involved depend on some parameter α, we write $f \lesssim_\alpha g$ and $f \simeq_\alpha g$. Also, for any $a, b \in \mathbb{R}$ such that $a < b$, we write $\sum_{n=a}^{b} = \sum_{n \in [a,b] \cap \mathbb{Z}}$ and $\sum_{n>a}^{b} = \sum_{n \in (a,b] \cap \mathbb{Z}}$.

Let us now gather and precise all definitions concerning structure functions, high-pass filters, flatness and intermittency we already saw in Section 1.4. We do that in all generality for functions $f : \mathbb{T} \to \mathbb{C}$ given by an absolutely convergent Fourier series

$$f(x) = \sum_{n \in \mathbb{Z}} a_n\, e_n(x), \qquad a_n \in \mathbb{C}. \tag{5.3}$$

We begin with high-pass filters by defining them and also the corresponding flatness. We follow the ideas in Subsection 1.4.2 and generalise them to any quotient between any L^p and L^q norms.

Definition 5.1. For $f : \mathbb{T} \to \mathbb{C}$ given by the Fourier series (5.3) and $N \in \mathbb{N}$, the high-pass filter and the low-pass filter are the projections of f on Fourier modes above N and below N respectively, given by

$$f_{\geq N}(x) = \sum_{|n| \geq N} a_n e_n(x) \qquad \text{and} \qquad f_{\leq N}(x) = \sum_{|n| \leq N} a_n e_n(x).$$

For $1 \leq q < p < \infty$, the (p,q)-flatness of f in the sense of high-pass filters is

$$F_f^{(p,q)}(N) = \frac{\|f_{\geq N}\|_{L^p(\mathbb{T})}^p}{\|f_{\geq N}\|_{L^q(\mathbb{T})}^p}.$$

[1] Boritchev, A., Eceizabarrena, D., and Vilaça da Rocha, V. "Riemann's non-differentiable function is intermittent". In: (2019). Preprint: http://arxiv.org/abs/1910.13191v1.

The values $p = 4$ and $q = 2$ correspond to the standard flatness

$$F_f(N) = \frac{\|f_{\geq N}\|^4_{L^4(\mathbb{T})}}{\|f_{\geq N}\|^4_{L^2(\mathbb{T})}}$$

that was defined in (1.55). We say that f is (p, q)-intermittent in the sense of high-pass filters if

$$\lim_{N\to+\infty} F_f^{(p,q)}(N) = +\infty,$$

and that it is simply intermittent if it is $(4, 2)$-intermittent, that is, if

$$\lim_{N\to+\infty} F_f(N) = +\infty.$$

If required, one can adapt the above definitions for high- and low-pass filters to work with strict inequalities

$$f_{>N}(x) = \sum_{|n|>N} a_n e_n(x), \qquad f_{<N}(x) = \sum_{|n|<N} a_n e_n(x).$$

We also give the analogue definitions for structure functions. Here as well, we generalise the definition of flatness and the corresponding concept of intermittency to the quotient between any L^p and L^q norms.

Definition 5.2. Let $p \geq 1$. The structure functions of $f : \mathbb{T} \to \mathbb{C}$ are

$$S_{f,p}(\ell) = \int_{\mathbb{T}} |f(x + \ell) - f(x)|^p \, dx, \qquad \ell \in [0, 1], \tag{5.4}$$

where the integral in $\mathbb{T}$ can be computed in any interval of length one. For $1 \leq q < p < \infty$, the (p, q)-flatness of f in the sense of structure functions is

$$G_f^{(p,q)}(\ell) = \frac{S_{f,p}(\ell)}{S_{f,q}(\ell)^{p/q}}.$$

The values $p = 4$ and $q = 2$ correspond to the standard flatness

$$G_f(N) = \frac{S_{f,4}(\ell)}{S_{f,2}(\ell)^2}$$

that was defined in (1.50). We say that f is (p, q)-intermittent in the sense of structure functions if

$$\lim_{\ell\to 0} G_f^{(p,q)}(\ell) = +\infty,$$

and that it is simply intermittent if it is $(4, 2)$-intermittent, this is, if

$$\lim_{\ell\to 0} G_f(\ell) = +\infty.$$

Remark 5.3. If there is no risk of confusion regarding f, as it will be the case with R, we write $S_p(\ell)$ instead of $S_{f,p}(\ell)$.

5.2 Statement of results

According to the definitions in the previous section, to decide whether a function is (p, q)-intermittent we need to have estimations of the L^p norms of the high-pass filters

$\|f_{\geq N}\|_p$ when $N \to \infty$ and also of the structure functions $S_{f,p}(\ell)$ when $\ell \to 0$. The main results in this chapter concern these estimations.

Regarding high-pass filters of Riemann's function, we prove the following theorem.

Theorem 5.4. *Let R be Riemann's non-differentiable function (5.1) and $1 < p < \infty$. Then, for $N > 0$ large enough,*

$$\|R_{\geq N}\|_{L^p}^p \simeq_p \begin{cases} N^{-3p/4}, & \text{if} \quad p < 4, \\ N^{-3} \log N, & \text{if} \quad p = 4, \\ N^{-(1+p/2)}, & \text{if} \quad p > 4. \end{cases}$$

Also,

$$\|R_{\geq N}\|_{L^\infty} \simeq N^{-1/2}.$$

The behaviour of the generalised flatness $F_R^{(p,q)}(N)$ when N tends to infinity can be readily computed.

Corollary 5.5. *Let R be Riemann's non-differentiable function (5.1) and $1 < q < p < \infty$. Then, there exists $N_{p,q} \in \mathbb{N}$ such that for $N \geq N_{p,q}$,*

$$F_R^{p,q}(N) \simeq_{p,q} \begin{cases} N^{p/q-1}, & \text{if} \quad 4 < q < p, \\ N^{p/4-1} (\log N)^{-p/4}, & \text{if} \quad 4 = q < p, \\ N^{p/4-1}, & \text{if} \quad q < 4 < p, \\ \log N, & \text{if} \quad q < p = 4, \\ 1, & \text{if} \quad q < p < 4, \end{cases}$$

and consequently R is (p,q)-intermittent in the sense of high-pass filters whenever $p \geq 4$.

Remark 5.6. The definition of (p,q)-flatness does not directly make sense when $p = \infty$, but $\left(F_f^{(p,q)}\right)^{1/p} = \|R_{\geq N}\|_{L^p} / \|R_{\geq N}\|_{L^q}$ does. If the definition of (∞, q)-flatness is understood this way, then Corollary 5.5 applies by setting $1/\infty = 0$.

Of course, the case $p = 4$ and $q = 2$ concerning the standard flatness and intermittency is included in the previous corollary. However, as we saw in Subsection 1.4.2, it was the main motivation for this study, so let us write for it an independent corollary.

Corollary 5.7. *Let R be Riemann's non-differentiable function (5.1). Then, there exists $N_0 \in \mathbb{N}$ such that for $N \geq N_0$,*

$$F_R(N) \simeq \log N.$$

Consequently, R is intermittent in the sense of high-pass filters.

Remark 5.8. The set $R([0,1])$, as a subset of the complex plane, is shown in Figure 1.2 up to some rotation and scaling. Even if this set is not exactly self-similar as the Cantor set or the Von Koch snowflake, the asymptotic behaviour in Duistermaat's work [29] and in Section 2.2, and also Figure 1.2 itself, reveal the presence of some approximate self-similar structure. Therefore, if as suggested in Subsection 1.4.2 intermittency is a measure of the lack of self-similarity, R should have weak intermittent properties, and its flatness should show this. The logarithmic growth of F_R in Corollary 5.7 agrees with this interpretation.

We now present the results concerning the structure functions.

Theorem 5.9. *Let R be Riemann's non-differentiable function (5.1) and $1 < p < \infty$. For $\ell > 0$ small enough,*

$$S_p(\ell) \simeq_p \begin{cases} \ell^{3p/4}, & \text{if} \quad p < 4, \\ \ell^3 \log\left(\ell^{-1}\right), & \text{if} \quad p = 4, \\ \ell^{1+p/2}, & \text{if} \quad p > 4. \end{cases}$$

As a corollary, we get the behaviour of the generalised flatness $G^{(p,q)}(\ell)$ when ℓ tends to zero.

Corollary 5.10. *Let R be Riemann's non-differentiable function (5.1) and $1 < q < p < \infty$. There exists $0 < \ell_{p,q} < 1$ such that for $0 < \ell < \ell_{p,q}$,*

$$G_R^{p,q}(\ell) \simeq_{p,q} \begin{cases} \ell^{1-p/q}, & \text{if} \quad 4 < q < p, \\ \ell^{1-p/4} \left(\log\left(\ell^{-1}\right)\right)^{-p/4}, & \text{if} \quad 4 = q < p, \\ \ell^{1-p/4}, & \text{if} \quad q < 4 < p, \\ \log\left(\ell^{-1}\right), & \text{if} \quad q < p = 4, \\ 1, & \text{if} \quad q < p < 4, \end{cases}$$

and consequently R is (p, q)-intermittent in the sense of structure functions whenever $p \geq 4$.

Like in the case of the high-pass filters, we write a separate corollary for the standard case of $p = 4$ and $q = 2$.

Corollary 5.11. *Let R be Riemann's non-differentiable function (5.1). There exists $0 < \ell_0 < 1$ such that for $0 < \ell < \ell_0$,*

$$G_R(\ell) \simeq \log\left(\ell^{-1}\right).$$

Consequently, R is intermittent in the sense of structure functions.

Remark 5.12. The same conclusion as in Remark 5.8 is valid here too: the logarithmic growth of the flatness can be interpreted as a weak intermittency that agrees with the fact that the image of R is not self-similar but almost.

A similar analysis as in Theorems 5.4 and 5.9 also seems reasonable for more general functions

$$R_\alpha(x) = \sum_{n=1}^{\infty} \frac{e^{2\pi i n^2 x}}{n^\alpha}, \quad x \in \mathbb{T}, \tag{5.5}$$

for different values of $\alpha \in \mathbb{R}$, which are on the one hand generalisations of R and also natural complex generalisations of the functions (1.3) considered by Hardy [47] among others. Hardy proved that (5.5) is not a Fourier series when $\alpha < 1/2$, but the analysis for $\alpha \geq 1/2$ seems feasible. This is part of the future work of this project.

5.3 Intermittency in the sense of high-pass filters

Let us prove Theorem 5.4. First of all, observe that the case $p = \infty$ is immediate because

$$\|R_{\geq N}\|_{L^\infty} = \sup_{x \in [0,1]} \left| \sum_{n=N}^{\infty} \frac{\sigma_n}{n} e_n(x) \right| = \sum_{n=\sqrt{N}}^{\infty} \frac{1}{n^2} \simeq \frac{1}{\sqrt{N}},$$

so let us focus on $p < \infty$. Theorem 5.19 in Section 5.5 will play an important role in the estimations we are looking for, so let us write here the function appearing there,

$$\psi_p(N) = \begin{cases} N^{p/2}, & p < 4, \\ N^2 \log N, & p = 4 \\ N^{p-2}, & p > 4, \end{cases}$$

for any $N > 1$. Also, we work with the Littlewood-Paley decomposition of R

$$R(x) = \sum_{k=1}^{\infty} \Delta_k R(x), \tag{5.6}$$

where $\Delta_k R(x)$ are the Littlewood-Paley pieces

$$\Delta_1 R(x) = \sum_{|n| \le A} \frac{\sigma_n}{n} e_n(x), \qquad \Delta_k R(x) = \sum_{A^k < |n| \le A^{k+1}} \frac{\sigma_n}{n} e_n(x)$$

with width ratio $A > 1$. The Littlewood-Paley theorem, which we state in Section 5.5, allows to compute the L^p norm of R by using these pieces that have disjoint frequencies. We choose the annulus width ratio $A = A_p$ as

$$A_p = \left(\frac{1 + C_p}{c_p} \right)^4 > 1, \tag{5.7}$$

where the constants $C_p > c_p > 0$ come from the Theorem 5.19 in Section 5.5. The reason for this choice will become evident along the proof. Theorem 5.4 will be then a consequence of Propositions 5.13 and 5.14.

Proposition 5.13. *Let R be Riemann's non-differentiable function (5.1), $1 \le p < \infty$ and its Littlewood-Paley decomposition (5.6) with A_p as in (5.7). There exists $k_p > 1$ such that for every $k \ge k_p$,*

$$\|\Delta_k R\|_{L^p}^p \simeq_p \frac{\psi_p\left(A_p^{k/2}\right)}{A_p^{kp}} = \begin{cases} A_p^{-3kp/4}, & \text{if } p < 4, \\ k A_4^{-3k}, & \text{if } p = 4, \\ A_p^{-k(p+2)/2}, & \text{if } p > 4. \end{cases}$$

Proof. The objective is to compute the L^p norm of the function

$$\Delta_k R(x) = \sum_{n > A_p^k}^{A_p^{k+1}} \frac{\sigma_n}{n} e_n(x).$$

Since this is a localised Fourier series, the idea is to take the denominator away by using Lemma 5.20 and then to use Theorem 5.19 to estimate the resulting L^p norm.

First of all, since $A_p^{k+1}/A_p^k = A_p$ is independent of k, we use Corollary 5.21 to write

$$\|\Delta_k R\|_{L^p} = \left\| \sum_{n > A_p^k}^{A_p^{k+1}} \frac{\sigma_n}{n} e_n \right\|_{L^p} \simeq_p \frac{1}{A_p^k} \left\| \sum_{n > A_p^k}^{A_p^{k+1}} \sigma_n e_n \right\|_{L^p} = \frac{1}{A_p^k} \left\| \sum_{n > A_p^{k/2}}^{A_p^{(k+1)/2}} e_{n^2} \right\|_{L^p}.$$

Then, the triangle inequality yields

$$\|\Delta_k R\|_{L^p} \lesssim_p \frac{1}{A_p^k}\left(\left\|\sum_{n=1}^{A_p^{\frac{k+1}{2}}} e_{n^2}\right\|_{L^p} + \left\|\sum_{n=1}^{A_p^{k/2}} e_{n^2}\right\|_{L^p}\right) \tag{5.8}$$

and

$$\|\Delta_k R\|_{L^p} \gtrsim_p \frac{1}{A_p^k}\left(\left\|\sum_{n=1}^{A_p^{\frac{k+1}{2}}} e_{n^2}\right\|_{L^p} - \left\|\sum_{n=1}^{A_p^{k/2}} e_{n^2}\right\|_{L^p}\right) \tag{5.9}$$

Let M_p be the constant from Theorem 5.19, and choose $k_p = \log_{A_p} M_p^2$, so $k > k_p$ implies $A_p^{k/2} > M_p$. Then, from (5.8) we obtain the upper bound

$$\|\Delta_k R\|_{L^p} \lesssim_p \frac{1}{A_p^k}\left(\psi_p^{1/p}\left(A_p^{(k+1)/2}\right) + \psi_p^{1/p}\left(A_p^{k/2}\right)\right) \simeq_p \frac{\psi_p^{1/p}\left(A_p^{k/2}\right)}{A_p^k}.$$

For the lower bound (5.9), Theorem 5.19 yields

$$\|\Delta_k R\|_{L^p} \gtrsim_p \frac{\psi_p^{1/p}\left(A_p^{k/2}\right)}{A_p^k}\left(c_p \frac{\psi_p^{1/p}\left(A_p^{(k+1)/2}\right)}{\psi_p^{1/p}\left(A_p^{k/2}\right)} - C_p\right).$$

One can check that

$$\frac{\psi_p^{1/p}\left(A_p^{(k+1)/2}\right)}{\psi_p^{1/p}\left(A_p^{k/2}\right)} = \begin{cases} A_p^{1/4}, & \text{if} \quad p < 4, \\ (1+\frac{1}{k})^{\frac{1}{4}} A_4^{1/4}, & \text{if} \quad p = 4, \\ A_p^{\frac{1}{2}-\frac{1}{p}}, & \text{if} \quad p > 4, \end{cases}$$

which has a uniform lower bound given by $A_p^{1/4}$. By the choice of A_p in (5.7), we get

$$c_p \frac{\psi_p^{1/p}\left(A_p^{(k+1)/2}\right)}{\psi_p^{1/p}\left(A_p^{k/2}\right)} - C_p \geq c_p A_p^{1/4} - C_p = 1,$$

and therefore,

$$\|\Delta_k R\|_{L^p} \gtrsim_p \frac{\psi_p^{1/p}\left(A_p^{k/2}\right)}{A_p^k}.$$

which concludes the proof. □

Proposition 5.14. *Let R be Riemann's non-differentiable function (5.2), $1 < p < \infty$, $N \geq 1$ and A_p as in (5.7). Define*

$$i_p(N) = \left\lfloor \frac{\log N}{\log A_p} \right\rfloor + 1 \qquad \textit{so that} \qquad A_p^{i_p(N)-1} \leq N < A^{i_p(N)}.$$

Then,

$$R_{\geq N}(x) = \Delta_{i_p(N)-1} R_{\geq N}(x) + \sum_{k=i_p(N)}^{\infty} \Delta_k R(x), \tag{5.10}$$

and there exists $N_p > 1$ such that for every $N \geq N_p$,

$$\|R_{\geq N}\|_{L^p}^p \simeq_p \|\Delta_{i_p(N)} R\|_{L^p}^p \simeq_p \begin{cases} N^{-\frac{3p}{4}}, & \text{if } p < 4, \\ N^{-3} \log N, & \text{if } p = 4, \\ N^{-\left(1+\frac{p}{2}\right)}, & \text{if } p > 4. \end{cases} \tag{5.11}$$

The upper estimate also holds for $p = 1$.

Proof. The Littlewood-Paley decomposition (5.10) is a direct consequence of the definition of $i_p(N)$. Indeed, since $R_{\geq N}$ has only modes greater than N, $\Delta_k R_{\geq N} = 0$ for all $k \leq i_p(N) - 2$, and $\Delta_k R_{\geq N} = \Delta_k R$ for $k \geq i_p(N)$. The intermediate block $\Delta_{i_p(N)-1} R_{\geq N}$ depends on where N lies in the interval $(A_p^{i_p(N)-1}, A_p^{i_p(N)})$.

Let us prove (5.11) now. According to the Littlewood-Paley Theorem 5.18, for $p > 1$ we have the lower bound

$$\|R_{\geq N}\|_{L^p} \simeq_p \left\| \left(\sum_{k \geq i_p(N)-1} |\Delta_k R_{\geq N}|^2 \right)^{\frac{1}{2}} \right\|_{L^p} \geq \|\Delta_{i_p(N)} R\|_{L^p}. \tag{5.12}$$

For the upper bound, for any $p \geq 1$ the triangle inequality yields

$$\|R_{\geq N}\|_{L^p} \leq \|\Delta_{i_p(N)-1} R_{\geq N}\|_{L^p} + \|\Delta_{i_p(N)} R\|_{L^p} + \sum_{k > i_p(N)} \|\Delta_k R\|_{L^p}. \tag{5.13}$$

The objective is to bound the first and the third terms by $\|\Delta_{i_p(N)} R\|_{L^p}$. Let us manage the first term first. Since $A_p^{i_p(N)}/N \leq A_p$, which is independent of N, Corollary 5.21 implies

$$\begin{aligned} \left\|\Delta_{i_p(N)-1} R_{\geq N}\right\|_{L^p} &= \left\| \sum_{n=N}^{A_p^{i_p(N)}} \frac{\sigma_n}{n} e_n \right\|_{L^p} \simeq_p \frac{1}{A_p^{i_p(N)}} \left\| \sum_{n=N}^{A_p^{i_p(N)}} \sigma_n e_n \right\|_{L^p} \\ &= \frac{1}{A_p^{i_p(N)}} \left\| \sum_{n=\sqrt{N}}^{A_p^{i_p(N)/2}} e_{n^2} \right\|_{L^p}, \end{aligned}$$

and using the triangle inequality we get

$$\left\|\Delta_{i_p(N)-1} R_{\geq N}\right\|_{L^p} \lesssim_p \frac{1}{A_p^{i_p(N)}} \left(\left\| \sum_{n=1}^{A_p^{i_p(N)/2}} e_{n^2} \right\|_{L^p} + \left\| \sum_{n=1}^{\sqrt{N}} e_{n^2} \right\|_{L^p} \right).$$

Then, use Theorem 5.19 and Proposition 5.13 to write

$$\begin{aligned} \left\|\Delta_{i_p(N)-1} R_{\geq N}\right\|_{L^p} &\lesssim_p \frac{\psi_p^{1/p}\left(A_p^{i_p(N)/2}\right) + \psi_p^{1/p}\left(\sqrt{N}\right)}{A_p^{i_p(N)}} \\ &\lesssim_p \frac{\psi_p^{1/p}\left(A_p^{i_p(N)/2}\right)}{A_p^{i_p(N)}} \simeq_p \|\Delta_{i_p(N)} R\|_p. \end{aligned}$$

This holds whenever $\sqrt{N} \geq M_p$ from Theorem 5.19 and when $i_p(N) > k_p = \log_{A_p} M_p^2$ from Proposition 5.13. Defining $N_p = M_p^2$, the two conditions are satisfied when

$N > N_p$.

Let us now consider the infinite sum in (5.13). We will need to separate cases depending on the value of p. Consider first the case $p \neq 4$. Then, if $N > N_p$, according to Proposition 5.13, we get

$$\|\Delta_k R\|_{L^p} \simeq_p r_p^k, \qquad \forall k \geq i_p(N),$$

where the constant $0 < r_p < 1$ is

$$r_p = \begin{cases} A_p^{-3/4}, & \text{if } p < 4, \\ A_p^{-\left(\frac{1}{2}+\frac{1}{p}\right)}, & \text{if } p > 4. \end{cases}$$

Then,

$$\sum_{k>i_p(N)} \|\Delta_k R\|_{L^p} \simeq_p \sum_{k>i_p(N)} r_p^k = \frac{r_p^{\lfloor i_p(N)\rfloor+1}}{1-r_p} = r_p^{i_p(N)} \frac{r_p^{1+\lfloor i_p(N)\rfloor-i_p(N)}}{1-r_p}, \tag{5.14}$$

where $r_p^{1+\lfloor i_p(N)\rfloor-i_p(N)} \in [r_p, 1]$. Again according to Proposition 5.13, this shows that

$$\sum_{k>i_p(N)} \|\Delta_k R\|_{L^p} \simeq_p r_p^{i_p(N)} \simeq_p \|\Delta_{i_p(N)} R\|_{L^p}.$$

which is what we wanted to prove. On the other hand, if $p = 4$, Proposition 5.13 says that

$$\|\Delta_k R\|_{L^4} \simeq k^{1/4} r^k, \qquad \forall k \geq i_p(N),$$

where $r = r_4 = A_4^{-3/4}$. Then, Hölder's inequality implies

$$\sum_{k>i_p(N)}^{\infty} \|\Delta_k R\|_{L^4} \leq \left(\sum_{k>i_p(N)}^{\infty} k\, r^k\right)^{\frac{1}{4}} \left(\sum_{k>i_p(N)}^{\infty} r^k\right)^{\frac{3}{4}}.$$

The second sum is identical to the sum (5.14) in the case $p \leq 4$, so $\sum_{k>i_4(N)}^{\infty} r^k \simeq r^{i_4(N)}$. For the first one, the differentiation theorem of power series shows that

$$\begin{aligned} \sum_{k>i_4(N)}^{\infty} k\, r^k \leq \sum_{k>i_4(N)}^{\infty} (k+1)\, r^k = \frac{d}{dr}\left(\sum_{k>i_4(N)+1}^{\infty} r^k\right) = \frac{d}{dr} \frac{r^{\lfloor i_4(N)\rfloor+2}}{1-r}. \\ \leq i_4(N) r^{i_4(N)} \frac{r}{1-r}\left(1 + \frac{1}{i_4(N)}\left(2 + \frac{r}{1-r}\right)\right) \\ \leq i_4(N) r^{i_4(N)} \frac{2r}{1-r}, \end{aligned}$$

where the last equality is satisfied if $N > A_4^{2+r/(1-r)}$. Together with the condition $N > M_4^2$ needed before, set $N_4 = \max\{M_4^2, A_4^{2+r/(1-r)}\}$ so that

$$\sum_{k>i_p(N)}^{\infty} \|\Delta_k R\|_{L^4} \lesssim i_4(N)^{\frac{1}{4}} r^{\frac{i_4(N)}{4}} r^{\frac{3i_4(N)}{4}} = i_4(N)^{\frac{1}{4}} r^{i_4(N)} \simeq \left\|\Delta_{i_4(N)} R\right\|_{L^4}$$

for every $N > N_4$.

In conclusion, all terms in (5.13) are bounded by $\|\Delta_{i_4(N)}R\|_{L^p}$ for every $p > 1$ whenever $N > N_p$, so $\|R_{\geq N}\|_{L^p} \lesssim_p \|\Delta_{i_p(N)}R\|_{L^p}$, which together with (5.12) gives

$$\|R_{\geq N}\|_{L^p} \simeq_p \|\Delta_{i_p(N)}R\|_{L^p}.$$

Finally, since the definition of $i_p(N)$ implies

$$A_p^{i_p(N)} \simeq_p N \qquad \text{and} \qquad i_p(N) \simeq_p \log N,$$

by Proposition 5.13 the proof is complete. □

5.4 Intermittency in the sense of structure functions

Let us prove Theorem 5.9. Recalling the definition of structure functions (5.4), we can do the elementary change of variables $x \to x - \ell/2$ so that

$$S_p(\ell) = \int_0^1 |R(x+\ell) - R(x)|^p \, dx = \int_0^1 |R(x+\ell/2) - R(x-\ell/2)|^p \, dx,$$

and hence define the increment function

$$I(\ell, x) = R(x+\ell/2) - R(x-\ell/2) = 2\,i \sum_{n=1}^{\infty} \frac{sin(\pi n \ell)}{n} \sigma_n \, e_n(x). \tag{5.15}$$

This way, writing $I(\ell) = I(\ell, \cdot)$, we have

$$S_p(\ell) = \|I(\ell)\|_p^p.$$

Recall that the objective is to compute the asymptotic behaviour of $S_p(\ell)$ when $\ell \to 0$.

We proceed as follows. First, we compute $S_p(\ell)$ for even values of p, cases in which we can use the Plancherel theorem. The idea then is to interpolate between these cases to extend the result to the rest of the values of p. However, because of the change of behaviour from $p < 4$ to $p > 4$, and specially because of the logarithmic term in $p = 4$, this technique will not give us the optimal results in some range of p around 4. To fix that, we will be able to prove the optimal upper estimate for all p avoiding the use of the Plancherel theorem. After that, interpolation will yield every lower estimate.

The case $p = 2$ is straightforward, but representative of the technique we use for a general even p. We show the argument of this simple case in the proof of the following lemma.

Lemma 5.15. *For $0 < \ell < 1/2$,*

$$S_2(\ell) \simeq \ell^{3/2}.$$

Proof. By Parseval's theorem and the definition of the increment function (5.15),

$$S_2(\ell) = \|I(\ell)\|_2^2 \simeq \sum_{n=1}^{\infty} \frac{\sin^2(\pi n \ell)}{n^2} \sigma_n^2.$$

We know that the $\sin x$ behaves like x when $x \to 0$. In this case, if $\ell \ll 1$ is small, then we will be able to approximate $\sin(\pi n \ell)$ for large values of n. Thus, we split the sum above in small frequencies $n \lesssim \ell^{-1}$, where we expect to use the estimation, and

large frequencies $n > \ell^{-1}$, which hopefully will be small enough. Thus,

$$\begin{aligned} S_2(\ell) &= \sum_{n\le(2\ell)^{-1/2}} \frac{\sin^2(\pi n^2\ell)}{n^4} + \sum_{n>(2\ell)^{-1/2}} \frac{\sin^2(\pi n^2\ell)}{n^4} \\ &= A_2(\ell) + B_2(\ell) \end{aligned}$$

On the one hand, since $\sin(x)/x \simeq 1$ for $|x| \le \pi/2$,

$$A_2(\ell) \simeq \sum_{n\le(2\ell)^{-1/2}} \frac{(\pi\, n^2\, \ell)^2}{n^4} \simeq \ell^{3/2}.$$

On the other hand, we have the upper bound

$$B_2(\ell) \le \sum_{n>(2\ell)^{-1/2}} \frac{1}{n^4} \simeq \int_{(2\ell)^{-1/2}}^{\infty} \frac{dx}{x^4} \simeq \ell^{3/2},$$

so the proof in complete because

$$\ell^{3/2} \simeq A_2(\ell) \le A_2(\ell) + B_2(\ell) \lesssim \ell^{3/2}.$$

□

We now generalise this reasoning to the rest of the even values of p.

Proposition 5.16. *Let $p \in 2\mathbb{N}$ be even. There exists $0 < \ell_p < 1/2$ such that*

$$S_p(\ell) \simeq_p \ell^{1+p/2}, \qquad \forall \ell \in (0, \ell_p), \qquad \text{when } p > 4,$$

and

$$S_4(\ell) \simeq \ell^3 \log(\ell^{-1}), \qquad \forall \ell \in (0, \ell_4).$$

Proof. Let $k \in \mathbb{N}$ such that $p = 2k$. Then, as in Lemma 5.15, split the increment function in small and large frequencies, this time with an indeterminate coefficient M, such that using the notation of the high- and low-pass filters in Definition 5.1 we get

$$I(\ell) = I_{\le M}(\ell) + I_{>M}(\ell). \tag{5.16}$$

This allows, by the triangle inequality, the upper bound

$$S_p^{1/p}(\ell) = \|I(\ell)\|_p \le \|I_{\le M}(\ell)\|_p + \|I_{>M}(\ell)\|_p. \tag{5.17}$$

Following the proof of Lemma 5.15, we should be able to get a lower bound by only $\|I_{\le M}(\ell)\|_p$ using the Plancherel theorem. For this, call the Fourier coefficients of I

$$a_n = \frac{\sin(\pi n\ell)}{n}\,\sigma_n, \qquad I(\ell) = \sum_{n=1}^{\infty} a_n\, e_n,$$

so that

$$S_p(\ell) = \Big\| \Big(\sum_{n=1}^{\infty} a_n\, e_n \Big)^k \Big\|_2^2 = \sum_{n=1}^{\infty} |b_n|^2, \quad \text{where} \quad \Big(\sum_{n=1}^{\infty} a_n\, e_n \Big)^k = \sum_{n=1}^{\infty} b_n\, e_n.$$

In the same way,

$$\|I_{\le M}(\ell)\|_p^p = \Big\| \Big(\sum_{n=1}^{M} a_n\, e_n \Big)^k \Big\|_2^2 = \sum_{n=1}^{kM} |b_n^M|^2, \qquad \text{where} \qquad \Big(\sum_{n=1}^{M} a_n\, e_n \Big)^k = \sum_{n=1}^{kM} b_n^M\, e_n. \tag{5.18}$$

More precisely,

$$b_n = \sum_{n_1+\ldots+n_k=n} a_{n_1} \ldots a_{n_k}, \qquad b_n^M = \sum_{\substack{n_1+\ldots+n_k=n \\ n_i \le M}} a_{n_1} \ldots a_{n_k}. \tag{5.19}$$

If $kM\ell \le 1/2$, then $1/2 \le \sin(\pi n\ell)/(\pi n\ell) \le 1$ for every $n \le kM$, which implies that $a_n, b_n, b_n^M > 0$ for all $n \le kM$. This positivity property implies

$$b_n^M = \sum_{\substack{n_1+\ldots+n_k=n \\ n_i \le M}} a_{n_1} \ldots a_{n_k} \le \sum_{n_1+\ldots+n_k=n} a_{n_1} \ldots a_{n_k} = b_n, \qquad \forall n \le kM,$$

which in turn implies

$$\|I_{\le M}(\ell)\|_p^p = \sum_{n=1}^{kM} (b_n^M)^2 \le \sum_{n=1}^{kM} b_n^2 = \sum_{n=1}^{kM} |b_n|^2 \le \sum_{n=1}^{\infty} |b_n|^2 = S_p(\ell).$$

Hence, (5.17) is completed by

$$\|I_{\le M}(\ell)\|_p \le S_p^{1/p}(\ell) = \|I(\ell)\|_p \le \|I_{\le M}(\ell)\|_p + \|I_{>M}(\ell)\|_p, \tag{5.20}$$

subject to the condition $\ell \le 1/(2kM)$. So we choose $M = 1/(2k\ell)$, but we keep the notation M for simplicity. Thus, we need both upper and lower estimates for the low-pass filter $\|I_M(\ell)\|_p$ but an upper estimate for the high-pass filter $\|I_{>M}(\ell)\|_p$ is enough.

Let us begin precisely with the latter case. By the definition of the increment function $I(\ell)$ in (5.15), and by the linearity of the high-pass filters, one can write

$$I_{>M}(\ell) = R_{>M}(x + \ell/2) - R_{>M}(x - \ell/2),$$

and therefore the triangle inequality as well as periodicity yield

$$\|I_{>M}(\ell)\|_p \le \|R_{>M}(\cdot + \ell/2)\|_p + \|R_{>M}(\cdot - \ell/2)\|_p = 2\|R_{>M}\|_p. \tag{5.21}$$

Thus, since $M = 1/(2k\ell) \simeq_p \ell^{-1}$, Theorem 5.4 gives the desired estimate

$$\|I_{>M}(\ell)\|_p \lesssim_p \begin{cases} \ell^{3/4}\, (\log \ell^{-1})^{1/4}, & \text{if } p = 4, \\ \ell^{1/2+1/p}, & \text{if } p > 4. \end{cases} \tag{5.22}$$

Let us analyse the low-pass filters $\|I_{\le M}(\ell)\|_p$. Looking at (5.18) and (5.19), we see that under the condition $M < 1/(2k\ell)$, we have

$$\frac{1}{2} \le \frac{\sin(\pi n_i \ell)}{\pi n_i \ell} \le 1, \qquad \Longrightarrow \qquad a_{n_i} \simeq \pi\, \ell\, \sigma_{n_i}, \qquad \forall n_i \le M = \frac{1}{2k\ell}.$$

That means that from (5.19) we have

$$b_n^M = (\pi\ell)^k \sum_{\substack{n_1+\ldots+n_k=n \\ n_i\le M}} \sigma_{n_1}\ldots\sigma_{n_k},$$

and therefore

$$\begin{aligned}\|I_{\le M}(\ell)\|_p^p &= (\pi\ell)^{2k} \sum_{n=1}^{kM} \left| \sum_{\substack{n_1+\ldots+n_k=n \\ n_i\le M}} \sigma_{n_1}\ldots\sigma_{n_k} \right|^2 \\ &\simeq \ell^{2k} \left\| \sum_{n=1}^{M} \sigma_n\, e_n \right\|_p^p = \ell^{2k} \left\| \sum_{n=1}^{\sqrt{M}} e_{n^2} \right\|_p^p,\end{aligned}$$

where in the penultimate equality we did nothing but to replace a_n by σ_n in (5.18) and (5.19). Thus, according to Theorem 5.19 in Section 5.5, remembering that $M \simeq_p \ell^{-1}$ and that $p = 2k$, we get

$$\|I_{\le M}(\ell)\|_p^p \simeq_p \begin{cases} \ell^p\,\ell^{-1}\,\log\ell^{-1/2} \simeq \ell^3\,\log\ell^{-1} & \text{if } p=4, \\ \ell^p\,\ell^{1-p/2} = \ell^{1+p/2} & \text{if } p>4. \end{cases} \tag{5.23}$$

This is the same expression as in (5.22), so according to (5.20), the behaviour of $S_p(\ell)$ is precisely that in (5.23), maybe up to some constant only depending on p. □

Once the result has been proved for even values of p, let us study the case of a general p.

Proposition 5.17. *Let $p \ge 1$. Then, for $\ell > 0$ small enough,*

$$S_p(\ell) \simeq_p \begin{cases} \ell^{3p/4}, & \text{if} \quad p<4, \\ \ell^{1+p/2}, & \text{if} \quad p>4. \end{cases}$$

As suggested, we will use interpolation between even cases. This technique suggest that $S_p(\ell)$ follows some rule related to $S_6, S_8, \ldots$ when $p > 4$ and related to S_2 when $p < 4$. However, this is not enough to conclude the results in Proposition 5.17 for values of p near 4 because the logarithmic term appearing in S_4 distorts the interpolation. We will solve this problem by proving the upper estimate directly. This is not trivial to generalise from the proof of Proposition 5.16 because in the case of the low-pass filter $I_{\le M}$, we will not be able to use the Plancherel theorem any more. Once we obtain the upper bound, we will interpolate to get the lower estimates.

Proof. Let us decompose the increment function in frequency as in (5.16) and bound it from above as in (5.20), again with $M = \ell^{-1}$. Observe that the upper bound for the high-pass filters in (5.21) holds, and since the upper estimate in Theorem 5.14 is valid for every $p \ge 1$, we have

$$\|I_{>M}(\ell)\|_p \lesssim_p \begin{cases} \ell^{3/4}, & \text{if } p<4, \\ \ell^{1/2+1/p}, & \text{if } p>4. \end{cases} \tag{5.24}$$

On the other hand, the proof of the upper bound for the low-pass filter $\|I_{\le M}(\ell)\|_p$ is mostly given in Corollary 5.23, which is based in other technical auxiliary results that we also use in other parts of this chapter and that also gathered in Section 5.5.3.

Using it with $A = M$, we get

$$\begin{aligned} \|I_{\le M}(\ell)\|_p &= \left\| \sum_{n=1}^{M} \frac{\sin(\pi n \ell)}{n}\, \sigma_n\, e_n \right\|_{L^p} \lesssim \ell\, \cosh(2\pi M \ell) \left\| \sum_{n=1}^{M} \sigma_n e_n \right\| |_{L^p} \\ &\simeq_p \ell \left\| \sum_{n=1}^{\ell^{-1/2}} e_{n^2} \right\|_{L^p}, \end{aligned} \tag{5.25}$$

which together with Theorem 5.19 in Section 5.5.2 yields

$$\|I_{\le M}(\ell)\|_p \lesssim_p \begin{cases} \ell^{3/4} & \text{if } p < 4, \\ \ell^{1/2+1/p} & \text{if } p > 4. \end{cases}$$

Since this is the same as (5.24), we get

$$S_p(\ell) \lesssim_p \begin{cases} \ell^{3p/4} & \text{if } p < 4, \\ \ell^{1+p/2} & \text{if } p > 4, \end{cases} \tag{5.26}$$

and the upper estimate in the statement is proved.

To obtain the lower bounds, we interpolate between the known cases of even p by means of Hölder's inequality, by which for any $q, q' \ge 1$ such that $1/q + 1/q' = 1$,

$$\|f\, g\|_1 \le \|f\|_q\, \|g\|_{q'} \qquad \text{for all } f \in L^q, \quad g \in L^{q'}.$$

The idea is that since $S_p(\ell) = \|I(\ell)\|_p^p$, we write

$$\int |I(\ell)|^A = \int |I(\ell)|^{a+b} \le \Big(\int |I(\ell)|^{aq} \Big)^{1/q} \Big(\int |I(\ell)|^{bq'} \Big)^{1/q'}, \tag{5.27}$$

and then we make $aq = p$ and $bq' = B$ and A, B even. Call $\theta = 1/q$, so the conditions are

$$\begin{cases} A = a + b, \\ aq = p, \\ bq' = B, \end{cases} \quad \Longrightarrow \quad \begin{cases} A = a + b, \\ a = p\theta, \\ b = B(1-\theta). \end{cases} \quad \Longrightarrow \quad \theta = \frac{B - A}{B - p}.$$

Of course, $\theta \in [0, 1]$ must hold. A simple and reasonable, but not the only, choice for A and B is that $A = 2m$ and $B = 2m+2$ for some $m \in \mathbb{N}$, so that $\theta = 2/(B-p)$ and then the condition for θ is satisfied in case $p \le B - 2$. In other words, if $p < 2m < 2m + 2$ and we interpolate $2m$ between p and $2m + 2$, we will get that

$$S_p^\theta(\ell) \ge \frac{S_{2m}(\ell)}{S_{2m+2}^{1-\theta}(\ell)}.$$

Since we know the upper and lower estimates for both S_{2m} and S_{2m+2}, this will yield a lower bound for S_p whenever $p < 2m$. Let us compute it by taking $m \ge 3$ so that $2m \ge 6$ and S_{2m} and S_{2m+2} behave like the first case in Proposition 5.16,

$$S_p(\ell) \gtrsim_p \ell^{\frac{1+m}{\theta}}\, \ell^{(2+m)(1-1/\theta)} = \ell^{2+m-1/\theta} = \ell^{2+m-m-1+p/2} = \ell^{1+p/2}.$$

According to the upper estimate we just obtained in (5.26), this is optimal when $p > 4$, but not when $p < 4$, since precisely $3p/4 < 1 + p/2$ when $p < 4$, and thus, $\ell^{1+p/2} < \ell^{3p/4}$. But of course, if we expect to have two different ranges of behaviour as shown in the statement, there is no way that we will get the correct estimate for

results for $p < 4$ using the behaviour for the other range $p > 4$.

For $p < 4$, we could think in using the above argument interpolating $p < 4 < 6$, for instance, or even $p < 2 < 4$ for smaller values of p. However, in these cases the interpolation will account for the logarithm in S_4, which we expect not to have in S_p when $p < 4$. However, for $1 \le p < 2$, this can be fixed thanks to the upper bounds obtained before for all values of p. Indeed, in (5.27) we need a lower estimate for S_A, which forces A to be even, but an upper estimate is enough for B. Thus, choose $A = 2$ and say, $B = 3$, so that the above argument yields

$$S_p(\ell)^\theta \gtrsim_p \frac{S_2(\ell)}{S_3^{1-\theta}}, \qquad \text{where} \qquad \theta = \frac{B-A}{B-p} = \frac{1}{3-p} < 1.$$

Thus, by Proposition 5.16 and the upper estimate for $S_3(\ell)$ in (5.26) we have established, we get

$$S_p(\ell) \gtrsim_p \ell^{\frac{3}{2\theta}}\, \ell^{\frac{9}{4}(1-1/\theta)} = \ell^{-\frac{3}{4}\frac{1}{\theta}+\frac{9}{4}} = \ell^{3p/4}, \qquad \text{when } 1 \le p < 2.$$

It is evident that the upper estimate of S_3 is vital here. Let us briefly explain here why interpolation does not work to get it and therefore why we need its direct computation as we did to get (5.26). One can write the arguments analogue to (5.27) for the upper estimates, now the power of the integral on the left hand side would have to be p, and both powers on the right hand side, some even numbers. With this we would obtain the optimal bound for $p > 6$, but $p \in (2, 6)$ need to be interpolated either between 2 and 4 or between 4 and 6, which will yield the unwanted logarithmic term present in S_4. Hence, an alternative was needed.

Yet the case $2 < p < 4$ is missing. The trick above does not work this time, since $0 < \theta < 1$ requires $p < A < B$ with A even, so either $A = 4$, which generates the logarithm, or $A \ge 6$, which is in the incorrect range for $p < 4$. However, there is a very simple argument based on the fact that we work in a space of finite measure that saves the situation, since

$$S_2(\ell) = \int_0^1 |I(\ell)|^2 \le \left(\int_0^1 |I(\ell)|^{2\,\frac{p}{2}} \right)^{2/p} \left(\int_0^1 1 \right)^{1/(p/2)'} = S_p(\ell)^{2/p},$$

which together with Proposition 5.15 immediately implies

$$S_p(\ell) \ge S_2(\ell)^{p/2} \simeq \ell^{\frac{3}{2}\frac{p}{2}} = \ell^{3p/4}, \qquad \text{when } 2 < p < 4.$$

The proof is now complete. □

5.5 Auxiliary results

In this section, we gather the famous Littlewood-Paley theorem in Subsection 5.5.1 and a number theoretical result by Zalcwasser in Subsection 5.5.2, both vital in the proofs of the results in this section. Finally, in Subsection 5.5.3, we gather several auxiliary lemmas needed in the proofs but whose inclusion in the main text might cause an unnecessarily heavy reading.

5.5.1 The Littlewood-Paley decomposition

We recall here the classical decomposition of functions by Littlewood and Paley [68, Theorem 3].

Theorem 5.18. *Let $p > 1$, $A > 1$ and $f(x) = \sum_{n\in\mathbb{Z}} a_n e^{2\pi i n x}$ a function in $L^p(0,1)$. Decompose*

$$f(x) = \sum_{k=1}^{\infty} \Delta_k f(x)$$

such that

$$\Delta_1 f(x) = \sum_{|n|\le A} a_n e^{2\pi i n x}, \qquad \Delta_k f(x) = \sum_{A^k < |n| \le A^{k+1}} a_n e^{2\pi i n x}$$

for every integer $k > 1$. There exist constants $B_1, B_2 > 0$ depending on p such that

$$B_1 \le \frac{\| \left(\sum_{k=1}^{\infty} |\Delta_k f|^2\right)^{1/2} \|_{L^p}}{\|f\|_{L^p}} \le B_2.$$

5.5.2 A theorem of Zalcwasser

The following result, proved by Zalcwasser in [99], estimates the L^p norm of the sum of square-phased oscillating functions.

Theorem 5.19. *Let $p > 0$. Then, there exist $M_p > 1$ and constants $C_p > c_p > 0$ such that for every $N > M_p$,*

$$c_p\, \psi_p(N) \le \int_0^1 \left| \sum_{m=1}^{N} e^{2\pi i m^2 x} \right|^p \mathrm{d}x \le C_p\, \psi_p(N)$$

where

$$\psi_p(N) = \begin{cases} N^{p/2}, & p < 4, \\ N^2 \log N, & p = 4 \\ N^{p-2}, & p > 4. \end{cases}$$

5.5.3 Other results

We present a lemma on estimates for the L^p norms of localised Fourier series of the kind of Riemann's function (5.2), very useful in the setting of high-pass filters in Section 5.3.

Lemma 5.20. *Let $p \ge 1$, $1 \le A < B$, $(a_n)_n \in \mathbb{C}^{\mathbb{N}}$ a sequence and $\gamma \in \mathbb{R}$. If $\gamma > 0$, we have*

$$A^\gamma \left\| \sum_{n=A}^{B} a_n e_n \right\|_{L^p} \lesssim_{|\gamma|, \frac{B}{A}} \left\| \sum_{n=A}^{B} n^\gamma a_n e_n \right\|_{L^p} \lesssim_{|\gamma|} B^\gamma \left\| \sum_{n=A}^{B} a_n e_n \right\|_{L^p}. \tag{5.28}$$

If $\gamma < 0$, we have

$$B^\gamma \left\| \sum_{n=A}^{B} a_n e_n \right\|_{L^p} \lesssim_{|\gamma|} \left\| \sum_{n=A}^{B} n^\gamma a_n e_n \right\|_{L^p} \lesssim_{|\gamma|, \frac{B}{A}} A^\gamma \left\| \sum_{n=A}^{B} a_n e_n \right\|_{L^p}. \tag{5.29}$$

Proof. Let us define

$$f = \sum_{n=A}^{B} n^\gamma a_n e_n \quad \text{and} \quad g = \sum_{n=A}^{B} a_n e_n,$$

so that the objective is to compare the L^p norms of f and g. We first prove the right-hand side inequality in (5.28), so assume $\gamma > 0$. Let $\chi_{(0,1)} \in \mathcal{S}(\mathbb{R})$ be a cut-off function satisfying

$$\chi_{(0,1)}(x) = \begin{cases} 1 & \text{if} \quad 0 \le x \le 1, \\ 0 & \text{if} \quad x \le -1 \quad \text{or} \quad x \ge 2, \end{cases} \tag{5.30}$$

and define the Fourier multiplier m_γ by

$$m_\gamma(\xi) = \xi^\gamma \chi_{(0,1)}(\xi), \qquad \xi \in \mathbb{R},$$

which is also a Schwartz function in $\mathcal{S}(\mathbb{R})$ because $\gamma > 0$. Define also the scaled multiplier $m_{\gamma,B}$ by

$$m_{\gamma,B}(\xi) = m_\gamma\left(\frac{\xi}{B}\right) = \frac{\xi^\gamma}{B^\gamma}\chi_{(0,1)}\left(\frac{\xi}{B}\right).$$

With these definitions, we can write

$$f = \sum_{n=A}^{B} n^\gamma a_n e_n = \sum_{n=A}^{B} n^\gamma \chi_{(0,1)}\left(\frac{n}{B}\right) a_n e_n = B^\gamma \sum_{n=A}^{B} m_{\gamma,B}(n) a_n e_n.$$

Let us now introduce the auxiliary function

$$h_{\gamma,B} = \sum_{n=-B}^{2B} m_{\gamma,B}(n)\, e_n. \tag{5.31}$$

We see that if $*$ denotes the convolution in $\mathbb{T}$, then

$$\begin{aligned} g * h_{\gamma,B}(x) &= \int_0^1 g(x-y)\, h_{\gamma,B}(y)\, dy = \sum_{n=A}^{B} \sum_{l=-B}^{2B} a_n\, m_{\gamma,B}(m)\, e_n(x) \int_0^1 e_{m-n}(y)\, dy \\ &= \sum_{n=A}^{B} a_n m_{\gamma,B}(n) e_n(x), \end{aligned}$$

since the last integral is 1 when $m = n$ and 0 otherwise. Therefore,

$$f = B^\gamma \left(g * h_{\gamma,B}\right). \tag{5.32}$$

Thus, by Young's convolution inequality, we have

$$\|f\|_{L^p} \le B^\gamma \|g\|_{L^p} \|h_{\gamma,B}\|_{L^1}, \tag{5.33}$$

so it suffices to bound $\|h_{\gamma,B}\|_{L^1}$. For that, let us define $H_\gamma \in \mathcal{S}(\mathbb{R})$ by

$$\widehat{H_\gamma}(\xi) := m_\gamma(\xi) = \xi^\gamma \chi_{(0,1)}(\xi),$$

and scale it by $H_{\gamma,B}(x) = BH_\gamma(Bx)$ so that $H_{\gamma,B}$ is an analogue of (5.31) in the real line. Indeed,

$$\widehat{H_{\gamma,B}}(\xi) = \widehat{H_\gamma}\left(\xi/B\right) = m_{\gamma,B}(\xi).$$

In view of (5.31), let us prove that

$$h_{\gamma,B}(x) = \sum_{j\in\mathbb{Z}} H_{\gamma,B}(x-j), \qquad \forall x \in \mathbb{T}. \tag{5.34}$$

For that, given $n \in \mathbb{Z}$, we compute the n-th Fourier coefficient of the right-hand side in (5.34), which is

$$\begin{aligned}\int_0^1 \sum_{j\in\mathbb{Z}} H_{\gamma,B}(x-j)e_{-n}(x)\,dx &= \sum_{j\in\mathbb{Z}} \int_0^1 H_{\gamma,B}(x-j)e_{-n}(x)\,dx \\ &= \sum_{j\in\mathbb{Z}} \int_{-j}^{-j+1} H_{\gamma,B}(y)e_{-n}(y)\,dy \\ &= \widehat{H_{\gamma,B}}(n) = m_{\gamma,B}(n),\end{aligned}$$

because $e_{-n}(x+j) = e_{-n}(x)$ for all $j \in \mathbb{Z}$, and therefore,

$$\sum_{j\in\mathbb{Z}} H_{\gamma,B}(\cdot - j) = \sum_{n\in\mathbb{Z}} m_{\gamma,B}(n)e_n = \sum_{n=-B}^{2B} m_{\gamma,B}(n)e_n = h_{\gamma,B},$$

since $m_{\gamma,B}(n) = 0$ whenever $n \le -B$ or $n \ge 2B$. Consequently,

$$\begin{aligned}\|h_{\gamma,B}\|_{L^1} &= \int_0^1 \left|\sum_{j\in\mathbb{Z}} H_{\gamma,B}(x-j)\right| dx \le \sum_{j\in\mathbb{Z}} \int_0^1 |H_{\gamma,B}(x-j)|\,dx \\ &= \int_{\mathbb{R}} |H_{\gamma,B}(x)|\,dx = \int_{\mathbb{R}} |H_\gamma(x)|\,dx = \|H_\gamma\|_{L^1(\mathbb{R})}.\end{aligned}$$

Hence, since $H_\gamma \in \mathcal{S}(\mathbb{R}) \subset L^1(\mathbb{R})$, substituting in (5.33) we obtain

$$\|f\|_{L^p} \le B^\gamma \, \|H_\gamma\|_{L^1(\mathbb{R})} \, \|g\|_{L^p}.$$

The constant $\|H_\gamma\|_{L^1(\mathbb{R})}$ depends only on γ, so the right-hand side of (5.28) is established. From this, the left-hand side inequality in (5.29) follows immediately since, if $\gamma < 0$, then $-\gamma > 0$ and defining $\tilde{a}_n = n^\gamma a_n$, we get

$$\left\|\sum_{n=A}^{B} a_n e_n\right\|_{L^p} = \left\|\sum_{n=A}^{B} n^{-\gamma}\tilde{a}_n e_n\right\|_{L^p} \lesssim_{|\gamma|} B^{-\gamma} \left\|\sum_{n=A}^{B} \tilde{a}_n e_n\right\|_{L^p} = B^{-\gamma} \left\|\sum_{n=A}^{B} n^{\gamma} a_n e_n\right\|_{L^p}. \tag{5.35}$$

The right-hand side of (5.29) is proved similarly with an alternative smooth cut-off function

$$\widetilde{\chi}_{(1,B/A)}(x) = \begin{cases} 1 & \text{if} \quad 1 \le x \le B/A, \\ 0 & \text{if} \quad x \le 1/2 \quad \text{or} \quad x \ge 2B/A. \end{cases}$$

Let us briefly explain it. Let $\gamma < 0$ and define

$$\widetilde{m}_\gamma(\xi) = \xi^\gamma \widetilde{\chi}_{(1,\frac{B}{A})}(\xi), \qquad \text{and} \qquad \widetilde{m}_{\gamma,A}(\xi) = \widetilde{m}_\gamma(\xi/A)$$

for $\xi \in \mathbb{R}$. Both functions are in $\mathcal{S}(\mathbb{R})$. Then,

$$f = \sum_{n=A}^{B} n^\gamma a_n\, e_n = \sum_{n=A}^{B} n^\gamma \tilde{\chi}_{(1,B/A)}\,(n/A)\, a_n\, e_n = A^\gamma \sum_{n=A}^{B} a_n\, \widetilde{m}_{\gamma,A}(n)\, e_n,$$

so defining $\widetilde{h}_{\gamma,A} = \sum_{n=A/2}^{2B} \widetilde{m}_{\gamma,A}(n)\, e_n$, in a similar way as in (5.32), by Young's inequality we have

$$\|f\|_{L^p} \le A^\gamma\, \|\widetilde{h}_{\gamma,A}\|_{L^1}\, \|g\|_{L^p}.$$

Then, define $\widetilde{H}_\gamma \in \mathcal{S}(\mathbb{R})$ such that $\widehat{\widetilde{H}_\gamma}(\xi) = \widetilde{m}_\gamma(\xi)$ and $\widetilde{H}_{\gamma,A}(x) = A\,\widetilde{H}(Ax)$ such that

$$\widehat{\widetilde{H}_{\gamma,A}}(\xi) = \widehat{\widetilde{H}_\gamma}(\xi/A) = \widetilde{m}_\gamma(\xi/A) = \widetilde{m}_{\gamma,A}(\xi).$$

Then, as in (5.34), we get

$$\widetilde{h}_{\gamma,A}(x) = \sum_{j\in\mathbb{Z}} \widetilde{H}_{\gamma,A}(x-j)$$

and

$$\|\widetilde{h}_{\gamma,A}\|_{L^1} \le \|\widetilde{H}_{\gamma,A}\|_{L^1(\mathbb{R})} = \|\widetilde{H}_\gamma\|_{L^1(\mathbb{R})}.$$

However, $\widetilde{H}_\gamma$ depends on $\widetilde{\chi}_{(1,B/A)}$, so $\|\widetilde{H}_\gamma\|_{L^1(\mathbb{R})}$ depends on γ and also on B/A. Hence, the right-hand side in (5.29) is established with the additional dependence on B/A. Finally, the right-hand side of (5.28) is proved by using the same trick as in (5.35). □

We immediately get the following corollary of Lemma 5.20, which we use in Section 5.3.

Corollary 5.21. *Let $0 < A < B$ be real numbers, possibly varying according to some parameter. Assume that the ratio B/A is bounded by a constant independent of that parameter. Then, for all $p \ge 1$ and $\gamma \in \mathbb{R}$,*

$$\left\| \sum_{n=A}^{B} n^\gamma\, a_n\, e_n \right\|_{L^p} \simeq A^\gamma \left\| \sum_{n=A}^{B} a_n e_n \right\|_{L^p} \simeq B^\gamma \left\| \sum_{n=A}^{B} a_n e_n \right\|_{L^p}.$$

Proof. If the constant bounding the ratio B/A is C, then the dependence on B/A in Lemma 5.20 can be dropped from the proof by choosing $\widetilde{\chi}_{(1,C)}$ instead of $\widetilde{\chi}_{(1,B/A)}$. Also, $A \simeq B$ holds independently of parameters. □

Lemma 5.20 will also be of use in the setting of structure functions, but for that we will need to combine it with the following lemma.

Lemma 5.22. *Let $C > 0$ and $M \ge 1$. Let also $f \in H^1(\mathbb{R})$ with support in $[-M, M]$. Then*

$$\sum_{k=0}^{\infty} \frac{C^{2k} \|\partial^{2k} \hat{f}\|_{L^1(\mathbb{R})}}{(2k+1)!} \lesssim \cosh(CM) \|f\|_{H^1(\mathbb{R})}.$$

Proof. First, we prove

$$\|g\|_{L^1(\mathbb{R})} \lesssim \|g\|_{L^2(\mathbb{R})}^{1/2}\, \|xg\|_{L^2(\mathbb{R})}^{1/2}, \qquad \forall g \in L^2(\mathbb{R}). \tag{5.36}$$

For that, let $R>0$ and $g\in L^2(\mathbb{R})$ a non-zero function. The Cauchy-Schwarz inequality implies that

$$\begin{aligned}\|g\|_{L^1(\mathbb{R})} &= \int_{|x|<R} g(x)\,dx + \int_{|x|>R} \frac{xg(x)}{x}\,dx \\ &\le \sqrt{2R}\,\|g\|_{L^2(\mathbb{R})} + \sqrt{\frac{2}{R}}\,\|xg\|_{L^2(\mathbb{R})},\end{aligned}$$

and choosing $R=\|xg\|_{L^2(\mathbb{R})}/\|g\|_{L^2(\mathbb{R})}$ (5.36) follows. Let now $M\ge 1$ and $f\in H^1(\mathbb{R})$ a non-zero function with support in $[-M,M]$. Let us show, using (5.36) for $\widehat{f}$, that

$$\|\partial^{2k}\widehat{f}\|_{L^1(\mathbb{R})} \lesssim \sqrt{2k+1}\,M^{2k}\,\|f\|_{H^1(\mathbb{R})}, \qquad \forall k\in\mathbb{N}\cup\{0\}. \tag{5.37}$$

The case $k=0$ follows immediately from (5.36) since

$$\|\widehat{f}\|_{L^1(\mathbb{R})} \lesssim \|\widehat{f}\|_{L^2(\mathbb{R})}^{1/2}\,\|\xi\widehat{f}\|_{L^2(\mathbb{R})}^{1/2} \le \|f\|_{H^1(\mathbb{R})}.$$

For $k>0$, since $\partial^{2k}\widehat{f}=i^{2k}\,(x^{2k}\,f)^\wedge$ and $i\,\xi\,\widehat{f}=(\partial f)^\wedge$, by the Plancherel theorem we have

$$\begin{aligned}\|\partial^{2k}\widehat{f}\|_{L^1(\mathbb{R})} &\lesssim \|x^{2k}f\|_{L^2(\mathbb{R})}^{1/2}\,\|\partial_x(x^{2k}f)\|_{L^2(\mathbb{R})}^{1/2} \\ &\le \|x^{2k}f\|_{L^2(\mathbb{R})}^{1/2}\,\Big(\|x^{2k}f'\|_{L^2(\mathbb{R})}+2k\|x^{2k-1}f\|_{L^2(\mathbb{R})}\Big)^{1/2}.\end{aligned}$$

Since f is supported in $[-M,M]$ and $M\ge 1$, we get

$$\|\partial^{2k}\widehat{f}\|_{L^1(\mathbb{R})} \lesssim M^{2k}\|f\|_{L^2(\mathbb{R})}^{1/2}\,(1+2k)^{1/2}\,\|f\|_{H^1(\mathbb{R})}^{1/2} \le M^{2k}\,\sqrt{2k+1}\,\|f\|_{H^1(\mathbb{R})},$$

which is (5.37). Thanks to it we conclude the proof of the lemma because

$$\sum_{k=0}^{\infty}\frac{C^{2k}\|\partial^{2k}\widehat{f}\|_{L^1(\mathbb{R})}}{(2k+1)!} \lesssim \sum_{k=0}^{\infty}\frac{C^{2k}M^{2k}\sqrt{2k+1}}{(2k+1)!}\|f\|_{H^1(\mathbb{R})} \le \cosh(CM)\|f\|_{H^1(\mathbb{R})}.$$

□

As a corollary of Lemmas 5.20 and 5.22, we get the following result which is critical in (5.25).

Corollary 5.23. *Let $p\ge 1$, $0<\ell<1/2$ and $A\ge 1$. Then, there exists a constant $c>0$ such that*

$$\left\|\sum_{n=1}^{A}\frac{sin(\pi n\ell)}{n}\sigma_n e_n\right\|_{L^p} \le c\,\ell\,\cosh(2\pi A\ell)\,\left\|\sum_{n=1}^{A}\sigma_n e_n\right\|_{L^p}.$$

Proof. By the Taylor series expansion of the sine and the triangular inequality, we obtain

$$\begin{aligned}\left\|\sum_{n=1}^{A}\frac{sin(\pi n\ell)}{n}\sigma_n e_n\right\|_{L^p} &= \left\|\sum_{n=1}^{A}\left(\sum_{k=0}^{\infty}\frac{(-1)^k(\pi\ell)^{2k+1}n^{2k}}{(2k+1)!}\right)\sigma_n e_n\right\|_{L^p} \\ &\le \sum_{k=0}^{\infty}\frac{(\pi\ell)^{2k+1}}{(2k+1)!}\left\|\sum_{n=1}^{A}n^{2k}\sigma_n e_n\right\|_{L^p}.\end{aligned}$$

We use Lemma 5.20 to bound the L^p norm. According to the proof of such lemma, we can keep the control of the constants depending on k, since

$$\left\| \sum_{n=1}^{A} n^{2k} \sigma_n e_n \right\|_{L^p} \leq A^{2k} \left\| H_{2k} \right\|_{L^1(\mathbb{R})} \left\| \sum_{n=1}^{A} \sigma_n e_n \right\|_{L^p},$$

where $\widehat{H_{2k}}(\xi) = \xi^{2k} \chi_{(0,1)}(\xi)$ and $\chi_{(0,1)}$ is the cut-off function (5.30). Consequently, since $H_{2k} = \mathcal{F}^{-1}\left(\xi^{2k} \chi_{(0,1)}\right) = (-2\pi i)^{-2k} \partial^{2k}(\widehat{\chi_{(0,1)}})$, we get

$$\left\| \sum_{n=1}^{A} \frac{sin(\pi n \ell)}{n} \sigma_n e_n \right\|_{L^p} \leq \pi \ell \sum_{k=0}^{\infty} \frac{(\ell A/2)^{2k} \left\| \partial^{2k} \widehat{\chi_{(0,1)}} \right\|_{L^1(\mathbb{R})}}{(2k+1)!} \left\| \sum_{n=1}^{A} \sigma_n e_n \right\|_{L^p}.$$

Applying Lemma 5.22 to $\chi_{(0,1)}$ with $M = 2$, we obtain

$$\left\| \sum_{n=1}^{A} \frac{sin(\pi n \ell)}{n} \sigma_n e_n \right\|_{L^p} \lesssim \left\| \chi_{(0,1)} \right\|_{H^1(\mathbb{R})} \ell \cosh(\ell A) \left\| \sum_{n=1}^{A} \sigma_n e_n \right\|_{L^p}.$$

□

APPENDIX A

The Talbot effect as a solution to the free Schrödinger equation

In Subsection 1.3.2, we saw that the Talbot effect can be mathematically described very accurately by means of a solution to the free Schrödinger equation

$$v(\xi,\zeta)=\sum_{n\in\mathbb{Z}} e^{2\pi i n\xi-2\pi i n^2\zeta}. \tag{A.1}$$

After a historic and physical account of the phenomenon, this expression was obtained in the final part of Subsection 1.3.1 from the solution (1.25) to the Helmholtz equation

$$u(\xi,\zeta)=\sum_{n\in\mathbb{Z}} e^{4\pi i(\frac{d}{\lambda})^2\zeta\sqrt{1-(\frac{\lambda n}{d})^2}}\, e^{2\pi i n\xi} \tag{A.2}$$

by means of the so called paraxial approximation, which consisted in nothing else than truncating the Taylor expansion of $\sqrt{1-x^2}$ as

$$\sqrt{1-x^2}\sim 1-\frac{x^2}{2}, \qquad \text{when} \quad |x|\ll 1 \tag{A.3}$$

and applying in the phase of (A.2). More precisely, if we denote

$$w(\xi,\zeta)=u(\xi,\zeta)\, e^{-4\pi i(\frac{d}{\lambda})^2\zeta}, \tag{A.4}$$

we saw in (1.28) that

$$w(\xi,\zeta)\approx v(\xi,\zeta). \tag{A.5}$$

Though physically reasonable, this approximation is rudimentary and suspicious from a mathematical point of view. The main objective in the present appendix is to decide whether it can be established with mathematical rigour in some sense that will have to be determined. With that goal in mind, we first explain in Subsection A.1 why it is acceptable from the physical point of view, while in Subsection A.2 we look for the correct mathematical setting and prove the corresponding results of convergence.

As we will see, even if (A.1) can be treated as a function, there is little doubt that the solution (A.2) we look for is not a function in the classical sense. Thus, we cannot expect convergence in the classical sense like as pointwise convergence, but in a much weaker sense. We will show that the setting of distributions, defined both in the real line and periodically in the torus, is an adequate setting for this analysis.

The reason for these results to be included in an appendix is that the mathematics needed to prove them are not too elaborate. In any case, the results in this appendix constitute an original work

A.1 The paraxial approximation

At the first glance, it might seem surprising that the Talbot effect, an optical effect that is a consequence of the wavy nature of light, and more precisely of the interference among the waves produced from the slits of the diffraction grating, is indeed described by means of the free Schrödinger equation. Certainly, the transition from the wave equation to the Schrödinger equation has been sketched in Subsection 1.3.1, based especially in a very permissive use of the paraxial approximation (A.3), since large indices n in (A.2) are clealy out of its range of validity. Even so, this approximation seems very reasonable from the physical point of view. Let us explain why in this section. We do this by very elementary means based on the Huygens principle, strongly inspired in the very didactical [27]. The same reasoning will yield an alternative, heuristic way to determine the Talbot distance z_T (1.20) that was computed by Rayleigh.

In Figure 1.7, the diffraction of a planar wave going against a wall with a tiny opening is shown and explained very accurately by the Huygens principle. The same principle was used by Young in Figure 1.8 to explain the double slit experiment. We suggested in Subsection 1.3.1 that the generalisation of this sketch to many slits would not be as fruitful as Young's, where the double slit effect can be distinguished at once, but chances are that it may lead to some information if we use slightly more elaborate arguments than simple visual observation. A simple picture of this generalisation, with a few slits and wavefronts, is shown in Figure A.1. There, the circular waves generated

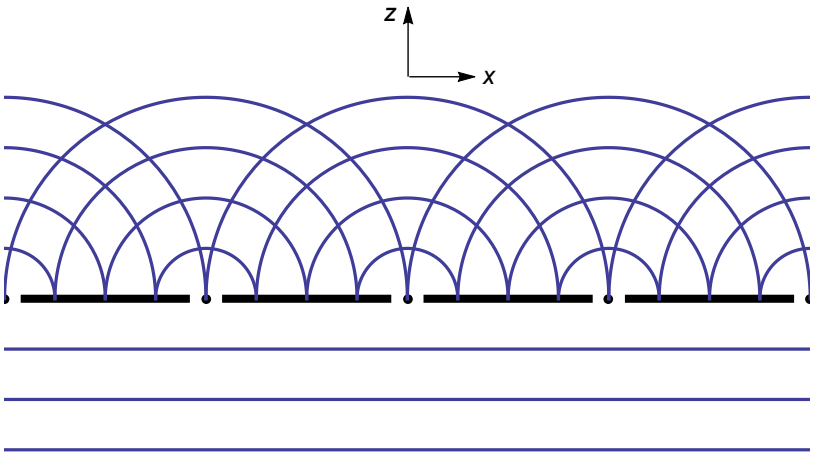

FIGURE A.1: By the Huygens principle, if a plane wave encounters a grating parallel to its wavefronts, each of the slits of the grating will behave as a source of a circular wave with the same wavelength.

from each of the slits interfere among themselves. In this situation, our objective is to detect new plane wavefronts generated from this interference. Figure A.2 is a visual aid for a better understanding of this geometric reasoning, which we proceed to explain.

We begin by remarking that, according to the Huygens principle, the circular waves created have the same wavelength λ as the original planar wave. Hence, the radius of every circular wavefront in Figure A.1 is a multiple of λ. This being said, having fixed $j \in \mathbb{N}$, a line parallel to the grating and tangent to every front of radius $j\lambda$ can be easily detected (Figure A.2A). Consider now some slit in the point $(s, 0)$, the front of radius λ centred in the next slit on the right hand side $(s + d, 0)$, the one of radius 2λ generated in the next hole $(s + 2d, 0)$, and so on. It is easy to see that the straight line beginning in the slit point and being tangent to the front of radius λ is also tangent to the front of radius 2λ and to every other front we are considering. In Figure A.2B, the red lines are all tangent to the circular fronts involved in each case. In the same way, if we pick the front with centre at $(s + d, 0)$ and of radius 2λ, the one with centre at $(s + 2d, 0)$ with radius 4λ and so on, another line, tangent to every one of them and more inclined that the previous one, can be drawn (Figure A.2C). Also, analogue figures with fronts centred in $(s - d, 0), (s - 2d, 0)$ and so on, so that fronts travelling to the right are formed, can be sketched as shown in Figure A.2D.

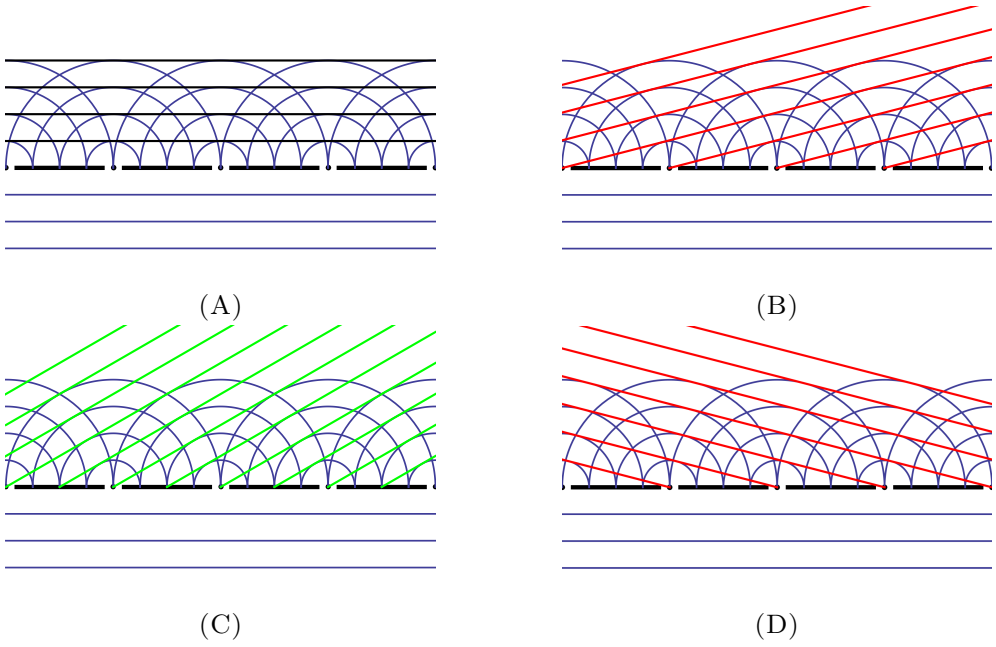

FIGURE A.2: The creation of planar wavefronts with different directions.

In each picture, each of these lines can be interpreted as a new wavefront corresponding to a plane wave of wavelength λ and travelling in a particular direction which is determined by the angle θ_n between the front and the grating. In Figure A.3, the case $n = 0$ corresponds to Figure A.2A, $n = 1$ to Figure A.2B, $n = 2$ to Figure A.2C and $n = -1$ to Figure A.2D.

These are not the only straight wavefronts that can be formed. We could also have chosen, for instance, the slit $(s, 0)$, the front of radius λ created in $(s + 2d, 0)$, the front of radius 2λ coming from $(s + 4d, 0)$ and so on, to get a wavefronts less inclined than those in Figure A.2B. In the setting of Figure A.3, this corresponds to changing d for Nd for some $N \in \mathbb{N}$. So, for a fixed $N \in \mathbb{N}$, straight wavefronts will appear with

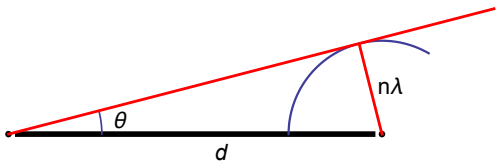

FIGURE A.3: The determination of θ_n corresponding to a wavefront.

direction $\theta_{N,n}$ such that

$$\sin\theta_{N,n} = \frac{n\lambda}{Nd}, \qquad n = \ldots, -2, -1, 0, 1, 2, \ldots. \tag{A.6}$$

It is clear, moreover, that the direction will be different from previous ones with a smaller N only if $\gcd(n, N) = 1$. On the other hand, this new plane wave will have wavelength λ/N.

Under this interpretation, the wave resulting from crossing the grating is the superposition of all these plane waves, which according to the previous paragraph are as many as rational numbers there are, each of them travelling in a different direction. However, since the waves with $N > 1$ are formed from wavefronts that are further away from each other than those with $N = 1$, they will be weaker, so it seems reasonable to neglect them. Therefore, we assume that after crossing the grating, the resulting wave is created from the interaction among all plane waves with $N = 1$. Let us call $\theta_{1,n} = \theta_n$.

Following (A.6) and Figure A.3, the maximum inclination of the wavefronts corresponds to $\theta_n = \pm\pi/2$. Those values would correspond to $n^* = \pm d/\lambda$, but since n has to be an integer, the construction of wavefronts depicted in Figure A.2 is valid for

$$n = -\left\lfloor \frac{d}{\lambda} \right\rfloor, \ldots, -2, -1, 0, 1, 2, \ldots, \left\lfloor \frac{d}{\lambda} \right\rfloor, \qquad \text{and} \qquad \sin\theta_n = \frac{n\lambda}{d},$$

which make a total of $2\lfloor d/\lambda \rfloor + 1$ plane waves.

Let us analyse one of these waves by fixing a value of n. For that, we will split the wave in parts parallel and perpendicular to the grating and will measure the phase in each of these directions. But what does it mean the phase in direction x or in direction z if the front is generally inclined? Assume $n \neq 0$ so that it is indeed the case that the wave is inclined. If we fix the position x_0 in the grating, then there is a wave travelling in direction z with some wavelength λ_z different from the original λ. In the same way, if we fix a vertical distance z_0, a wave travels in direction x with wavelength λ_x. This is shown in Figure A.4.

The wavelength in the horizontal direction, λ_x, can be easily deduced. Indeed, the grating is equidistant with separation d, so if some distance z_0 is fixed, then two points separated horizontally by a distance d are in the same situation with respect to the grating. From this we deduce that for each fixed z, the wave travelling in direction x will have spatial period d. Since λ_x is by definition is the minimal horizontal period, then

$$m\lambda_x = d \tag{A.7}$$

must hold for some $m \in \mathbb{N}$. Moreover, Figure A.2 shows that $m = |n|$. On the other hand, the blue arcs in the Figure A.4 indicate all the same angle θ_n, so it is clear that

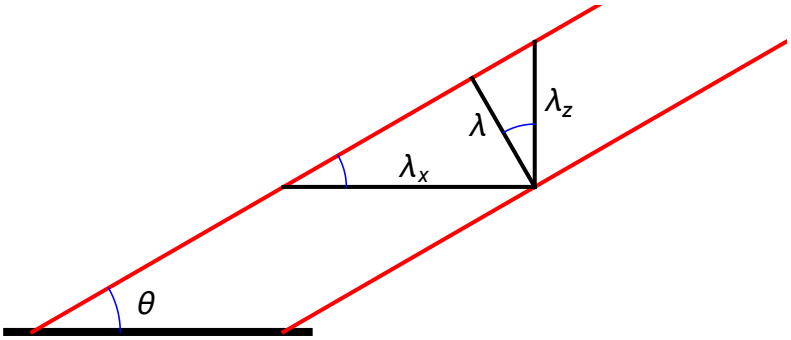

FIGURE A.4: The decomposition in directions x and z of the wavelength of the inclined plane wave corresponding to some $n \neq 0$.

$\lambda = \lambda_x \sin\theta_n$ and $\lambda = \lambda_z \cos\theta_n$. Therefore,

$$\frac{1}{\lambda^2} = \frac{1}{\lambda_x^2} + \frac{1}{\lambda_z^2}, \qquad \Longrightarrow \qquad \frac{1}{\lambda_z} = \sqrt{\frac{1}{\lambda^2} - \frac{1}{\lambda_x^2}} = \frac{1}{\lambda}\sqrt{1 - \frac{\lambda^2\, n^2}{d^2}}. \tag{A.8}$$

Once these coordinate wavelengths have been determined, it is easy to compute the phase. Indeed, a wave travelling in direction y with wavelength λ, with phase in $[0, 2\pi)$ that is set to be 0 in $y = 0$, will have phase $2\pi y_0/\lambda$ in position y_0, hence the wavenumber $k = 2\pi/\lambda$. Take this concept to the x and z directions so that by (A.7) and (A.8),

$$\text{phase}_n(x) = \frac{2\pi}{\lambda_x}\, x = \frac{2\pi n x}{d}, \qquad \text{phase}_n(z) = \frac{2\pi}{\lambda_z}\, z = \frac{2\pi z}{\lambda}\sqrt{1 - \frac{\lambda^2\, n^2}{d^2}}. \tag{A.9}$$

These are trivially valid also for the vertically directed wave $n = 0$, for which $\lambda = \lambda_z$. Rescale them according to (1.23) to get

$$\text{phase}_n(\xi) = 2\pi n \xi, \qquad \text{phase}_n(\zeta) = 4\pi \left(\frac{d}{\lambda}\right)^2 \zeta \sqrt{1 - \frac{\lambda^2\, n^2}{d^2}},$$

and compare them with the phases of the Helmholtz solution (A.2). They are the same. This suggests that the oscillating terms in (A.2) with $|n| < d/\lambda$ correspond to the plane waves with wavefronts like in Figure A.2 and which form an angle θ_n with the grating. Exactly this is also suggested by Figure 15 in [8, Section 6], where they consider the experiment with a diffraction grating of finitely many slits.

Now, in what consists the approximation (A.3) that was baptised as *paraxial*? In geometric optics, where light is represented by rays that indicate its direction and that are perpendicular to the wavefronts (like in Figure 1.7), a paraxial ray is a ray that is either parallel to the optical axis or close to be so. In the case of a lens, the optical axis is the axis of rotational symmetry, and in the case of Talbot's experiment, it is the vertical direction. The paraxial approximation consists in assuming that all rays are paraxial so that, since the angle with the optical axis is small, approximations such as $\sin\theta \sim \theta$, $\tan\theta \sim \theta$ and $\cos\theta \sim 1 - \theta^2/2$ are extensively used. In our situation, consider a wave with small n so that θ_n is small. The wavefronts are close to be parallel to the grating and therefore the ray that indicates the direction of the propagation of the wave is almost vertical; indeed, the angle with respect to the optical (vertical) axis is precisely θ_n, so it is a paraxial ray. On the contrary, the waves with large n

have very inclined wavefronts and the rays are close to be horizontal, the angle with the optical axis θ_n being very close to $\pi/2$. Therefore, these rays are not paraxial.

However, if we fix a distance $z_0 > 0$, the distance that the non-paraxial and inclined ray with large n has to travel to reach the height z_0 is much larger than the distance that a paraxial ray has to travel to reach there. It is therefore expectable that the non-paraxial rays will suffer a stronger dispersion by the time they reach z_0. Also, in the practical case of a grating with finitely many slits, the resulting waves can be considered to have a finite width (see figure A.5, where only paraxial waves are depicted). Thus, if a finite screen is put at distance z_0, the non-paraxial rays are too inclined to hit the screen and therefore will have no effect on the received image. These reasons suggest that the effect of the non-paraxial rays and of their corresponding planar waves is very small, negligible comparing to the contribution of the paraxial ones.

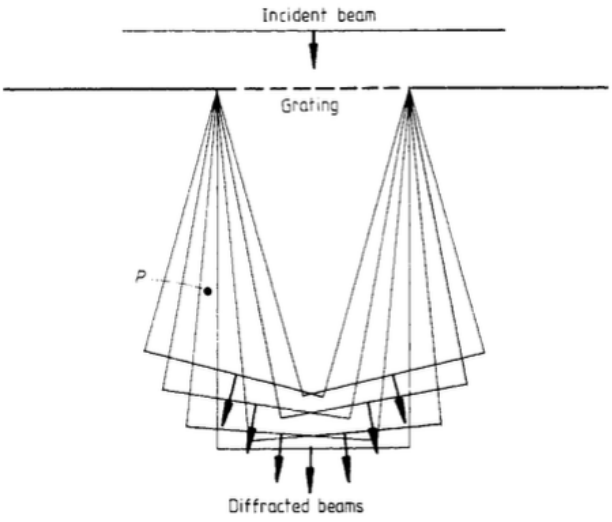

FIGURE A.5: The paraxial waves, with their corresponding rays, coming out from a finite grating. Non-paraxial waves, which travel more horizontally and which will not hit a finite screen placed in front of the grating, are not shown. This figure is [8, Figure 15].

Therefore, only the contribution of the paraxial waves, those corresponding to small values of n, needs to be taken into account in (A.2). For them, the approximation (A.3) in the phase of z can be used. On the other hand, the waves with $n \simeq d/\lambda$, which are not paraxial and are out of the approximation, are negligible compared to the previous ones, so whatever we do with their phase, they will contribute nothing. For even larger n, the waves in (A.2) have an exponential behaviour and rapidly vanish.

Apart from justifying the use of the paraxial approximation, the argument of the wavefronts also allows to compute the estimation (1.20) for the Talbot distance. Indeed, having into account that all waves have phase zero when they leave the grating, if we find a distance z in which the phase of all wavefronts is the same, the observed light pattern at that distance will be identical to the one emitted from the grating. For that, the paraxial approximation in the phase in z (A.9) gives

$$\operatorname{phase}_n(z) = \frac{2\pi z}{\lambda} - 2\pi \frac{z\lambda n^2}{2\,d^2}.$$

The second term alone depends on n, and if we consider z such that

$$\frac{z\lambda}{2d^2} = 1, \tag{A.10}$$

the dependence on n disappears because $2\pi n^2$ is a multiple of 2π and does not contribute. So if (A.10) holds, all waves have the same phase in z, and the grating image gets reproduced. This distance is

$$z = z_T = \frac{\lambda}{2d^2},$$

identical to the simplification (1.20) of the Talbot distance that Rayleigh obtained by means of more elaborated means.

From the point of view of getting an approximate result and for laboratory experiments, this procedure and therefore the result (A.5) seem reasonable. This was probably the position of the authors of the physically oriented articles [8, 9, 72] which we already mentioned. In [9], also a *post-paraxial* analysis of the Helmholtz solution (A.2) is carried out by taking one more term in the Taylor expansion in (A.3), with the objective of measuring the error of the paraxial approximation and identify the blurring observed in the experiments. In any case, several doubts arise about the mathematical validity of truncating the Taylor expansion, and especially in the very common use of the paraxial approximation (A.3). The terms of low index $n \ll d/\lambda$ in (A.2) really are paraxial and thus subject to the approximation, while the exponential functions corresponding to indices $n > d/\lambda$ can probably be managed naturally by means of their own decay. But the behaviour of the oscillating terms corresponding to values of n close to d/λ is not paraxial, and therefore the use of such an approximation is far from being mathematically acceptable. The question is then clear: is there any way to justify the transition from the Helmholtz solution (A.2) to the Schrödinger solution (A.1) in a mathematically rigorous way? In other words, is there any way to establish (A.5) rigorously? We will see in Subsection A.2 that this is possible through some convergence procedure involving the physical magnitudes λ or d, albeit in quite a weak form that comes imposed by the structure of w and v themselves.

A.2 A rigorous mathematical approximation

In this section, we study in which sense (A.5) can be mathematically correct. As we suggested in the previous section, two are the main issues:

- In view of (A.2), the terms of w with large n are real exponentials which do not appear in v.
- The Schrödinger solution v was found by means of the paraxial approximation (A.3) in the phase of the rest of oscillating indices $|n| < d/\lambda$, but this can only be used when $|n| \ll d/\lambda$ and not when $|n| \simeq d/\lambda$.

In any case, there are three regions that can be clearly distinguished, which are delimited by the ratio d/λ. Moreover, rather than in λ and d as independent parameters, w depends in that ratio, which we denote by $r = d/\lambda$. Accordingly, let us denote (A.4) by

$$w_r(\xi,\zeta) = w(\xi,\zeta) = e^{-4\pi i r^2 \zeta} \sum_{n\in\mathbb{Z}} e^{4\pi i r^2 \zeta \sqrt{1-\frac{n^2}{r^2}}}\, e^{2\pi i n \xi} \tag{A.11}$$

One possible way to maximise the number of indices subject to the paraxial approximation is to make this ratio tend to infinity. Hence, we could think that (A.5) should be understood as an equality in the limit when $r \to \infty$.

Let us do this splitting of w_r. The first part is for the lowest $|n| \ll r$ where the paraxial approximation works; the second one, the middle and most problematic range $|n| \sim r$; and finally, the part with largest $|n| > r$ where the contribution is exponentially decaying. To be more precise on this, let us define $\mu(r)$ the function that will delimit the validity range of the paraxial approximation. Let it satisfy

$$\lim_{r\to\infty} \mu(r) = +\infty \qquad \text{and} \qquad \lim_{r\to\infty} \mu(r)/r = 0, \tag{A.12}$$

where the second condition is the precise expression for the informal $\mu(r) \ll r$ that we need. With this, let

$$w_r = w_{r,1} + w_{r,2} + w_{r,3},$$

where

$$w_{r,1}(\xi,\zeta) = e^{-4\pi i r^2 \zeta} \sum_{|n|\le\mu(r)} e^{4\pi i r^2 \zeta\sqrt{1-\frac{n^2}{r^2}}}\, e^{2\pi i n\xi},$$

is a low-pass filter of w_r,

$$w_{r,2}(\xi,\zeta) = e^{-4\pi i r^2 \zeta} \sum_{\mu(r)<|n|\le r} e^{4\pi i r^2 \zeta\sqrt{1-\frac{n^2}{r^2}}}\, e^{2\pi i n\xi},$$

a band-pass filter, and

$$w_{r,3}(\xi,\zeta) = e^{-4\pi i r^2 \zeta} \sum_{|n|>r} e^{-4\pi r^2 \zeta\sqrt{\frac{n^2}{r^2}-1}}\, e^{2\pi i n\xi}$$

a high-pass filter. The idea is that the low-pass filter $w_{r,1}$, which can be paraxially approximated, converges to some form of v when $r \to \infty$. Since the paraxial approximation does not hold for the other two, there is no hope for them to converge to v, so they should converge to zero. We may have hope with $w_{r,3}$ because of the exponential decay in r present in the ζ-depending part, but problems will arise in the case of $w_{r,2}$ because it tends to a sum of more and more oscillating functions that do not decay.

Before guessing the result, we need to find the proper environment of convergence. For that, let us have a closer look at the structure of both w_r and v. For every finite r, $w_{r,1}$ and $w_{r,2}$ are clearly functions, but w_r and $w_{r,3}$ are infinite sums of functions, which in principle need not be functions themselves. However, the tails, which correspond to $w_{r,3}$, can be bounded by

$$\begin{aligned} |w_{r,3}(\xi,\zeta)| &\le 2 \sum_{n=r+1}^{\infty} e^{-4\pi r^2 \zeta\sqrt{\frac{n^2}{r^2}-1}} \\ &\simeq \sum_{n=r+1}^{100r} e^{-4\pi r^2 \zeta\sqrt{\frac{n^2}{r^2}-1}} + \sum_{n=100r+1}^{\infty} e^{-4\pi r\zeta n} < \infty, \end{aligned}$$

because $\sqrt{n^2/r^2-1} \simeq n$ when $n \ge 100r$ and because the infinite sum is a convergent geometric sum whenever $\zeta > 0$. Thus, w_r is indeed a function for $\zeta > 0$, so it makes sense to ask for its pointwise convergence when $r \to \infty$. On the other hand, the limit that we are seeking, v, is an infinite sum of oscillating functions which does not

converge absolutely. It is definitely not a function, at least not a well-behaved one. In order to have an idea of what kind of object we are dealing with, let us consider $v(\xi,0)$, which is

$$v(\xi,0)=\sum_{n\in\mathbb{Z}} e^{2\pi i n\xi}=\sum_{n\in\mathbb{Z}}\delta(\xi-n).$$

This is a tempered distribution, an element of the dual space $\mathcal{S}'(\mathbb{R})$ of the space of rapidly decreasing Schwartz functions

$$\mathcal{S}(\mathbb{R})=\left\{\quad \varphi\in C^\infty(\mathbb{R}) \quad | \quad \sup_{x\in\mathbb{R}}|x^\alpha\, D^\beta f(x)|<\infty \quad \forall \alpha,\beta\in\mathbb{N}\cup\{0\} \quad \right\},$$

where D^β is the differentiation operator. More precisely, we have

$$\langle v(\cdot,0),\varphi\rangle=\sum_{n\in\mathbb{Z}}\widehat{\varphi}(n)=\sum_{n\in\mathbb{Z}}\varphi(n), \qquad \forall\varphi\in\mathcal{S}(\mathbb{R}).$$

In the same way, $v(\cdot,\zeta)$ can be interpreted to be a tempered distribution in the variable ξ for every $\zeta>0$, whose action in $\mathcal{S}$ is

$$\langle v(\cdot,\zeta),\varphi\rangle=\sum_{n\in\mathbb{Z}} e^{-4\pi i n^2\zeta}\,\widehat{\varphi}(n), \qquad \forall\varphi\in\mathcal{S}(\mathbb{R}). \tag{A.13}$$

Of course, $v(\xi,\zeta)$ could also be interpreted as a distribution in $\mathcal{S}(\mathbb{R}^2)$ where the image would be

$$\langle v,\varphi\rangle=\sum_{n\in\mathbb{Z}}\widehat{\varphi}(n,-2\pi n^2), \qquad \forall\varphi\in\mathcal{S}(\mathbb{R}^2),$$

or even as a distribution in ζ for every fixed $\xi\in\mathbb{R}$. However, from the perspective of the Talbot effect, it only makes sense to consider $v(\xi,\zeta)$ for $\zeta>0$. Moreover, since according to its mathematical expression (1.32), the Talbot effect is a phenomenon that happens in the ξ axis for every fixed $\zeta>0$, it is most natural to consider both w_r and v as distributions in ξ for every fixed $\zeta>0$.

In this sense, if the candidate for the limit $v(\xi,\zeta)$ is a distribution rather a function, asking for pointwise convergence of w_r to v makes not much sense. Therefore, the results that we seek and which we are able to prove will be in a distributional sense. In this context, recall that a sequence of distributions $T_n\in\mathcal{S}'$ is said to converge to $T\in\mathcal{S}'$ if

$$\lim_{n\to\infty}\langle T_n,\varphi\rangle=\langle T,\varphi\rangle, \qquad \forall\varphi\in\mathcal{S}. \tag{A.14}$$

The first result we obtain is the following.

Theorem A.1. *Let $\zeta>0$. Let $w_r=w_r(\cdot,\zeta)$ defined in (A.11) be considered as a function of ξ alone, and v defined in (A.1) as a distribution of ξ alone. Then,*

$$\lim_{r\to\infty} w_r(\cdot,\zeta)=v(\cdot,\zeta) \qquad\qquad \text{in} \quad \mathcal{S}'(\mathbb{R}).$$

Also, $v(\cdot,\zeta)$ is a Fourier series, thus 1-periodic, so it can be regarded as a periodic distribution in $\mathbb{R}$. The space of periodic distributions, in this case of period 1, is usually denoted by $\mathcal{P}'(\mathbb{T})$, where $\mathbb{T}=\mathbb{R}/\mathbb{Z}$ is the torus. This is because if $\mathcal{P}(\mathbb{T})$ is the space of smooth and periodic test functions in $\mathbb{T}$, then there is an identification between the dual space $(\mathcal{P}(\mathbb{T}))'$ and the space of periodic distributions $\mathcal{P}'(\mathbb{T})$, hence this notation. The reader can check [100] for details.

In this setting, we will be able to be more precise about the space of distributions where the convergence holds. Indeed, in a similar way that in (A.13) the image of

$\varphi \in \mathcal{S}(\mathbb{R})$ depends in its Fourier transform evaluated in the integers, in this case the image of $\varphi \in \mathcal{P}(\mathbb{T})$ by w_r and v will depend on its Fourier coefficients $\widehat{\varphi}_n$. In this sense, very convenient will be the Sobolev spaces

$$H^s(\mathbb{T}) = \left\{ f \in L^2(\mathbb{T}) \quad | \quad \|f\|^2_{H^s(\mathbb{T})} = \sum_{n\in\mathbb{Z}} (1+n^2)^s \, |\widehat{f}_n|^2 < \infty \right\}, \qquad \forall s \geq 0, \tag{A.15}$$

definition which can be generalised to $s \in \mathbb{R}$ if instead of $f \in L^2(\mathbb{T})$ we consider $f \in \mathcal{P}'(\mathbb{T})$. Moreover, it is known that $(H^s(\mathbb{T}))' = H^{-s}(\mathbb{T})$. In this setting, the result we prove is the following:

Theorem A.2. *Let $s > 1/2$ and $\zeta > 0$. Let $w_r = w_r(\cdot, \zeta)$ as above be considered as a function of ξ alone, and v in (A.1) as a periodic distribution also in ξ alone. Then,*

$$\lim_{r\to\infty} w_r(\cdot,\zeta) = v(\cdot,\zeta) \qquad\qquad \text{in} \quad H^{-s}(\mathbb{T}).$$

In the following subsections we prove these results on weak convergence. We prove Theorem A.1 in Subsection A.2.2 and Theorem A.2 in Subsection A.2.3. However, before that, we think it convenient to analyse to what extent pointwise results can be established, at least for the parts of w_r where it makes sense. We do this in Subsection A.2.1.

A.2.1 Partial pointwise convergence

According to the above, we do not expect to obtain a pointwise convergence result similar to Theorems A.1 and A.2, especially because of the middle range $w_{r,2}$, where the paraxial approximation cannot be used. But can we work pointwise at least with $w_{r,1}$? And can we say something about the exponential tails $w_{r,3}$?

Remember that we said that v is not a function, so in case we want to prove some pointwise convergence result, we will need to turn it into a function first. For that, in a similar way as we defined $w_{r,1}$, let us also define a low-pass filter of v,

$$v_r(\xi,\zeta) = \sum_{|n|\leq\mu(r)} e^{2\pi i n\xi - 2\pi i n^2 \zeta}.$$

Let us measure how the error $w_{r,1} - v_r$ behaves when $r \to 0$ by writing

$$w_{r,1}(\xi,\zeta) - v_r(\xi,\zeta) = \sum_{|n|\leq\mu(r)} \left(e^{-4\pi i r^2\zeta} \, e^{4\pi i r^2 \zeta \sqrt{1-\frac{n^2}{r^2}}} - e^{-2\pi i n^2 \zeta} \right) e^{2\pi i n\xi}.$$

Since $n \leq \mu(r)$ and $\lim_{r\to\infty} \mu(r)/r = 0$, the paraxial approximation is valid in the form

$$\sqrt{1-\frac{n^2}{r^2}} = 1 - \frac{n^2}{2r^2} + O\left(\frac{n^3}{r^3}\right),$$

and we get

$$w_{r,1}(\xi,\zeta) - v_r(\xi,\zeta) = \sum_{|n|\leq\mu(r)} \left(e^{4\pi i r^2 \zeta O\left(\frac{n^3}{r^3}\right)} - 1 \right) e^{-2\pi i n^2\zeta} \, e^{2\pi i n\xi}. \tag{A.16}$$

Then, by using the Taylor expansion of the exponential, the absolute error of the approximation is bounded like

$$|w_{r,1}(\xi,\zeta) - v_r(\xi,\zeta)| \leq C \sum_{n=1}^{\mu(r)} \frac{n^3}{r} \leq C\, \frac{\mu(r)^4}{r}, \tag{A.17}$$

where $C > 0$ is some constant. This error converges to zero when $r \to \infty$ if the additional condition

$$\lim_{r\to\infty} \frac{\mu(r)^4}{r} = 0 \qquad \Longleftrightarrow \qquad \lim_{r\to\infty} \frac{\mu(r)}{r^{1/4}} = 0 \tag{A.18}$$

is set for the function μ, which informally reads $\mu(r) \ll r^{1/4}$. We have thus proved the following lemma:

Lemma A.3. *If μ defined in (A.12) satisfies the additional condition (A.18), then*

$$\lim_{r\to\infty} \|w_{r,1} - v_r\|_{L^\infty_{\xi,\zeta}(\mathbb{R}\times(0,+\infty))} = 0.$$

So in some sense, we may say that the low-pass filter of w that allows the paraxial approximation converges to v pointwise. Thus, weaker concepts of convergence should follow easily by this lemma.

Let us work now with the high frequencies in $w_{r,3}$. As we suggested, we should try to prove that it tends to zero. We hope that the exponential decay will be enough, so by the triangle inequality we write

$$|w_{r,3}(\xi,\zeta)| \leq 2 \sum_{n>r} e^{-4\pi r^2 \zeta \sqrt{\frac{n^2}{r^2} - 1}}. \tag{A.19}$$

The summand is a decreasing function of n, so related to the convergence of the sum, we prove the following lemma.

Lemma A.4. *Let $\zeta > 0$. Then,*

$$\lim_{r\to\infty} \int_r^\infty e^{-4\pi r^2 \zeta \sqrt{\frac{x^2}{r^2} - 1}}\, dx = 0.$$

Proof. By changing variables $x = ry$ first and $r^2\sqrt{y^2-1} = z$ later, we get

$$\int_r^\infty e^{-4\pi r^2 \zeta \sqrt{\frac{x^2}{r^2} - 1}}\, dx = \int_1^\infty e^{-4\pi r^2 \zeta \sqrt{y^2-1}}\, r\, dy = \int_0^\infty \frac{z\, e^{-4\pi\zeta z}}{r^3 \sqrt{1 + \frac{z^2}{r^4}}}\, dz.$$

Call $f_r(z) = r^{-3}\, e^{-4\pi\zeta z}\, z/\sqrt{1 + z^2/r^4}$, so that when r is large enough we have

$$|f_r(z)| \leq z e^{-4\pi\zeta z} \in L^1((0,\infty)).$$

Moreover, since for every fixed $z \geq 0$ we have $\lim_{r\to 0} f_r(z) = 0$, the theorem of dominated convergence gives the result. □

However, this lemma is not enough to prove that $\lim_{r\to\infty} w_{r,3}(\xi,\zeta) = 0$. Indeed, since the function $e^{-4\pi r^2\zeta\sqrt{\frac{x^2}{r^2}-1}}$ is decreasing in x, its integral bounds every term in

the sum (A.19) except the first one. Then, we can write

$$\lim_{r\to\infty} \sum_{n>r+1} e^{-4\pi r^2\zeta\sqrt{\frac{n^2}{r^2}-1}} \leq \lim_{r\to\infty} \int_r^\infty e^{-4\pi r^2\zeta\sqrt{\frac{x^2}{r^2}-1}}\, dx = 0,$$

so since the first term corresponds to $n = \lfloor r\rfloor + 1$, where $\lfloor r\rfloor \in \mathbb{N}$ is the integer part of r, we get

$$\lim_{r\to\infty} w_{r,3}(\xi,\zeta) = \lim_{r\to\infty} e^{4\pi i r^2\zeta}\, e^{-4\pi r^2\zeta\sqrt{\frac{(\lfloor r\rfloor+1)^2}{r^2}-1}}\, e^{2\pi i(\lfloor r\rfloor+1)\xi},$$

and consequently,

$$\lim_{r\to\infty} |w_{r,3}(\xi,\zeta)| = \lim_{r\to\infty} e^{-4\pi r^2\zeta\sqrt{\frac{(\lfloor r\rfloor+1)^2}{r^2}-1}}.$$

This term does not converge to zero. Indeed, let $r = \lfloor r\rfloor + \{r\}$, where $\{r\} \in [0,1)$ is the fractional part of r. When $r\to\infty$, then $\lfloor r\rfloor \to \infty$ in the integers, while $\{r\}$ oscillates in the unit interval as a sawtooth function. In particular,

$$\begin{aligned} e^{-4\pi r^2\zeta\sqrt{\frac{(\lfloor r\rfloor+1)^2}{r^2}-1}} &= e^{-4\pi r\zeta\sqrt{(\lfloor r\rfloor+1)^2-r^2}} = e^{-4\pi r\zeta\sqrt{(\lfloor r\rfloor+1)^2-(\lfloor r\rfloor+\{r\})^2}} \\ &= e^{-4\pi r\zeta\sqrt{(1-\{r\})(1+\{r\}+2\lfloor r\rfloor)}} \to 1 \end{aligned} \tag{A.20}$$

whenever $\{r\}\to 1$, which happens infinitely many times. Hence, when $r\to\infty$, it oscillates and is very close to 1 whenever r approaches an integer value, and $w_{r,3}$ does not converge to zero when $r\to\infty$.

As a remark, this problem can be solved if instead of taking the limit $r\to\infty$ continuously, we take it discretely by setting $r = m + r_0$ with $m\in\mathbb{N}$ and a fixed $r_0\in(0,1)$ and we do $m\to\infty$. In this case, $\{r\} = r_0$ so the square root in (A.20) is always positive and hence the exponential tends to zero.

Lemma A.5. *Let $\xi\in\mathbb{R}$, $\zeta>0$, $m\in\mathbb{N}$ and $r_0\in(0,1)$. Then,*

$$\lim_{m\to\infty} w_{m+r_0,3}(\xi,\zeta) = 0,$$

but

$$\lim_{r\to\infty} w_{r,3}(\xi,\zeta) \neq 0.$$

Regarding $w_{r,2}$, there is little we can do, since as we said it is a sum of oscillating functions that gets wider and wider because the measure of the interval $(\mu(r), r)$ is $r-\mu(r)\simeq r\to\infty$. This forces us to relax the convergence conditions to the sense of distributions. As we already said, for each $\zeta>0$ both $w_r(\cdot,\zeta)$ and $v(\cdot,\zeta)$ can be seen as distributions in $\xi\in\mathbb{R}$. We analyse this setting in Section A.2.2. Also, since they are periodic of period 1, they can be seen as periodic distributions in $\mathcal{P}'(\mathbb{T})$, a situation which we study in Section A.2.3.

A.2.2 Convergence in the sense of distributions

In this subsection, we will work with $w_r(\cdot,\zeta)$ and $v(\cdot,\zeta)$ as distributions in $\mathbb{R}$ all the time, so for simplicity, we denote the space of Schwartz functions simply by $\mathcal{S}$ and the space of tempered distributions by $\mathcal{S}'$.

We also recall that locally integrable functions of slow growth f, that is, functions that satisfy $\lim_{\xi\to\infty}|\xi|^{-N}f(\xi)=0$ for some $N\in\mathbb{N}$, yield a tempered distribution by means of

$$\langle f,\varphi\rangle=\int_{\mathbb{R}}f(x)\,\varphi(x)\,dx,\qquad\forall\varphi\in\mathcal{S}. \tag{A.21}$$

Examples of these functions are, for instance, the exponentials $f_n(x)=e^{2\pi inx}$ for every $n\in\mathbb{N}$.

Let us first work with the problematic $w_{r,2}$. In this case, the decay of the Schwartz function will make the work that the function is not able to do by itself. Indeed, let $\zeta\geq 0$ so that $w_{r,2}(\cdot,\zeta)\in\mathcal{S}'$ such that

$$\begin{aligned}\langle w_{r,2}(\cdot,\zeta),\varphi\rangle&=e^{-4\pi ir^2\zeta}\sum_{\mu(r)<|n|\leq r}e^{4\pi ir^2\zeta\sqrt{1-\frac{n^2}{r^2}}}\,\langle e^{2\pi in\xi},\varphi\rangle\\&=e^{-4\pi ir^2\zeta}\sum_{\mu(r)<|n|\leq r}e^{4\pi ir^2\zeta\sqrt{1-\frac{n^2}{r^2}}}\,\widehat{\varphi}(-n)\end{aligned} \tag{A.22}$$

for any $\varphi\in\mathcal{S}$, because according to (A.21), $\langle e^{2\pi inx},\varphi\rangle=\widehat{\varphi}(-n)$. Also, the first equality holds for linearity of distributions. Now use the triangle inequality so that

$$|\langle w_{r,2}(\cdot,\zeta),\varphi\rangle|=\left|\sum_{\mu(r)<|n|\leq r}e^{4\pi ir^2\zeta\sqrt{1-\frac{n^2}{r^2}}}\,\widehat{\varphi}(-n)\right|\leq\sum_{\mu(r)<|n|\leq r}|\widehat{\varphi}(n)|\,.$$

Since $\varphi\in\mathcal{S}$ implies $\widehat{\varphi}\in\mathcal{S}$, the sequence $\widehat{\varphi}(n)$ decays faster than the inverse of any polynomial sequence, for instance, than n^{-2}. Since $\lim_{r\to\infty}\mu(r)=\infty$, we can write

$$\lim_{r\to\infty}|\langle w_{r,2}(\cdot,\zeta),\varphi\rangle|\leq\lim_{r\to\infty}\sum_{n=\mu(r)}^{\infty}|\widehat{\varphi}(n)|+|\widehat{\varphi}(-n)|\leq C_\varphi\lim_{r\to\infty}\sum_{n=\mu(r)}^{\infty}\frac{1}{n^2}=0, \tag{A.23}$$

where $C_\varphi>0$ is a constant depending on φ. According to (A.14), this means that $w_{r,2}$ converges to zero in $\mathcal{S}'$. On the other hand, for $w_{r,3}$, we also avoid the problem (A.20) in the proof of Lemma A.5 by letting the test function $\varphi\in\mathcal{S}$ do the work for the decay. By the triangle inequality, we write

$$|\langle w_{r,3}(\cdot,\zeta),\varphi\rangle|\leq\sum_{|n|>r}e^{-4\pi r^2\zeta\sqrt{\frac{n^2}{r^2}-1}}\left|\langle e^{2\pi in\xi},\varphi\rangle\right|\leq\sum_{|n|>r}|\widehat{\varphi}(n)|\,, \tag{A.24}$$

and for the same reasons as in (A.23), we conclude that

$$\lim_{r\to\infty}|\langle w_{r,3}(\cdot,\zeta),\varphi\rangle|\leq\lim_{r\to\infty}\sum_{n=r}^{\infty}|\widehat{\varphi}(n)|+|\widehat{\varphi}(-n)|\leq C_\varphi\lim_{r\to\infty}\sum_{n=r}^{\infty}\frac{1}{n^2}=0,\quad\forall\varphi\in\mathcal{S}.$$

Thus, we have proved the following lemma:

Lemma A.6. *Let $\zeta\geq 0$. Then,*

$$\lim_{r\to\infty}w_{r,2}(\cdot,\zeta)=0=\lim_{r\to\infty}w_{r,3}(\cdot,\zeta)\qquad\text{in }\mathcal{S}'.$$

In the case of $w_{r,1}$, since the convergence holds pointwise, the same proof as for Lemma A.3 will yield the weaker distributional convergence. Indeed, from (A.16) and

(A.17), and also because the Fourier transform of $\varphi \in \mathcal{S}$ is bounded, we can write

$$\begin{aligned}|\langle w_{r,1}(\cdot,\zeta) - v_r(\cdot,\zeta), \varphi\rangle| &\leq \sum_{|n|\leq\mu(r)} \left|e^{4\pi i r^2 \zeta O\left(\frac{n^3}{r^3}\right)} - 1\right| \left|\langle e^{2\pi i n\xi}, \varphi\rangle\right| \\ &\leq C \sum_{|n|\leq\mu(r)} \frac{|n|^3}{r} |\widehat{\varphi}(n)| \leq C_\varphi \frac{\mu(r)^4}{r} \to 0\end{aligned}$$

when $r \to \infty$ if condition (A.18) for $\mu(r)$ is satisfied. Thus, we have

Lemma A.7. *Let $\zeta \geq 0$. If $\mu(r)$ satisfies (A.18), then*

$$\lim_{r\to\infty} \Big(w_{r,1}(\cdot,\zeta) - v_r(\cdot,\zeta)\Big) = 0 \qquad \text{in} \quad \mathcal{S}'.$$

Then, Theorem A.1 is just a corollary of Lemmas A.6 and A.7.

Corollary A.8. *Let $\zeta \geq 0$. Then,*

$$\lim_{r\to\infty} w_r(\cdot,\zeta) = v(\cdot,\zeta) \qquad \text{in} \quad \mathcal{S}'.$$

Proof. From Lemmas A.6 and A.7 we have

$$\lim_{r\to\infty} \Big(w_r(\cdot,\zeta) - v_r(\cdot,\zeta)\Big) = 0,$$

so it is enough to prove that $\lim_{r\to\infty} v_r(\cdot,\zeta) = v(\cdot,\zeta)$. Let $\varphi \in \mathcal{S}$ so that

$$\langle v_r(\cdot,\zeta), \varphi\rangle = \sum_{|n|\leq\mu(r)} e^{-2\pi i n^2\zeta} \langle e^{2\pi i n\xi}, \varphi\rangle = \sum_{|n|\leq\mu(r)} e^{-2\pi i n^2\zeta} \widehat{\varphi}(n). \tag{A.25}$$

Since

$$\langle v(\cdot,\zeta), \varphi\rangle = \sum_{n\in\mathbb{Z}} e^{-2\pi i n^2\zeta} \widehat{\varphi}(n),$$

we want to use the theorem of dominated convergence in (A.25) when we take the limit $r \to \infty$. For that, observe that

$$\left|\chi_{[-\mu(r),\mu(r)]}(n)\, e^{-2\pi i n^2\zeta} \widehat{\varphi}(n)\right| \leq |\widehat{\varphi}(n)|\,,$$

which is independent of r. Moreover, it is summable because $\widehat{\varphi} \in \mathcal{S}$ implies for instance that $|\xi|^2|\widehat{\varphi}(\xi)| \leq C_\varphi$ and, therefore,

$$\sum_{n\in\mathbb{Z}} |\widehat{\varphi}(n)| \leq \widehat{\varphi}(0) + 2C_\varphi \sum_{n=1}^{\infty} \frac{1}{n^2} < \infty.$$

Hence, taking limits $r \to \infty$ in (A.25), we get

$$\lim_{r\to\infty} \langle v_r(\cdot,\zeta), \varphi\rangle = \sum_{n\in\mathbb{Z}} e^{-2\pi i n^2\zeta} \widehat{\varphi}(n) = \langle v(\cdot,\zeta), \varphi\rangle,$$

which completes the proof. □

A.2.3 Convergence in the sense of periodic distributions

Let us now study the convergence in the sense of periodic distributions by using periodic test functions. Since the period of our distributions is 1, we work in the torus

$\mathbb{T} = \mathbb{R}/\mathbb{Z}$ all along this subsection, and for simplicity, we denote the space of smooth and periodic test functions of period 1 by $\mathcal{P}$. As we said in the beginning of the section, there is an identification between the dual of $\mathcal{P}$ and the usual distributions in $\mathcal{D}'(\mathbb{R})$ that are 1-periodic, reason by which we simply denote this space as $\mathcal{P}'$.

Since our distributions can be regarded both as elements of $\mathcal{S}'$ and of $\mathcal{P}'$, to avoid confusion let us denote by $\langle T, \varphi\rangle_{\mathbb{T}}$ the image of the test function $\varphi \in \mathcal{P}$ by $T \in \mathcal{P}'$. In case that a locally integrable function f that defines a distribution in $\mathcal{S}$ by (A.21) is 1-periodic, then it is identified with the corresponding distribution in $\mathcal{P}'$, which acts as

$$\langle f, \varphi\rangle_{\mathbb{T}} = \int_{\mathbb{T}} f(x)\,\varphi(x)\,dx, \qquad \forall \varphi \in \mathcal{P},$$

where the integral can be taken in any interval of length one. In the case of v and w_r, it is important to know how to work with $e^{2\pi i n x}$. While if $e^{2\pi i n x} \in \mathcal{S}'$ we saw that $\langle e^{2\pi i n \xi}, \varphi\rangle = \widehat{\varphi}(-n)$ for a test function $\varphi \in \mathcal{S}$, in case that $e^{2\pi i n \xi} \in \mathcal{P}'$ we have

$$\langle e^{2\pi i n \xi}, \varphi\rangle = \int_{\mathbb{T}} \varphi(\xi)\, e^{2\pi i n \xi}\, d\xi = \widehat{\varphi}_{-n}, \qquad \forall \varphi \in \mathcal{P}.$$

where by $\widehat{\varphi}_n$ we denote the n-th Fourier coefficient of φ. Again, for more detailed information we refer to [100].

Having said this, let us analyse the convergence of w_r to v. As in Subsection A.2.2, we begin our analysis with the most problematic piece $w_{r,2}$ which needs the assistance of the test functions to converge. As in (A.22), we have for $\varphi \in \mathcal{P}$

$$|\langle w_{r,2}(\cdot,\zeta), \varphi\rangle_{\mathbb{T}}| = \left| \sum_{\mu(r)<|n|\leq r} e^{4\pi i r^2 \zeta \sqrt{1-\frac{n^2}{r^2}}}\, \langle e^{2\pi i n \xi}, \varphi\rangle_{\mathbb{T}} \right| \leq \sum_{\mu(r)<|n|\leq r} |\widehat{\varphi}_n|\,.$$

In view of this, we might be asking for regularity in excess, since it will be enough that the sum of the Fourier coefficients be finite. Spaces very convenient for this are the Sobolev spaces introduced in (A.15). Indeed, if $\varphi \in H^s(\mathbb{T})$, then the Cauchy-Schwarz inequality gives

$$\begin{aligned} \sum_{\mu(r)<|n|\leq r} |\widehat{\varphi}_n| &\leq \left(\sum_{\mu(r)<|n|\leq r} |\widehat{\varphi}_n|^2\, (1+n^2)^s \right)^{1/2} \left(\sum_{\mu(r)<|n|\leq r} \frac{1}{(1+n^2)^s} \right)^{1/2} \\ &\leq C\|\varphi\|_{H^s(\mathbb{T})} \left(\sum_{\mu(r)<|n|\leq r} \frac{1}{n^{2s}} \right)^{1/2}. \end{aligned} \tag{A.26}$$

The series $\sum_{n=1}^{\infty} n^{-2s}$ is convergent if and only is $2s > 1$, in which case its tail goes to zero when $r \to 0$ and hence

$$\lim_{r\to\infty} |\langle w_{r,2}(\cdot,\zeta), \varphi\rangle_{\mathbb{T}}| = 0, \qquad \forall \varphi \in H^s(\mathbb{T}), \quad \forall s > 1/2.$$

When it comes to $w_{r,3}$, as in (A.24) we avoid the problems with the first term by bounding the exponential by one and using the decay of the test function as with

$w_{r,2}$. That way, we get

$$|\langle w_{r,3}(\cdot,\zeta),\varphi\rangle_{\mathbb{T}}| = \left|\sum_{|n|>r} e^{-4\pi r^2\zeta\sqrt{\frac{n^2}{r^2}-1}}\,\langle e^{2\pi in\xi},\varphi\rangle_{\mathbb{T}}\right| \leq \sum_{|n|>r}|\widehat{\varphi}_n|$$
$$\leq C\|\varphi\|_{H^s(\mathbb{T})}\left(\sum_{|n|>r}\frac{1}{n^{2s}}\right)^{1/2},$$

whenever $\varphi\in H^s(\mathbb{T})$ with $2s>1$, showing that

$$\lim_{r\to\infty}|\langle w_{r,3}(\cdot,\zeta),\varphi\rangle_{\mathbb{T}}| = 0, \qquad \forall\varphi\in H^s(\mathbb{T}), \quad \forall s>1/2.$$

Hence, we have proved the following lemma.

Lemma A.9. *Let $\zeta\geq 0$ and $2s>1$. Then,*

$$\lim_{r\to\infty} w_{r,2}(\cdot,\zeta) = 0 = \lim_{r\to\infty} w_{r,3}(\cdot,\zeta) \qquad \text{in} \quad H^s(\mathbb{T}).$$

For $w_{r,1}$, the pointwise convergence should yield the weaker result we are looking for, and indeed, if $\varphi\in\mathcal{P}$, according to (A.16) we have

$$|\langle w_{r,1}(\cdot,\zeta)-v_r(\cdot,\zeta),\varphi\rangle_{\mathbb{T}}| = \left|\sum_{|n|\leq\mu(r)}\left(e^{4\pi ir^2\zeta O\left(\frac{n^3}{r^3}\right)}-1\right)e^{-2\pi in^2\zeta}\,\langle e^{2\pi in\xi},\varphi\rangle_{\mathbb{T}}\right|$$
$$\leq \sum_{|n|\leq\mu(r)}\left|e^{4\pi ir^2\zeta O\left(\frac{n^3}{r^3}\right)}-1\right||\widehat{\varphi}_{-n}|$$
$$\leq C\sum_{|n|\leq\mu(r)}\frac{n^3}{r}|\widehat{\varphi}_{-n}|.$$

If μ satisfies (A.18), the paraxial approximation does the work and it is enough that the Fourier coefficients $|\widehat{\varphi}_n|$ do not grow. If this is the case, then

$$\lim_{r\to\infty}|\langle w_{r,1}(\cdot,\zeta)-v_r(\cdot,\zeta),\varphi\rangle_{\mathbb{T}}| \leq C_\varphi\lim_{r\to\infty}\frac{\mu(r)^4}{r} = 0,$$

so we have proved the following result:

Lemma A.10. *Let $\zeta\geq 0$ and assume that μ satisfies (A.12) and (A.18). Then, if φ is a periodic function such that $|\widehat{\varphi}_n|\leq C_\varphi$ for some constant $C_\varphi>0$ and for all $n\in\mathbb{Z}$, then*

$$\lim_{r\to\infty}\langle w_{r,1}(\cdot,\zeta)-v_r(\cdot,\zeta),\varphi\rangle_{\mathbb{T}} = 0.$$

In particular, if $s\geq 0$,

$$\lim_{r\to\infty}\Big(w_{r,1}(\cdot,\zeta)-v_r(\cdot,\zeta)\Big) = 0 \qquad \text{in } H^s(\mathbb{T}).$$

Lemmas A.9 and A.10 imply Theorem A.2 as a corollary:

Corollary A.11. *Let $\zeta>0$ ans $s>1/2$. Then,*

$$\lim_{r\to\infty} w_r(\cdot,\zeta) = v(\cdot,\zeta) \qquad \text{in} \quad H^{-s}(\mathbb{T}).$$

Proof. The proof is the same as that of Corollary A.8. Based on Lemmas A.9 and A.10, we have

$$\lim_{r\to\infty}\Big(w_r(\cdot,\zeta)-v_r(\cdot,\zeta)\Big)=0 \qquad \text{in } H^s(\mathbb{T})$$

for every $s>1/2$, so it is enough to prove that $\lim_{r\to\infty} v_r(\cdot,\zeta)=v(\cdot,\zeta)$ holds in $H^{-s}(\mathbb{T})$. Since for $\varphi\in H^s(\mathbb{T})$ we have

$$\langle v_r(\cdot,\zeta),\varphi\rangle_{\mathbb{T}}=\sum_{|n|\le\mu(r)} e^{-2\pi i n^2\zeta}\,\widehat{\varphi}_n \qquad \text{and} \qquad \langle v(\cdot,\zeta),\varphi\rangle_{\mathbb{T}}=\sum_{n\in\mathbb{Z}} e^{-2\pi i n^2\zeta}\,\widehat{\varphi}_n,$$

the theorem of dominated convergence implies that

$$\lim_{r\to\infty}\langle v_r(\cdot,\zeta),\varphi\rangle_{\mathbb{T}}=\sum_{n\in\mathbb{Z}} e^{-2\pi i n^2\zeta}\,\widehat{\varphi}_n=\langle v(\cdot,\zeta),\varphi\rangle_{\mathbb{T}}, \qquad \forall\varphi\in H^s(\mathbb{T}),$$

because $\Big|\chi_{[-\mu(r),\mu(r)]}(n)\,e^{-2\pi i n^2\zeta}\,\widehat{\varphi}_n\Big|\le|\widehat{\varphi}_n|$ and as in (A.26),

$$\sum_{n\in\mathbb{Z}}|\widehat{\varphi}_n|\le\|\varphi\|_{H^s(\mathbb{T})}\left(\sum_{n\in\mathbb{Z}}\frac{1}{(1+n^2)^s}\right)^{1/2}<\infty$$

whenever $2s>1$. □

APPENDIX B

Continued fractions

Continued fractions are, in simplest terms, one way to represent real numbers, whose utility lies in finding rational approximations. Of course, they would lack of any kind of interest if this were their only property, for many methods exist to approximate real numbers by means of rationals. However, this procedure gives, somehow, the best rational approximations for any given real number.

Definition B.1. Let $N \in \mathbb{N}$, $a_0 \in \mathbb{Z}$, $a_1, \ldots, a_N \in \mathbb{N}$ and $a_N \neq 1$. Then,

$$[a_0, a_1, a_2, \ldots, a_N] = a_0 + \cfrac{1}{a_1 + \cfrac{1}{a_2 + \cfrac{1}{\ddots + \cfrac{1}{a_N}}}}.$$

is called a continued fraction.

The motivation for this definition comes probably from the celebrated Euclidean algorithm, which states that given $a, b \in \mathbb{N}$, then there exist $a_0 \in \mathbb{N}$ and $0 \leq r_0 < b$ such that $a = ba_0 + r_0$, and moreover that $\gcd(a, b) = \gcd(b, r_0)$. Of course, this process can be repeated with b and r_0 so that there exist $a_1 \in \mathbb{N}$ and $0 \leq r_1 < r_0$ such that $b = a_1 r_0 + r_1$. Iterating this process, we get

$$\frac{a}{b} = a_0 + \frac{r_0}{b} = a_0 + \frac{1}{b/r_0} = a_0 + \cfrac{1}{a_1 + \cfrac{r_1}{r_0}} = a_0 + \cfrac{1}{a_1 + \cfrac{1}{a_2 + \cfrac{r_2}{r_1}}} = \ldots,$$

and since the sequence r_n is decreasing, this process will end when for some n, $r_n = 1$. Moreover, with this method one can find approximations

$$\rho_0 = a_0, \qquad \rho_1 = a_0 + \frac{1}{a_1}, \qquad \rho_2 = a_0 + \cfrac{1}{a_1 + \cfrac{1}{a_2}}, \qquad \cdots$$

It is clear that every finite simple continued fraction is a rational number. Reversely, according to the Euclidean algorithm, every rational number can be written as a finite simple continued fraction. But what happens with infinite fractions, and what happens with irrationals? For $\rho \in \mathbb{R}\setminus\mathbb{Q}$, one may adapt the Euclidean algorithm by calling $a_0 = \lfloor \rho \rfloor$ so that since $0 \leq \{\rho\} < 1$, we can write

$$\rho = \lfloor \rho \rfloor + \{\rho\} = a_0 + \frac{1}{r_1}, \qquad r_1 = 1/\{\rho\} > 1.$$

Then let $a_1 = \lfloor r_1 \rfloor \in \mathbb{N}$ so that calling $r_2 = 1/\{r_1\} > 1$,

$$\rho = a_0 + \cfrac{1}{a_1 + \cfrac{1}{r_2}} = \dots \tag{B.1}$$

and this can be iterated without end. It seems, then, that the irrational ρ is connected to an infinite continued fraction $[a_0; a_1, a_2, \dots]$ formed as above.

Definition B.2. Let $a_0 \in \mathbb{Z}$, $a_n \in \mathbb{N}$ for $n \in \mathbb{N}$. Then, the continued fraction $\rho_n = [a_0; a_1, \dots, a_n]$ is called the n-th convergent. If $\lim_{n\to\infty} \rho_n$ exists, then the infinite continued fraction $[a_0; a_1, a_2, a_3, \dots]$ is defined as the limit of its convergents,

$$[a_0; a_1, a_2, a_3, \dots] = a_0 + \cfrac{1}{a_1 + \cfrac{1}{a_2 + \cfrac{1}{a_3 + \ddots}}} = \lim_{n\to\infty} \rho_n.$$

The main result concerning the representation of real numbers by continued fractions is the following well-known theorem which we prove in Subsection B.2.

Theorem B.3. *Every infinite continued fraction converges to an irrational number. Also, every irrational number has a unique representation as a continued fraction.*

In this sense, if $x \in \mathbb{R}$ has the continued fraction $[a_0; a_1, a_2, \dots, a_N]$, where $N \in \mathbb{N} \cup \{\infty\}$, and if p_n/q_n is the n-th convergent, then

- if x is rational, that is, if $N \in \mathbb{N}$, then $x = p_N/q_N$.
- if x is irrational, that is, if $N = \infty$, then $\lim_{n\to\infty} p_n/q_n = x$.

We remark here, and we will prove, that the convergents are always irreducible fractions.

Moreover, the advantage of the rational approximations by continued fractions of a real number is that they are, in some sense, the best approximations one may have. For a proof of this theorem, see [65, Theorem 17].

Theorem B.4. *Let $x \in \mathbb{R}$, $n \in \mathbb{N}$ and $\rho_n = p_n/q_n$ the n-th convergent of its expression as a continued fraction. Let also $p' \in \mathbb{Z}, q' \in \mathbb{N}$ be coprime integers. Then,*

$$|q'x - p'| < |qx - p| \qquad \Longrightarrow \qquad q' > q.$$

Consequently,

$$\left|x - \frac{p'}{q'}\right| < \left|x - \frac{p}{q}\right| \qquad \Longrightarrow \qquad q' > q.$$

In the following subsections, we state and prove the basic properties of continued fractions that we use along the dissertation.

B.1 Basic properties

Definitions B.1 and B.2 also make sense if $a_i \in \mathbb{R}$ for any $n \in \mathbb{N}$, the only change being that in that case the convergents need not be rationals. The assumption of this generality allows to prove very nice properties of continued fractions. In words of Khinchin [65], it allows to establish the *formal apparatus* of continued fractions. Unless otherwise stated, along this section all continued fractions will be of this kind.

Almost all properties are a consequence of the following result concerning the convergents.

Proposition B.5. *Let $N \in \mathbb{N}$ and $a_0, a_1, \dots a_N \in \mathbb{R}^N$, and define the recursive sequences*

$$\begin{array}{lll} p_0 = a_0, & p_1 = a_0 a_1 + 1, & p_n = a_n p_{n-1} + p_{n-2}, \quad \forall n \geq 2, \\ q_0 = 1, & q_1 = a_1, & q_n = a_n q_{n-1} + q_{n-2}, \quad \forall n \geq 2. \end{array}$$

Then,

$$[a_0, a_1, a_2, \dots, a_n] = \frac{p_n}{q_n}, \qquad \forall n \leq N.$$

We remark that now p_n/q_n need no longer be rational numbers, but we still call them convergents of the continued fraction.

Proof. The proof works by induction on the length of the fraction n. For $n = 0$, we just have $[a_0] = a_0$, so $p_0 = a_0$ and $q_0 = 1$ satisfy the property. For $n = 1$, we see that

$$[a_0; a_1] = a_0 + \frac{1}{a_1} = \frac{a_0 a_1 + 1}{a_1},$$

so $p_1 = a_0 a_1 + 1$ and $q_1 = a_1$ are also correct. Now let $n \geq 1$ and assume that the property is true for every $k \leq n$. Then,

$$[a_0; a_1, \dots, a_n, a_{n+1}] = a_0 + \cfrac{1}{a_1 + \cfrac{1}{\ddots + \cfrac{1}{a_n + \cfrac{1}{a_{n+1}}}}} = [a_0; a_1, \dots, a_{n-1}, a_n + \tfrac{1}{a_{n+1}}],$$

the last expression being of length n. Then, since $[a_0; a_1, \dots, a_{n-1}] = p_{n-1}/q_{n-1}$ such that p_{n-1} and q_{n-1} satisfy the recurrence relation, by the inductive hypothesis we have that $[a_0; a_1, \dots, a_{n-1}, a_n + \frac{1}{a_{n+1}}] = p'_n/q'_n$ such that

$$p'_n = \left(a_n + \frac{1}{a_{n+1}}\right) p_{n-1} + p_{n-2}, \qquad q'_n = \left(a_n + \frac{1}{a_{n+1}}\right) q_{n-1} + q_{n-2}.$$

If we compute the quotient

$$\begin{aligned} \frac{p'_n}{q'_n} &= \frac{\left(a_n + \frac{1}{a_{n+1}}\right) p_{n-1} + p_{n-2}}{\left(a_n + \frac{1}{a_{n+1}}\right) q_{n-1} + q_{n-2}} = \frac{(a_{n+1}a_n + 1)\, p_{n-1} + a_{n+1} p_{n-2}}{(a_{n+1}a_n + 1)\, q_{n-1} + a_{n+1} q_{n-2}} \\ &= \frac{a_{n+1}(a_n p_{n-1} + p_{n-2}) + p_{n-1}}{a_{n+1}(a_n q_{n-1} + q_{n-2}) + q_{n-1}} = \frac{a_{n+1} p_n + p_{n-1}}{a_{n+1} q_n + q_{n-1}}, \end{aligned}$$

where $[a_0; a_q, \dots, a_n] = p_n/q_n$. Then, $p_{n+1} = a_{n+1}p_n + p_{n-1}$ and $q_{n+1} = a_{n+1}q_n + q_{n-1}$ satisfy $[a_0; a_1, \dots, a_n, a_{n+1}] = p_{n+1}/q_{n+1}$. □

In what follows, we state and prove a bunch of propositions, corollaries of Proposition B.5.

Proposition B.6. *If $[a_0; a_1, \dots, a_N]$ is a continued fraction and p_n, q_n are the sequences of numbers defined in Proposition B.5, then*

$$p_n q_{n-1} - p_{n-1} q_n = (-1)^{n-1}, \qquad \forall n = 1, \dots, N.$$

Also,

$$\frac{p_n}{q_n} - \frac{p_{n-1}}{q_{n-1}} = \frac{(-1)^{n-1}}{q_n q_{n-1}}, \qquad \forall n = 1, \dots, N.$$

Proof. Also by induction on n. If $n = 1$, we get

$$p_1 q_0 - p_0 q_1 = (a_0 a_1 + 1) - a_0 a_1 = 1 = (-1)^0.$$

Now assuming the property holds for $k \leq n-1$, we see by Proposition B.5

$$\begin{aligned} p_n q_{n-1} - p_{n-1} q_n &= (a_n p_{n-1} + p_{n-2}) q_{n-1} - p_{n-1}(a_n q_{n-1} + q_{n-2}) \\ &= p_{n-2} q_{n-1} - p_{n-1} q_{n-2} = -(p_{n-1} q_{n-2} - p_{n-2} q_{n-1}) \\ &= -(-1)^{n-2} = (-1)^{n-1}. \end{aligned}$$

Also,

$$\frac{p_n}{q_n} - \frac{p_{n-1}}{q_{n-1}} = \frac{p_n q_{n-1} - p_{n-1} q_n}{q_n q_{n-1}} = \frac{(-1)^{n-1}}{q_n q_{n-1}}.$$

□

A similar result is the following.

Proposition B.7. *If $[a_0; a_1, \dots, a_N]$ is a continued fraction and p_n, q_n are the sequences of numbers defined in Proposition B.5, then*

$$p_n q_{n-2} - p_{n-2} q_n = (-1)^n a_n, \qquad \forall n = 2, \dots, N.$$

Also,

$$\frac{p_n}{q_n} - \frac{p_{n-2}}{q_{n-2}} = \frac{(-1)^n a_n}{q_n q_{n-2}}, \qquad \forall n = 2, \dots, N.$$

Proof. It comes as a consequence of Propositions B.5 and B.6, since

$$\begin{aligned} p_n q_{n-2} - p_{n-2} q_n &= (a_n p_{n-1} + p_{n-2}) q_{n-2} - p_{n-2}(a_n q_{n-1} + q_{n-2}) \\ &= a_n (p_{n-1} q_{n-2} - p_{n-2} q_{n-1}) = a_n (-1)^{n-2} \\ &= a_n (-1)^n. \end{aligned}$$

As a consequence,

$$\frac{p_n}{q_n} - \frac{p_{n-2}}{q_{n-2}} = \frac{p_n q_{n-2} - p_{n-2} q_n}{q_n q_{n-2}} = \frac{(-1)^n a_n}{q_n q_{n-2}}.$$

□

This last result allows to know more about the behaviour of the convergents.

Proposition B.8. *Let $N \in \mathbb{N}$ and $[a_0; a_1, \dots, a_N]$ be a continued fraction such that $a_1, \dots, a_N > 0$ with convergents p_n/q_n given by Proposition B.5. Then,*

- *the sequence of even-indexed convergents* $(p_n/q_n)_{n\in 2\mathbb{N}}$ *is strictly increasing, and*
- *the sequence of odd-indexed convergents* $(p_n/q_n)_{n\in 2\mathbb{N}+1}$ *is strictly decreasing.*

Also, any odd-indexed convergent is greater than any even-indexed convergent, and consequently, the two subsequences tend toward each other. Shortly, for every $n < N/2$,

$$\frac{p_0}{q_0} < \frac{p_2}{q_2} < \ldots < \frac{p_{2n}}{q_{2n}} < \ldots \leq [a_0; a_1, \ldots, a_N] \leq \ldots < \frac{p_{2n+1}}{q_{2n+1}} < \ldots < \frac{p_3}{q_3} < \frac{p_1}{q_1},$$

where the equality only holds with the last convergent p_N/q_N.

For simplicity, let us call the even-indexed convergents simply even convergents, and the odd-indexed convergents simply odd convergents.

Proof. First of all, if $a_1, \ldots a_N > 0$, then it is clear from the recurrence relation in Proposition B.5 that $q_n > 0$ for all $n = 0, 1, \ldots, N$. Assume now n is even. Proposition B.7 shows that

$$\frac{p_n}{q_n} - \frac{p_{n-2}}{q_{n-2}} = \frac{(-1)^n a_n}{q_n q_{n-2}} = \frac{a_n}{q_n q_{n-2}} > 0,$$

so the even convergents increase strictly, whereas if n is odd, then

$$\frac{p_n}{q_n} - \frac{p_{n-2}}{q_{n-2}} = \frac{(-1)^n a_n}{q_n q_{n-2}} = -\frac{a_n}{q_n q_{n-2}} < 0,$$

and the odd convergents decrease strictly. On the other hand, if n is even, then according to Proposition B.6

$$\frac{p_n}{q_n} - \frac{p_{n-1}}{q_{n-1}} = \frac{(-1)^{n-1}}{q_n q_{n-1}} = \frac{-1}{q_n q_{n-1}} < 0,$$

so every even convergent is smaller than its previous odd convergent. Then, for any $n, k \in \mathbb{N}$, we have

$$\frac{p_{2n}}{q_{2n}} < \frac{p_{2k-1}}{q_{2k-1}}.$$

Indeed, if $k \leq n$, then

$$\frac{p_{2n}}{q_{2n}} < \frac{p_{2n-1}}{q_{2n-1}} \leq \frac{p_{2k-1}}{q_{2k-1}},$$

and if $k > n$, then

$$\frac{p_{2n}}{q_{2n}} < \frac{p_{2k}}{q_{2k}} < \frac{p_{2k-1}}{q_{2k-1}}.$$

Since the last convergent is $p_N/q_N = [1_0, a_1, \ldots, a_N]$, all even convergents are below it, and all odd convergents, above it. □

B.2 Approximation of real numbers

We said in the beginning that rationals can be expressed as continued fractions with integer coefficients thanks to the Euclidean algorithm, and that this could be adapted to the irrational numbers so that an infinite continued fraction was obtained. In this section, we come back to the problem of approximation, for which we work with finite and infinite fractions with $a_0 \in \mathbb{Z}$ and $a_n \in \mathbb{N}$ for every $n \in \mathbb{N}$.

Proposition B.9. *Let $N \in \mathbb{N}$ and $[a_0; a_1, \dots, a_N]$ be a continued fraction such that $a_0 \in \mathbb{Z}$ and $a_1, \dots, a_N \in \mathbb{N}$. Then, the convergents p_n/q_n given by Proposition B.5 satisfy:*

- $p_n \in \mathbb{Z}$, $q_n \in \mathbb{N}$.
- $\gcd(p_n, q_n) = 1$ *for all* $n \in \mathbb{N}$.
- *The sequence $(q_n)_{n\in\mathbb{N}}$ is strictly increasing when $n \geq 2$, and moreover*

$$q_n \geq 2^{(n-1)/2}, \qquad \forall n \leq N.$$

Proof. It is evident from the recurrence relations in Proposition B.5 that both p_n and q_n are integers, and moreover that $q_n > 0$. Assume that $d \in \mathbb{N}$ divides both p_n and q_n. Then, d also divides $p_n q_{n-1} - p_{n-1} q_n$, and by Proposition B.6 d divides $(-1)^{n-1}$. Hence, $d = 1$ and $\gcd(p_n, q_n) = 1$. Finally, $q_n = a_n q_{n-1} + q_{n-2} > a_n q_{n-1} \geq q_{n-1}$, so $(q_n)_n$ is a strictly increasing sequence when $n \geq 2$. As a consequence,

$$q_n = a_n q_{n-1} + q_{n-2} > 2q_{n-2} \qquad \Longrightarrow \qquad q_n > 2^k q_{n-2k}, \quad \forall k \leq n/2.$$

Hence, if n is even, then $q_n > 2^{n/2} q_0 = 2^{n/2}$, and if n is odd, then $q_n > 2^{(n-1)/2} q_1 \leq 2^{(n-1)/2}$. □

The situation for rationals is clear by the Euclidean algorithm, there is a one to one correspondence between them and finite continued fractions. The above Proposition, as well as the ones in the previous section, allow to prove the same characterisation for irrational numbers, as stated in Theorem B.3.

Proof of Theorem B.3. Let us first prove that an arbitrary infinite continued fraction is always convergent. For that, let $a_0 \in \mathbb{Z}$ and $a_n \in \mathbb{N}$ for all $n \in \mathbb{N}$. We want to see that sequence of convergents $p_n/q_n = [a_0; a_1, \dots, a_n]$ is convergents. For that, by Proposition B.8 we know that the sequence of even convergents $(p_{2n}/q_{2n})_n$ is strictly increasing and moreover bounded above by p_1/q_1, hence it is convergent. In the same way, the sequence $(p_{2n+1}/q_{2n+1})_n$ is strictly decreasing and bounded below by p_0/q_0, so it is also convergent. Now, by Propositions B.6 and B.9,

$$\frac{p_{2n+1}}{q_{2n+1}} - \frac{p_{2n}}{q_{2n}} = \frac{(-1)^{2n}}{q_{2n} q_{2n+1}} < \frac{1}{2^{2n-1/2}} \to 0$$

when $n \to \infty$. This shows that the limits of the two subsequences are equal, and hence the sequence of convergents is convergent.

Now, let $\rho \in \mathbb{R} \setminus \mathbb{Q}$, build the infinite continued fraction $[a_0; a_1, \dots, a_n, \dots]$ as in (B.1) and let p_n/q_n be the corresponding convergents. Then, with the sequence r_n there, we have

$$r_n = a_n + \frac{1}{r_{n+1}}, \qquad \rho = [a_0; a_1, \dots, a_{n-1}, r_n], \qquad \forall n \in \mathbb{N}$$

Then, following the recurrence relation in Proposition B.5,

$$\rho = \frac{r_n p_{n-1} + p_{n-2}}{r_n q_{n-1} + q_{n-2}} \qquad \text{and} \qquad \frac{p_n}{q_n} = \frac{a_n p_{n-1} + p_{n-2}}{a_n q_{n-1} + q_{n-2}},$$

so

$$\rho - \frac{p_n}{q_n} = (-1)^n \frac{r_n - a_n}{q_n (r_n q_{n-1} + q_{n-2})}.$$

Since $r_n - a_n = 1/r_{n+1} < 1$ and $r_n > a_n$ implies $r_n q_{n-1} + q_{n-2} > q_n$, we get

$$\lim_{n\to\infty} \left| \rho - \frac{p_n}{q_n} \right| < \lim_{n\to\infty} \frac{1}{q_n^2} = 0,$$

so $\rho = [a_0; a_1, \ldots, a_n, \ldots]$.

Finally, we want to see that it this continued fraction is unique. Assume that there is one more continued fraction $[a'_0; a'_1, \ldots, a'_n, \ldots] = \rho$. Analysing the integer part of ρ, we get $a'_0 = \lfloor \rho \rfloor = a_0$. Now, assume the inductive hypothesis that $a_k = a'_k$ for every $k < n$. Then, by Proposition B.5, all the corresponding convergents satisfy $p_k = p'_k$ and $q_k = q'_k$ for every $k < n$. Then, define

$$r_n = [a_n; a_{n+1}, \ldots], \qquad r'_n = [a'_n; a'_{n+1}, \ldots]$$

so that

$$\rho = [a_0; a_1, \ldots, a_{n-1}, r_n] = \frac{r_n p_{n-1} + p_{n-2}}{r_n q_{n-1} + q_{n-2}}$$

and

$$\rho = [a_0; a_1, \ldots, a_{n-1}, r'_n] = \frac{r'_n p_{n-1} + p_{n-2}}{r'_n q_{n-1} + q_{n-2}}.$$

We deduce from this equality that $r_n = r'_n$, and therefore $a_n = \lfloor r_n \rfloor = \lfloor r'_n \rfloor = a'_n$, which concludes the proof. □

Once we have established that every real number corresponds to a continued fraction and viceversa, we measure the error of the convergents. The main estimate can already be distinguished in Proposition B.6.

Proposition B.10. *Let $x \in \mathbb{R}$ and its continued fraction, finite or infinite depending on whether x is rational or irrational, be given by the sequence $a_0 \in \mathbb{N}$, $a_n \in \mathbb{N}$. Let p_n/q_n be the n-th convergent. Then,*

$$\frac{1}{q_n(q_{n+1} + q_n)} \leq \left| x - \frac{p_n}{q_n} \right| \leq \frac{1}{q_{n+1} q_n}$$

for all n. In particular,

$$\left| x - \frac{p_n}{q_n} \right| < \frac{1}{q_n^2}, \qquad \forall n. \tag{B.2}$$

Proof. Proposition B.8 shows that two consecutive convergents of x are each on one side of it, so it is clear that

$$\left| x - \frac{p_n}{q_n} \right| < \left| \frac{p_{n+1}}{q_{n+1}} - \frac{p_n}{q_n} \right| = \frac{1}{q_{n+1} q_n},$$

the last equality being a consequence of Proposition B.6. Observe that the strict inequality is an equality if and only if the continued fraction is finite and if $n = N - 1$. Since $q_{n+1} > q_n$, the last conclusion of the proposition follows immediately.

For the lower bound, assume that n is even, so that $p_n/q_n < x < p_{n+1}/q_{n+1}$. Then, it is a general fact that

$$\frac{p_n}{q_n} < \frac{p_n + p_{n+1}}{q_n + q_{n+1}} < \frac{p_{n+1}}{q_{n+1}}.$$

Let us iterate this a_{n+2} times, so that

$$\frac{p_n}{q_n} < \frac{p_n + p_{n+1}}{q_n + q_{n+1}} < \frac{p_n + 2p_{n+1}}{q_n + 2q_{n+1}} < \dots \frac{p_n + a_{n+2}p_{n+1}}{q_n + a_{n+2}q_{n+1}} < \frac{p_{n+1}}{q_{n+1}}.$$

According to the recurrence relations in Proposition B.5, we have shown that

$$\frac{p_n}{q_n} < \frac{p_n + p_{n+1}}{q_n + q_{n+1}} < \frac{p_{n+2}}{q_{n+2}} < x.$$

Thus,

$$\left| x - \frac{p_n}{q_n} \right| > \frac{p_n + p_{n+1}}{q_n + q_{n+1}} - \frac{p_n}{q_n} = \frac{q_n(p_n + p_{n+1}) - p_n(q_n + q_{n+1})}{q_n(q_n + q_{n+1})} = \frac{1}{q_n(q_n + q_{n+1})}.$$

If n is odd, the proof is completely analogous. □

Related to the approximation result in Proposition B.10, the following theorem states that if an arbitrary irreducible fraction approaches an irrational a little bit better than (B.2), then it must be a convergent. Even if the proof is not too complicated, it is related to the concept of best approximation in Theorem B.4, so as we did there, we refer to [65, Theorems 16 and 19].

Theorem B.11. *Let $x \in \mathbb{R}$ and an irreducible fraction p/q such that*

$$\left| x - \frac{p}{q} \right| < \frac{1}{2q^2}.$$

Then, p/q is a convergent of x.

In Section 4.6, when we prove the non-existence of tangents in irrational points of the image of Riemann's non-differentiable function $\phi(\mathbb{R})$, we claim that we can always work with convergents p_n/q_n such that q_n is odd. We show that in the following proposition.

Proposition B.12. *Let $\rho \in \mathbb{R} \setminus \mathbb{Q}$, its continued fraction $[a_0; a_1, \dots, a_n, \dots]$ and the convergents p_n/q_n. Then, for any $n \in \mathbb{N}$, q_n and q_{n+1} are not both even. Consequently, there exists a subsequence of convergents p_{n_j}/q_{n_j} such that q_{n_j} is odd for all $j \in \mathbb{N}$.*

Proof. By contradiction, let $N \in \mathbb{N}$ be such that q_N and q_{N+1} are both even. Then, the recurrence relation in Proposition B.5 shows that

$$q_{N-1} = q_{N+1} - a_{N+1}q_N = 0 \pmod 2,$$

so q_{N-1} is even. By induction, q_n is even for every $n \leq N$. But $q_0 = 1$, which is a contradiction. Hence, there are never two consecutive convergents with even denominator, and convergents with odd denominator are infinitely many. □

Also when analysing the tangents, it is important to measure the error in Proposition B.10 in a more precise way. We do that by analysing the behaviour of the sequence K_n defined in (4.4) as

$$\left| \rho - \frac{p_n}{q_n} \right| = \frac{K_n}{q_n^2}, \qquad \forall n \in \mathbb{N},$$

which is a sequence that satisfies $0 < K_n < 1$. The first result we show is the relationship between K_n and the sequence of the coefficients of the continued fraction a_n.

Proposition B.13. *Let $\rho \in \mathbb{R} \setminus \mathbb{Q}$, its continued fraction $[a_0; a_1, \ldots, a_n, \ldots]$ and the convergents p_n/q_n. Let $K_n = q_n^2 \, |\rho - p_n/q_n|$. Then,*

$$\frac{1}{a_{n+1}+2} < K_n < \frac{1}{a_{n+1}}, \qquad \forall n \in \mathbb{N}.$$

This result is, of curse, valid also for finite continued fractions in the corresponding range of n.

Proof. The recurrence formula for q_n shows that

$$q_{n+1} = a_{n+1}q_n + q_{n-1} > a_{n+1}q_n$$

and

$$q_{n+1} + q_n = a_{n+1}q_n + q_{n-1} + q_n < (a_{n+1}+2)q_n.$$

Hence, from Proposition B.10 we get for all $n \in \mathbb{N}$

$$\frac{1}{(a_{n+1}+2)q_n^2} < \left|\rho - \frac{p_n}{q_n}\right| = \frac{K_n}{q_n^2} < \frac{1}{a_{n+1}q_n^2}.$$

□

Hence, we see that the behaviour of K_n when $n \to \infty$ completely depends on the behaviour of a_n when $n \to \infty$. In Section 4.6, we needed to work with the limit of K_n because the situation was different whether it was zero or not. Proposition B.13 shows that there are plenty of irrationals such that $\lim_{n\to\infty} K_n = 0$, but one can also conclude that the limit may not exist.

Corollary B.14. *Let $\rho = [a_0; a_1, \ldots, a_n, \ldots] \in \mathbb{R} \setminus \mathbb{Q}$. Then*

$$\lim_{n\to\infty} K_n = 0 \quad \Longleftrightarrow \quad \lim_{n\to\infty} a_n = +\infty.$$

On the other hand, there exist irrational numbers for which the limit of K_n does not exist.

Proof. According to Proposition B.13, $\lim_{n\to\infty} K_n = 0$ implies $\lim_{n\to\infty} 1/(a_{n+1} + 2) = 0$, which implies $\lim_{n\to\infty} a_n = +\infty$. Reversely, if $\lim_{n\to\infty} a_n = 0$ holds, then $\lim_{n\to\infty} K_{n-1} = 0$.

To find a number whose K_n does not have a limit, it is enough to let the sequence a_n be such that

$$\frac{1}{a_{2n}} < \frac{1}{a_{2n+1}+2}, \qquad \forall n \in \mathbb{N}.$$

This is achieved, for instance, if $a_{2n} = 4$ and $a_{2n+1} = 1$, so that

$$\rho = [0, 1, 4, 1, 4, 1, 4, \ldots] = 2(\sqrt{2} - 1).$$

For this number, $K_{2n+1} < 1/4 < 1/3 < K_{2n}$ for all $n \in \mathbb{N}$, so $\lim_{n\to\infty} K_n$ does not exist. □

This is the reason for which we needed to subtract a subsequence, in order to be able to work with some limit that exists, such as the limit inferior. A characterisation analogue to Corollary B.14 is the followng

Corollary B.15. *Let $\rho = [a_0; a_1, \ldots, a_n, \ldots] \in \mathbb{R} \setminus \mathbb{Q}$. Then*

$$\liminf_{n\to\infty} K_n = 0 \quad \Longleftrightarrow \quad (a_n)_{n=1}^{\infty} \text{ is unbounded.}$$

Proof. If there exists a subsequence K_{n_j} converging to zero, then the subsequence a_{n_j+1} diverges to infinity so the sequence a_n is unbounded. Reversely, if a_n is unbounded, then there exists a subsequence a_{m_j} diverging to infinity, which means that $lim_{j\to\infty} K_{m_j-1} = 0$, and hence $\liminf_{n\to\infty} K_n = 0$. □

A good bound for it is given in the following result whose proof, which we do not reproduce here, can be found in [65, Theorem 20].

Proposition B.16. *Given a real number $x \in \mathbb{R}$ and its continued fraction convergents $(p_n/q_n)_n$, then for a given n, at least one of the bounds*

$$\left|x - \frac{p_n}{q_n}\right| < \frac{1}{\sqrt{5}\, q_n^2}, \quad \text{or} \quad \left|x - \frac{p_{n-1}}{q_{n-1}}\right| < \frac{1}{\sqrt{5}\, q_{n-1}^2} \quad \text{or} \quad \left|x - \frac{p_{n-2}}{q_{n-2}}\right| < \frac{1}{\sqrt{5}\, q_{n-2}^2}$$

must hold.

We deduce immediately the following.

Corollary B.17. *For an irrational $\rho \in \mathbb{R} \setminus \mathbb{Q}$, $\liminf_{n\to\infty} K_n \le 1/\sqrt{5}$.*

It is known that this bound cannot be improved. A very nice result that shows this is, for instance, the computation of the limit of K_n for continued fractions that are constant from some coefficient on.

Proposition B.18. *Let $a, N \in \mathbb{N}$ and $\rho = [a_0; a_1, \ldots, a_n, \ldots] \in \mathbb{R} \setminus \mathbb{Q}$ be such that $a_n = a$ for all $n \ge N$. Then,*

$$\lim_{n\to\infty} K_n = \frac{1}{\sqrt{a^2+4}}.$$

In particular, for the golden number $\varphi = [1; 1, 1, 1, \ldots] = (1+\sqrt{5})/2$, $\lim_{n\to\infty} K_n = 1/\sqrt{5}$.

This result, and others of the kind, can be found in a very nice exposition by Hurwitz [52] and Koksma [67, Section III.2], who denoted $M(\theta) = \limsup_n 1/K_n = 1/\liminf_n K_n$.

All these results concerning the behaviour of the sequence K_n show that all possibilities for $K = \liminf_{n\to\infty} K_n$ that was defined in (4.6) need to be studied in the proof of Proposition 4.21, since either $K = 0$ or $0 < K \le 1/\sqrt{5}$ may happen.

APPENDIX C

Some symmetries of the Schrödinger equation

A symmetry of a differential equation is a transformation from the space of the solutions to the equation to itself. In other words, we say that transformation S is a symmetry the image Su of any solution is also a solution. In this case, we are interested in symmetries of the free Schrödinger equation

$$u_t = i\,\Delta u, \tag{C.1}$$

where $u = u(x,t)$ and $x \in \mathbb{R}^n, t \in \mathbb{R}$. We begin by recalling that the Cauchy problem of the equation

$$\begin{cases} u_t = i\,\Delta u, & x \in \mathbb{R}^n, \quad t \in \mathbb{R}, \\ u(x,0) = f(x), & x \in \mathbb{R}^n, \end{cases}$$

can be solved, for instance, taking the Fourier transform only in space so that the equation turns into $\widehat{u}_t(\xi,t) = -4\pi^2 i|\xi|^2\widehat{u}(\xi,t)$. Together with the initial datum $\widehat{u}(\xi,0) = \widehat{f}(\xi)$, it constitutes an ODE problem that is satisfied by

$$\widehat{u}(\xi,t) = \widehat{f}(\xi)\, e^{-4\pi^2 i|\xi|^2 t}. \tag{C.2}$$

The inverse Fourier transform yields then the solution

$$u(x,t) = \int_{\mathbb{R}^n} \widehat{f}(\xi)\, e^{2\pi i x\xi - 4\pi^2 i|\xi|^2 t}\, d\xi. \tag{C.3}$$

One more option is to compute first the fundamental solution, which corresponds to the initial datum given by the Dirac delta. Set $f = \delta \in \mathcal{S}'$ which satisfies $\widehat{f} = 1$. Hence, denoting the fundamental solution by F, from (C.2) we get

$$\widehat{F}(\xi,t) = e^{-4\pi^2 i|\xi|^2 t} \quad \Longrightarrow \quad F(x,t) = \frac{1}{(4\pi i t)^{n/2}}\, e^{i|x|^2/(4t)}, \tag{C.4}$$

and the solution to the Cauchy problem can be expressed by

$$u(x,t) = \frac{1}{(4\pi i t)^{n/2}} \int_{\mathbb{R}^n} f(y)\, e^{\frac{i|x-y|^2}{4t}}\, dy. \tag{C.5}$$

Remark C.1. The choice of $\sqrt{it}$ in the fundamental solution is determined by the integral

$$\int_{-\infty}^{\infty} e^{ix^2}\, dx = \frac{1+i}{\sqrt{2}}\sqrt{\pi},$$

which we could denote by $\sqrt{\pi i}$. Indeed, since no generality is lost if in (C.4) we work with $n = 1$, computing the Fourier transform directly and completing the square, one gets

$$F(x,t) = \int_{\mathbb{R}} e^{-4\pi^2 i\xi^2 t}\, e^{2\pi i x\xi}\, d\xi = e^{i\frac{x^2}{4t}} \int_{-\infty}^{\infty} e^{-4\pi^2 i t\xi^2}\, d\xi.$$

If $t > 0$, then change variables $\eta = 2\pi\sqrt{t}\xi$ so that

$$F(x,t) = \frac{e^{i\frac{x^2}{4t}}}{2\pi\sqrt{t}} \int_{-\infty}^{\infty} e^{-i\eta^2}\, d\eta = \frac{e^{i\frac{x^2}{4t}}}{2\pi\sqrt{t}}\sqrt{\pi}\frac{1-i}{\sqrt{2}} = \frac{e^{i\frac{x^2}{4t}}}{\sqrt{4\pi t}\frac{1+i}{\sqrt{2}}}.$$

On the other hand, if $t < 0$, then change variables $\eta = 2\pi\sqrt{-t}\xi$ so that

$$F(x,t) = \frac{e^{i\frac{x^2}{4t}}}{2\pi\sqrt{-t}} \int_{-\infty}^{\infty} e^{i\eta^2}\, d\eta = \frac{e^{i\frac{x^2}{4t}}}{\sqrt{-4\pi t}}\frac{1+i}{\sqrt{2}} = \frac{e^{i\frac{x^2}{4t}}}{\sqrt{4\pi t}\sqrt{-1}\frac{1-i}{\sqrt{2}}} = \frac{e^{i\frac{x^2}{4t}}}{\sqrt{4\pi t}\frac{1+i}{\sqrt{2}}},$$

if we choose $\sqrt{-1} = i$. Alternatively, it is now evident that the solution can also be written as

$$F(x,t) = \frac{e^{i\frac{x^2}{4t}}}{\sqrt{4\pi|t|}\frac{1+\mathrm{sign}(t)i}{\sqrt{2}}}.$$

C.1 Most basic symmetries

Let us briefly review some simple symmetries that can be immediately deduced from the equation or the expressions for the solution above.

C.1.1 Translations in space and time

Let $u(x,t)$ be a solution to the free Schrödinger solution and $x_0 \in \mathbb{R}^n$, $t_0 \in \mathbb{R}$. Then,

$$v(x,t) = u(x + x_0, t + t_0)$$

is also a solution to the (C.1). Moreover, the initial datum is $v_0(x) = u(x + x_0, t_0)$.

C.1.2 Dilations

The correct scaling for dilations of the variables with respect to a parameter $\lambda \in \mathbb{R}$ is also easily guessed from the equation itself. If u is a solution with initial datum f, we

can also use (C.3), where if v is the solution with the initial datum $\widehat{f}(\xi/\lambda)$, then

$$\begin{aligned} v(x,t) &= \int_{\mathbb{R}^n} \widehat{f}(\xi/\lambda) e^{2\pi i x\xi - 4\pi^2 i|\xi|^2 t}\, d\xi = \lambda^n \int_{\mathbb{R}^n} \widehat{f}(\eta) e^{2\pi i(\lambda x)\eta - 4\pi^2 i|\eta|^2(\lambda^2 t)}\, d\eta \\ &= \lambda^n\, u(\lambda x, \lambda^2 t). \end{aligned}$$

Since multiplication by constants is evidently also a symmetry, then

$$w(x,t) = \lambda^\alpha\, u(\lambda x, \lambda^2 t), \qquad \forall \lambda \in \mathbb{R}, \quad \forall \alpha \in \mathbb{R} \tag{C.6}$$

is also a solution, with initial datum $w_0(x) = \lambda^\alpha\, u_0(\lambda x)$.

C.1.3 Conjugation

Conjugating (C.3), one gets

$$\begin{aligned} \overline{u(x,t)} &= \int_{\mathbb{R}^n} \overline{\widehat{f}(\xi)}\, e^{-2\pi i x\xi + 4\pi^2 i|\xi|^2 t}\, d\xi = \int_{\mathbb{R}^n} \widehat{\overline{f}}(-\xi)\, e^{-2\pi i x\xi + 4\pi^2 i|\xi|^2 t}\, d\xi \\ &= \int_{\mathbb{R}^n} \widehat{\overline{f}}(\xi)\, e^{2\pi i x\xi + 4\pi^2 i|\xi|^2 t}\, d\xi \\ &= v(x,-t). \end{aligned}$$

Hence,

$$v(x,t) = \overline{u(x,-t)}$$

is also a solution to the free Schrödinger equation such that $v_0(x) = \overline{u_0}(x)$.

C.2 The Galilean symmetry

We have seen how very simple and certainly trivial symmetries can also be deduced from altering the Fourier transform of the initial datum of the solution. We can thus expect that other variations in $\widehat{f}$ will yield more complicated and not so evident symmetries for the equation. The Galilean symmetry corresponds to translations in the Fourier space. Indeed, if v is taken to be the solution corresponding to $\widehat{f}(\xi + \xi_0)$ for some $\xi_0 \in \mathbb{R}^n$, then

$$\begin{aligned} v(x,t) &= \int_{\mathbb{R}^n} \widehat{f}(\xi+\xi_0)\, e^{2\pi i x\xi - 4\pi^2 i|\xi|^2 t}\, d\xi = \int_{\mathbb{R}^n} \widehat{f}(\eta)\, e^{2\pi i x(\eta-\xi_0) - 4\pi^2 i|\eta-\xi_0|^2 t}\, d\xi \\ &= e^{-2\pi i x\xi_0 + 4\pi^2 i|\xi_0|^2 t} \int_{\mathbb{R}^n} \widehat{f}(\eta)\, e^{2\pi i x\eta - 4\pi^2 i(|\eta|^2 - 2\eta\xi_0)t}\, d\xi \\ &= e^{-2\pi i x\xi_0 + 4\pi^2 i|\xi_0|^2 t} \int_{\mathbb{R}^n} \widehat{f}(\eta)\, e^{2\pi i(x+4\pi\xi_0 t)\eta - 4\pi^2 i|\eta|^2 t}\, d\xi \\ &= e^{-2\pi i x\xi_0 + 4\pi^2 i|\xi_0|^2 t}\, u(x + 4\pi\xi_0 t, t). \end{aligned}$$

Thus,

$$v(x,t) = e^{-2\pi i x\xi_0 + 4\pi^2 i|\xi_0|^2 t}\, u(x + 4\pi\xi_0 t, t), \qquad \forall \xi_0 \in \mathbb{R}^n \tag{C.7}$$

is a solution to the free Schrödinger equation with initial datum $v_0(x) = e^{-2\pi i x\xi_0}\, u_0(x)$.

From the expression of this symmetry in (C.7), one can understand why it is called the way it is. Indeed, it makes reference to the Galilean invariance, the physical principle asserting that movement follows the same laws in any frame of reference which is allowed to move but not to accelerate. Galileo explained this principle in

the 17th century in terms of a sailing ship; he claimed that if a big boat were sailing at a constant speed, then a sailor shut below decks would not be able to distinguish whether the boat was indeed sailing in the open sea or docked in the port, since the movement of people, objects, animals, or liquids around him would be exactly the same in the two circumstances. The movement of the ship with respect to some point of reference x would be given by $x + \overrightarrow{v}t$, where $\overrightarrow{v}$ is its constant speed. In the setting of (C.7), that motion corresponds to $x + 4\pi\xi_0 t$, in which case the solution u is being preserved even if it is being translated by a velocity $4\pi\xi_0$.

Remark C.2. The Galilean symmetry also holds for the nonlinear Schrödinger equation appearing in the vortex filament problem (1.13).

C.3 The pseudoconformal symmetry

The pseudoconformal symmetry corresponds to changing the initial datum f by its Fourier transform $\widehat{f}$, and it is more or less easily obtained combining the two expressions (C.3) and (C.5) we wrote in the beginning. Indeed, let v be a solution with its initial datum v_0, and try to arrive to u. Start from (C.3) and complete the square to get

$$\begin{aligned}
v(x,t) &= \int_{\mathbb{R}^n} \widehat{v_0}(\xi)\, e^{2\pi i x\xi - 4\pi^2 i|\xi|^2 t}\, d\xi = e^{\frac{i|x|^2}{4t}} \int_{\mathbb{R}^n} \widehat{v_0}(\xi)\, e^{-4\pi^2 it|\xi - \frac{x}{4\pi t}|^2}\, d\xi \\
e^{\frac{i|x|^2}{4t}} &\int_{\mathbb{R}^n} \widehat{v_0}(\xi)\, e^{\frac{i|\frac{x}{4\pi t} - \xi|^2}{4/(-16\pi^2 t)}}\, d\xi = e^{\frac{i|x|^2}{4t}} \overline{\int_{\mathbb{R}^n} \overline{\widehat{v_0}(\xi)}\, e^{\frac{i|\frac{x}{4\pi t} - \xi|^2}{4/(16\pi^2 t)}}\, d\xi} \\
&= e^{\frac{i|x|^2}{4t}} \left(\frac{i}{4\pi t}\right)^{n/2} \left(\frac{4\pi t}{i}\right)^{n/2} \overline{\int_{\mathbb{R}^n} \overline{\widehat{v_0}(\xi)}\, e^{\frac{i|\frac{x}{4\pi t} - \xi|^2}{4/(16\pi^2 t)}}\, d\xi} \\
&= \frac{e^{\frac{i|x|^2}{4t}}}{(4\pi i t)^{n/2}}\, \overline{u}\left(\frac{x}{4\pi t}, \frac{1}{16\pi^2 t}\right),
\end{aligned}$$

if we denote $u_0(x) = f(x) = \overline{\widehat{v_0}(x)}$. Thus, we get a new solution

$$v(x,t) = \frac{e^{\frac{i|x|^2}{4t}}}{(4\pi i t)^{n/2}}\, \overline{u}\left(\frac{x}{4\pi t}, \frac{1}{16\pi^2 t}\right) \tag{C.8}$$

with initial datum $v_0(x) = \overline{\widehat{u_0}(x)}$.

On the other hand, to match the expression we use in (2.16) in Subsection 2.2.2, we combine (C.8) with the dilation symmetry (C.6) with $\lambda = 4\pi$ to get one more solution

$$w(x,t) = \frac{1}{4\pi}\, v\left(\frac{x}{4\pi}, \frac{t}{16\pi^2}\right) = \frac{e^{\frac{i|x|^2}{4t}}}{(4\pi i t)^{n/2}}\, \overline{u}\left(\frac{x}{t}, \frac{1}{t}\right),$$

so that $w_0(x) = \frac{1}{4\pi}\, v_0(x/4\pi) = \frac{1}{4\pi}\, \overline{\widehat{u_0}(x/4\pi)}$.

Bibliography

[1] Ampère, A.-M. "Recherche sur quelques points de la théorie des fonctions dérivées qui conduisent à une nouvelle démonstration du théorème de Taylor, et à l'expression finie des termes qu'on néglige lorsqu'on arrête cette série à un terme quelconque". *J. Éc. polytech.* 13 (1806), pp. 148–181. URL: https://gallica.bnf.fr/ark:/12148/bpt6k433669p/f149.image (cit. on p. 2).

[2] Apostol, T. M. *Modular functions and Dirichlet series in number theory*. Second. Vol. 41. Graduate Texts in Mathematics. Springer-Verlag, New York, 1990. DOI: 10.1007/978-1-4612-0999-7 (cit. on p. 40).

[3] Arms, R. J. and Hama, F. R. "Localized-Induction Concept on a Curved Vortex and Motion of an Elliptic Vortex Ring". *Phys. Fluids* 8 (4) (1965), pp. 553–559. DOI: 10.1063/1.1761268 (cit. on p. 9).

[4] Banica, V. and Vega, L. "The initial value problem for the binormal flow with rough data". *Ann. Sci. Éc. Norm. Supér. (4)* 48 (6) (2015), pp. 1423–1455. DOI: 10.24033/asens.2273 (cit. on p. 10).

[5] Banica, V. and Vega, L. "Evolution of polygonal lines by the binormal flow". *Ann. PDE* 6 (1) (2020), p. 6. DOI: 10.1007/s40818-020-0078-z (cit. on p. 10).

[6] Berndt, B. C., Evans, R. J., and Williams, K. S. *Gauss and Jacobi sums*. Canadian Mathematical Society Series of Monographs and Advanced Texts. A Wiley-Interscience Publication. John Wiley & Sons, Inc., New York, 1998 (cit. on p. 43).

[7] Berry, M. V. "Quantum fractals in boxes". *J. Phys. A* 29 (20) (1996), pp. 6617–6629. DOI: 10.1088/0305-4470/29/20/016 (cit. on p. 8).

[8] Berry, M. V. and Goldberg, J. "Renormalisation of curlicues". *Nonlinearity* 1 (1) (1988), pp. 1–26. DOI: 10.1088/0951-7715/1/1/001 (cit. on pp. 133–135).

[9] Berry, M. V. and Klein, S. "Integer, fractional and fractal Talbot effects". *J. Modern Opt.* 43 (10) (1996), pp. 2139–2164. DOI: 10.1080/09500349608232876 (cit. on pp. 8, 20, 23, 135).

[10] Berry, M., Marzoli, I., and Schleich, W. "Quantum carpets, carpets of light". *Phys. World* 14 (6) (2001), pp. 39–46. DOI: 10.1088/2058-7058/14/6/30 (cit. on p. 17).

[11] Bolzano, B. *Functionenlehre*. Vol. 1. Spisy Bernarda Bolzano - Bernard Bolzano's Schriften. Královská Ceská Spolecnost Nauk, 1930 (cit. on p. 3).

[12] Boritchev, A., Eceizabarrena, D., and Vilaça da Rocha, V. "Riemann's non-differentiable function is intermittent" (2019). Preprint: http://arxiv.org/abs/1910.13191v1 (cit. on p. 108).

[13] Buckmaster, T. and Vicol, V. "Convex integration and phenomenologies in turbulence". *EMS Surv. Math. Sci.* 6 (1) (2019), pp. 173–263. DOI: 10.4171/emss/34 (cit. on p. 27).

[14] Butzer, P. L. and Stark, E. L. ""Riemann's example" of a continuous non-differentiable function in the light of two letters (1865) of Christoffel to Prym". *Bull. Soc. Math. Belg. Sér. A* 38 (1986), 45–73 (1987) (cit. on p. 5).

[15] Cellérier, M. C. "Note sur les principes fondamentaux de l'analyse". *B. Sci. Math.* 14 (1890), pp. 142–160. URL: https://gallica.bnf.fr/ark:/12148/bpt6k9621739d/f146.item.r=140 (cit. on p. 4).

[16] Chamizo, F. and Córdoba, A. "Differentiability and dimension of some fractal Fourier series". *Adv. Math.* 142 (2) (1999), pp. 335–354. DOI: 10.1006/aima.1998.1792 (cit. on p. 8).

[17] Chamizo, F. and Ubis, A. "Some Fourier series with gaps". *J. Anal. Math.* 101 (2007), pp. 179–197. DOI: 10.1007/s11854-007-0007-z (cit. on p. 8).

[18] Chamizo, F. and Ubis, A. "Multifractal behavior of polynomial Fourier series". *Adv. Math.* 250 (2014), pp. 1–34. DOI: 10.1016/j.aim.2013.09.015 (cit. on p. 8).

[19] Chousionis, V., Erdoğan, M. B., and Tzirakis, N. "Fractal solutions of linear and nonlinear dispersive partial differential equations". *Proc. Lond. Math. Soc. (3)* 110 (3) (2015), pp. 543–564. DOI: 10.1112/plms/pdu061 (cit. on p. 8).

[20] Da Rios, L. S. "Sul moto d'un liquido indefinito con un filetto vorticoso di forma qualunque". *Rend. Circ. Mat. Palermo* 22 (1) (1906), pp. 117–135. DOI: 10.1007/bf03018608 (cit. on pp. xi, xvii, xxiii, 9).

[21] Darboux, G. "Mémoire sur les fonctions discontinues". *Ann. Sci. École Norm. Sup. (2)* 4 (1875), pp. 57–112. URL: http://www.numdam.org/item?id=ASENS_1875_2_4__57_0 (cit. on p. 2).

[22] Daubechies, I. and Lagarias, J. C. "On the thermodynamic formalism for multifractal functions". *Rev. Math. Phys.* 6 (5A) (1994), pp. 1033–1070. DOI: 10.1142/S0129055X94000353 (cit. on pp. 27–29).

[23] de la Hoz, F., García-Cervera, C. J., and Vega, L. "A numerical study of the self-similar solutions of the Schrödinger map". *SIAM J. Appl. Math.* 70 (4) (2009), pp. 1047–1077. DOI: 10.1137/080741720 (cit. on p. 10).

[24] de la Hoz, F. and Vega, L. "On the relationship between the one-corner problem and the M-corner problem for the vortex filament equation". *J. Nonlinear Sci.* 28 (6) (2018), pp. 2275–2327. DOI: 10.1007/s00332-018-9477-7 (cit. on p. 14).

[25] de la Hoz, F., Kumar, S., and Vega, L. "On the evolution of the vortex filament equation for regular M-polygons with nonzero torsion". *SIAM J. Appl. Math.* 80 (2) (2020), pp. 1034–1056. DOI: 10.1137/19M1272755 (cit. on p. 14).

[26] de la Hoz, F. and Vega, L. "Vortex filament equation for a regular polygon". *Nonlinearity* 27 (12) (2014), pp. 3031–3057. DOI: 10.1088/0951-7715/27/12/3031 (cit. on pp. xi, xii, xvii, xviii, xxiii, xxiv, 9–11, 14, 24, 25, 42, 77).

[27] Dr. SkySkull. "Rolling out the (optical) Talbot carpet: the Talbot effect". *Skulls in the Stars* (2010). Visited on 2020-04-10. URL: https://skullsinthestars.com/2010/03/04/rolling-out-the-optical-carpet-the-talbot-effect/ (cit. on p. 130).

[28] Du Bois-Reymond, P. "Versuch einer Classification der willkürlichen Functionen reeller Argumente nach ihren Aenderungen in den kleinsten Intervallen." *J. Reine Angew. Math.* (79) (1875), pp. 21–37. DOI: 10.1515/crll.1875.79.21 (cit. on p. 3).

[29] Duistermaat, J. J. "Self-similarity of "Riemann's nondifferentiable function"". *Nieuw Arch. Wisk.* 9 (3) (1991), pp. 303–337 (cit. on pp. xiv, xx, xxvi, 6, 29, 39, 48, 53, 79, 102, 110).

[30] Eceizabarrena, D. "Asymptotic behaviour and Hausdorff dimension of Riemann's non-differentiable function" (2019). Preprint: http://arxiv.org/abs/1910.02530v1 (cit. on pp. 38, 66).

[31] Eceizabarrena, D. "Some geometric properties of Riemann's non-differentiable function". *C. R. Math. Acad. Sci. Paris* 357 (11-12) (2019), pp. 846–850. DOI: 10.1016/j.crma.2019.10.007 (cit. on pp. 38, 66, 80).

[32] Eceizabarrena, D. "Geometric differentiability of Riemann's non-differentiable function". *Adv. Math.* 366 (2020), p. 107091. DOI: 10.1016/j.aim.2020.107091 (cit. on p. 80).

[33] Erdoğan, M. B. and Shakan, G. "Fractal solutions of dispersive partial differential equations on the torus". *Selecta Math. (N.S.)* 25 (1) (2019), Paper No. 11, 26. DOI: 10.1007/s00029-019-0455-1 (cit. on p. 8).

[34] Erdoğan, M. B. and Tzirakis, N. "Talbot effect for the cubic non-linear Schrödinger equation on the torus". *Math. Res. Lett.* 20 (6) (2013), pp. 1081–1090. DOI: 10.4310/MRL.2013.v20.n6.a7 (cit. on p. 8).

[35] Euler, L. *Introductio in Analysin Infinitorum*. 1748. URL: http://eulerarchive.maa.org/pages/E101.html (cit. on p. 1).

[36] Euler, L. "Principes généraux du mouvement des fluides". *Mémoires de l'académie des sciences de Berlin* 11 (1757), pp. 274–315. URL: http://eulerarchive.maa.org/pages/E226.html (cit. on p. 1).

[37] Eyink, G. L. "Besov spaces and the multifractal hypothesis". *J. Statist. Phys.* 78 (1-2) (1995). Papers dedicated to the memory of Lars Onsager, pp. 353–375. DOI: 10.1007/BF02183353 (cit. on pp. 28, 29).

[38] Falconer, K. *Fractal geometry: Mathematical foundations and applications*. Third. John Wiley & Sons, 2014 (cit. on pp. 7, 66, 67, 80).

[39] Fourier, J. *Théorie analytique de la chaleur*. 1822. URL: https://archive.org/details/thorieanalytiq00four/page/n7/mode/2up (cit. on p. 2).

[40] Frisch, U. *Turbulence*. The legacy of A. N. Kolmogorov. Cambridge University Press, Cambridge, 1995. DOI: 10.1017/cbo9781139170666 (cit. on pp. 27, 30, 31).

[41] Frisch, U. and Parisi, G. "On the singularity structure of fully developed turbulence." In: *Proc. Enrico Fermi International Summer School in Physics*. Appendix to 'Fully developed turbulence and intermittency', by U. Frisch. 1985, pp. 84–88. URL: https://www.researchgate.net/publication/284646749 (cit. on pp. xiii, xix, xxv, 7, 27).

[42] Gerver, J. "The differentiability of the Riemann function at certain rational multiples of π". *Amer. J. Math.* 92 (1970), pp. 33–55. DOI: 10.2307/2373496 (cit. on pp. xi, xvii, xxiii, 5, 39, 53, 78).

[43] Gerver, J. "More on the differentiability of the Riemann function". *Amer. J. Math.* 93 (1971), pp. 33–41. DOI: 10.2307/2373445 (cit. on pp. 5, 39, 78).

[44] Grafakos, L. *Classical Fourier analysis*. Second. Vol. 249. Graduate Texts in Mathematics. Springer, 2008 (cit. on p. 48).

[45] Gutiérrez, S., Rivas, J., and Vega, L. "Formation of singularities and self-similar vortex motion under the localized induction approximation". *Comm. Partial Differential Equations* 28 (5-6) (2003), pp. 927–968. DOI: 10.1081/PDE-120021181 (cit. on p. 9).

[46] Gutmark, E. J. and Grinstein, F. F. "Flow control with noncircular jets". *Annu. Rev. Fluid Mech.* 31 (1) (1999), pp. 239–272. DOI: 10.1146/annurev.fluid.31.1.239 (cit. on p. 10).

[47] Hardy, G. H. "Weierstrass's non-differentiable function". *Trans. Amer. Math. Soc.* 17 (3) (1916), pp. 301–325. DOI: 10.2307/1989005 (cit. on pp. xvii, 5, 111).

[48] Hardy, G. H. and Littlewood, J. E. "Some problems of diophantine approximation". *Acta Math.* 37 (1) (1914), pp. 193–239. DOI: 10.1007/BF02401834 (cit. on p. 5).

[49] Hasimoto, H. "A soliton on a vortex filament". *J. Fluid Mech.* 51 (3) (1972), pp. 477–485. DOI: 10.1017/S0022112072002307 (cit. on p. 12).

[50] Hiedemann, E. A. and Breazeale, M. A. "Secondary Interference in the Fresnel Zone of Gratings". *J. Opt. Soc. Am.* 49 (4) (1959), p. 372. DOI: 10.1364/josa.49.000372 (cit. on p. 20).

[51] Holschneider, M. and Tchamitchian, P. "Pointwise analysis of Riemann's "nondifferentiable" function". *Invent. Math.* 105 (1) (1991), pp. 157–175. DOI: 10.1007/BF01232261 (cit. on pp. 5, 6).

[52] Hurwitz, A. "Ueber die angenäherte Darstellung der Irrationalzahlen durch rationale Brüche". *Math. Ann.* 39 (2) (1891), pp. 279–284. DOI: 10.1007/BF01206656 (cit. on p. 156).

[53] Huygens, C. *Traité de la lumière*. 1690. URL: https://gallica.bnf.fr/ark:/12148/bpt6k5659616j.texteImage (cit. on p. 17).

[54] Itatsu, S. "Differentiability of Riemann's function". *Proc. Japan Acad. Ser. A Math. Sci.* 57 (10) (1981), pp. 492–495. DOI: 10.3792/pjaa.57.492 (cit. on p. 5).

[55] Jaffard, S. "The spectrum of singularities of Riemann's function". *Rev. Mat. Iberoamericana* 12 (2) (1996), pp. 441–460. DOI: 10.4171/RMI/203. URL: https://doi.org/10.4171/RMI/203 (cit. on pp. xiii, xx, xxvi, 7, 26, 28, 30, 45, 70, 71, 79, 107).

[56] Jaffard, S. "Multifractal formalism for functions. I. Results valid for all functions". *SIAM J. Math. Anal.* 28 (4) (1997), pp. 944–970. DOI: 10.1137/S0036141095282991 (cit. on pp. 27–29).

[57] Jaffard, S. "Multifractal formalism for functions. II. Self-similar functions". *SIAM J. Math. Anal.* 28 (4) (1997), pp. 971–998. DOI: 10.1137/S0036141095283005 (cit. on pp. 28, 29).

[58] Jaffard, S. "Exposants de Hölder en des points donnés et coefficients d'ondelettes". *C. R. Acad. Sci. Paris Sér. I Math.* 308 (4) (1989), pp. 79–81. URL: https://gallica.bnf.fr/ark:/12148/bpt6k56756371/f15.item (cit. on p. 6).

[59] Jaffard, S. "Sur la dimension de Hausdorff des points singuliers d'une fonction". *C. R. Acad. Sci. Paris Sér. I Math.* 314 (1) (1992), pp. 31–36. URL: https://gallica.bnf.fr/ark:/12148/bpt6k58688425/f35.item (cit. on p. 29).

[60] Jaffard, S. "Old friends revisited: the multifractal nature of some classical functions". *J. Fourier Anal. Appl.* 3 (1) (1997), pp. 1–22. DOI: 10.1007/s00041-001-4047-y (cit. on pp. 28, 29).

[61] Jaffard, S. and Meyer, Y. "Wavelet methods for pointwise regularity and local oscillations of functions". *Mem. Amer. Math. Soc.* 123 (587) (1996). DOI: 10.1090/memo/0587 (cit. on p. 7).

[62] Jaffard, S., Meyer, Y., and Ryan, R. D. *Wavelets: Tools for science & technology*. Revised. Society for Industrial and Applied Mathematics (SIAM), Philadelphia, PA, 2001. DOI: 10.1137/1.9780898718119 (cit. on p. 29).

[63] Jerrard, R. L. and Smets, D. "On the motion of a curve by its binormal curvature". *J. Eur. Math. Soc. (JEMS)* 17 (6) (2015), pp. 1487–1515. DOI: 10.4171/JEMS/536 (cit. on pp. 10, 25, 26, 77).

[64] Kapitanski, L. and Rodnianski, I. "Does a quantum particle know the time?" In: *Emerging applications of number theory (Minneapolis, MN, 1996)*. Vol. 109. IMA Vol. Math. Appl. Springer, New York, 1999, pp. 355–371. DOI: 10.1007/978-1-4612-1544-8_14 (cit. on p. 8).

[65] Khinchin, A. Y. *Continued fractions*. Reprint of the 1964 translation. Dover Publications, 1997 (cit. on pp. 148, 149, 154, 156).

[66] Kleckner, D., Scheeler, M. W., and Irvine, W. T. M. "The life of a vortex knot". *Phys. Fluids* 26 (9) (2014), p. 091105. DOI: 10.1063/1.4893590 (cit. on pp. xi, xvii, xxiii, 10, 77).

[67] Koksma, J. F. *Diophantische Approximationen*. Springer, 1936. DOI: 10.1007/978-3-642-65618-7 (cit. on p. 156).

[68] Littlewood, J. E. and Paley, R. E.A. C. "Theorems on Fourier series and power series". *J. London Math. Soc.* 6 (3) (1931), pp. 230–233. DOI: 10.1112/jlms/s1-6.3.230 (cit. on p. 121).

[69] Luther, W. "The differentiability of Fourier gap series and "Riemann's example" of a continuous, nondifferentiable function". *J. Approx. Theory* 48 (3) (1986), pp. 303–321. DOI: 10.1016/0021-9045(86)90053-5 (cit. on p. 5).

[70] Mandelbrot, B. "How long is the coast of Britain? Statistical self-similarity and fractional dimension". *Science* 156 (3775) (1967), pp. 636–638. DOI: 10.1126/science.156.3775.636 (cit. on p. 27).

[71] Mandelbrot, B. *The fractal geometry of nature*. W. H. Freeman and Co., San Francisco, Calif., 1982 (cit. on p. 27).

[72] Matsutani, S. and Ônishi, Y. "Wave-particle complementarity and reciprocity of Gauss sums on Talbot effects". *Found. Phys. Lett.* 16 (4) (2003), pp. 325–341. DOI: 10.1023/A:1025309708569 (cit. on pp. 20, 23, 135).

[73] Mattila, P. *Geometry of sets and measures in Euclidean spaces: Fractals and rectifiability*. Vol. 44. Cambridge Studies in Advanced Mathematics. Cambridge University Press, Cambridge, 1995. DOI: 10.1017/CBO9780511623813 (cit. on pp. 66, 67).

[74] Medvedev, F. A. *Scenes from the history of real functions*. Vol. 7. Science Networks. Historical Studies. Birkhäuser Verlag, Basel, 1991, p. 265. DOI: 10.1007/978-3-0348-8660-4 (cit. on p. 2).

[75] Neuenschwander, E. "Riemann's example of a continuous, 'nondifferentiable' function". *Math. Intelligencer* 1 (1) (1978/79), pp. 40–44. DOI: 10.1007/BF03023045 (cit. on p. 5).

[76] Newton, I. *Opticks: or, A Treatise of the Reflexions, Refractions, Inflexions and Colours of Light*. 1704. URL: https://gallica.bnf.fr/ark:/12148/bpt6k3362k/f1.image (cit. on p. 17).

[77] Oskolkov, K. I. "A class of I. M. Vinogradov's series and its applications in harmonic analysis". In: *Progress in approximation theory (Tampa, FL, 1990)*. Vol. 19. Springer Ser. Comput. Math. Springer, New York, 1992, pp. 353–402. DOI: 10.1007/978-1-4612-2966-7_16 (cit. on p. 8).

[78] Oskolkov, K. I. "The Schrödinger density and the Talbot effect". In: *Approximation and probability*. Vol. 72. Banach Center Publ. Polish Acad. Sci. Inst. Math., Warsaw, 2006, pp. 189–219. DOI: 10.4064/bc72-0-13 (cit. on p. 8).

[79] Oskolkov, K. I. and Chakhkiev, M. A. "On Riemann 'nondifferentiable' function and Schrödinger equation". *Proc. Steklov Inst. Math.* 269 (1) (2010), pp. 186–196. DOI: 10.1134/s0081543810020161 (cit. on pp. 8, 48).

[80] Oskolkov, K. I. and Chakhkiev, M. A. "Traces of the discrete Hilbert transform with quadratic phase". *Proc. Steklov Inst. Math.* 280 (1) (2013), pp. 248–262. DOI: 10.1134/s0081543813010185 (cit. on p. 8).

[81] Pastor, C. "On the regularity of fractional integrals of modular forms". *Trans. Amer. Math. Soc.* 372 (2) (2019), pp. 829–857. DOI: 10.1090/tran/7418 (cit. on p. 8).

[82] Perrin, J. *Les atomes*. 1913 (cit. on p. 4).

[83] Poincaré, H. "La logique et l'intuition dans la science mathématique et dans l'enseignement". *Enseign. Math.* 1 (1899), pp. 157–162. URL: https://www.e-periodica.ch/digbib/view?pid=ens-001:1899:1#309 (cit. on p. 4).

[84] Queffelec, H. "Dérivabilité de certaines sommes de séries de Fourier lacunaires". *C. R. Acad. Sci. Paris Sér. A-B* 273 (1971), A291–A293. URL: https://gallica.bnf.fr/ark:/12148/bpt6k5728931c/f29.item (cit. on p. 5).

[85] Rayleigh, L. *The Theory of Sound*. 1877. URL: https://archive.org/details/theorysound06raylgoog/page/n8/mode/2up (cit. on p. 20).

[86] Rayleigh, L. "On copying diffraction-gratings, and on some phenomena connected therewith". *Philos. Mag.* 11 (67) (1881), pp. 196–205. DOI: 10.1080/14786448108626995. URL: https://archive.org/details/londonedinburg5111881lond/page/196/mode/2up (cit. on p. 19).

[87] Rodnianski, I. "Fractal solutions of the Schrödinger equation". In: *Nonlinear PDE's, dynamics and continuum physics (South Hadley, MA, 1998)*. Vol. 255. Contemp. Math. Amer. Math. Soc., Providence, RI, 2000, pp. 181–187. DOI: 10.1090/conm/255/03981 (cit. on p. 8).

[88] Schwarz, K. W. "Three-dimensional vortex dynamics in superfluid He4: Line-line and line-boundary interactions". *Phys. Rev. B* 31 (9) (1985), pp. 5782–5804. DOI: 10.1103/physrevb.31.5782 (cit. on p. 10).

[89] Segal, S. L. "Riemann's example of a continuous 'nondifferentiable' function. II". *Math. Intelligencer* 1 (2) (1978/79), pp. 81–82. DOI: 10.1007/BF03023065 (cit. on p. 5).

[90] Smith, A. "The differentiability of Riemann's functions". *Proc. Amer. Math. Soc.* 34 (1972), pp. 463–468. DOI: 10.2307/2038391 (cit. on pp. 5, 11, 48).

[91] Stein, E. M. and Shakarchi, R. *Complex analysis*. Vol. 2. Princeton Lectures in Analysis. Princeton University Press, 2003 (cit. on p. 40).

[92] Talbot, H. F. "Facts relating to optical science. No. IV". *Philos. Mag.* 9 (56) (1836), pp. 401–407. DOI: 10.1080/14786443608649032 (cit. on pp. 15, 19).

[93] Tennekes, H. and Lumley, J. L. *A first course in turbulence*. MIT Press, 1972 (cit. on pp. 30–32).

[94] University of Vienna. "The Talbot effect". *Quantum Interactive* (2016). Visited on 2020-03-23. URL: https://interactive.quantumnano.at/advanced/quantum-experiments/talbot-effect/ (cit. on p. 16).

[95] Weierstrass, K. "Über continuirliche Functionen eines reellen Arguments, die für keinen Werth des letzteren einen bestimmten Differentialquotienten besitzen." In: *Mathematische Werke. II. Abhandlungen 2*. 1895, pp. 71–74 (cit. on p. 2).

[96] Westfall, P. H. "Kurtosis as peakedness, 1905–2014. *R.I.P.*" *Amer. Statist.* 68 (3) (2014), pp. 191–195. DOI: 10.1080/00031305.2014.917055 (cit. on p. 31).

[97] Winthrop, J. T. and Worthington, C. R. "Theory of Fresnel Images. I. Plane Periodic Objects in Monochromatic Light". *J. Opt. Soc. Am.* 55 (4) (1965), pp. 373–381. DOI: 10.1364/josa.55.000373 (cit. on p. 20).

[98] Young, T. "The Bakerian Lecture. Experiments and calculations relative to physical optics". *Phil. Trans. R. Soc.* 94 (1804), pp. 1–16. DOI: 10.1098/rstl.1804.0001 (cit. on p. 18).

[99] Zalcwasser, Z. "Sur les polynomes associés aux fonctions modulaires". *Studia Math.* 7 (1) (1938), pp. 16–35. DOI: 10.4064/sm-7-1-16-35 (cit. on p. 122).

[100] Zemanian, A. H. *Distribution theory and transform analysis: an introduction to generalized functions, with applications*. Second. Dover Publications, Inc., New York, 1987 (cit. on pp. 137, 143).